# Proceedings of the First Italian Meeting on Environmental Micropaleontology

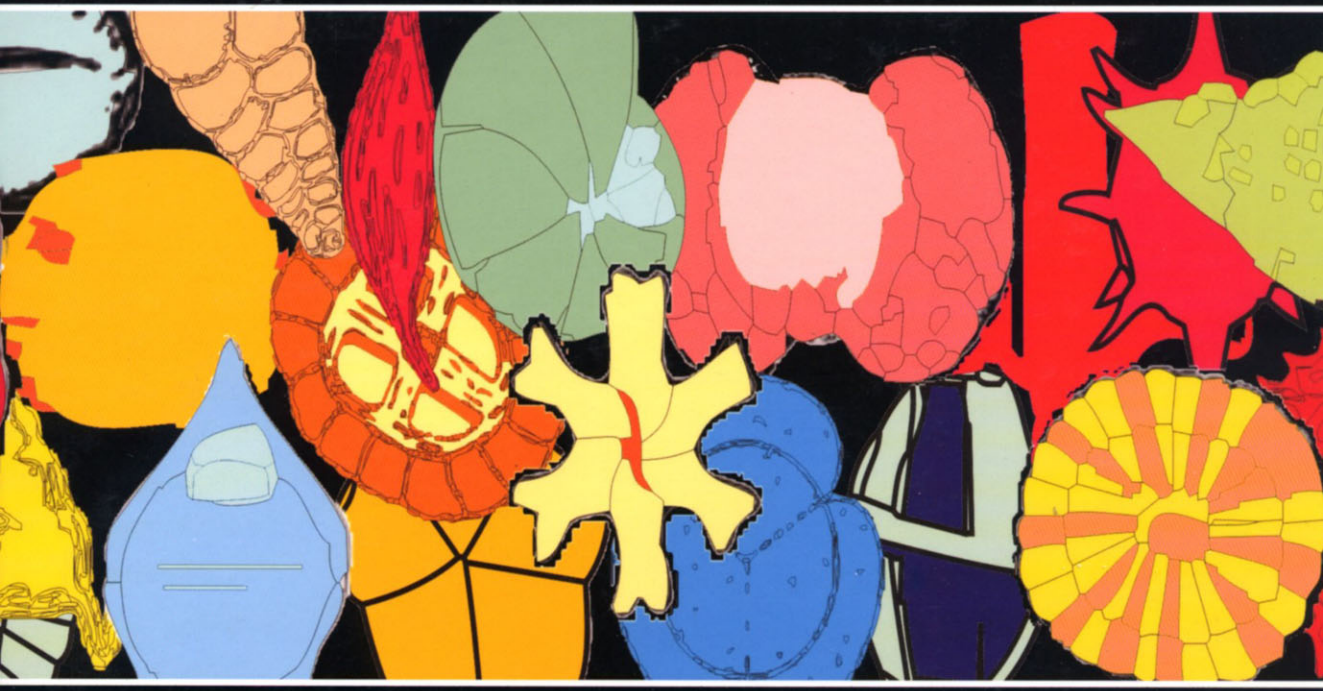

Edited by:
R. Coccioni
S. Galeotti
F. Lirer

# Proceedings of the First Italian Meeting on Environmental Micropaleontology

**Urbino, Italy, June 4-6, 2002**

*Edited by:*
**R. Coccioni, S. Galeotti, & F. Lirer**


**Grzybowski Foundation, 2004**

# Proceedings of the First Italian Meeting on Environmental Micropaleontology

(Urbino, Italy, June 4-6, 2002)

Edited by

**Rodolfo Coccioni**
Istituto di Geologia e Centro di Geobiologia,
Università degli Studi di Urbino "*Carlo Bo*",
Campus Scientifico, Località Crocicchia, 61029 Urbino, Italy

**Simone Galeotti**
Istituto di Geologia e Centro di Geobiologia,
Università degli Studi di Urbino "*Carlo Bo*",
Campus Scientifico, Località Crocicchia, 61029 Urbino, Italy

and

**Fabrizio Lirer**
Istituto per l'Ambiente Marino Costiero (IAMC),
Geomare – CNR,
Calata Porta di Massa, Interno Porto di Napoli, 80133 Napoli, Italy

Published by

**The Grzybowski Foundation**

**Grzybowski Foundation Special Publication No. 9**

First published in 2004 by the

**Grzybowski Foundation**

a charitable scientific foundation which associates itself with the Geological Society of Poland, founded in 1992.
The Grzybowski Foundation promotes and supports education and research in the field of Micropalaeontology through its Library (located at the Geological Museum of the Jagiellonian University), Special Publications, Student Grant-in-Aid Programme, and by organising symposia at scientific conferences. Visit our website:

**www.es.ucl.ac.uk/Grzybowski/**



**Distributors:**

The Special Publications Editor (Email: m.kaminski@ucl.ac.uk), or any of the Trustees of the Grzybowski Foundation

North America: Micropaleontology Project, 256 Fifth Avenue - 4th Floor, New York, N.Y. 10021 [1-212-481-2997]

Poland: The Grzybowski Foundation, c/o Geological Museum, Jagiellonian University, ul. Oleandry 2a, 30-063 Kraków, Poland.

**This book can be cited as:**
Coccioni R., Galeotti S. & Lirer F. (eds), 2004. Proceedings of the First Italian Meeting on Environmental Micropaleontology. *Grzybowski Foundation Special Publication*, 9, 96 + x pp.



**British Library Cataloguing in Publication Data**
Proceedings of the First Italian Meeting on Environmental Micropaleontology
1. Fossil Foraminifera
I. Coccioni, R. (Rodolfo), 1948 -
II. Galeotti, S. (Simone), 1965 –
III. Lirer, F. (Fabrizio), 1970 -

**ISBN:** 83-912385-5-5

Printed in Italy by:
Arti Grafiche Editoriali srl, Urbino.
Publication Date: May 20, 2004.

## Preface

The Italian Meetings on Environmental Micropaleontology (IMEM) at the University of Urbino "Carlo Bo" are intended to promote scientific interaction between Italian specialists in a broad spectrum of fossil and recent microorganismal taxa that share environmental applications.

The 1st meeting held in July, 2002 has seen the participation of 44 micropaleontologists attending over 20 oral presentation on the various aspects the paleoenvironmental reconstruction and environmental monitoring based on microorganismal distribution. This thematic collection consisting of seven of the many papers presented on Recent and fossil foraminiferal distribution from a wide variety of depositional settings and environments, is very welcome as a first in what will hopefully be a long-standing series.

We wish to thank the many people that helped making the 1st IMEM meeting a great success, most important among which were the participants who gave some outstanding presentations during the meeting.

Finally, we wish to thank all those that assisted in the review process, the authors who responded to the comments in good spirit, and Andrea Marsili for his assistance with the final preparation of the book.

***The Editors***

**Participants at the First Italian Meeting on Environmental Micropaleontology**
**Campus Scientifico, Università degli Studi di Urbino "*Carlo Bo*", Urbino**

## TABLE OF CONTENTS



## *LIST OF REVIEWERS*

## *LIST OF REVIEWERS*

R. Coccioni (Urbino, Italy); S. Galeotti (Urbino, Italy); M.B. Hart (Plymouth, United Kingdom); S. Iaccarino (Parma, Italy); M.A. Kaminski (London, United Kingdom); I. Premoli Silva (Milan, Italy); R. Spejer (Bremen, Germany); S. Spezzaferrri (Fribourg, Switzerland); R. Sprovieri (Palermo, Italy); D. Violanti (Torino, Italy).

## 1st ITALIAN MEETING ON ENVIRONMENTAL MICROPALEONTOLOGY
*Università degli Studi di Urbino "Carlo Bo", Urbino*

## *LIST OF PARTICIPANTS*

| | |
|---|---|
| **BERGAMIN LUISA** | **Università di Roma "La Sapienza"** |
| **BIONDI RICCARDO** | **Università di Chieti** |
| **CAMILLETTI LUCIA** | **Università di Ancona** |
| **CARUSO ANTONIO** | **Università di Palermo** |
| **CASCELLA ANTONIO** | **Università di Pisa** |
| **CATTABIANI FABRIZIO** | **Università di Parma** |
| **CAVALAZZI BARBARA** | **Università di Bologna** |
| **COCCIONI RODOLFO** | **Università di Urbino** |
| **DALL'ANTONIA BARBARA** | **Università di Pisa** |
| **DI BELLA LETIZIA** | **Università di Roma "La Sapienza"** |
| **DI STEFANO AGATA** | **Università di Catania** |
| **FERRARO LUCIANA** | **CNR - IAMC Napoli** |
| **FONTANESI GIULIA** | **Università di Parma** |
| **FREZZA VIRGILIO** | **Università di Roma "La Sapienza"** |

| | |
|---|---|
| **GALEOTTI SIMONE** | **Università di Urbino** |
| **GIUNTA SIMONA** | **Università di Ancona** |
| **GUASTI ELISA** | **Università di Brema** |
| **IACCARINO SILVIA** | **Università di Parma** |
| **IACOVONE VALERIA** | **CNR - IGM Bologna** |
| **IAMUNDO FABRIZIA** | **Università di Roma "La Sapienza"** |
| **LIRER FABRIZIO** | **Università di Parma** |
| **MANISCALCO ROSANNA** | **Università di Catania** |
| **MARINO MARIA CONCETTA** | **Università di Bari** |
| **MICUCCI ALESSANDRO** | **Università di Ancona** |
| **MORABITO SIMONA** | **Università di Benevento** |
| **MORIGI CATERINA** | **Università di Ancona** |
| **MOTTA YLENIA** | **Università di Ancona** |
| **MURANO INCORONATA** | **Università di Ancona** |
| **NEGRI ALESSANDRA** | **Università di Ancona** |
| **PANCOTTI IRENE** | **Università di Ancona** |
| **PANIERI GIULIANA** | **Università di Bologna** |
| **PAOLIZZI ELISA** | **CNR - IGM Bologna** |
| **PERSICO DAVIDE** | **Università di Parma** |
| **PRINCIPATO MARIA SPERANZA** | **Università di Milano Bicocca** |
| **PUCCI FRANCESCA** | **Università Ancona** |
| **RETTORI ROBERTO** | **Università di Perugia** |
| **RIDOLFI VALERIA** | **Università di Ancona** |
| **SABBATINI ANNA** | **Università di Ancona** |
| **SMEDILE ALESSANDRA** | **Università di Catania** |

| | |
|---|---|
| **SOROLDONI ENRICA** | **CNR - IGM Bologna** |
| **STEFANELLI SIMONA** | **Università di Bari** |
| **VENTURATI ALBERTO** | **Università di Urbino** |
| **VIOLANTI DONATA** | **Università di Torino** |
| **ZERMANI ANNALISA** | **Università di Parma** |

# Late Quaternary planktonic foraminiferal distributions: problems related to size fraction

*LUCILLA CAPOTONDI[1], ENRICA SOROLDONI[2], MARIA SPERANZA PRINCIPATO[3] and CESARE CORSELLI[3]*

1. ISMAR - C.N.R. - Sezione di Geologia Marina - Bologna, Italy
2. Collaboratrice esterna ISMAR - C.N.R. - Sezione di Geologia Marina - Bologna, Italy
3. Dipartimento di Scienze Geologiche e Geotecnologiche - Universita' di Milano - Bicocca, Italy

**ABSTRACT**

Planktonic foraminifera from marine sediment cores collected in different regions of the Mediterranean Sea were size-fractioned at 63, 125 and 150 μm in order to asses the effect of the sieve mesh size on the faunal composition. In most cases the fraction > 63 μm includes a notable mineralogical component and specimens that have not reached the adult stage of ontogeny, consequently many specimens are too small and difficult to identify. The census counts performed in the >125 and >150 μm fractions show a sensitive decrease of small species such as *Turborotalita quinqueloba*.
This study documents that the choice of the sieve size may affect the results of the investigation, influencing the percentage composition of the assemblages and consequently the paleoceanographic interpretation based on the counts. We propose the use of the 125 μm mesh sieve size for quantitative analysis in paleoclimatic and paleoceanographic reconstructions since it has allowed us to obtain, with the standard number of 300 individuals, a more realistic spectrum of the assemblage in the Mediterranean Sea.

**Keywords**: planktonic foraminifera, size fraction, sieve mesh size

## INTRODUCTION

The Late Quaternary climatic record is characterised by well dated significant fluctuations from glacial to interglacial conditions that affected the global marine plankton distribution. Planktonic foraminiferal distribution is closely related to physical-chemical properties of water masses and it depends on specific temperature and salinity ranges (Thunell, 1978). Therefore, the statistical analysis of planktonic foraminiferal assemblages provides a reliable and detailed tool for the Late Quaternary paleoceanographic and paleoclimatic reconstructions.

For this kind of investigations a standard procedure is used, based on counts of planktonic foraminifera in the dry residues after sieving through different sieve mesh size. The results of countings allow to reconstruct the relative magnitude of climatic changes that occurred in the marine environment.

For example, a very detailed study performed in the central Mediterranean Sea pointed out that the relative abundance of planktonic foraminifera *Globigerinoides* ex gr. *ruber* is in phase with the GRIP ice core record during the Last Glacial Maximum - Holocene transition (Asioli *et al.*, 1999).

In the Atlantic Ocean, the massive increase of polar planktonic species, as *Neogloboquadrina pachyderma* left, in the fraction >125 and >150 μm characterises the occurrence of Heinrich layers with Ice-Rafted Detritus (Bond *et al.*, 1993). At the same time, distribution patterns of other species are associated with the rapid climatic variations called Dansgaard - Oeschger cycles (Hendy & Kennett, 2000). Temporal changes in *Globigerina bulloides* and isotopic tracers have been successfully used to understand upwelling trends in the Somali Basin (Northwest Indian Ocean) (Vergnaud - Grazzini *et al.*,1995).

The distribution of planktonic foraminifera assemblages in surface sediment (core tops) is extensively used to develop a transfer function which helps in estimating past sea surface temperature (SST) and salinity (SSS) (CLIMAP, 1981). The quantitative distribution trends are used also as

*In*: Coccioni R., Galeotti S., & Lirer F., (eds), 2004. Proceedings of the First Italian Meeting on Environmental Micropaleontology. *Grzybowski Foundation Special Publication*, 9, 1-6.

**Table 1.** Location and characteristics of the studied sediment cores.

| Core | Water depth (m) | Lat.N | Long.E | Time interval (average age K. y.) | Research project |
|---|---|---|---|---|---|
| B74-12 | 1069 | 39°42'06" | 00° 55' 07" | S1 (8.5) | SINAPSI |
| ODP 975 C | 2500 | 58°53'79" | 04° 30' 9" | S6 (172) | ODP |
| ET99-M11 | 850 | 36°44'04" | 15° 50' 94" | S1 (8.5) | SINAPSI |
| SL9-BC | 2302 | 34°17.167' | 31° 31.361' | Holocene | SAP |

stratigraphic record: the ecozonal method offers a very high resolution time (millennial scale) and provides a detailed biochronological subdivision of the last deglacial time (Capotondi *et al.*, 1999; Asioli *et al.*, 1999; Sbaffi *et al.*, 2001).

Different counting experiments indicate that the relative abundance and the microfauna compositions are affected by the different choices of sieve mesh size among different working groups (inter alias Huber *et al.*, 1999; Smart *et al.*, 2002). The choice of the sieve may affect the results of the investigation, influencing the percentage composition of the assemblages and consequently the paleoceanographic/paleoclimatic interpretation based on the counting (Peeters *et al.*, 1999). In this work we underline the importance of the size of the sieve used for quantitative analyses.

The aim of this paper is to present some remarks on the necessity of a careful choice and our observations derived from comparative studies.

## MATERIAL AND METHODS

The samples considered in this paper were taken from cores investigated for different research projects (SAP - Sapropel And Paleoceanography, SINAPSI - Seasonal, Interannual and decAdal variability of the atmosPhere, oceanS and related marIne ecosystems and ODP - Ocean Drilling Program, Leg 161). The cores are derived from different Mediterranean basins and are related to different time periods. The stratigraphic frame was provided by radiocarbon dating and oxygen isotope stratigraphy. Details and core locations are summarised in Table 1 and Figure 1.

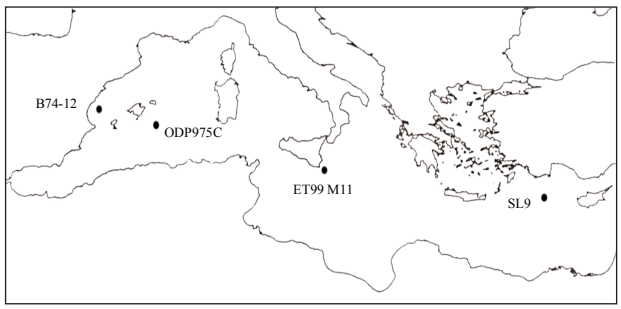


**Figure 1.** Location map of the investigated sediment cores.

All samples were washed on a >63 μm sieve and the dry residues were weighed. For each sample, we repeated the counting procedure on different fractions, >63 μm, >125 μm, >150 μm, according to the most common sieves used for micropaleontological investigations in the Mediterranean Sea. The residues of each fraction were split into aliquots containing at least 300 planktonic foraminifera individuals.

Planktonic foraminifera were identified using a binocular microscope following the taxonomy of Hemleben et al (1989).

## RESULTS

In Figure 2 we report the counting result performed on sapropel S1 (cores B 74-12, ET 99 M11, SL 9) and sapropel S6 (Hole 975 C) deposited during warm (isotopic stage 1) and cold (isotopic stage 6) climatic conditions respectively. Sapropels are organic-rich layers deposited periodically in the Mediterranean Sea caused by a brackish water lens on the surface and bottom water stagnation (Olausson, 1961).

The planktonic content reasults are comparable in the three different basins investigated and the total abundance of planktonic foraminifers reveals some dissimilarities between the different size fractions. In detail, the fraction > 63 μm includes a notable mineralogical component, sometimes prevailing over the biological one, and specimens that have not reached the adult stage of ontogeny. As a result, most many specimens are too small and difficult to identify. The counting performed in the same sample using sieve sizes >125 or >150 μm showed a significant decrease of small species, in particular *Turborotalita quinqueloba*.

In Figure 3 we report the relative abundance (plotted versus depth) of the most common taxa identified in core SL 9 spanning the last 10000 yr. The comparison between the two size fractions used for the counting (>63 and >150 μm) shows a similar trend for many species but with different values. The relative abundance and ranges of *Globigerinoides ruber* (var. *alba* and *rosea*),

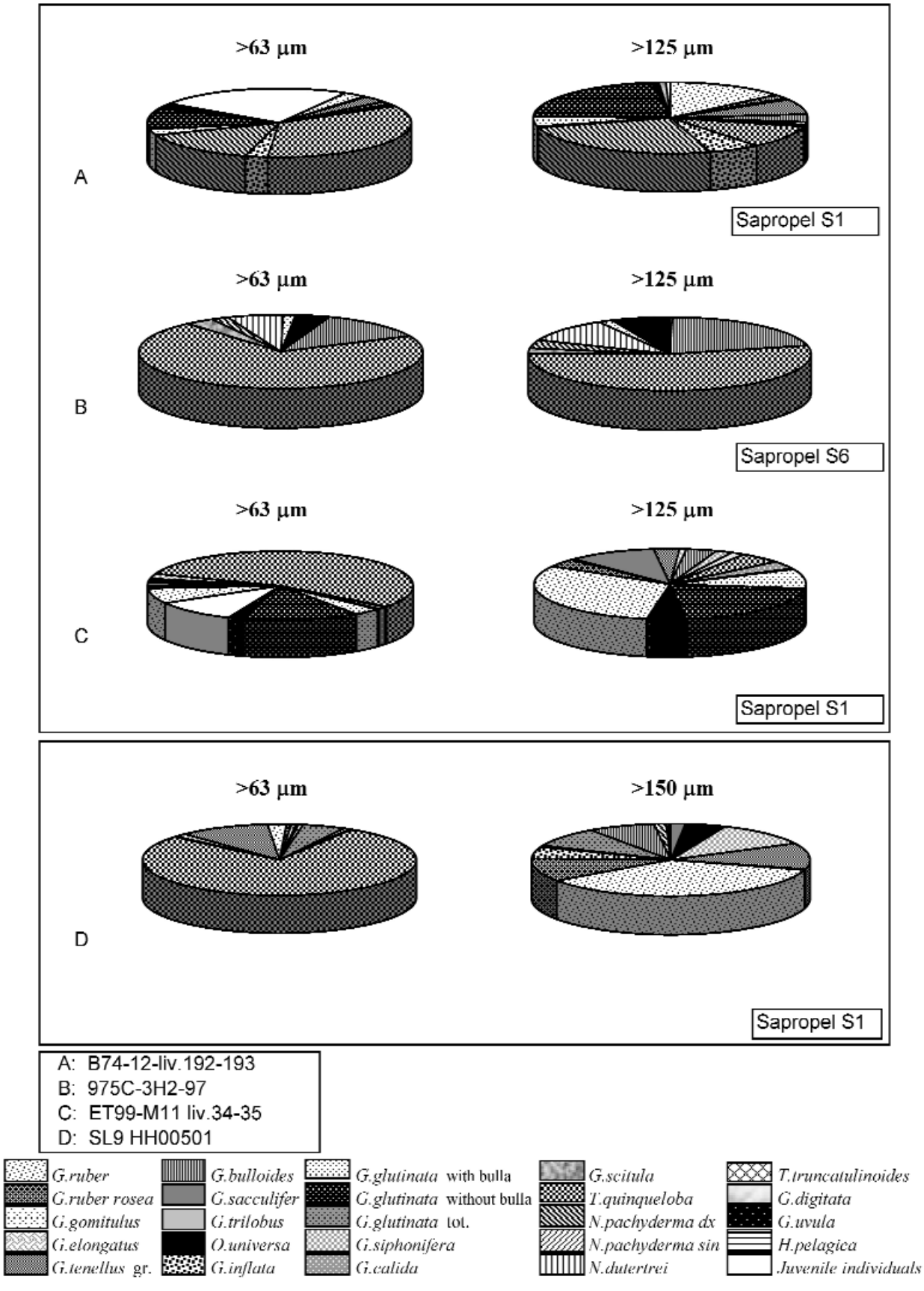


**Figure 2**. Percentages of the different species of planktic foraminifera identified in the middle part of the sediment coming from the sapropel layers (see Tab.1). Comparison between >63 μm, >125 μm and >150 μm fractions.

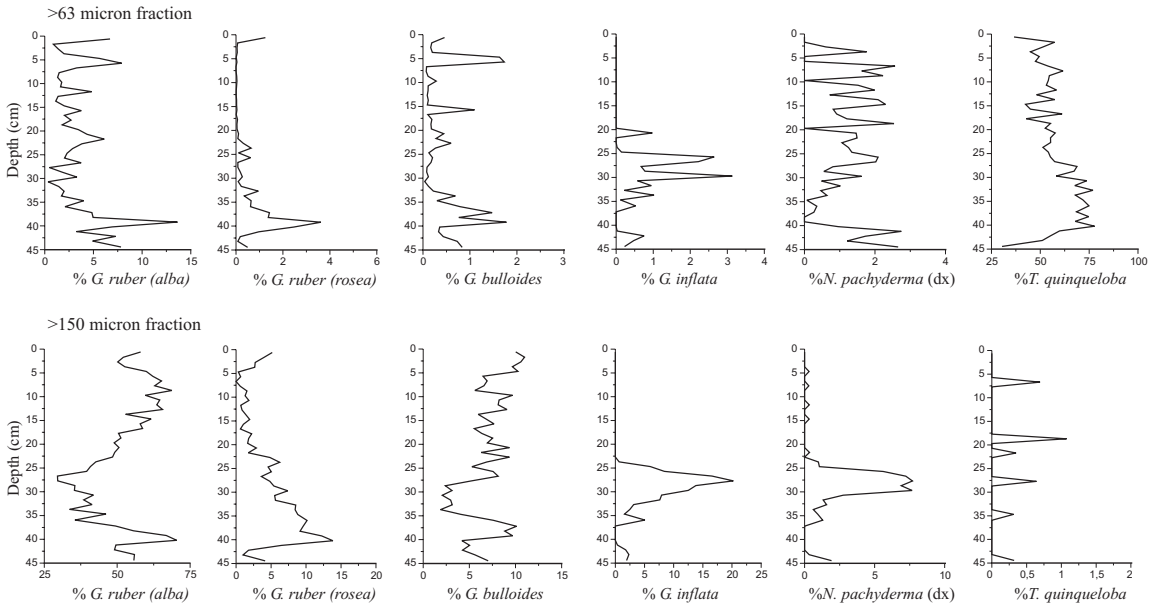


**Figure 3.** Relative abundance of the most common taxa identified in core SL 9. Comparison between >63 μm and >150 μm fractions.

*Neogloboquadrina pachyderma* (dex), *Globorotalia inflata* and *Globigerina bulloides* are higher in the >150 μm size-fraction compared with the >63 μm size fraction, whereas *Turborotalita quinqueloba* is more abundant in the >63 μm size fraction, compared with the > 150 μm size fraction (Fig. 3). At certain intervals, some species such as *Globigerinoides ruber alba*, *Neogloboquadrina pachyderma* dex and *Turborotalita quinqueloba* are under-represented or even absent from the larger size-fraction (>150 μm) while they have high abundances in the smaller size-fraction (>63 μm) (Fig. 3). Peaks in abundance of *Globorotalia inflata* in the >63 μm are consistent with peaks in abundance in the >150 μm. (Fig. 3).

## DISCUSSION AND CONCLUSIONS

The variations in size of a species can be related to the chemical - physical conditions of the surface water which controls the dynamics of the population: an increase in the average test size of a species can be achieved if temperature and salinity parameters are close to the optimum of the species (Heecht, 1976). Previous studies on size variations of planktonic foraminifera indicated that variations are related to geographical regions. Tropical species are larger in warmer waters than in cool waters and decrease in size with increasing latitude, while polar species behave in an opposite way (Bè *et al.*, 1973). On a regional scale, the environmental factors such as primary productivity and environmental dynamics of frontal systems cause deviations from this trend (Bijma *et al.*, 1992; Schiebel *et al.*, 2001).

The size of the tests taken from sediment samples can also depend on the different sedimentation rate: for example, large specimens belonging to non-spinose species usually reach the seafloor faster than the small spinose species which can remain for longer periods in the water column and are more frequently subject to dissolution or predation (Takahashi & Bé, 1984, Bijma *et al.*, 1994, Peeters *et al.*, 1999).

Using a sieve with a large mesh size it is possible to lose not only juvenile individuals of problematic classification but also a lot of individuals belonging to those species that can reach moderate dimensions. In this case a species could be overestimated affecting the composition percentage of the entire assemblage: in the larger size fraction warm species usually prevail over cold species (Bè & Hutson, 1977).

Results show that the relative abundance and the species composition of the assemblages change as a function of the sieve mesh size used during micropaleontological sample preparation.

In this study, the counting performed at >63 and >125 μm size fractions does not show a significant compositional changes; the dissimilarities became evident comparing the >63 and the >150 μm size fractions. In particular, the small foraminifer *Turborotalita quinqueloba* dominates at 63 μm while it almost disappears at >150 μm.

*Turborotalita quinqueloba* lives in the photic zone, bears symbionts (Bè & Tolderlund 1971; Hemleben *et al.*, 1989) and characterises the cold water masses assemblages; it is abundant in high fertility conditions (Bè & Tolderlund 1971; Hemleben *et al.*, 1989). Plankton tows collected in the Mediterranean Sea, showed that this species is abundant during June

around Sardinia and in the Tyrrhenian Sea (Cifelli, 1974). This species also tolerates lowered salinity: it is the dominant planktonic foraminifera in the Marmara Sea, where surface water salinity is as low as 20‰ (Aksu *et al.*, 2002). The increase of this small species in the sapropel layers deposited during both warm and cold SST conditions suggests its strong link with periods of low water density, highly stratified water column in concurrence with high nutrients and terrestrial organic material input. The correct evaluation of *Turborotalita quinqueloba* occurrence is very important for paleoenvironmental reconstruction; in this case, in the >150 μm fraction, this information has been lost and, on the other side, in the >63 μm fraction the signal is over-estimated, even considering taxonomic complications.

The distribution pattern (percentages versus depth) of the most important taxa identified in core SL 9 (Fig. 3) points out additional considerations concerning the choice of the size fraction.

The bioevents, defined as temporary occurrence or absence, or increase and decrease (following the nomenclature introduced by Pujol & Vergnaud Grazzini, 1989; Capotondi *et al.*, 1999) are not at the same stratigraphic level. Therefore, it is difficult to correlate directly the upper Quaternary eco-stratigraphical schemes based on data sets performed on different size fractions.

The observed different percentages of the same species between the >63 and >150 μm fractions from the same sample can change the climatic signal based on "warm" and "cold" water planktonic foraminifera. Paleotemperatures based on the >150 μm fraction foraminiferal assemblage can indicate colder or warmer surface temperatures than sea surface temperatures derived from the >63 μm fraction as recently documented by Niebler & Gersonde (1998) studyng the distributions of planktonic foraminifera from the southern South Atlantic Ocean.

Different authors suggest the use of >150 μm fractions for standard analysis of faunal associations because in this fraction the majority of individuals have reached the adult stage of ontogeny. Otherwise, for comparative studies on the relative abundance of small and large test size species, the use of >125 μm and >150 μm is recommended (Peeters *et al.* 1999). Based on our results, we suggest to consider more carefully the >63 μm fraction in the Mediterranean Sea. This basin is characterized by different biogeographic zones ranging from tropical to subpolar (sensu Thunell, 1978) with a large variability in the size of species. We found that the use of a 125 μm mesh sieve size allows to obtain, with the standard number of 300 individuals, a more realistic spectrum of the assemblage and consequently a reliable paleoclimatic and paleoceanographic reconstruction. In order to achieve reliable interpretations and reconstructions only the comparison between the results obtained with the same size fraction should be considered.

## ACKNOWLEDGEMENTS

The authors want to express their gratitude to the MAS III funded SAP Project (MAS3CT970137), SINAPSI (Seasonal, Interannual and decAdal variability of the atmosPhere, oceanS and related marIne ecosystems) and ODP (Ocean Drilling Program, Leg 161) Projects for the support provided. We thank Francesca Sangiorgi and Anna Maria Borsetti for stimulating discussions and Cecilia Negrini for her help. Simone Galeotti and an anonymous referee provided suggestions that helped to improve the manuscript. This publication is ISMAR - IGM - BO scientific contribution n. 1349.

## REFERENCES

Aksu, A.E., Hiscott, R.N., Kaminski, M.A., Mudie, P.J., Gillespie, H., Abrajano, T., & Yasar, D. 2002. LAst glacial-Holocene paleoceanography of the Black Sea and Marmara Sea: stable isotopic, foraminiferal and coccolith abundance. *Marine Geology*, **190**, 119-149.

Asioli, A., Trincardi, F., Lowe, J.J, & Oldfield F. 1999. Short - term climate changes during the last Glacial-Holocene transition: comparison between Mediterranean records and the GRIP event stratigraphy. *Journal of Quaternary Science*, **14**(4), 373-381.

Bè, A.W.H, & Tolderlund, D.S. 1971. Distribution and ecology of living planktonic Foraminifera in surface waters of the Atlantic and Indian oceans. In: Funnel B.M. & Riedel W.R. (Eds.), *The Micropaleontology of the Oceans*, Cambridge University Press, 105-149.

Bè, A.W.H., Harrison S.M., & Lott, L. 1973. *Orbulina universa* d'Orbigny in the Indian Ocean. Micropaleontology, **19**, 150-192.

Bè, A.W.H., & Hutson, W.H. 1977. Ecology of planktonic foraminifera and biogeographic patterns of life and fossil assemblages in the Indian Ocean. *Micropaleontology*, **23**, 369-414.

Bijma, J., Hemleben, C., Oberhänsli, H., & Spindler M. 1992. The effect of increased water fertility on tropical spinose planktonic foraminifers in laboratory cultures. Journal of Foraminiferal Research, **22**, 242-256.

Bijma, J., Hemleben, C., & Wellnitz, K. 1994. Lunar-influenced carbonate flux of the planktic foraminifer Globigerinoides sacculifer (Brady) from the central Red Sea. *Deep - Sea Res*, I, **41**, 511-530.

Bond, G., Broecker, W., Johnson, S., McManus, J., Labeyrie, L., Jouzel, J., & Bonani, G. 1993. Correlations between climate records from North Atlantic sediments and Greenland ice. *Nature*, **365**, 143-147

Capotondi, L., Borsetti, A.M., & Morigi, C. 1999. Foraminiferal ecozones, a high resolution proxy for the late Quaternary biochronology in the Central Mediterranean Sea. *Marine Geology*, **153**, 253-274.

Cifelli, R. 1974. Planktonic foraminifera from the Mediterranean and adjacent Atlantic waters (Cruise 49 of the Atlantic II, 1969). *Journal of Foraminiferal Research*, **4**, 171-183.

CLIMAP 1981. Seasonal reconstruction of the earth's surface at the last glacial maximum. *Geological Society of*

*America Map Chart Ser*. MC-36.

Dansgaard, W., Johnsen, S.J., Clausen, H.B., Dahl-Jensen, D., Gundestrup, N.S., Hammer, C.U., Hvidberg, C.S., Steffensen, J.P., Sveinbjornsdottir, A.E., Jouzel, J., & Bond, G. 1993. Evidence for general instability of past climate from a 250-kyr ice-core record. *Nature*, **364**, 218-220.

Hecht, A.D. 1976. An ecologic model for test size variation in recent planktonic foraminifera: applications to the fossil record. *Journal of Foraminiferal Research*, **6**, 295-311.

Hemleben, C., Spindler, M., & Anderson, O.R. 1989. *Modern Planktonic Foraminifera*. Springer, New York, 363pp.

Hendy, I.L., & Kennett, J.P. 2000. Dansgaard - Oeschger cycles and the California Current System: planktonic foraminiferal response to rapid climate change in Santa Barbara Basin, Ocean Drilling Program hole 893A. *Paleoceanography*, 15, 1, 30-42.

Huber, R., Baumann, K.H., Beyer, J.,Brüning, J., & Hüneke, S. 1999. Data Report: counting experiments on different size fractions: examples from Site 984, *Proceeding of the Ocean Drilling Program, Scientific Results*, **162**, 191-194.

Niebler, H.S. & Gersonde, R. 1998. A planktic foraminiferal transfer function for the southern South Atlantic Ocean. *Marine Micropaleontology*, **34**, 213-234.

Olausson, E. 1961. Studies of deep - sea cores. *Reports of the Swedish Deep-Sea Expedition* 1947-1948, **8**(4), 323-438.

Peeters, F., Ivanova, K., Conan, S., Brummer, G.J., Ganssen, G., Troelstra, S., Van Hinte, J. 1999. A size analysis of planktic foraminifera from the Arabian Sea. *Marine Micropaleontology*, **36**, 31-63.

Pujol, C., Vergnaud-Grazzini, C. 1989. Paleoceanography of the Last Deglaciation in the Alboran Sea (Western Mediterranean). Stable isotopes and planktic foraminiferal records. *Marine Micropaleontology*, **15**, 153-179.

Sbaffi, L., Wezel, F.C., Kallel, N., Paterne, M., Cacho, I., Ziveri, P., & Shackleton, N. 2001. Response of the pelagic environment to paleoclimatic changes in the central Mediterranean Sea during the Late Quaternary. *Marine Geology*, **178**, 39-62.

Schiebel, R., Waniek, J., Bork, M., & Hemleben C. 2001. Planktic foraminiferal production stimulated by chlorophyll. *Deep Sea Research Part I*, **48**, 72-740.

Smart, C.W. 2002. A comparison between smaller (>63 μm) and larger (>150 μm) planktonic foraminiferal faunas from the Pleistocene of ODP Site 1073 (Leg 174 A), New Jersey margin, NW Atlantic Ocean. *Journal of Micropaleontology*, **21**, 137-147.

Takahashi, K. & Bé, A.D. 1984. Planktonic foraminifera: factors controlling sinking speeds. *Deep-Sea Research*, **1**, 1477-1500.

Thunell, R.C. 1978. Distribution of recent planktonic foraminifera in surface sediments of the Mediterranean Sea. *Marine Micropaleontology*, **3**, 147-173.

Vergnaud - Grazzini, C., Venec-Peire, M.T., Caulet, J.P., & Lerasle, N. 1995. Fertility tracers and monsoon forcing at an equatorial site of the Somali Basin (Northwest Indian Ocean). *Marine Micropaleontology*, **26**, 137-152.

# Distribution of Recent benthic foraminifers in the Ombrone River Basin (Tuscany Continental shelf, Tyrrhenian Sea, Italy): Relations with fluvial run-off

**M. GABRIELLA CARBONI[1,2], VIRGILIO FREZZA[1] *and* LUISA BERGAMIN[3]**

1. Earth Science Department. Università di Roma "La Sapienza". P.le A. Moro, 5 - 00185 - Roma.
e-mail: gabriella.carboni @uniroma1.it;
2. IGAG (CNR)- Environmental Geology and Geoengineering Institute. Earth Science Department, Università di Roma "La Sapienza". P.le A. Moro, 5 - 00185 - Roma.
3. ICRAM - Central Institute for Marine Research. Via di Casalotti, 300 - 00166 - Roma.

**ABSTRACT**

The Ombrone River basin and its delta (Tyrrhenian Sea, Italy) have been the subject of an important interdisciplinary project, focused on reconstructing the paleoenvironmental and paleogeographic evolution during the last climatic/eustatic semi-cycle. In this context, the study of Recent benthic foraminiferal assemblages provides useful proxies for the paleoecological reconstruction of the delta environment. In addition, such studies lead to an important contribution to the reconstruction of distributional patterns of fluvial contributions. Principal Component Analysis and Cluster Analysis are utilised in order to study the assemblages in relation to water depth and river delta effects. Statistical analyses show that a very important factor in determining the species distribution is distance from the river-mouth. The typical *Valvulineria bradyana* assemblage, characterised by relatively low species diversity, high dominance and benthic number, marks the most eutrophicated area running parallel to the coast, as in the Adriatic Sea. The results of this study suggest an environmental model, common to basins characterised by river-mouth and morphological setting typical of a nutrient-trap, useful for paleogeographic reconstruction.

**Keywords**: benthic foraminifera, statistical analysis, organic flux, Recent sediments, Tyrrhenian Sea

## INTRODUCTION

The part of the Tuscan continental shelf named the "Ombrone River Basin" is a confined marine sector, situated between Monte Piombino-Isola d'Elba to the north and the Argentario-Isola del Giglio to the south (Fig. 1). The coast is dominated by the Ombrone River Delta, which shows an extremely cuspidate morphology. The Ombrone River is the main contributor in this area, having a considerable load discharge of 2,000,000 t/yr, especially if compared with the limited drainage basin area of 3,500 km² (Carboni *et al*., 2000); the Ombrone is responsible for the coastal evolution of the entire basin (Ferretti & Manfredi Frattarelli, 1993). Fine deltaic sediments are dispersed along a wide area between Monte Argentario and Isola d'Elba (Chiesi *et al*., 1993). In the second half of the '90s the Ombrone River Delta and its basin were the subject of an important interdisciplinary project, focused on reconstructing its paleoenvironmental and paleogeographic evolution during the last climatic/eustatic semi-cycle (Chiocci *et al*., 1997). This area was selected for three main reasons: the presence of a small delta that includes all the typical morpho-depositional elements of larger delta complexes (Tortora, 1999); its geographical setting, whereby the basin is well protected by external factors; and the presence of the "Uccellina Natural Park", whereby a large portion of the Ombrone River drainage basin is not conditioned by human interference. In this context, benthic foraminiferal assemblages provide useful proxies for the paleoecological reconstruction of the delta environment. In addition, such assemblages offer an important contribution to the reconstruction of distributional patterns of fluvial contributions (Bergamin, 1998). The detailed study of benthic assemblages permitted to highlight, especially in the delta area, assemblages characterised by the dominance of one opportunistic species, low diversity, and high benthic productivity typical of eutrophic basins (Bergamin *et al*., 1999). Similar assemblages were singled out in the pelitic belt produced in the Adriatic Sea by the Po run-off and in other extensively studied basins over the world

*In*: Coccioni R., Galeotti S., & Lirer F., (eds), 2004. Proceedings of the First Italian Meeting on Environmental Micropaleontology. *Grzybowski Foundation Special Publication*, 9, 7-16.

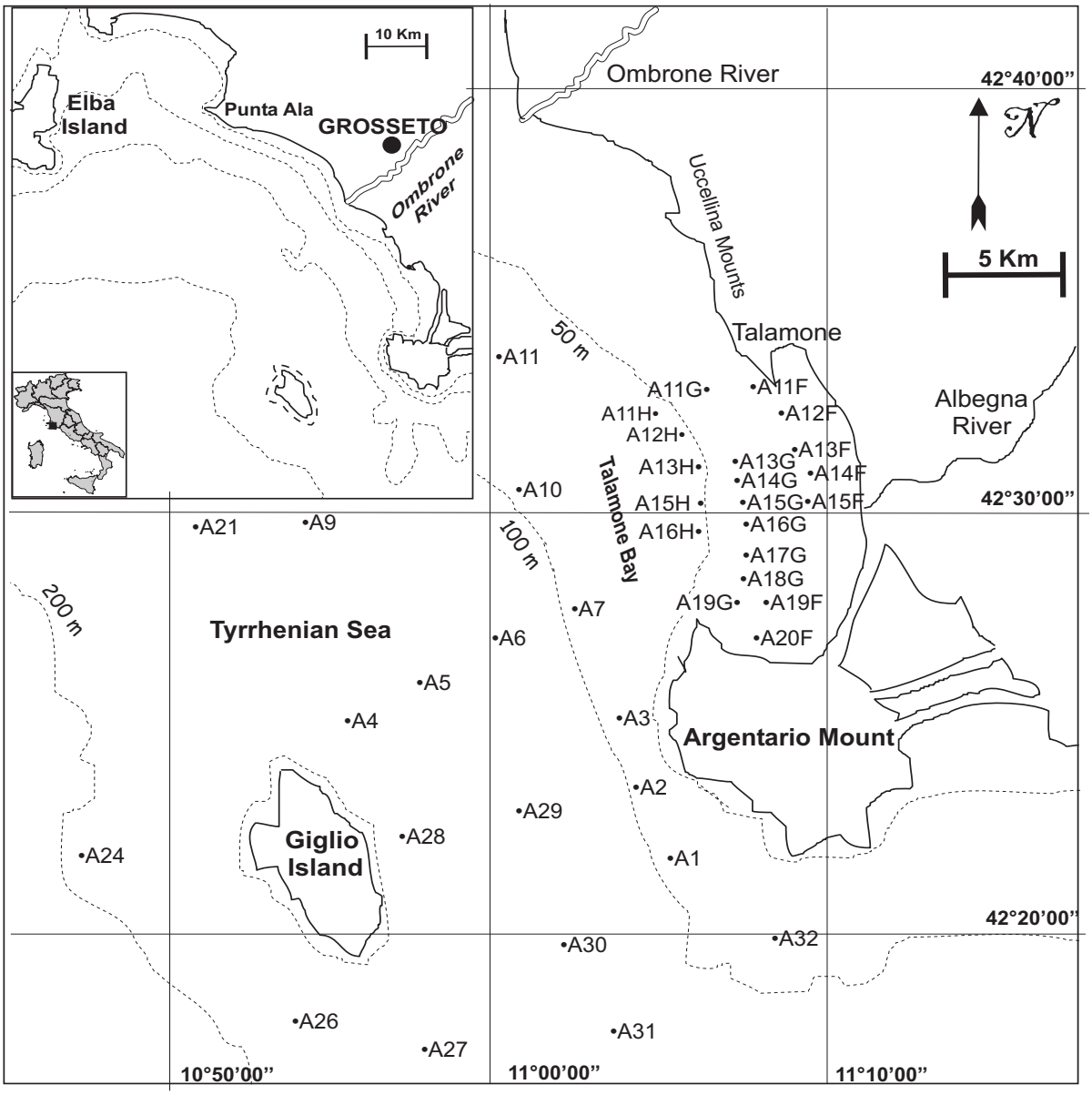


**Figure 1**. The study area. Location of sampling sites.

(Jorissen, 1987; 1988; Van der Zwaan & Jorissen, 1991; Barmavidjaja *et al*., 1992; Jorissen *et al*., 1992). Mechanisms determining the development of such assemblages are linked to the high availability of nutrients and the related low oxygen concentration at the sea bottom and within deep-water column layers (Jorissen *et al*., 1995; Van der Zwaan *et al*., 1999).

In this study we analyse benthic foraminiferal assemblages from the southern sector of the Ombrone River Basin (located between the Talamone and Argentario promontories) (Fig. 1); the goal is to analyse the assemblages in relation to water depth and river delta effects. This kind of research can be useful for marine paleo-environmental reconstruction, especially in shallow eutrophic basins. Such environments were widespread in the Italian Pliocene-Pleistocene; the geological setting of Italian coasts during these times was particularly suitable to the establishment of semi-enclosed and organic matter enriched basins, characterised by restricted water circulation (Di Bella, 1997; Borzi *et al*., 1998).

## MATERIALS AND METHODS

During the "Maremma '96" expedition of the CNR "Urania" oceanographic boat (November 23-27, 1996), several dozen grab samples were collected for micropaleontological and sedimentological analyses. In this study, 39 samples, taken at water depths ranging from 30 to 184 m are analysed. The micropaleontological samples were stored in ethanol containing Rose Bengal (2 gr/l) to distinguish between living and dead foraminifera. For this study, 19 Rose Bengal stained samples were analysed. As the percentages of living foraminifera were

**Table 1.** Geographic coordinates and water-depth of sampling sites.

| Samples | Latitude | Longitude | Water-depth (m) |
|---|---|---|---|
| A20F | 42°26'44" | 11°07'20" | 30,3 |
| A12F | 42°31'59" | 11°07'37" | 30,8 |
| A19F | 42°27'32" | 11°07'45" | 30,8 |
| A13F | 42°31'27" | 11°07'58" | 31,3 |
| A14F | 42°30'45" | 11°08'04" | 31,3 |
| A15F | 42°30'09" | 11°08'15" | 31,9 |
| A11F | 42°32'43" | 11°06'47" | 32,0 |
| A19G | 42°27'38" | 11°06'57" | 41,0 |
| A15G | 42°30'08" | 11°07'19" | 41,1 |
| A13G | 42°31'07" | 11°07'08" | 41,5 |
| A17G | 42°28'55" | 11°07'13" | 42,0 |
| A16G | 42°29'24" | 11°07'14" | 42,1 |
| A18G | 42°28'16" | 11°07'03" | 42,3 |
| A14G | 42°30'31" | 11°07'10" | 42,5 |
| A11G | 42°32'24" | 11°06'06" | 43,0 |
| A12H | 42°31'31" | 11°05'54" | 51,4 |
| A13H | 42°30'59" | 11°06'07" | 51,7 |
| A15H | 42°30'04" | 11°06'23" | 52,0 |
| A16H | 42°29'25" | 11°06'21" | 52,1 |
| A11H | 42°32'07" | 11°05'27" | 53,0 |
| A11 | 42°33'16" | 11°01'13" | 84,0 |
| A10 | 42°30'50" | 11°01'57" | 89,0 |
| A32 | 42°19'56" | 11°08'09" | 89,2 |
| A 7 | 42°28'07" | 11°02'22" | 90,0 |
| A 3 | 42°24'53" | 11°03'45" | 94,0 |
| A 1 | 42°21'18" | 11°04'17" | 95,0 |
| A 2 | 42°23'00" | 11°03'46" | 99,0 |
| A 6 | 42°26'54" | 11°00'07" | 107,0 |
| A31 | 42°17'44" | 11°03'55" | 116,0 |
| A 5 | 42°26'00" | 10°58'09" | 118,0 |
| A30 | 42°19'47" | 11°01'20" | 118,0 |
| A29 | 42°22'29" | 11°01'10" | 120,0 |
| A9 | 42°29'26" | 10°54'58" | 122,0 |
| A 4 | 42°24'43" | 10°55'49" | 127,0 |
| A21 | 42°29'59" | 10°51'23" | 135,0 |
| A27 | 42°17'34" | 10°57'20" | 137,5 |
| A28 | 42°21'49" | 10°57'01" | 153,0 |
| A26 | 42°17'46" | 10°51'30" | 172,5 |
| A24 | 42°21'46" | 10°46'37" | 183,9 |

very low, we preferred to study the total benthic assemblage, which represents the prevailing environmental conditions over the year. On the contrary, the living assemblage is free from taphonomic processes, but it is strongly influenced by seasonality and only a time-series of sampling over the whole year gives a complete idea of the entire assemblage (Scott & Medioli, 1980). It was consequently possible to increase the detail of the research by using 20 unstained samples.

All 39 samples (Table 1) were wet-sieved over 63 and 125 μm; in this study data from the >125 μm size fraction are used. Following the generic classification of Loeblich & Tappan (1987), approximately 300 specimens for each sample were counted and classified.

In accordance with the SPSS (10.1) statistical program, a hierarchical clustering (R-mode and Q-mode Cluster Analysis) was performed using the relative abundance of 26 common taxa. Distance is given in percentage by the Pearson correlation, while the similarities of the new fused clusters were calculated by adopting the most widely used method in statistical ecology, i.e., the Average Linkage method (within group) (Pielou, 1984; Parker & Arnold, 1999). In addition, two Principal Component Analyses were carried out utilising as variables both species and samples with the Canoco program (4.0). In order to simplify the matrix, some species were grouped on the basis of their taxonomy when they had homogeneous environmental significance, so that only species or groups more abundant than 4% in at least one sample were considered for statistical analysis.

To delineate in detail the assemblage structure several parameters were calculated: α-Fisher index, indicating the relationship between number of species and number of individuals in an assemblage (Fisher *et al*., 1943; Murray, 1973); Shannon H' and Shannon $H'_{(max)}$ indexes, which are indicators of heterogeneity (Murray, 1991); Percentage Dominance (PD), which is the percentage of the most abundant species in a sample (Walton, 1964); number of species compounding 80% of association; Benthic Number (BN), which is the total number of specimens per 1 gr dry sediment.

## RESULTS

### *Hierarchical clustering*

The data set containing the relative abundances of 26 common species or groups of species, was used to perform R-mode and Q-mode Cluster Analysis.

The R-mode CA (Fig. 2) groups taxa with similar environmental preferences by singling out distinct associations. In the dendrogram, two main clusters (A and B), enclosing two lower hierarchical clusters each, can be distinguished. Cluster A includes typical circalittoral to epibathyal taxa, while cluster B is constituted by infralittoral taxa. The first inferior cluster (A1) includes the deep-water foraminifera (*Uvigerina mediterranea*, *U. peregrina*, *Sphaeroidina bulloides* and *Textularia* spp.) and the second one (A2) includes *Bulimina sublimbata*, *B. marginata*, *Melonis barleeanus*, *M. pompilioides* and *Hyalinea balthica*, among others. Cluster B1 consists of taxa typical of vegetated substrate (*Rosalina bradyi*, *Lobatula*

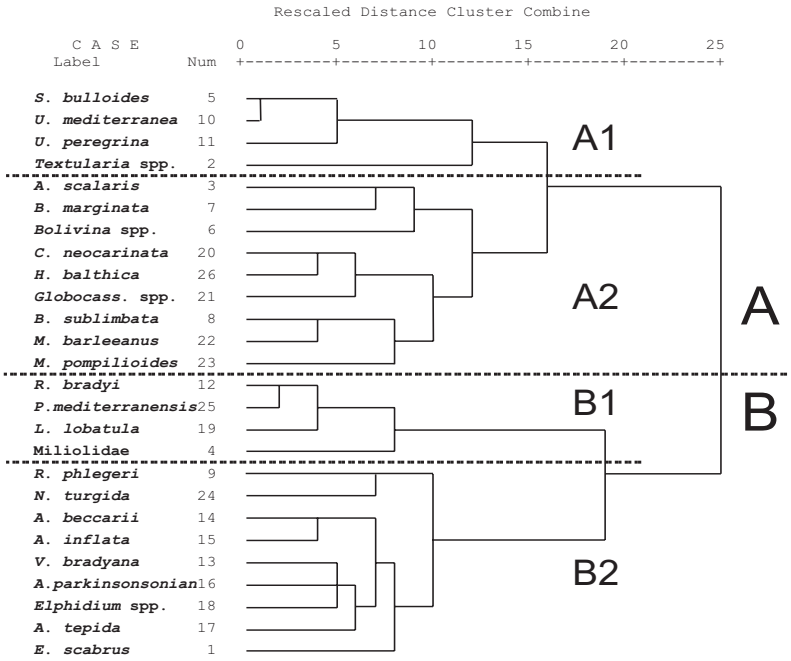


**Figure 2**. Dendrogram of 26 taxa, based on an R-mode Cluster Analysis.

*lobatula*, *Planorbulina mediterranensis* and the miliolid group). The last cluster (B2) consists of shallow water species, mainly *Ammonia* spp., *Elphidium* spp., *Eggerelloides scabrus* and *Valvulineria bradyana*. While *Ammonia* spp. and *Elphidium* spp. are typical infralittoral taxa, *V. bradyana* is characteristic of circalittoral mud (Blanc-Vernet, 1969), but it can also be found at shallower depth, near the river mouths, in substrates with high organic matter content (Jorissen, 1987).

In order to group samples characterised by homogeneous ecological conditions, the Q-mode Cluster Analysis (Fig. 3) was performed so that clusters may be viewed as biofacies. Parameters related to the assemblage structure are plotted following the sample order of Figure 3 to better characterise such groups (Fig. 4).

The outcome of the Cluster Analysis, performed with respect to the 39 samples, singles out two main clusters (X, Y). The largest one (X) is structured in two sub-clusters (X1 and X2). The succession of samples from the upper to the lower part of X1, marks the transition from assemblages where *V. bradyana* dominates (30-40%), with *Elphidium* spp. and *Ammonia* spp. less abundant, to assemblages where the equilibrium between *V. bradyana* and other taxa (*Elphidium* spp., *Ammonia* spp. and, occasionally, *E. scabrus* or *Textularia* spp.) is singled out. Samples from A15G to A13F are very similar and are mainly characterised by high BN and PD and relatively low α-index and heterogeneity (Fig. 4). Other species prevail on *V. bradyana* in five heterogeneous samples at cluster X1 bottom. Among them, A13H sample presents abundant typical epiphytic taxa (i.e., *L. lobatula*, *R. bradyi* and miliolids). These five samples show a significant distance in the dendrogram. Nevertheless, relatively low BN

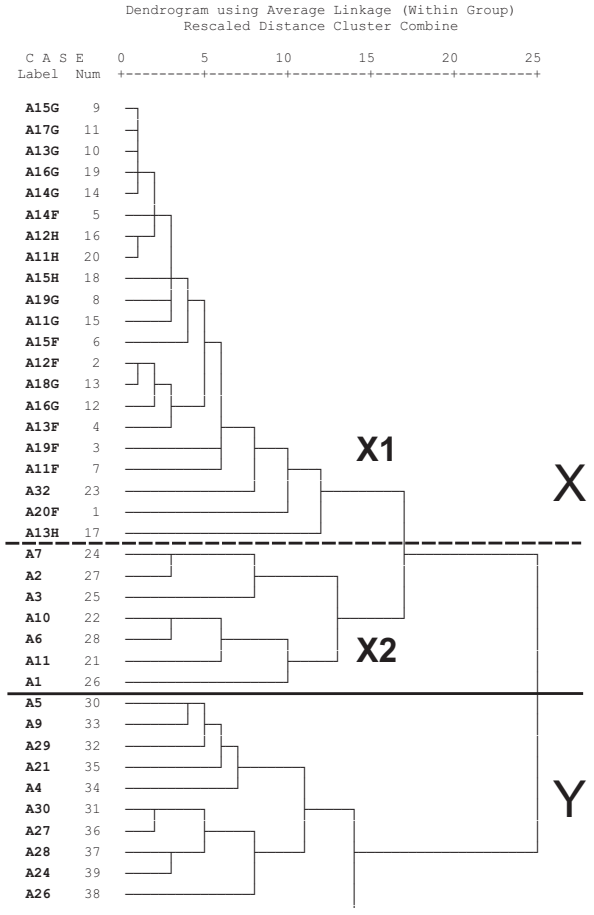


**Figure 3**. Dendrogram of 39 samples, based on a Q-mode Cluster Analysis.

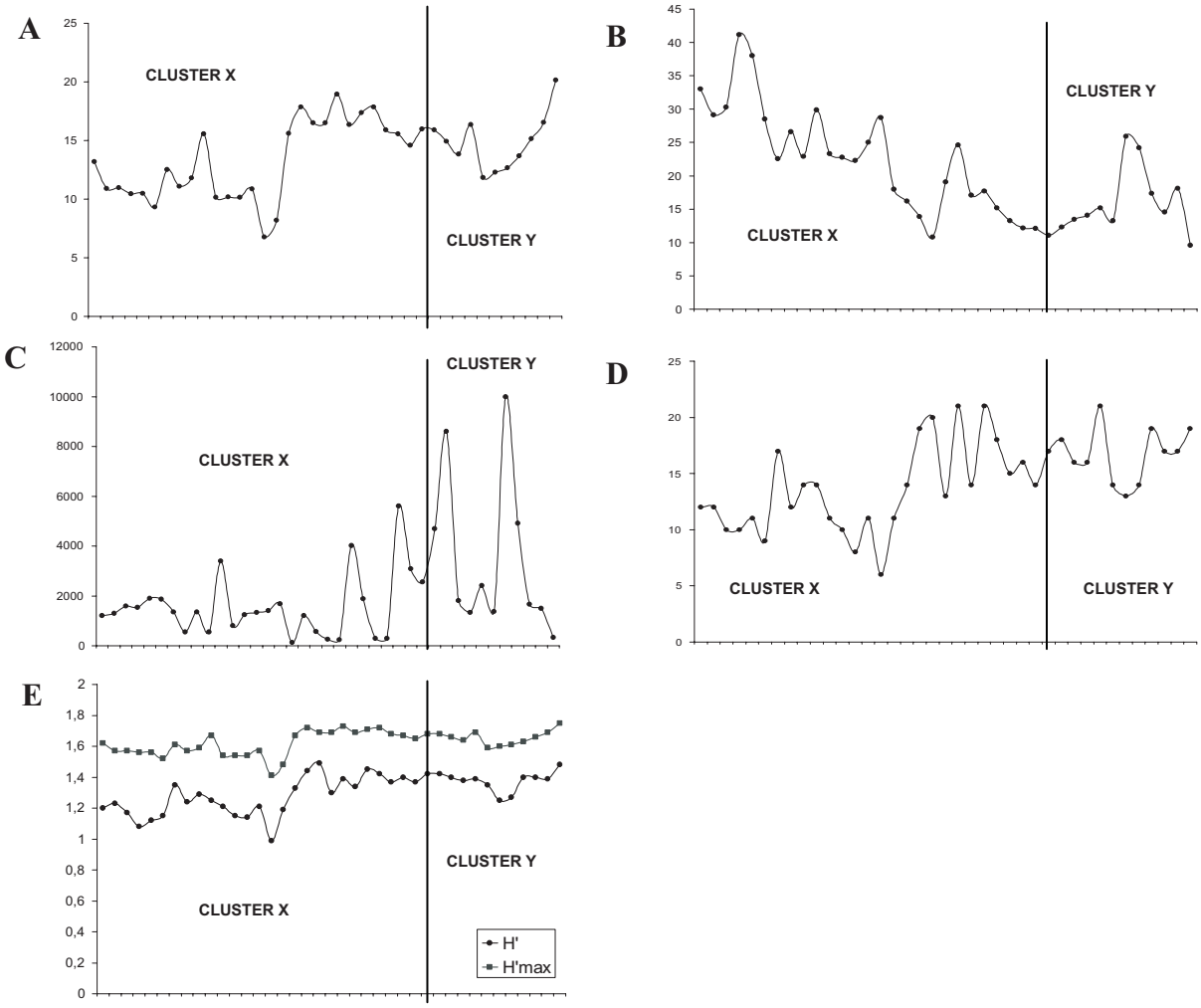


**Figure 4.** Assemblage parameters: A) a-Fisher index; B) PD - Percentage Dominance; C) BN - Benthic Number; D) Number of species forming 80% of the assemblage; E) Shannon H' and H'max. Samples order follows that of Q-mode Cluster Analysis.

and PD, high species diversity and heterogeneity are a common features of such samples.

Samples of the second smaller subcluster (X2) display a balanced upper circalittoral assemblage enclosing *V. bradyana* together with *Cassidulina neocarinata*, *B. marginata*, *M. pompilioides* and *M. barleeanus*. Such samples are characterised by variable BN, low PD, high species diversity and heterogeneity.

In cluster Y a lower circalittoral assemblage with *B. marginata*, *U. peregrina*, *U. mediterranea* and *S. bulloides* is singled out. These samples show high BN and species diversity and the highest heterogeneity and the lowest PD are also recorded.

### *Principal Component Analysis*

The Principal Component Analysis output is plotted in Figures 5 and 6. The first and second axis of PCA account for 55.4% and 12.5% of the variance respectively. Next to the PCA scores of the 26 taxa, three variables were included and plotted as vectors. The variables are the sample water-depth and, to test a possible influence of river run-off, the differences between samples latitude and longitude versus those of the Ombrone River mouth, located north of the sampling area.

Considering the geographical setting of the coast, the data show that the longitude difference almost coincides with the distance from the Ombrone River Delta. In addition, the latitude difference almost coincides with the distance from the coast and, consequently, water-depth.

The three vectors, D (depth), LOD (longitude-difference = distance from coast) and LAD (latitude-difference = distance from the Ombrone River mouth) plot negatively on the first axis. Vector LAD coincides with such axis meaning that Component 1 is strictly linked to the distance from the Ombrone River mouth. Consequently, the latitude-difference is independent from the second axis. Vectors D and LOD plot also negatively on the second axis.

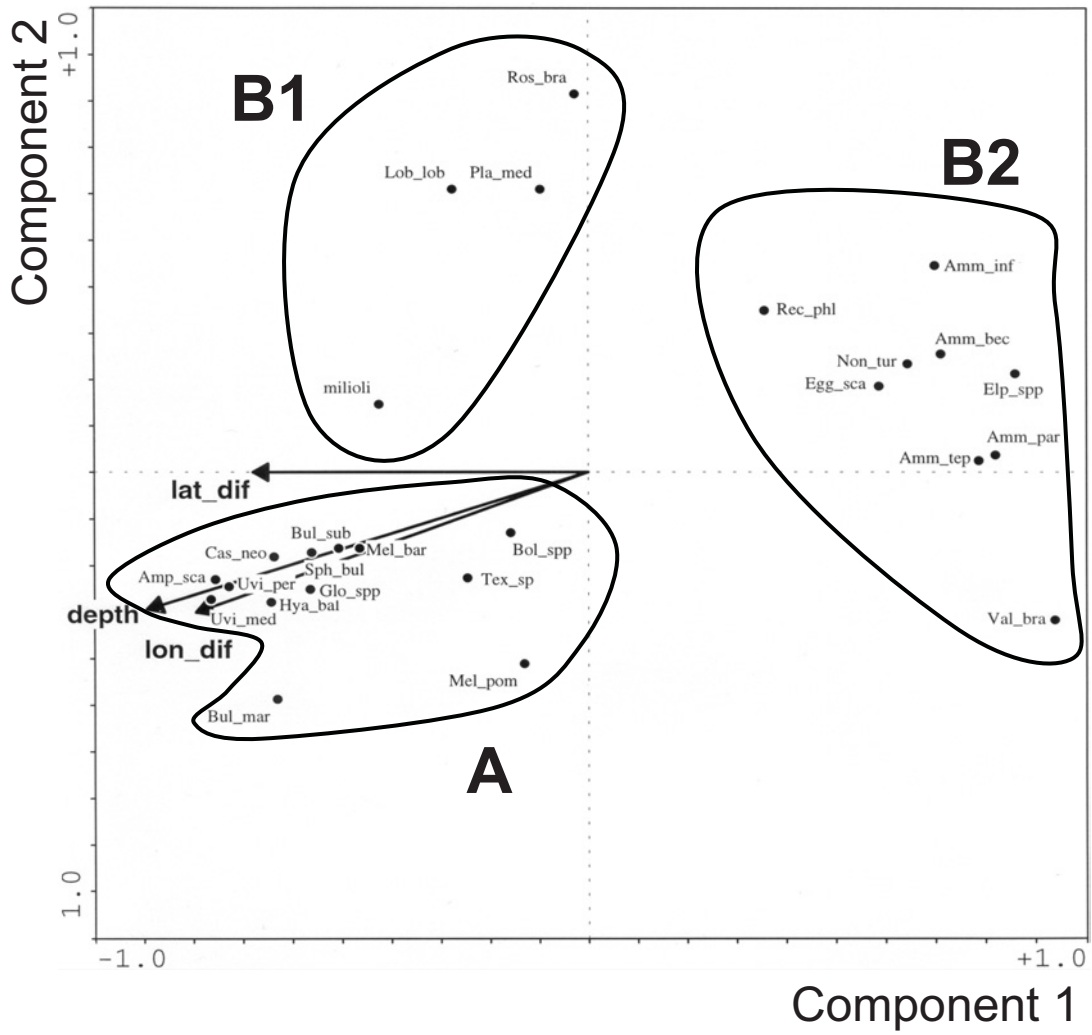


**Figure 5**. Principal Component Analysis on taxa. The clustering follows that of R-mode CA. Legend: Ros_bra = *Rosalina bradyi*; Lob_lob = *Lobatula lobatula*; Pla_med = *Planorbulina mediterranensis*; Amm_inf = *Ammonia inflata*; Rec_phl = *Rectuvigerina phlegeri*; Amm_becc = *Ammonia beccarii*; Non_tur = *Nonionella tugida*; Egg_sca = *Eggerelloides scabrus*; Elp_spp = *Elphidium* spp.; milioli = *Miliolidae*; Amm_par = *Ammonia parkinsoniana*; Amm_tep = *A. tepida*; Bol_spp = *Bolivina* spp.; Bul_sub = *Bulimina sublimbata*; Mel_bar = *Melonis barleeanus*; Sph_bul = *Sphaeroidina bulloides*; Cas_neo = *Cassidulina neocarinata*; Tex_sp = *Textularia* spp.; Amp_sca = *Amphicoryna scalaris*; Uvi_per = *Uvigerina peregrina*; Glo_spp = *Globocassidulina* spp.; Hya_bal = *Hyalinea balthica*; Uvi_med = *Uvigerina mediterranea*; Mel_pom = *Melonis pompilioides*; Bul_mar = *Bulimina marginata*.

The groups of species singled out by the PCA (Fig. 5) may be referred to the clusters of the R-mode Cluster Analysis (Fig. 2). Epiphytic taxa (cluster B1 of Fig. 2) plot negatively on the first axis and positively on the second axis. They are not clearly correlated to the three vectors. Because of their distribution related to the shallow-water environment (infralittoral zone), species of cluster B2 (Fig. 2) appear to be more closely related to Component 1, plotting positively on it. Among species of cluster B2, only *V. bradyana* seems correlated in the PCA with the negative side of the second axis, while the others taxa plot oppositely to the three vectors (water-depth, latitude and longitude).

Species of clusters A1 and A2 (Fig. 2) are not clearly separated in the two dimensional PCA-diagram (Fig. 5), in which they plot negatively on the first and second axis and are correlated with water-depth increase and latitude-longitude difference. Species included in this cluster are categorised as living between intermediate and deep water-depths (i.e., upper circalittoral environment).

The first PCA component might represent the living water depth of foraminifera, with the shallower taxa in cluster B2 (positive side) and deeper taxa in clusters A and B1 (negative side). This component might also be positively related to the grain size. The second PCA component might represent the pore water oxygenation: in fact, while on the positive side there are taxa living in well-oxygenated or vegetated environments (i.e. *R. bradyi*, miliolids), taxa typical of poorly oxygenated sediments (i.e. *V. bradyana*, *Uvigerina* spp.) are present on the negative side.

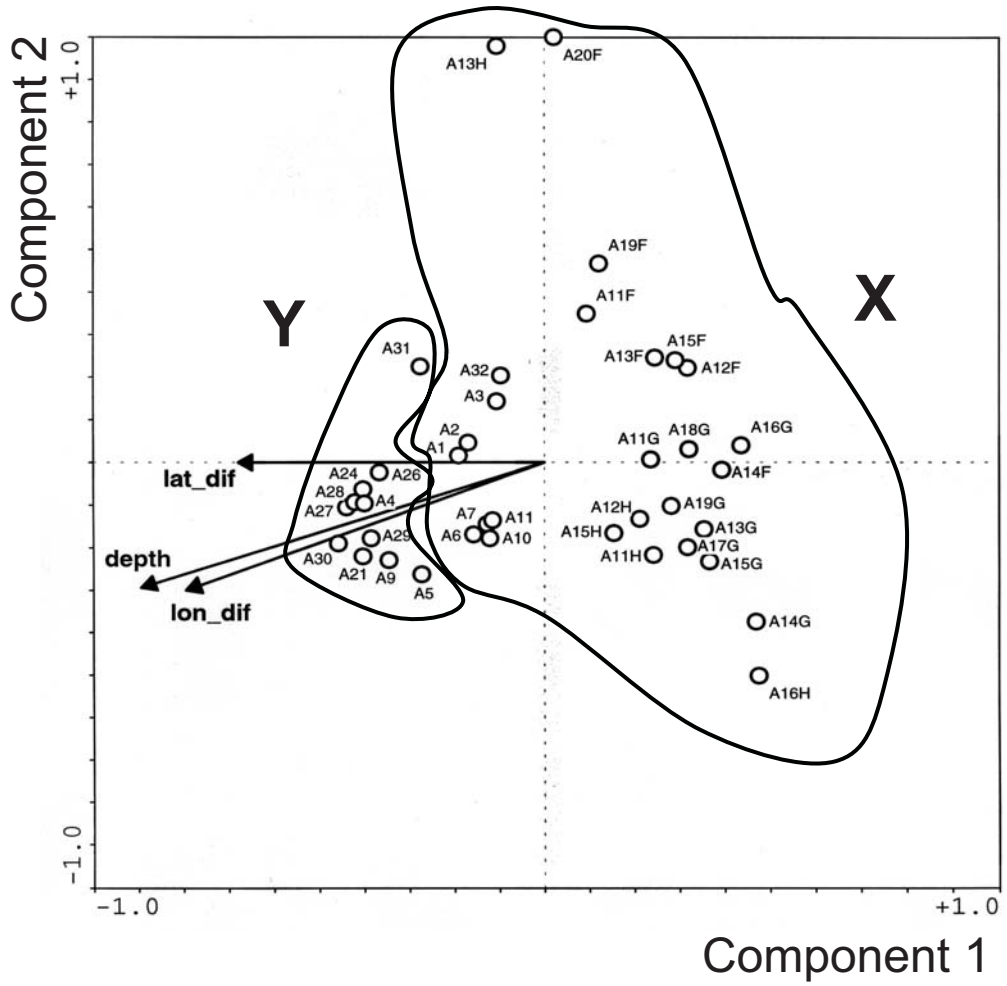


**Figure 6.** Principal Component Analysis on samples. The clustering follows that of Q-mode Cluster Analysis.

The groups of samples singled out by the PCA (Fig. 6) may be referred to the clusters of the Q-mode Cluster Analysis (Fig. 3). PCA plot is presented with samples and the three (D, LOD and LAD) vectors. While samples of cluster Y plot negatively with the first axis, those of cluster X appear not clearly linked to this component. Nevertheless, within cluster X, samples characterised by the highest percentages of *V. bradyana* plot clearly positively with the first axis. Cluster Y only shows a clear positive relation to the D, LOD and LAD vectors.

## DISCUSSION

Clustering of the 26 most common foraminiferal groups (or species) results in two large clusters (Fig. 2). Cluster A taxa plot negatively on the PCA first axis (Fig. 5), which seems positively related to grain size and/or inversely linked to water-depth. Therefore, taxa of cluster A are interpreted to prefer relatively deep, muddy sediments. As cluster A plots negatively on the second axis too, probably representing oxygenation level of the sea bottom, it may be assumed that this group of foraminifera tolerate dysoxic environments.

Cluster B1 (Fig. 2, 5) includes epiphytic taxa (i.e., *R. bradyi*, *P. mediterranensis*, and miliolids) and loads strongly on the second axis (oxygenation), being rather independent from the first axis. The apparent scarce influence of grain-size/water-depth on distribution of these taxa may be attributed to the heavy influence of the type of substrate for their attached lifestyle. Finally, cluster B2 plots positively on the first axis as it includes taxa living in shallow water. This cluster shows a large variation range for Component 2; while the other species preferring normal oxygen content plot positively on the second axis, *V. bradyana* plots negatively on the second axis, because of its connection with low bottom oxygenation and high organic matter content.

The three clusters singled out by the PCA show a different relationship with the D, LAD and LOD vectors. In cluster A, including among others *Bolivina* spp., *Bulimina* spp., *Uvigerina* spp., and *Melonis* spp., species show a marked positive correlation with the three vectors. Cluster B2, enclosing species like *V. bradyana*, *Ammonia* spp. and *Elphidium* spp., show a negative correlation with the

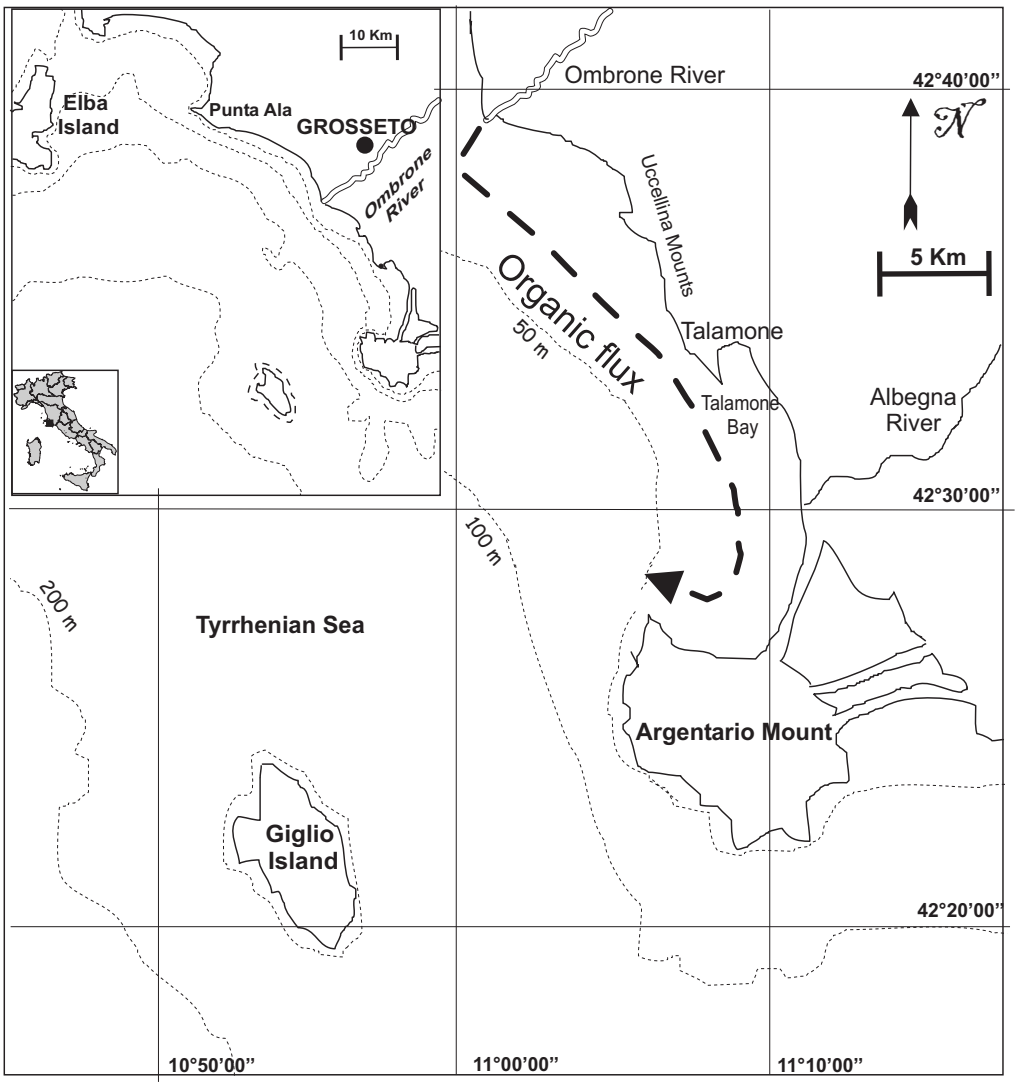


**Figure 7.** Reconstruction of the organic flux in the Talamone Bay.

three vectors. In detail, *V. bradyana* seems more oppositely linked to the LAD vector, while the other taxa are more negatively related to the LOD, D vectors. Taxa of cluster B1 (*R. bradyi*, *L. lobatula*, *P. mediterranensis* and miliolids) seem not clearly related to the vectors because their abundance is strongly conditioned by the substratum.

The PCA on samples (Fig. 6) shows evidence of two main groups, probably related to grain-size. Samples of cluster X have positive or low negative values for Component 1 and are mainly characterised by silty sediments, while samples of Cluster Y have relatively high negative values for Component 1 and are characterised by clayey sediments (Ferretti & Manfredi Frattarelli, 1993). An epiphytic assemblage implying well-oxygenated sea bottoms characterises both samples that show a strong correlation with the second axis. Furthermore, samples with abundant low-oxygen tolerant species have negative values for Component 2. Component 2 may consequently, be related to the oxygen concentration. High percentage of variance used by the first axis indicates that grain-size is the main environmental factor determining the type of assemblage.

Samples of cluster Y plot positively with D, LAD and LOD vectors: the increasing distance from the river mouth and the related increase in the water-depth favour their assemblage. Samples of cluster X do not highlight a well-defined correlation with the three vectors. Nevertheless, samples with high similarity in the Q-mode CA (Fig. 3) and characterised by high percentages of *V. bradyana*, plot negatively with respect to such three vectors. The decreasing distance from the river mouth and the related decrease in the water-depth favour consequently their assemblage.

## CONCLUSIONS

The season of samples collection probably influences the very low percentage of living (Rose Bengal stained) specimens in all the samples. Nevertheless, the total assemblages are well diversified, with high alpha index, confirming average favourable

condition for foraminiferal life.

The assemblages of several shallow samples, dominated by the typical opportunistic species *V. bradyana* (up to 40%), are characterised by relatively low species diversity, high dominance and high benthic number. Such assemblages are similar to those found near the Ombrone River mouth and recognised as determined by the eutrophicated environment related to the fluvial input (Bergamin *et al*., 1999). Nevertheless, the structure of the Talamone assemblages seems more indicative of smaller amounts of organic matter and accordingly of less stressed environmental conditions than those in the Ombrone Delta. PCA revealed in fact, that the studied *V. bradyana* assemblage might be linked to oxygen-poor bottoms, but the percentages of variance attribute a stronger importance to grain-size. On the other hand, a relationship between *V. bradyana* assemblage and the river input is confirmed by its negative correlation with the distance from the Ombrone River mouth. This feature also confirms that organic flux decreases with latitude. The comparison between samples collected near the Ombrone River mouth (Bergamin *et al*., 1999) and those from Talamone Bay shows a gradual transition, from north to south, from more to less eutrophicated and stressed environments. In this research, samples characterised by the highest percentage of *V. bradyana* are located within the bay; nevertheless the shallowest samples do not show such a feature. It may then be supposed that the organic flux flows southward, parallel to the coast, bypassing without entering the inner bay (Fig. 7). The Ombrone River, running off north of the sampling sector, is probably the source of organic matter, while the small Albegna River, flowing in Talamone Bay, does not affect the assemblages in proximity to its mouth.

From 90 m water depth we found an assemblage with *C. neocarinata*, *Melonis* spp. and *B. marginata*. From approximately 120 m water-depth assemblages are dominated by *U. mediterranea*, *B. marginata* and *S. bulloides*. The presence of *Uvigerina* spp. might suggest relatively low oxygen content, but *S. bulloides* is often considered as oxyphilic. Such assemblages show higher species diversity and heterogeneity and lower dominance than those dominated by *V. bradyana*. These features indicate that the organic flux from the Ombrone River is limited to shallower water-depth.

Finally, a remark on the *E. scabrus* autoecology may be interesting. The statistical analysis revealed its relation with high organic flux. Nevertheless, the reason for its patchy distribution is unclear.

The sediment dispersion path reconstructed in this study is similar to the sediment dispersion found by Jorissen (1988) and Barmawidjaja *et al*. (1992) in the Adriatic Sea. They recognised benthic assemblages with abundant opportunistic species (mainly *V. bradyana* and *Nonionella turgida*) in the pelitic belt running parallel to the coast and caused by the Po run-off. Our actualistic research suggests an environmental model useful for paleogeographic reconstruction, common to basins characterised by the presence of river-mouths and geographical setting typical of a nutrient-trap.

## ACKNOWLEDGEMENTS

Authors thank Prof. B. Van der Zwaan for his support in realisation and interpretation of statistical analysis and the referees, Prof. D. Violanti and Prof. M. Kaminski, for their useful advice. This work was supported by COFIN 1998/2000 "Il bilancio in sistemi costieri alimentati da apporti fluviali. Il delta del Fiume Ombrone".

## REFERENCES

Barmawidjaja, D.M., Jorissen, F.J., Puskaric, S. & Van der Zwaan, G.J. 1992. Microhabitat selection by benthic foraminifera in the northern Adriatic Sea. *Journal of Foraminiferal Research*, **22**, 297-317.

Bergamin, L. 1998. *Associazioni a foraminiferi bentonici attuali e subfossili della costa tirrenica centrale (area del fiume Ombrone e di Terracina)*, 161 pp. Tesi di Dottorato inedita, Università "La Sapienza" Roma, Italy

Bergamin, L., Di Bella, L. & Carboni, M.G. 1999. *Valvulineria bradyana* (Fornasini) in organic matter-enriched environment. *Il Quaternario, Italian Journal of Quaternary Sciences*, **12**, 51-56.

Blanc - Vernet L. 1969, *Contribution à l'étude des foraminifères de Méditerranée,* Travaux de la Station Marine d'Endoume, 281 pp.

Borzi, M., Carboni, M.G., Cilento, G., Di Bella, L., Florindo, F., Girotti, O., Piccardi, E. & Sagnotti, L. 1998. Bio- and magneto-stratigraphy in the Tiber valley revised. *Quaternary International*, **47/48**, 65-72.

Carboni, M.G., Bellotti, P., Bergamin, L., Di Bella, L. & Matteucci, R. 2000. Benthic foraminiferal assemblages from the Ombrone and Tiber deltas: a preliminary comparison. *Géologie Méditerranéenne*, **27**, 3-13.

Chiesi, R., Immordino, F. & Forti, S. 1993. Composizione mineralogica e tessiturale dei sedimenti recenti dell'area del "Bacino Centrale" dell'Arcipelago Toscano. In: Furia, S. (ed.), *Arcipelago Toscano. Studio sedimentologico, geochimico e biologico*. 197-211. ENEA.

Chiocci, F.L., La Monica, G.B. & Ombrone Scientific Party 1997. Present day sedimentary processes on Central Tyrrhenian continental shelf as the result of a 20 kyr environmental evolution. *Progress in Oceanography of the Mediterranean Sea*. Abstract book, 264-265.

Di Bella, L. 1997. Plio/Pleistocene *Bolivina* assemblages in the Tiber Valley. Stratigraphic and paleoecological implications. *Geologica Romana*, **32**, 47-57.

Ferretti, O. & Manfredi Frattarelli, F.M. 1993. Caratterizzazione granulometrica e mineralogica dei sedimenti marini superficiali tra l'Isola d'Elba e l'Argentario (Tirreno settentrionale). In: Furia, S. (ed.), *Arcipelago Toscano. Studio sedimentologico, geochimico e biologico*. 171-184. ENEA.

Fisher, R.A., Corbet, A.S. & Williams, C.B. 1943. The rela-

tion between the number of species and the number of individuals in a random sample of an animal population. *Journal of Animal Ecology*, **12**, 42-58.

Jorissen, F.J. 1987. The distribution of benthic foraminifera in the Adriatic Sea. *Marine Micropaleontology*, **12**, 21-48.

Jorissen, F.J. 1988. Benthic foraminifera from the Adriatic Sea; principles of phenotypic variations. *Utrecht Micropaleontological Bulletin*, **37**, 1-174.

Jorissen, F.J., Barmawidjaja, D.M., Puskaric, S. & Van der Zwaan, G.J. 1992. Vertical distribution of benthic foraminifera in the northern Adriatic Sea: the relation with the organic flux. *Marine Micropaleontology*, **19**, 131-146.

Jorissen, F.J., de Stiger, H.C. & Widmark, J.G.V. 1995. A conceptual model explaning benthic foraminiferal microhabitats. *Marine Micropaleontology*, **26**, 3-15.

Loeblich, A.R. & Tappan, H. 1987. *Foraminiferal Genera and their Classification*, Van Nostrand Reinhold Company, 970 pp.

Murray, J.W. 1973. *Distribution and Ecology of Living Benthonic Foraminiferids*, Heinemann Educational Books, 288 pp.

Murray, J.W. 1991. *Ecology and Paleoecology of Benthic Foraminifera*, Longman Scientific & Technical, 312 pp.

Parker, W.C. & Arnold, A.J. 1999. Quantitative analysis in foraminiferal ecology. In: Sen Gupta, B. (ed.), *Modern Foraminifera*, Kluwer Academic Publishers, 71-79.

Pielou, E.C. 1984. *The interpretation of Ecological Data*, Wiley & Sons, 263 pp.

Scott, D.B. & Medioli, F.S. 1980. Living vs. total foraminiferal populations: their relative usefulness in paleoecology. *Journal of Paleontology*, **54**, 814-831.

Tortora, P. 1999. Sediment distribution on the Ombrone River delta seafloor and related dispersal processes. *Geologica Romana*, **35**, 211-218.

Van der Zwaan, G.J. & Jorissen, F.J. 1991. Biofacial patterns in river-induced shelf anoxia. In: Tyson, R.V. & Pearson, T.H. (eds), *Modern and Ancient Continental Shelf Anoxia*, Geological Society Special Publication, **58**, 65-82.

Van der Zwaan, G.J., Duijnstee, I.A.P., den Dulk, M., Ernst, S.R., Jannik, N.T. & Kouwenhoven, T.J. 1999. Benthic foraminifers: proxies or problems? A review of paleoecological concepts. *Earth Science Review*, **46**, 213-236.

Walton, W.R. 1964. Recent foraminiferal ecology and paleoecology. In: Imbrie, J., Newell, N.D. (eds), *Approaches to Paleoecology*. 151-237. John Wiley.

# Climatic changes during Late Pliocene and Early Pleistocene at Capo Rossello (Sicily, Italy): response from planktonic foraminifera

*ANTONIO CARUSO*

Dipartimento di Geologia e Geodesia, Università di Palermo corso Tukory 131, 90134 Palermo
e-mail: acaruso@unipa.it

**ABSTRACT**

A micropaleontological study has been carried out on the marls of the Monte Narbone Formation outcropping at Capo Rossello (Sicily). The studied sediments span the interval from the base of Gelasian stage, in correspondence of the sapropel A5, dated at 2.588 Ma (isotopic stage 103), to the base of the Emilian (sub-stage of lower Pleistocene) in correspondence of the first occurrence (FO) of *Hyalinea balthica*, dated at 1.552 Ma (isotopic stage 53). The studied interval includes obliquity cycles (o-cycle) 129 to 78, and insolation cycles (i-cycle) 250 to 150 of Laskar *et al*., (1993) solution $90_{(1,1)}$.

The identified bioevents allowed to correlate with extreme detail the studied section with those of Vrica (Plio/Pleistocene boundary stratotype), Singa (Southern Italy) and Site 964 (Ionian Sea). Planktonic foraminifera abundance fluctuations are mainly related to paleoenvironmental changes, induced by climatic variations, tied to Milankovitch periodicities. In particular, precession minima/insolation maxima and obliquity maxima coincide with abundance peaks of the *Globigerinoides ruber* group, while precession maxima/insolation minima and obliquity minima coincide with abundance peaks of neogloboquadrinids.

Fluctuation in abundance of neogloboquadrinids and *G. ruber* group highlighted the dominant role of obliquity frequency, and the interference between obliquity, precession and eccentricity.

Five different intervals have been described based on planktonic foraminiferal distribution. An increasing abundance trend of cool species started at 2.57 Ma, in coincidence of o-cycle (128). *Neogloboquadrina atlantica*, *N. pachyderma* (sinistral forms) and *Globorotalia bononiensis* are abundant between 2.57 and 2.40 Ma. This interval coincides with the expansion of northern hemisphere ice sheets, and with the input of North Atlantic cool-polar waters into the Mediterranean area. In particular, the strongest glaciations occurs at 2.535 Ma, within the isotopic stage 100 (o-cycle 126), and well correlated with insolation/obliquity/eccentricity minima. In the Mediterranean area this glacial event is well identified by changes in abundance of calcareous plankton, and in particular coincides with decrease of discoasterids and increase of *Neogloboquadrina atlantica*. Between 2.40 and 1.99 Ma increasing abundances of warm oligotrophic species coincide with maxima of eccentricity curve; this interval is characterised by strong glacial/interglacial cyclicities, dominated by obliquity periodicities, and clearly marked by fluctuating abundances of the *G. ruber* group and neogloboquadrinids.

Between 1.99 and 1.67 Ma temperate and cool species developed progressively; the Plio/Pleistocene boundary is well marked by the increase of sinistral forms of neogloboquadrinids, and the absence of *Globigerinoides* spp. The Plio/Pleistocene boundary is placed at 1.805 Ma in coincidence with isotopic stage 64, i-cycle 176 and o-cycle (90/91).

Ultimately variations in abundances of planktonic foraminifera enabled the reconstruction, cycle by cycle, the climatic history of the central Mediterranean, in the interval spanning 2.60 to 1.55 Ma.

**Keywords**: Plio/Pleistocene boundary, Milankovitch periodicities, climatic changes, planktonic foraminifera

## INTRODUCTION

Detailed biostratigraphy (Cita & Gartner 1973; Colalongo & Sartoni, 1979; Spaak, 1983; Iaccarino, 1985; Sprovieri 1993; Sprovieri *et al*., 1998) and astrochronological time scales, from the Late Pliocene to the Early Pleistocene in the Mediterranean area, have been published by many authors (e.g., Hilgen *et al*. 1991a,b; Lourens *et al*.,

*In*: Coccioni R., Galeotti S., & Lirer F., (eds) 2004. Proceedings of the First Italian Meeting on Environmental Micropaleontology. *Grzybowski Foundation Special Publication*, 9, 17-36.

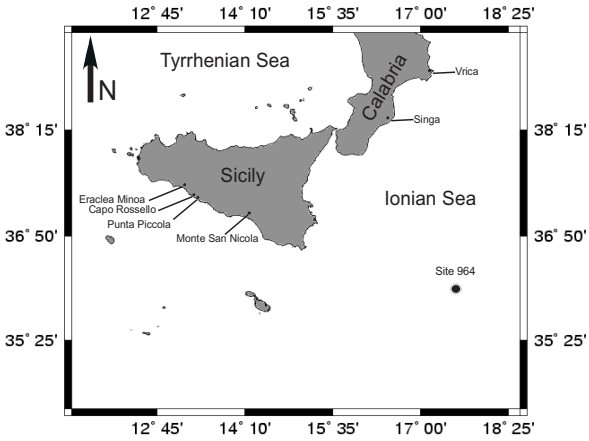


**Figure 1.** Location map of the sections discussed in the paper: Faro Rossello, Punta Piccola, Monte San Nicola, Singa and Vrica.

1996). The most important calcareous plankton bioevents identified in these stratigraphic intervals have been dated at Vrica and Singa composite sections on the basis of astronomical calibration of sedimentary sequences (Lourens *et al*., 1996), and at Site 964 (ODP, Leg 160) on the basis of fluctuations in abundance of *Globigerinoides* spp. (Sprovieri *et al*., 1998).

Plio/Pleistocene boundary is commonly recognised in the Mediterranean area by the increase in abundance of *N. pachyderma* left coiling (Di Stefano *et al*., 1993; Lourens *et al*., 1996; Sprovieri *et al*., 1998), that occurs in the isotopic stage 64 at 1.80 Ma (Lourens *et al*., 1996). The identification of this boundary approximates the top of the Olduvai Subchron (Aguirre & Pasini, 1985), which occurs in correspondence of the isotopic stage 63 at 1.785 Ma (Lourens *et al*., 1996), and it is approximated by the first occurrence of *Gephyrocapsa* medium size, dated at about 1.7 Ma (Lourens *et al*., 1996; Raffi, 2002). In extra-Mediterranean successions the Plio/Pleistocene boundary is not easily recognizable, and its position is currently in debate. In particular Naish *et al*., (1997) proposed a conglomerate layer outcropping at Hautawa Shellbed (New Zealand) to mark the Plio/Pleistocene boundary; this layer was correlated to isotopic stage 100 at 2.5 Ma, very close to Gauss/Matuyama inversion (2.582 Ma). Suc *et al*., (1997) proposed the isotopic stage 104 (2.61 Ma) to place the Plio/Pleistocene boundary almost coincident with the Gauss/Matuyama polarity inversion.

The Plio/Pleistocene (P/P) boundary is usually equated to the timing of the expansion of glaciations in the northern hemisphere, and many authors described important glacial events at 3.1 and 2.4 Ma (Shackleton & Cita, 1979, Ruddiman *et al*., 1986; Zachariasse *et al*., 1990), even if Larsen *et al*., (1994) considered the start of boreal glaciations at 7 Ma, on the basis of ice-rafted detritus recognised in North Atlantic Sites. After many debates in the scientific community, at the 27th International Geological Congress (Moscow, 1984) was decided to use the

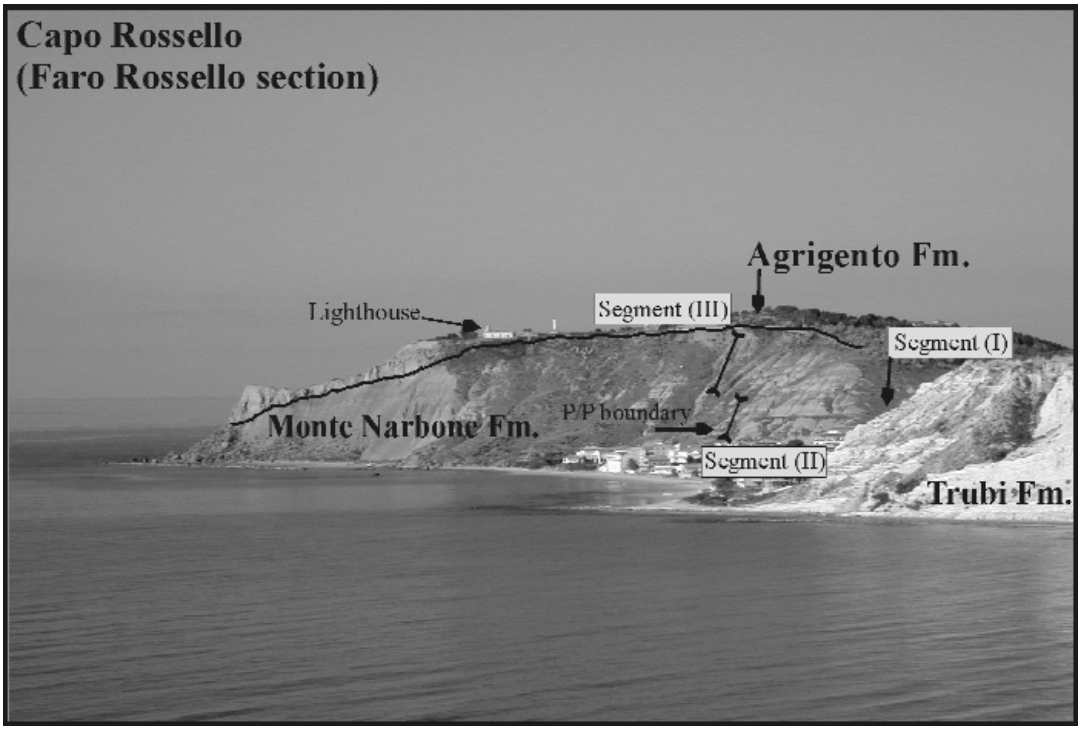


**Figure 2.** Photo of the Capo Rossello area, general view of the Faro Rossello section;


**Figure 3.** Punta Piccola section, with progressive numbers 95-112 and A1 (Lourens et al., 1996) corresponding to the lithological cycles recognised on the field in the Monte Narbone Fm; stars correspond to palygorskite layers of Foucault & Mélières (2000).

isotopic stage 64 to define the Plio/Pleistocene boundary, successively identified in the sapropel "e" of the Vrica section, (Aguirre & Pasini, 1985), isotopic stage 64 and i-cycle 176 (Lourens *et al*., 1996; Hilgen *et al*., 1999). The P/P boundary is also approximated by the increase of abundance of *N. pachyderma* left coiling that occurs within i-cycle 175 (Hilgen *et al*., 1999). As Cita *et al*., (1999) pointed out, the Vrica section is probably the best location to define the P/P boundary.

The Capo Rossello area (Southern Sicily, Italy) represents one of the most beautiful and complete sedimentary successions of upper Messinian to lower Pleistocene, and is particularly suitable for the study of the P/P boundary (Figs. 1 and 2). Hilgen (1991a; 1991b) proposed an astronomical time scale for the whole lower-middle Pliocene in this area. Cita & Gartner (1973) described the Miocene/Pliocene boundary stratotype to the contact Arenazzolo-Trubi Formation which outcrops along Capo Rossello Beach. Successively Hilgen & Langereis (1993) proposed to place the Miocene/Pliocene boundary at Eraclea Minoa (20 Km NW of the Capo Rossello area), based on more reliable paleomagnetic data, obtaining an astronomical age of 5.33 Ma. During the field trip of "Mediterranean Neogene Paleoceanography" Congress at Erice in 1997, the "golden spike" for the Zanclean/Piacenzian GSSP was placed at Punta Piccola within the uppermost part of Trubi Fm, in the lithological cycle 77 (Fig. 3) (Castradori *et al*., 1998, Van Couvering *et al*., 2000), astronomically dated at 3.60 Ma, almost coincident with the Gilbert/Gauss inversion (3.596 Ma). Cita *et al*., (1999) erroneously indicated, at Punta Piccola, the Zanclean/Piacenzian boundary to the Trubi/Monte Narbone Fms contact, which instead coincides with cycle 95/96 aged 3.18 Ma (see Fig. 4b of Cita *et al*., 1999). The Trubi/Monte Narbone Fms contact represents a drastic change in sedimentation rate, and coincides with the climatic cooling described by Zachariasse *et al*., (1989). During this period precession (lithological cycles 102-109 and A1-A5) and obliquity periodicities (lithological cycles 110-A1) triggered sapropel formation in the Mediterranean Sea (Figs. 4 and 5).

The transition from the Trubi Fm to the Monte Narbone Fm gradually changes between lithological cycles 95 to 101 of Lourens *et al*., (1996), from 3.18 to 3.06 Ma (Fig. 3). In the central part of Mediterranean Sea sapropel formation started at 3.06 Ma with lithological cycle 102 (Figs. 3 and 6), and endured almost constantly about 400 kyr, until 2.588 Ma (sapropel A5). During the middle Pliocene, between 3.1 and 2.5 Ma, Haug & Tiedemann (1998) proposed major closure of Panamian Isthmus. The clousure caused a marked reorganization of ocean circulation, favouring ther-

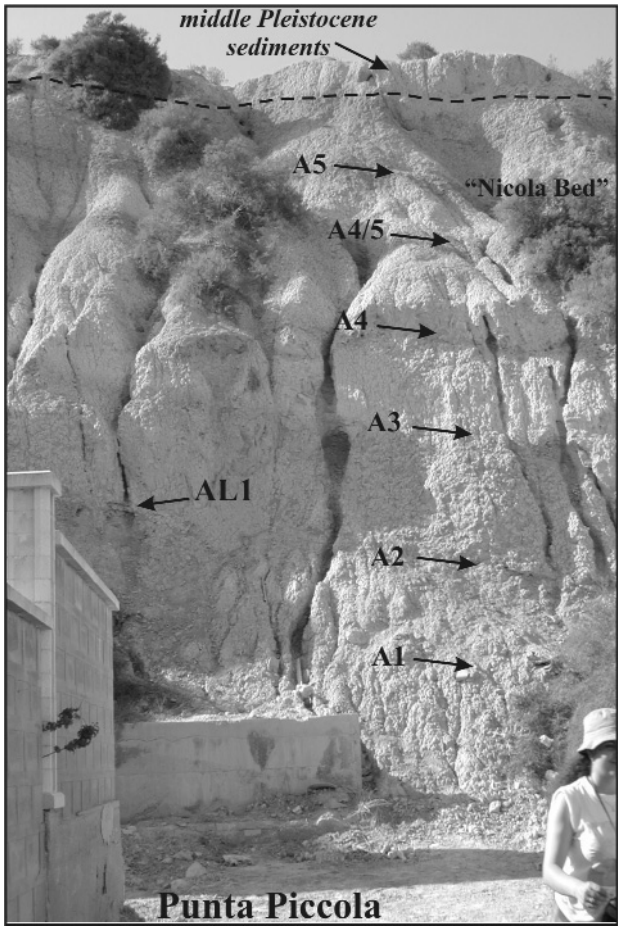


**Figure 4.** Punta Piccola, particular photo of sapropels A1-A5; sapropel A5 corresponds to the "Nicola Bed", base of Gelasian stage (2.588 Ma). AL1 indicates the volcanic ash layer at 2.676 Ma.

mohaline circulation in Atlantic Ocean and increased atmospheric moisture content, that was a favorable condition for ice-sheet growth. These events were triggered by incremental changes in the Earth orbital obliquity. According to Zhisheng *et al*., (2001) during this period the evolution of Asian monsoons, tied to phases of the Himalaya-Tibetan plateau uplift, played also an important role in the climatic cooling of Earth; the authors supposed that the increasing of atmospheric dust, associated with strong winter winds, may have helped a global cooling and contributed to the intensification of glaciation. During the deposition of sapropels, between 3.06 and 2.6 Ma, monsoonal activity was strong in the central Mediterranean area, with important input of Saharian dust (Foucault & Mélières, 2000).

This paper presents a climatic reconstruction from 2.6 Ma to 1.55; this interval recovers the whole Gelasian stage and lower part of Pleistocene just above the base of Emilian sub-stage. The study has been carried out using fluctuations in abundance of planktonic foraminifera and major nannofossils bioevents, across the Plio/Pleistocene boundary. The studied samples come from the marls of the Monte Narbone Formation, outcropping at Capo Rossello. The data of calcareous plankton was compared with $\delta^{18}O$ variations described by Sprovieri *et al*., (1998) for Site 964 (ODP Leg 160), and correlated with the astronomical curves of Laskar *et al*., (1993) solution $90_{(1,1)}$.

## GEOLOGICAL SETTING OF THE CAPO ROSSELLO AREA

The Capo Rossello area is located in the southern part of Sicily in the Caltanissetta basin (Fig. 1), where compressive and extensive tectonic disturbances are related to the stacking of nappes thrusted southward during the uplift of the Appenninic-Maghrebid belt (Catalano & D'Argenio, 1982). Due to tectonic activity some low angle compressive faults are present along the sections, and displace slightly the stratigraphic sequence.

Along the Capo Rossello Beach outcrops the Arenazzolo-Trubi contact, corresponding to the Miocene/Pliocene boundary (Cita & Gartner 1973; Hilgen & Langereis, 1993). This contact coincides with the return to normal marine conditions in the Mediterranean area after the "Salinity Crisis" (Ruggieri & Sprovieri, 1976). The Trubi Formation is here represented by a spectacular sequence, 120m thick, of clear lithological cycles.

Trubi Formation is followed in continuity by marls of the Monte Narbone Fm, 220m thick, well represented in the Capo Rossello area (Fig. 2). The uppermost part of the Neogene sequence finishes with sandstones and calcarenite sediments of the Agrigento Formation up to 100m.

## STUDIED SECTIONS

### *Punta Piccola (Figs. 3 and 4)*

This section was studied in extreme detail by many authors (Zachariasse *et al*., 1989; 1990; Hilgen, 1991; Sprovieri, 1993; Lourens *et al*., 1996). Punta Piccola is 38m thick; the first 13m (cycle 75 to 95 of Lourens *et al*., 1996) are here represented by a classic quadruplets of whitish marly limestone and whitish calcareous marls of the Trubi Fm, forced by precessional cycles (Hilgen 1991a; 1991b). The uppermost 25m of the Monte Narbone Fm are grey whitish marls, grey marls and dark marls, sometimes laminated, usually known as "sapropels". The marls of the Monte Narbone Fm include lithological cycle 96 to sapropel A5 (Lourens *et al*., 1996; Castradori *et al*., 1998). The marls of Monte Narbone Fm, 1 m above the top of sapropel A5, are truncated by middle Pleistocene sandstone and calcarenite sediments (Fig. 4). The sapropel A5 corresponds to the base of Gelasian stage (Fig. 4), which occurs in isotopic

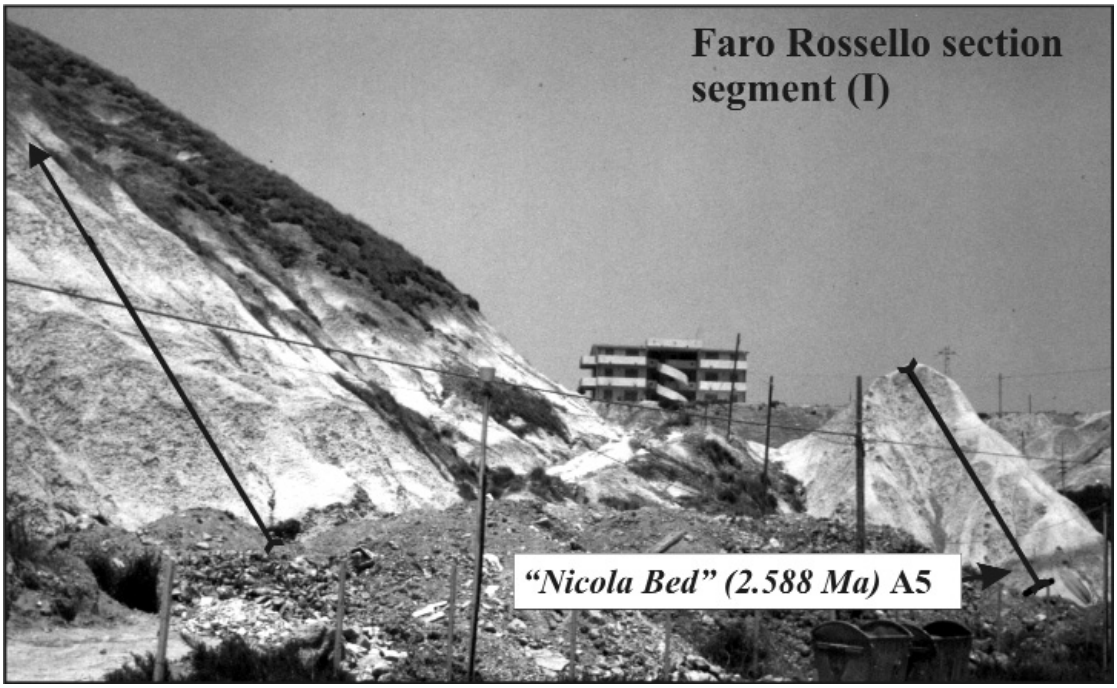


**Figure 5**. Details of first 28 m of segment (I) at Faro Rossello; only one sapropel is present (A5). Sapropel A5 is equivalent to the "Nicola Bed" .

stage 103 (i-cycle 250, o-cycle 129, following the numeration of Lourens *et al*. (1996), and pratically coincides with the "Nicola bed" layer of Rio *et al*., (1994; 1998) that outcrops at Monte San Nicola near Gela town (Fig. 1). Lourens *et al*., (1996) obtained an astronomical age of 2.588 Ma for sapropel A5, very close to the Gauss/Matuyama inversion (2.582 Ma). The base of the Gelasian stage is almost coincident to the age of development of northern hemisphere ice sheet at 2.4 Ma (Cita *et al*., 1999). According to Rio *et al*., (1990) this glacial event is easily recognizable in the marine and continental succession.

The sapropel A5 (Fig. 4) was used as marker bed to correlate the uppermost part of Punta Piccola with the base of the Faro Rossello section studied herein (Figs. 5 and 6). A volcanic ash layer (AL1), 15 cm thick, is present just above sapropel A2 (Figs. 4 and 5).

***Faro Rossello (Figs. 2 and 6)***

This section outcrops near the lighthouse of Capo Rossello, (Lat. 37°17'53''; Long. 13°27'20'') 4 km NW of Punta Piccola (Fig. 1), and consists of marls belonging to the Monte Narbone Fm. The 198 m thick studied section is composed of three segments (Figs. 2, 5 and 6) partially overlapped, which are well exposed in a series of gullies along the southern slope, 150-300m away from the lighthouse.

Segment (I) is characterised by 109 m thick grey homogeneous marls (Figs. 5 and 6); this interval includes three laminated dark marls (sapropels) progressively numbered (A5, A6 and A7), and one ash layer (AL2). The first sapropel is 0.90 cm thick and corresponds A5 layer of Lourens *et al*., (1996) (Figs. 5 and 6), correlated also with "Nicola bed" of Rio *et al*., (1994) dated at 2.588 Ma (Rio *et al*., 1998). At Faro Rossello, sapropel A5 outcropped 1m just above the base of the section (Fig. 6), but unfortunately is now missing because the first 7 m were recently removed for building purposes; therefore, sapropel A5 is presently missing. The second sapropel (A6), 30 cm thick, is located 53 m above the base of segment (I). Just above this sapropel an ash layer (AL2), 10 cm thick, is present (Fig. 6). The third sapropel (A7) is 35 cm thick and lies 97 m above the base of segment (I).

In the first segment (I) some faults may have displaced some sediments, between 15 and 45 m.

Segment (II) is 35 m thick, and outcrops 100 m SW of segment (I) (Figs. 2 and 5). It is characterised by grey and grey-yellow homogeneous marls. This interval includes three laminated dark marls (sapropels A7, A8 and A9); the first one has been correlated with sapropel A7 of segment (I). Sapropels A8 and A9, respectively 30 and 90 cm thick, outcrop 16 m and 24 m above the base of the section (Fig. 6).

Segment (III) is 85 m thick and is characterised, in the first 35 m, by grey and grey-yellow homogeneous marls. Only two sapropels (A9 and A10) are present. Sapropel A9 is 90 cm thick, and represents the base of this segment; 24 m above this level sapropel (A10) is present, 35 cm thick (Fig. 6). The uppermost 35 m of segment (III) are characterised by yellow silty marls rapidly changing to sandsto-

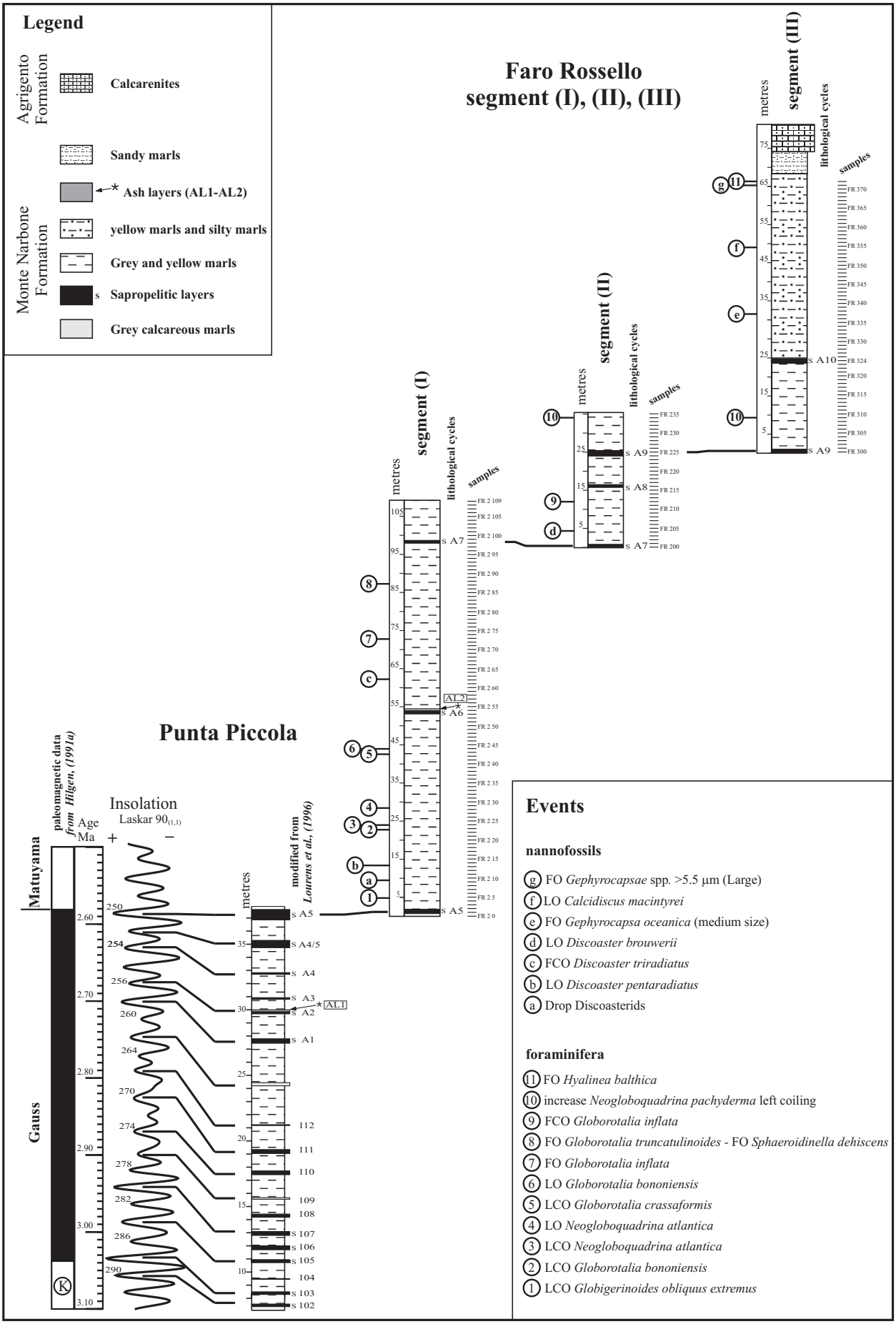


**Figure 6.** Correlation between the studied sedimentary sequences of Faro Rossello (segment I, II and III) with Punta Piccola section. Bioevents are reported on the left of the lithological column. Progressive numbers (102-112 and A1-A5) mark the lithological cycles of Figs. 3 and 4.

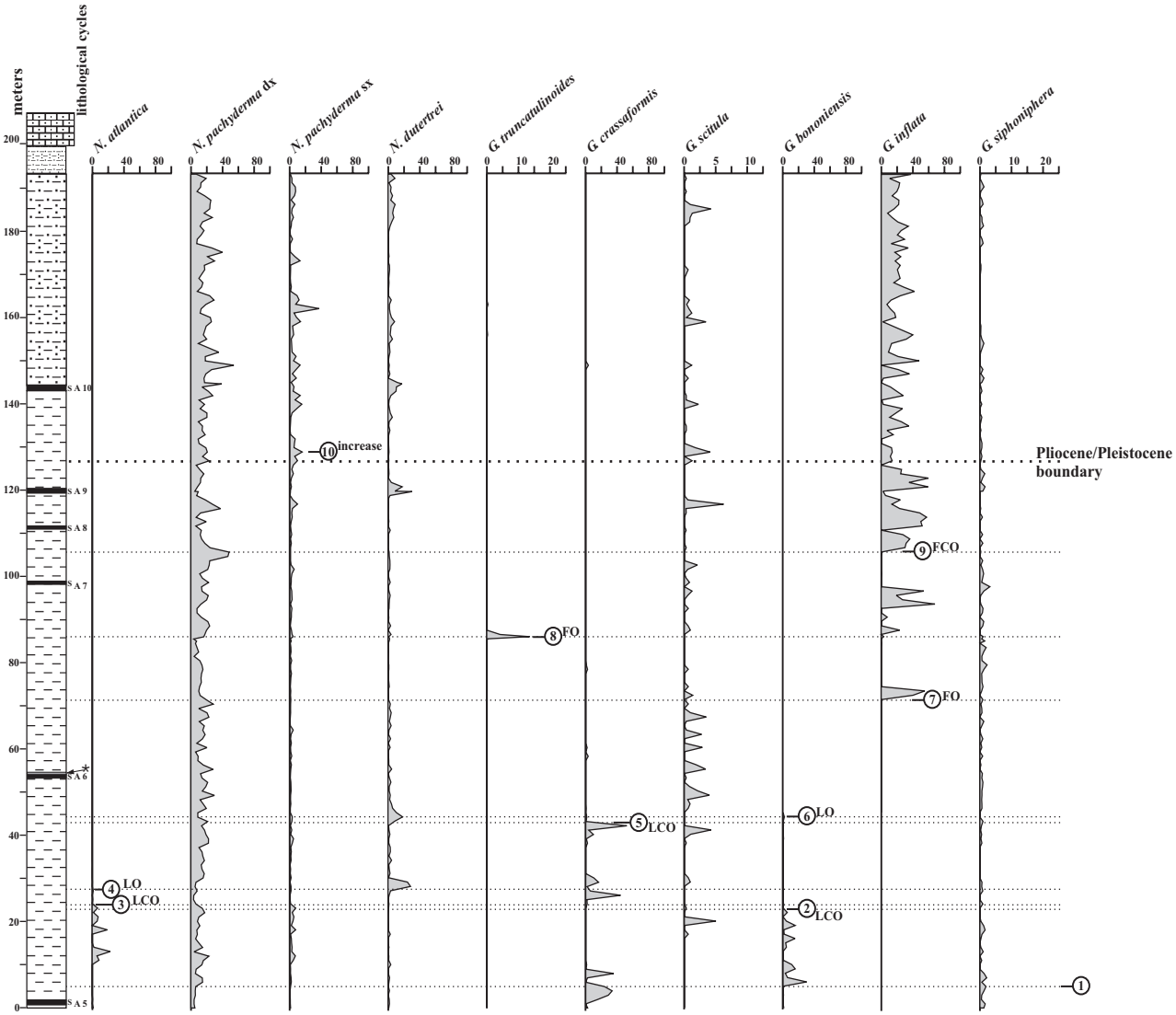


**Figure 7.** Quantitative distribution of the planktonic foraminiferal taxonomic units identified in the studied section. Number encircled correspond to foraminifera bioevents reported on Fig. 3.

nes and calcarenites of the Agrigento Fm (Figs. 2 and 6).

Biostratigraphic and lithological controls allowed the correlation of the three segments, and finally a 198m thick composite lithological log has been constructed (Fig. 6).

## METHODS AND DATA

### *Planktonic foraminifera*

The Faro Rossello section was sampled with a 1 m resolution (Fig. 6), but between 75 and 105 m above the base, the sampling was intensified every 50 cm. A total of 220 samples were collected. One hundred grams of dried sediment, for each sample were washed through a 63 μm sieve for foraminiferal studies. Quantitative data are obtained by counting about 300 specimens from the residue fraction greater than 125 μm. Identification of the bio-events of planktonic foraminifera is also based on a semi-quantitative study of the fraction greater than 63 μm.

A preliminary plankton biostratigraphy, based on quantitative analyses of planktonic foraminifera and calcareous nannofossil assemblages, was reported by Di Stefano et al. (1993).

A total of 25 species have been recognised: *Globigerinoides sacculifer*, *G. quadrilobatus*, *G. trilobus*, *G. ruber*, *G. elongatus*, *G. conglobatus*, *G. obliquus extremus*, *Orbulina universa*, *Globigerinella siphonifera*, *Globigerinita glutinata*, *Turborotalita quinqueloba*, *Globorotalia bononienis*, *G. crassaformis*, *G. inflata*, *G. scitula*, *G. tosaensis*, *G. truncatulinoides*, *Sphaeroidinella dehiscens*, *Globigerina bulloides*, *G. apertura*, *G. falconensis*, *Neogloboquadrina atlantica*, *N. acostaensis*, *N. pachyderma*, *N. dutertrei*.

The *G. quadrilobatus* group contains *G. sacculifer*,

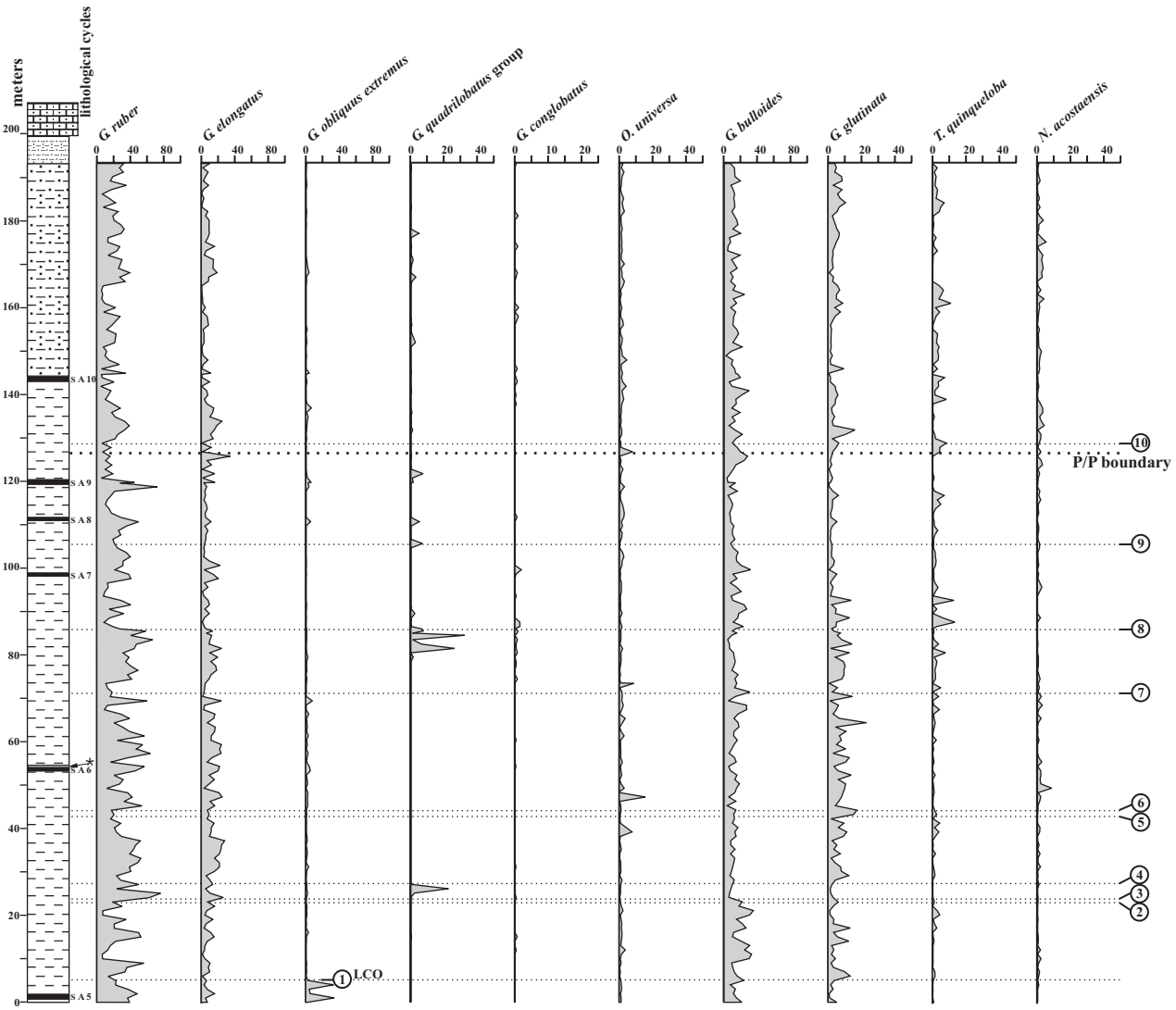


**Figure 8.** Quantitative distribution of other planktonic foraminiferal taxonomic units identified in the studied section. Numbers encircled correspond to foraminiferal bioevents reported on Figure 6.

*G. quadrilobatus*, *G. trilobus*. *N. pachyderma* have been subdivided in dextral and sinistral forms. *G. ruber* and *G. elongatus* are grouped together. *G. truncatulinoides* and *G. tosaensis* are grouped together. Relative abundance fluctuations of the most important taxonomic units are plotted in Figures 7 and 8.

### *Warm/cold ratio*

The ratio of warm-water versus cool-water species, using modern habitat characteristics described by Pujol & Vergnaud-Grazzini, (1995) Lourens *et al*., (1996) and Pérez-Folgado *et al*., (2003) herein following. Warm-water species include *G. conglobatus*, *G. sacculifer*, *G. quadrilobatus*, *G. ruber*, *G. elongatus*, *G. obliquus extremus*, *O. universa*, *G. siphoniphera*, while *T. quinqueloba*, *G. scitula*, *G. glutinata*, *N. atlantica*, *N. acostaensis*, *N. pachyderma* were taken as representative of cool-water species. The resulting warm versus cold ratio record is reported in Figure 9.

### *Calcareous nannofossils*

Additional smear slides were prepared from unprocessed sediments following standard techniques, in order to integrate the sampling of Di Stefano *et al*., (1993). The distribution of selected calcareous nannofossil taxa was obtained by light microscope analysis (transmitted light and crossed nicols) at about 1000 X magnification. Abundance data were collected using the methodology described by Backman & Shackleton, (1983) and Rio *et al*., (1990), and are extensively used in Mediterranean or extra-Mediterranean quantitative biostratigraphic studies of Neogene marine records, in ODP sequences and land sections (Lourens *et al*., 1996; Sprovieri *et al*., 1998; Raffi, 2002).

In Figure 6 the most important calcareous nanno-

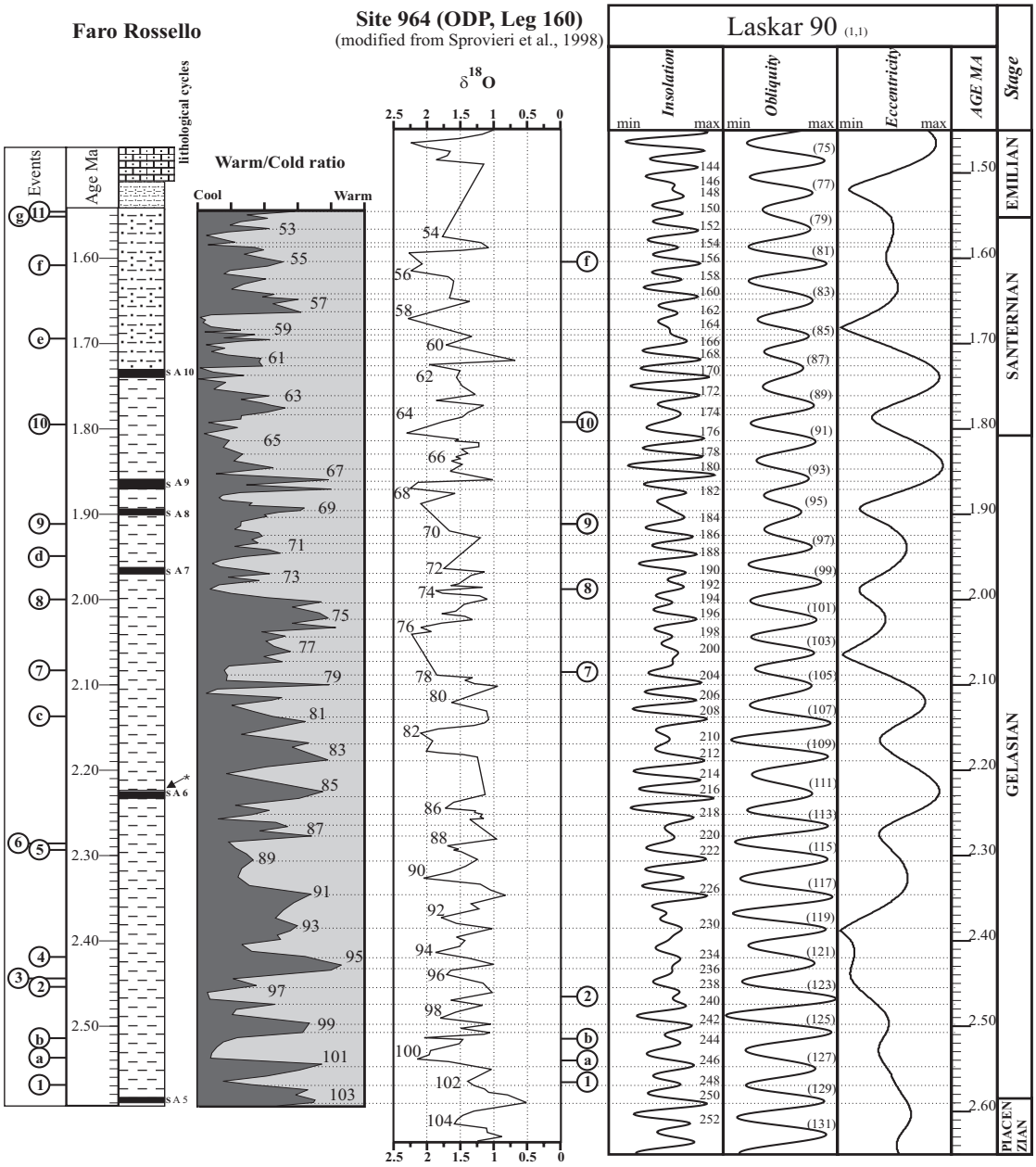


**Figure 9.** Distribution of warm versus cold foraminifera, compared and correlated with $\delta^{18}O$ values from ODP Site 964 (Leg 160) modified from Sprovieri et al., (1998).

fossil bioevents recognised along the sedimentary sequence are plotted.

***Oxygen Isotopes***

The stable isotopes record obtained from Site 964 (ODP, Leg 160) by Sprovieri *et al*., (1998) on *G. ruber* tests were used. The $\delta^{18}O$ fluctuations have been recalibrated in age scale by comparing of Site 964 bio-events with those of Vrica and Faro Rossello sections. Finally the $\delta^{18}O$ curve has been correlated with warm/cold species ratio of Faro Rossello section.

***Spectral analysis and cyclicity***

The study was carried out with a medium sampling every 1 m. Because of high variation in the sedimentation rates, 18.7 cm/kyr in the first segment (I), and 21.7-24.4 cm/kyr in the other two segments (II and III), the sampling has been intesified in some intervals in which the sedimentation rate was higher, obtaining an average sampling each ~5 kyr. The frequency of sampling has permitted to highlight the Milankovitch periodicities for the whole section.

Sprovieri (1993), Caruso *et al*., (2002) and Sprovieri *et al*., (2002) have demonstrated that astronomical cycles (21, 41 and 100 kyr) are responsible for planktonic foraminifera fluctuations.

In particular, the abundances curves of *G. ruber* and neogloboquadrinids show Milankovitch periodicities (Fig. 10). These fluctuactions have been calibrated to the astronomical tuning of Laskar *et al*.,

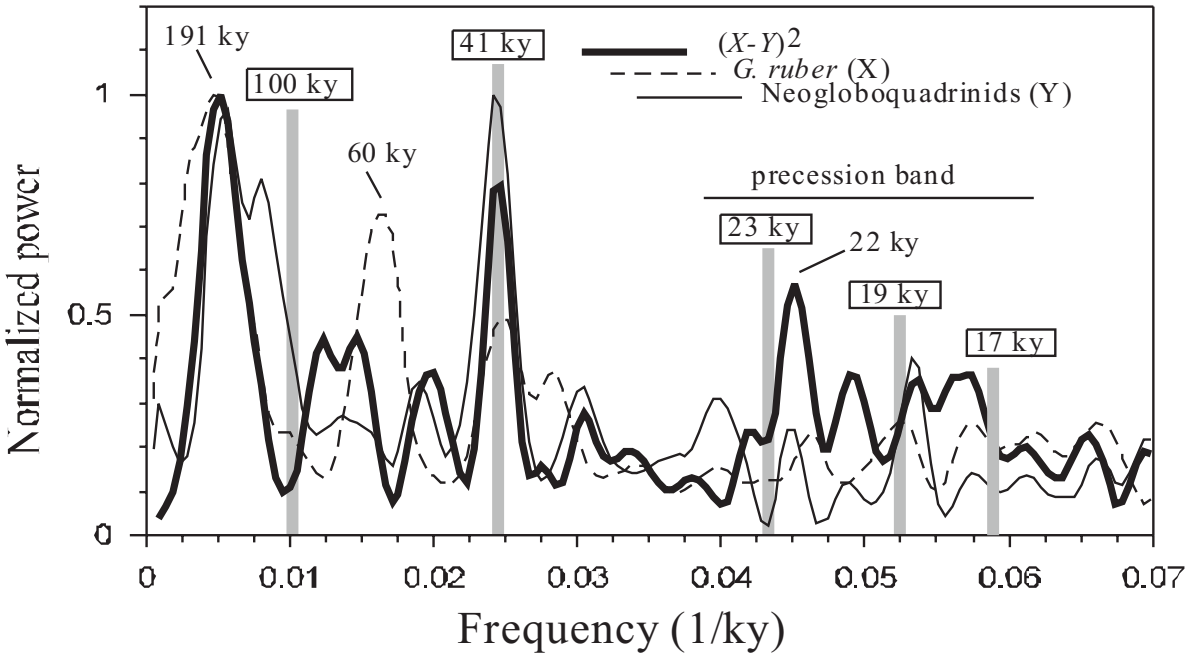


**Figure 10**. Power spectra of the *Globigerinoides ruber* group (X) and neogloboquadrinid (Y) signals are reported. Following the methods of Schulz & Stattegger, (1997) power spectrum of function (*G. ruber* group-neogloboquadrinids)$^2$ indicates the 191, 41 and 22 kyr periodicities.

(1993). *Globigerinoides ruber* is a typical species of warm surface water, and blooms during maxima insolation in the spring/summer periods. Neogloboquadrinids are typical species of cool/cold water, and bloom during minima insolation and autumn/winter periods. In particular, the lowest abundances of the *G. ruber* group coincide with precessional maxima/insolation minima, while *G. ruber* group high abundances coincide with precessional minima/insolation maxima (Fig. 11). Neogloboquadrinids show an opposite trend to *G. ruber* (Fig. 11); in fact highest abundances of neogloquadrinids coincide with insolation/ obliquity/eccentricity minima.

Since the classic lithologic cycles, recognised in the coeval Singa/Vrica sections and Site 964, are not present in the Faro Rossello section, spectral and filtering methodologies of Schulz & Stattegger (1997) have been applied to the curves of the relative abundance fluctuations of *G. ruber* group and neogloboquadrinids, in order to reconstruct the sequence of precession and obliquity cycles. The astronomical calibration previously obtained by lithological tuning of the section, allowed to represent the succession of the faunal signals with an age model (Fig. 11).

The power spectra of the *G. ruber* group (X) and neogloboquadrinids (Y) signals (Fig. 10) show dominant frequencies at 191 and 41 kyr. The precession (22 kyr) signal is weak. In order to highlight the Milankovitch periodicities, a comparison of the abundance curves of the *G. ruber* group and neogloboquadrinids has been carried out to obtain a power spectrum in function of the balance percentage (X-Y)$^2$, between *G. ruber* group (X) and neogloboquadrinids (Y) fluctuations, following the methods of Schulz & Stattegger, (1997). This spectrum highlighted the 41 and 22 kyr periodicities (Fig. 10).

The ages of the bioevents obtained, compared with those reported by Lourens *et al*., (1996), confirm the reliability of this calibration, although not all ages corresponds (Tab. 1). The studied section recovers the interval time from 2.60 to 1.552 Ma, which includes i-cycles 250-150 and o-cycles (129-78) (Figs. 9 and 11).

## ASH LAYERS

Two volcanic ash layers were recognised between Punta Piccola and Faro Rossello sections, the first one (AL1) outcrops at Punta Piccola 5 cm above the sapropel A2 of Lourens *et al*., (1996). Using Laskar $90_{(1,1)}$ solution an astronomical age of 2.676 Ma was obtained for AL1 (Fig. 4 and Tab. 1).

The second volcanic ash layer (AL2) is present in the Faro Rossello section just above sapropel A6. An astronomical age of 2.225 Ma was obtained for this ash layer (Fig. 9 and Tab. 1).

## DISCUSSION

On the basis of the faunal, floral and geochemical signals, the studied sequence has been subdivided

| | Lourens et al., (1996) | | | | Sprovieri et al., (1998) | | | Raffi (2002) - *Site 607* | | | This work | | | | |
|---|---|---|---|---|---|---|---|---|---|---|---|---|---|---|---|
| **nannofosils** | **Event** | **insolation cycles** | **obliquity cycles** | **Age (Ma)** | **Event** | **Isotopic stage** | **Age (Ma)** | **Event** | **Isotopic stage** | **Age (Ma)** | **Event** | **insolation cycles** | **obliquity cycles** | **Isotopic stage** | **Age (Ma)** |
| ⓖ Large *Gephyrocapsa* | **FO** | 157 | (81/82) | 1.61 | **FO** | 49/51? | 1.50 | FO | 54/55 | 1.595 | **FO** | 150/151 | (78/79) | 53 | 1.556 ± 0.004 |
| ⓕ *Calcidiscus macintyrei* | **LO** | 164 | (83/84) | 1.67 | **LO** | 56 | 1.62 | LO | 55 | 1.601-1.610 | **LO** | 156 | (81) | 55/56 | 1.611 ± 0.005 |
| ⓔ *Gephyrocapsa oceanica* | **FO** | 167 | (86) | 1.71 | **FO** | 61 | 1.75 | FO | 60 | 1.7 | **FO** | 166 | (85) | 59 | 1.694 ± 0.005 |
| ⓓ *Discoaster brouwerii* | **LO** | 189 | (97/98) | 1.95 | **LO** | 1.95 | 1.95 | | | | **LO** | 188/189 | (98) | 72 | 1.948 ± 0.004 |
| ⓒ *Discoaster triradiatus* | | | | | | | | | | | **FO** | 208 | (107) | 81 | 2.139 ± 0.006 |
| ⓑ *Discoaster pentaradiatus* | **LO** | 244 | (126) | 2.51 | **LO** | 99 | 2.51 | | | | **LO** | 244 | (125/126) | 99 | 2.515 ± 0.005 |
| ⓐ Drop Discoasterids | | | | | **Drop** | 100 | 2.53 | | | | **LCO** | 245 | (126) | 100 | 2.542 ± 0.004 |
| **foraminifera** | | | | | | | | | | | | | | | |
| ⑪ *Hyalinea balthica* | | | | | | | | | | | **FO** | 150 | (78) | 53 | 1.552 ± 0.004 |
| ⑩ *N. pachyderma* left coiling | **increase** | 175 | (90/91) | 1.80 | increase | 64 | 1.81 | | | | **increase** | 175 | (90) | 64 | 1.797 ± 0.005 |
| ⑨ *Globorotalia inflata* | | | | | | | | | | | **FCO** | 185 | (96) | 70 | 1.911 ± 0.005 |
| ⑧ *G. truncatulinoides - S. dehiscens* | **FO** | 193/195 | (101) | 2.00 | **FO** | 77 | 2.07 | | | | **FO** | 193/194 | (100) | 74 | 2.000 ± 0.005 |
| ⑦ *Globorotalia inflata* | **FO** | 203 | (104) | 2.09 | **FO** | 80 | 2.13 | | | | **FO** | 203 | (104) | 78 | 2.085 ± 0.005 |
| ⑥ *Globorotalia bononiensis* | **LO** | 230 | (121/122) | 2.41 | | | | | | | **LO** | 220 | (114) | 87/88 | 2.286 ± 0.007 |
| ⑤ *Globorotalia crassaformis* | | | | | | | | | | | **LCO** | 221 | (114/115) | 88 | 2.293 ± 0.007 |
| ④ *Neogloboquadrina atlantica* | **LO** | 230/231 | (121/122) | 2.41 | | | | | | | **LO** | 231/232 | (120/121) | 94 | 2.418 ± 0.005 |
| ③ *Neogloboquadrina atlantica* | | | | | | | | | | | **LCO** | 237 | (122) | 96/97 | 2.442 ± 0.007 |
| ② *Globorotalia bononiensis* | | | | | **LO** | 96 | 2.45 | | | | **LCO** | 237/238 | (122) | 96/97 | 2.450 ± 0.007 |
| ① *Globigerinoides obliquus extremus* | | | | | | | | | | | **LCO** | 248 | (128) | 102 | 2.573 ± 0.006 |
| **Faro Rossello** | **Singa/Vrica** | | | | | | | | | | | | | | |
| *Sapropels* | | | | | | | | | | | | | | | |
| A 10 | C 8/f | 170 | (87) | 1.736 | | | | | | | | 170 | (87) | 618 | 1.736 |
| A 9 | C 4/c | 180 | (93) | 1.851 | | | | | | | | 180 | (93) | 67 | 1.851 |
| A 8 | | | | | | | | | | | | 184 | (95) | 69 | 2.384 |
| A 7 | C 0/* | 190 | (99) | 1.965 | | | | | | | | 237 | (99) | 73 | 1.965 |
| A 6 | B 2 | 216 | (111) | 2.229 | | | | | | | | 216 | (111) | 85 | 2.229 |
| A 5 | A 5 | 230/231 | (129) | 2.588 | | | | | | | | 250 | (129) | 103 | 2.588 |
| ***Volcanic Ash Layers*** | | | | | | | | | | | | | | | |
| AL2 | | | | | | | | | | | | 216 | (111) | 85 | 2.225 ±0.002 |
| AL1 | | | | | | | | | | | | 258 | (129) | 107 | 2.676 ±0.002 |

**Table 1**. Astronomical ages of: i) calcareous plankton bioevents; ii) sapropel layers; iii) volcanic ash layers. Comparation with other authors.

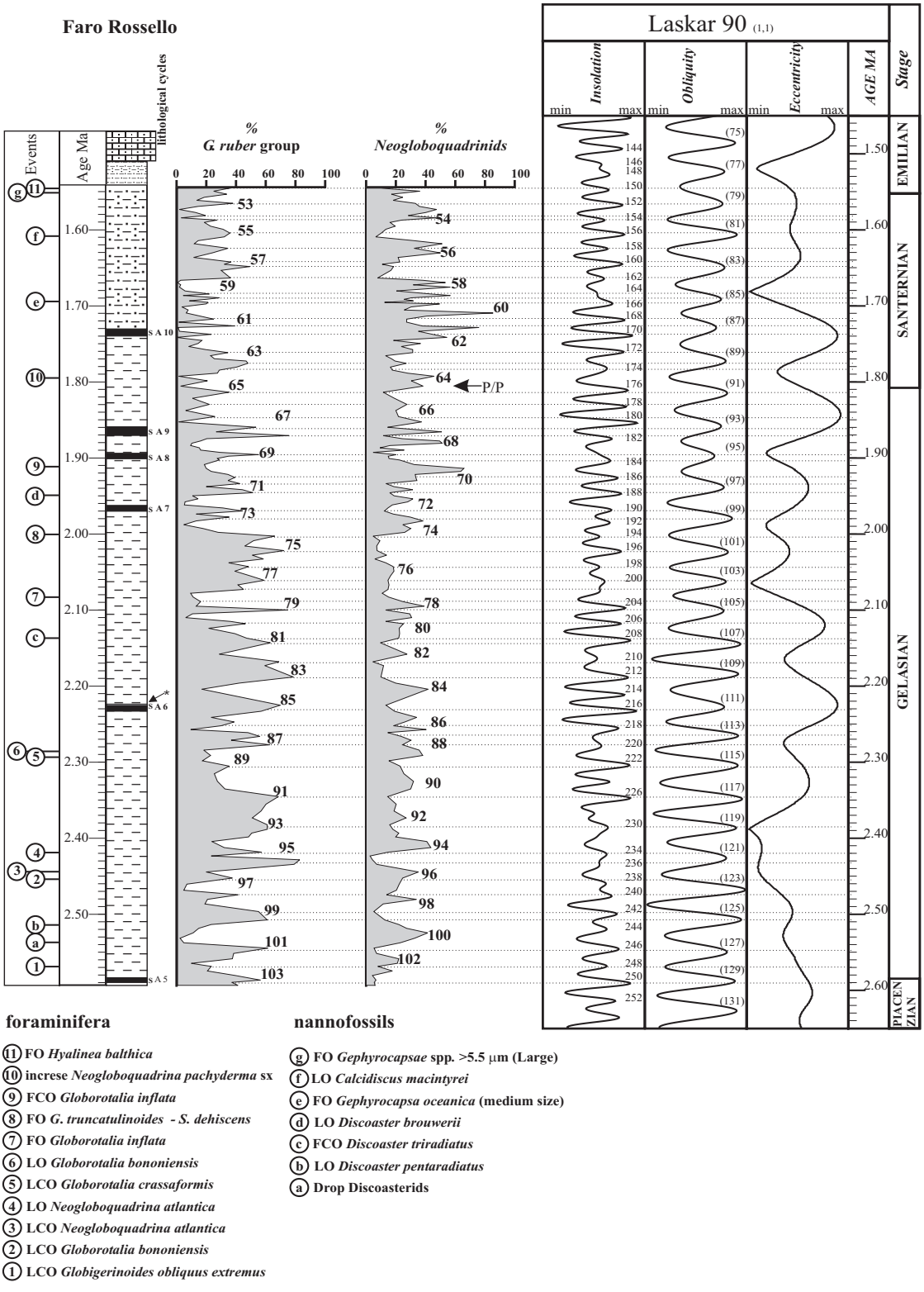


**Figure 11.** Comparison between *Globigerinoides ruber* group and neogloboquadrinids, correlation with Laskar 90 $_{(1,1)}$ curves. The lithological log is plotted versus the age model.

into five climatic intervals.

***Interval 1 from 2.60 to 2.57 Ma (tropical-temperate)*** This interval is characterised by: a) high percentages of the *G. ruber* group and *G. obliquus extremus*, typical species of tropical surface water (Fig. 11); b) abundant discoasterids (*D. pentaradiatus*, *D. surculus* and *D. brouwerii*), and low percentages of cool species. *G. obliquus extremus* is abundant in the first 4.50 m, corresponding to 30 kyr of the section; its

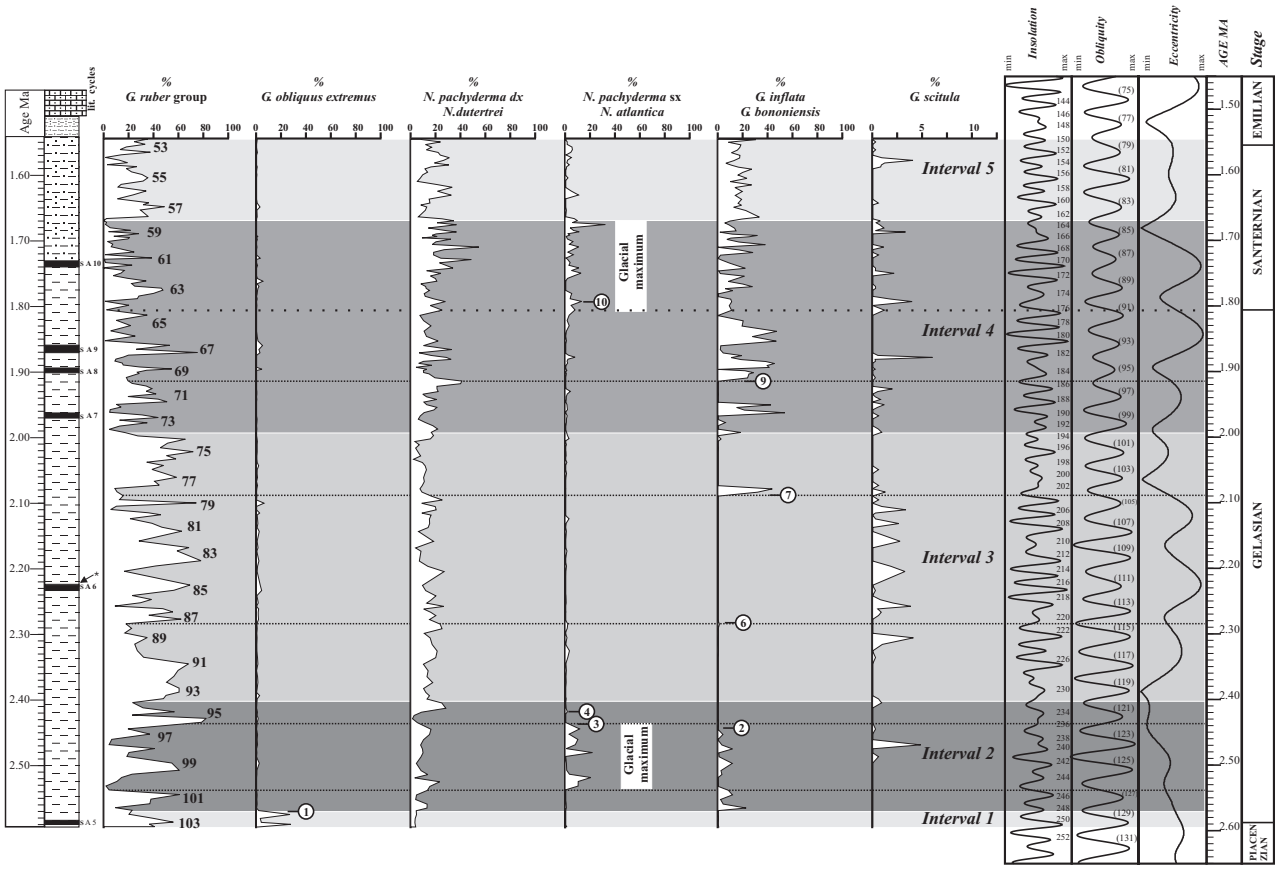


**Figure 12**. Five different climatic intervals have been recognised by correlating planktonic foraminifera abundances with astronomical curves. Interval 1 (tropical-temperate cool); Interval 2 (glacial-temperate); Interval 3 (glacial-interglacial); Interval 4 (glacial trend); Interval 5 (glacial-temperate). White rectangles indicate glacial maxima.

higher abundances were recognised in coincidence of i-cycle 250 (sapropel A5) and i-cycle 248 (Fig. 12). In particular isotopic stage 103 display the lowest value of $\delta^{18}O$ (Fig. 9). Sapropel A5 corresponds to i-cycle 250/o-cycle (129) maxima. Tropical condition ended in coincidence of the Last Common Occurrence (LCO) of *G. obliquus extremus*, within isotopic stage 102 at 2.573 Ma (Fig. 12).

***Interval 2 from 2.57 to 2.40 Ma (temperate-glacial)***

According to many authors (Hays *et al*., 1976; Imbrie *et al*., 1984; Weedon, 2003), during the Late Pliocene obliquity amplitudes were very strong and produced glacial/interglacial climate oscillations. During this interval *G. ruber* gr. and neogloboquadrinid fluctuations were dominated by obliquity forcing (Fig. 11).

This interval is characterised by the drastic reduction of warm tropical species and by an increase in polar and cool forms (Figs. 9 and 12). In particular, *N. atlantica* and *N. pachyderma* sinistral forms (pl. 1) are common and their abundance are up to 20% (Figs. 7a and 11). Cyclical fluctuations in the abundance of *G. bononiensis* were also emphasized (Figs. 7 and 12).

In each precessional cycle a particular trend in *G. ruber-G. bononiensis-N. atlantica* is present (Fig. 13a). Perez-Folgado *et al*., (2003) and Sierro *et al*., (2003) described similar event successions in the sapropel cyclicity of the lower Messinian with *Globigerinoides quadrilobatus-Globorotalia miotumida-N. acostaensis*. Neogloquadrinids are only abundant when winter temperatures are colder than 13.5°C, and proliferate in the presence of a shallow nutricline (Pérez-Folgado *et al*., 2003; Pujol & Vergnaud-Grazzini, 1995).

*Globorotalia bononiensis* belongs to the *G. bononiensis-inflata* phyletic lineage (Spaak, 1983; Zachariasse *et al*., 1989). *Globorotalia inflata* is typical of transitional water (Bé & Tonderlund, 1971) and blooms during the winter period in the modern Mediterranean area (Pujol & Vergnaud-Grazzini, 1995). *Globorotalia inflata* prefers a deep mixed layer without a thermocline, when the temperature ranges from 13 to 16-17°C (Pujol & Vergnaud-Grazzini, 1995). *Globigerinoides ruber* is typical of warm oligotrophic surface waters and prefers water masses warmer than 17°C, with relative lower (<34.5‰) or higher (>36‰) salinity (Bé & Tonderlund, 1971; Pujol & Vergnaud-Grazzini, 1995).

*Neogloboquadrina atlantica* is typical of North Atlantic polar waters (Poore & Bergreen, 1975;

Zachariasse *et al*., 1990; Zijderveld, 1990) and *N. pachyderma* left coiling actually lives in polar regions (Bé & Tonderlund, 1971).

The highest values of neogloboquadrinids (sinistral forms) and *N. atlantica* fall within isotopic stage 100, with values of $\delta^{18}O$ up to 2.2‰, well correlated to obliquity minima, in which i-cycle 245/o-cycle (126)/eccentricity minima are in phase (Figs. 11 and 12). The co-occurrence of the three minima in Milankovitch periodicities has amplified the glacial event, producing the expansion of the Northern hemisphere ice sheet, astronomically dated at 2.535 Ma. This glacial event has been recognised in Mediterranean and extra-Mediterranean areas, and reported at 2.4 or 2.5 Ma (Shackleton & Cita, 1979; Zachariasse *et al*., 1989; Rio *et al*., 1990; Naish *et al*., 1997; Cita *et al*., 1999). Haug & Tiedemann, (1998) proposed that the final closure of Panamian Isthmus caused favorable condition for ice-sheet growth, at 2.5 Ma.

During this interval a drastic reduction of discoasterids, typical nannofossils of the tropical area (Cheptow-Lusty *et al*., 1989), was also observed in isotopic stage 100/99. This observation is in good agreement with the positive shift of $\delta^{18}O$, and with higher abundance of polar-temperate planktonic foraminifera (Figs. 9 and 12).

In summary, isotopic stage 100 corresponds to the maximal contraction in the ecological niche of tropical species in the Mediterranean Sea, even if the cooling trend, regulated by eccentricity, continued up to 2.40 Ma.

***Interval 3 from 2.40 to 1.99 Ma (glacial-interglacial)***
This interval includes i-cycles from 233 to 193 and o-cycles (119 to 100) (Figs. 11 and 12). *Globorotalia bononiensis* is absent or rare, and disappears at 2.286 Ma. *Globorotalia scitula* is cyclically present, with abundance fluctuating from 4 to 6%. *Globorotalia scitula* is a typical form of intermediate-deep cool water and is common during glacial intervals in the Mediterranean Sea (Rohling *et al*. 1997; Capotondi *et al*. 1999; Negri *et al*., 2002). *Globorotalia scitula* and neogloquadrinid high abundances are negatively correlated to those of the *G. ruber* group. The abundance of the *G. ruber* group shows an increasing trend well correlated with the strongest amplitudes of the eccentricity curve, in correspondence with dominant obliquity forcing, and lower $\delta^{18}O$ values (Fig. 9). The highest peaks in the abundance of *G. ruber* (isotopic stage 91, 87, 85, 83 and 81) correspond to climatic amelioration, well marked by the increase of eccentricity, and these peaks are also in phase with the insolation/obliquity maxima (Fig. 9). Only one sapropel is present (A6) within isotopic stage 85, perfectly correlated to i-cycle 216/o-cycle(111)/eccentricity maxima (Figs. 11 and 12).

The *Discoaster triradiatus* FCO was recognised in isotopic stage 81; this event correspond to i-cycle 208/o-cycle (107)/ eccentricity maxima, astronomically dated at 2.14 Ma. *Discoaster brouwerii* and *D. triradiatus* are the only two species of discoasterids that survived to the cooling related to the glacial event at 2.535 Ma.

In the interval from 2.30 to 2.10 Ma, in which the *G. inflata* group is absent, the *G. ruber* group is alternatively replaced by cool species like *T. quinqueloba*, *G. scitula* and *N. pachyderma* (Fig. 13b). These fluctuations are well correlated to the Milankovitch periodicities. In fact, peaks of warm species are positively correlated to the insolation or obliquity maxima, while cool and polar species are correlated with insolation/obliquity minima.

*Globorotalia inflata* appears with only one peak around 40% in isotopic stage 78 at 2.085 Ma, in coincidence with i-cycle 203/o-cycle (104). Just above the *G. inflata* peak, an increase in the abundance of warm species and a contemporaneous decrease in $\delta^{18}O$ values, have been observed corresponding to o-cycle (101)/i-cycle 198 to 194. This particular warmer trend is well evident (Fig. 9). In summary in this interval, obliquity forcing and eccentricity trends produced strong climatic variations, with an alternation of tropical and temperate-cool phases.

***Interval 4 from 1.99 to 1.67 Ma (glacial trend and Plio/Pleistocene boundary)***
This interval includes i-cycles from 192 to 163 and o-cycles (99-84), and starts with a reduction of warm species in correspondence with isotopic stage 74 (Figs. 9 and 12). A gradual cooling trend starts at 1.99 Ma, marked by the re-appearance of *G. inflata*, in coincidence with the extinction of discoasterids, astronomically dated at 1.948 Ma. Also the abundance of neogloboquadrinids increases in correspondence of a positive shift of $\delta^{18}O$ values within isotopic stage 70 (Figs. 9 and 11). In particular, left coiled *N. pachyderma* increases in abundance in isotopic stage 64, i-cycle 175/176 astronomically dated at 1.797 Ma, in correspondence of the lowest values of *G. ruber* and high abundance peaks of *G. scitula* (Fig. 12). *Neogloboquadrina pachyderma* sinistral is very close to the P/P boundary, which at the Vrica section, has an estimated age of 1.805 Ma (i-cycle 176).

In the four sapropelitic layers (A7-A10) benthic foraminifera are absent or very rare, and represented by oligothypic assemblages typical of dysoxic conditions. These sapropels are characterised by an abundance of warm oligotrophic planktonic foraminifera. In sapropels (A9-A10) *N. dutertrei* is abundant with percentages up to 25%; *N. dutertrei* sometimes is interpreted as a species of low salinity and high nutrients in an upwelling system (Jian *et al*., 2003). *Gephyrocapsa oceanica* (medium size) appears at 1.694 Ma in the isotopic stage 59. This age is very

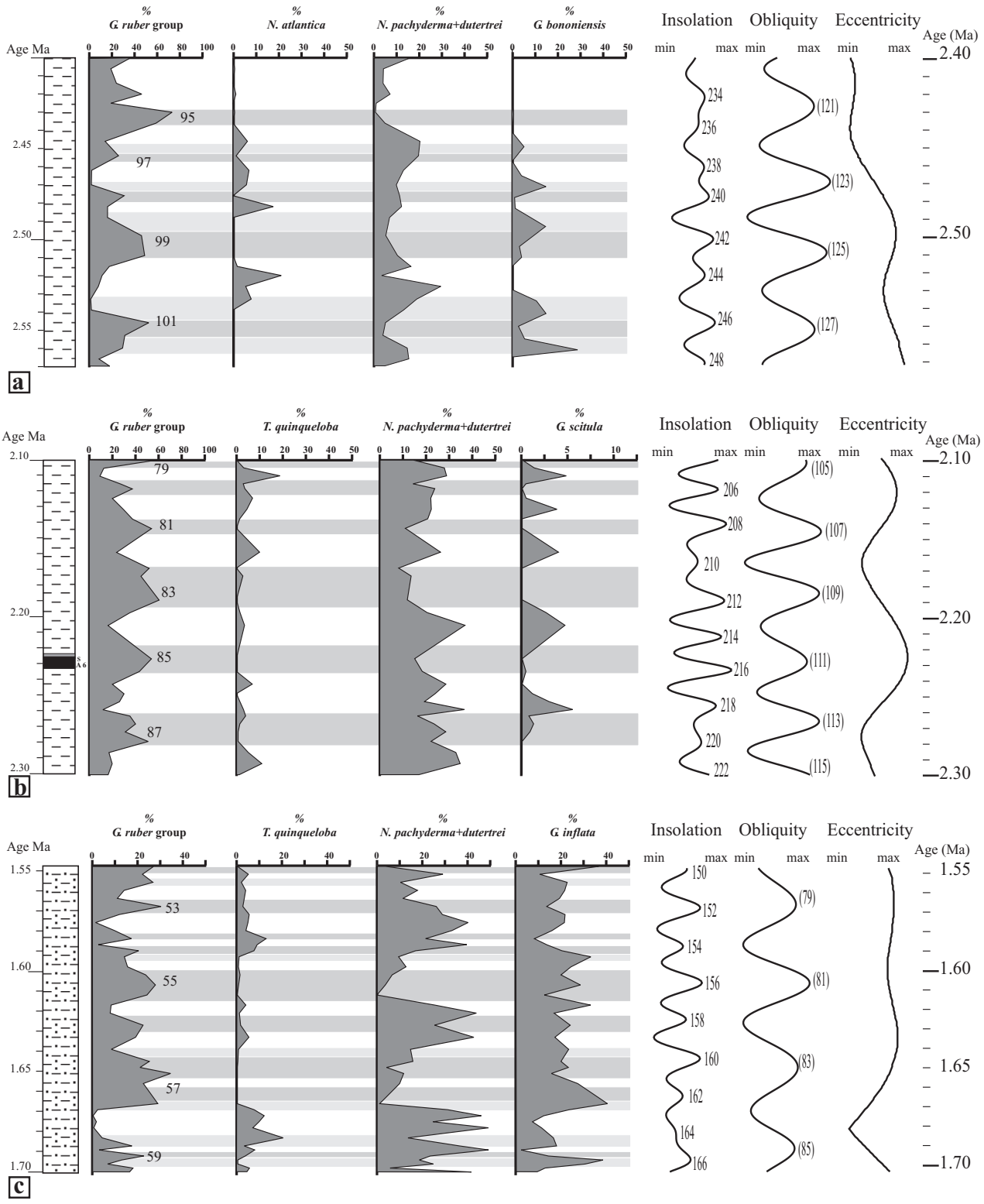


**Figure 13.** Relative abundance of warm, cold and temperate planktonic foraminifera species tuned with insolation/obliquity/eccentricity curves; a) interval 2.57-2.40 Ma, b) interval between 2.30-2.10 Ma; c) interval between 1.66-1.54 Ma.

close to the age proposed by Raffi (2002) in the Site 607, while Lourens *et al*., (1996) reported an age 15 kyr older for the same event (Tab. 1). The glacial trend ended with the increase in abundance of *G. ruber* gr., in coincidence of i-cycle 162/o-cycle (83/84)/eccentricity minima (Fig. 5).

***Interval 5 from 1.66 to 1.54 Ma (temperate-glacial period)***

An amelioration of climatic conditions started at

1.66 Ma, well comparable with high percentages of warm (*G. ruber*) and temperate species (*G. inflata*) (Figs. 11 and 12). This period shows a gradual warming trend, alternating with cold episodes. Temperate and warm species (Fig. 12c), in particular cold surface species (neogloboquadrinids), are replaced by *G. inflata*, typical of deep mixed layer (Capotondi *et al*., 1999), and subsequently replaced by surface warm oligotrophic species (*G. ruber*). A similar trend has been described in the sapropel c of Vrica section, i-cycle 180 by Negri *et al*., (2002). Interval 5 ended just above *C. macintyrei* LO (1.611 Ma), with the input of two boreal species into the Mediterranean Sea: *Gephyrocapsa* >5.5µm (FO) and *Hyalinea balthica* (FO), astronomically dated at 1.556 and 1.552 Ma respectively, within isotopic stage 53 (Tab. 1).

## SUMMARY AND CONCLUSION

The study of planktonic foraminifera has permitted to recognize five climatic different intervals over the upper Pliocene to lower Pleistocene (2.6 to 1.55 Ma). After the deposition of sapropel A5 (2.588 Ma), sapropels were rare and irregularly distributed in the central Mediterranean (Faro Rossello and Monte San Nicola Gela), and formed only during some particular eccentricity/obliquity maxima. On the other hand, in the Ionian area and in eastern part of Mediterranean Basin, sapropels were constantly present, and their deposition was triggered by precessional forcing (Singa/Vrica composite section; Site 964 and other eastern Sites). The drastic change between the western, central, and eastern parts of the Mediterranean Basin in marine sedimentation, is probably due to the maxima expansion of the northern Hemisphere ice sheet, which produced important changes in the atmospheric and oceanic circulation. The interactions of astronomic and tectonic events: a) Panamian Isthmus closure; b) major amplitudes of obliquity forcing; c) major phase of Himalaya-Tibetan plateau uplift, produced global climatic changes, with the intensification of monsoonal activity. Moonsonal activity was also strong in the southern and southeastern Mediterranean area, with important input of palygorskite/kaolinite from North African sources. The presence of palygorskite/kaolinite, during the Middle Pliocene, was interpreted as an arid phase during precessional maxima/insolation minima (Foucalt & Mélières, 2000). To these global events it is necessary to add the geodynamic evolution of the Appennine-Maghrebid belt, which during the Middle and Late Pliocene produced the uplift of the Caltanissetta basin. The uplift of Appennine-Maghrebid belt had an important role in the paleoceanographic differentiation between the eastern and western part of the Mediterranean basin.

The expansion of the northern Hemisphere ice sheet at 2.57 Ma (Interval 2), culminated between 2.535 and 2.43 Ma. This glacial event favored the input of North Atlantic temperate and polar water, driving cooler species (*G. bononiensis* and *N. atlantica*) into the Mediterranean area, and causing the extinction of tropical forms (discoasterids decrease in abundance and *G. obliquus extremus* LCO). This interval was characterised by high amplitudes of obliquity forcing, endured until 2.385 Ma, which produced glacial-interglacial events; moreover, a cyclical alternation of warm-temperate-cool species was constant in each precessional cycle.

Interval 3, between 2.40 to 1.99 Ma, was marked by high fluctuations of warm/cool species, in which dominant obliquity forcing produced high seasonality.

A clear glacial trend between 1.99 and 1.66 Ma (Interval 4) was identified based on the increase of abundance of *G. inflata* and *N. pachyderma* sinistral, and the contemporaneous decrease in abundance of the *G. ruber* group. A glacial maximum, between 1.805 and 1.67 Ma, contains the P/P boundary, astronomically dated at 1.805 Ma. A climatic warmer trend, started at 1.66 Ma, and persisted until 1.55 Ma, at top of the studied section (Interval 5).

Additionally, the *G. ruber* and neogloboquadrinid abundance fluctuations contain strong obliquity periodicities (41 kyr), precession (22 kyr) and 191 kyr cycles probably related to Earth's eccentricity periodicity.

## ACKNOWLEDGEMENTS

I am are very grateful to Frèderic Mélières (MNHN, Paris) for stimulanting discussion on clay minerals of Punta Piccola, and Jaume Dinares-Tùrell (INGV, Rome) for useful suggestions on spectral analysis. This paper was substantially improved by the thorough and constructive remarks of Silvia Iaccarino and Silvia Spezzaferri. This research is supported by the grants of Regione Siciliana Ass. Beni Culturali ed Ambientali n. 77502 "Geositi della Sicilia".

## REFERENCES

Aguirre, E. & Pasini G. 1985. The Pliocene-Pleistocene boundary. *Episodes*, **8**, 116-120.

Backman, J. & Shackleton, N.J. 1983. Quantitative biochronology of Pliocene and early Pleistocene calcareous nannofossils from the Atlantic, Indian and Pacific oceans. *Marine Micropaleontology*, **8**, 141-170.

Bé, A.W.H. & Tolderlund, D.S. 1971. Distribution and ecology of living planktonic foraminifera in surface waters of the Atlantic and Indian oceans. In: Funnell, B.M. & Riedel, W.R. (eds), *Micropaleontology of the Oceans*, Cambridge University Press, Cambridge, UK, 105-149.

Capotondi, L., Borsetti, A.M. & Morigi, C. 1999. Foraminiferal ecozones: a high resolution proxy for the late Quaternary biochronology in the central Mediterranean Sea. *Marine Geology*, **153,** 253-274.

Caruso A., Sprovieri, M., Bonanno, A. & Sprovieri, R. 2002. Astronomical calibration of the upper Serravallian/Tortonian boundary at Case Pelacani Section (Sicily, Italy). In: Iaccarino S. (ed.), Integrated stratigraphy and paleoceanography of the Mediterranean Middle Miocene. *Rivista Italiana Paleontologia e Stratigrafia*, **108**, 297-306.

Castradori, D., Rio, D., Hilgen, F.J. & Lourens, L.J. 1998. The global standard Stratotype-section and point (GSSP) of the Piacenzian Stage (Middle Miocene). *Episodes*, **21**, 2, 88-93.

Catalano, R. & D'Argenio, B. 1982. Guida alla geologia della Sicilia occidentale. In: Catalano, R. & D'Argenio, B. (eds.), *Guida alla geologia della Sicilia Occidentale*. Società Geologica Italiana, 9-41.

Cheptow-Lusty, A., Backman, J. & Shackleton, N.J. 1989. Comparison of upper Pliocene *Discoaster* abundance variations from North Atlantic Site 552, 607, 658, 659 and 662: Further evidence for marine plankton responding to orbital forcing. *Proceedings of the Ocean Drilling Program, Scientific Results*, **108**, 461-478.

Cita, M.B. & Gartner, S. 1973. Studi sul Pliocene e gli strati di passaggio dal Miocene al Pliocene. IV. The stratotype Zanclean foraminiferal and nannofossil biostratigraphy. *Rivista Italiana Paleontologia e Stratigrafia*, **79**, 503-558.

Cita, M.B., Rio, D. & Sprovieri, R. 1999. The Pliocene series: Chronology of the type Mediterranean record and standard chronostratigraphy. In Wrenn, J.H., Suc, J.-P. and Leroy, S.A.G. (eds), *The Pliocene: Time of change*; American Association of Stratigraphic Palynoligists Foundation, 49-63.

Colalongo, M.L. & Sartoni, S. 1979. Schema biostratigrafico per il Pliocene e il basso Pleistocene in Italia. Progetto Finalizzato Geodinamica. *Contributi Carta Neotettonica Italia*, **251**, 645-654.

Di Stefano, E., Sprovieri, R. & Caruso, A. 1993. High resolution biochronology in the Monte Narbone Formation of the Capo Rossello section and the Mediterranean first occurrence of *Globorotalia truncatulinoides*. *Rivista Italiana Paleontologia e Stratigrafia*, **99**, 357-370.

Foucault, A. & Mélières, F. 2000. Palaeoclimatic cyclicity in central Mediterranean Pliocene sediments: the mineralogical signal. *Palaeogeography, Palaeoclimatology, Palaeoecology*, **158**, 311-323

Haug, G.H. & Tiedemann R. 1998. Effect of the formation of the Isthmus of Panama on Atlantic Ocean thermoaline circulation. *Nature*, **393**, 673-676.

Hays, J.D., Imbrie, I. & Shackleton, N.J. 1976. Variations in the Earth's orbit: pacemaker of the ice ages. *Science*, **194**, 1121-32.

Hilgen, F.J. 1991a. Astronomical calibration of Gauss to Matuyama sapropels in the Mediterranean and implication for the Geomagnetic Polarity Time scale. *Earth and Planetary Science Letters*, **104**, 226-244.

Hilgen, F.J. 1991b - Extension of the astronomically calibrated (polarity) time scale to the Miocene/Pliocene boundary. *Earth and Planetary Science Letters*, **107**, 349-368.

Hilgen, F.J. & Langereis, C.G. 1993. A critical (r)evaluation of the Miocene/Piocene boundary as defined in the Mediterranean. *Earth and Planetary Science Letters*, **118**, 167-179.

Hilgen, F.J., Abdul Aziz, H., Krijgsman, W., Langereis, C.G., Lourens, L.J., Meulenkamp, J.E., Raffi, I., Steenbrink, J., Turco, E., van Vugt, N., Wijbrans, JR. & Zachariasse, W.J. 1999. Present status of the astronomical (polarity) time-scale for the Mediterranean Late Neogene. *Philosophical Transaction of the Royal Society of London A*, **357**, 1931-1947.

Jian, Z., Zhao, Q., Cheng, X., Wang, J., Wang, P. & Su, X. 2003. Pliocene-Pleistocene isotope and paleoceanographic changes in the northern South China Sea. *Palaeogeography, Palaeoclimatology, Palaeoecology*, **193**, 425-442

Iaccarino, S. 1985. Mediterranean Miocene and Pliocene plantkic foraminifera. In: Bolli, J.B., Saunders, K. & Perch-Nielsen, H.M. (eds.), *Plantkon Stratigraphy*. Cambridge University Press, Cambridge, UK, **1**, 283-314.

Imbrie, J., Hays, J.D., Martinson, D.G., McIntyrei, A.C., Mix, A.C., Morley, J.J. Pisias, N.G., Prell, W.L. & Shackleton, N.J., 1984. The orbital theory of Pleistocene climate: support from revised chronology of the marine $\delta^{18}O$ record. In: Berger, A., Imbrie, J., Hays, J.D., Kukla, G. & Slatzman, B. (eds.), *Milankovitch and Climate*, Reidel, Dordrecht, **1**, 269-305.

Larsen, H.C., Beget, J., Clift, P., Wei, W. & Spezzaferri S. 1994. Seven million years of glaciations in Greenland. *Science*, **264**, 952-955.

Laskar, J., Joutel, F. & Boudin, F. 1993. Orbital, precessional, and insolation quantities for the Earth from -20 Myr to +10Myr. *Astronomical and Astrophysic*, **270**, 522-533.

Lourens, L.J., Antonarakou, A., Hilgen, F.J., Van Hoof, A.A.M., Vergnaud Grazzini, C. & Zachariasse, W.J., 1996. Evaluation of the Pliocene to early Pleistocene astronomical time scale. *Paleoceanography*, **11**, 391-413.

Naish, R.T., Abbott, S.T., Alloway, B.V., Beu, A.G., Carter, R.M., Edwards, A.R., Journeaux, T.D., Kamp, J.J., Pillans, B.J., Saul, G. & Woolfe, K.J. 1997. Astronomical calibration of a southern hemisphere Plio-Pleistocene reference section, Wanganui Basin, New Zealand. *Quaternary Research*, **17**, 695-710.

Negri, A., Morigi, C. & Giunta, S. 2003. Are productivity and stratification important to sapropel deposition? Microfossil evidence from late Pliocene insolation cycle 180 at Vrica, Calabria. *Palaeogeography, Palaeoclimatology, Palaeoecology*, **190**, 243-255.

Pérez-Folgado, M., Sierro, F.J., Bàrcena, M.A., Flores, J.A., Vasquez, A., Utrilla, R., Hilgen, F.J., Krijgsman, W. & Filippelli, G.M. 2003. Western versus eastern Mediterranean paleoceanographic response to astronomical forcing: a high-resolution microplankton study of precession-controlled sedimentary cycles during the Messinian. *Palaeogeography, Palaeoclimatology, Palaeoecology*, **190**, 317-334.

Poore, R., Z. & Berggren, W.A. 1975. The morphology and classification of *Neogloboquadrina atlantica* (Berggren). *Journal Foraminiferal Research*, **29**, 76-84.

Pujol, C. & Vergnaud-Grazzini, C. 1995. Distribution patterns of live planktic foraminifers as related to regional hydrography and productive systems of the Mediterranean Sea. *Marine Micropaleontology*, **25**, 187-215.

Raffi, I. 2002. Revision of the early-middle pleistocene calcareous nannofossil biochronology (1.75-0.85 Ma). *Marine Micropaleontology*, **45**, 25-55.

Rio, D., Sprovieri, R., Castradori, D. & Di Stefano, E. 1998. The Gelasian stage (Upper Pliocene): A new unit of the global standard chronostratigraphic scale. *Episodes*, **21**, 82-87.

Rio, D., Sprovieri, R. & Di Stefano, E. 1994. The Gelasian Stage: a new chronostratigraphic unit of the Pliocene series. *Rivista Italiana Paleontologia e Stratigrafia*, **100**, 103-124.

Rio, D., Raffi, I., Villa, G. 1990 - Pliocene-Pleistocene calcareous nannofossils distribution patterns in the western Mediterranean, *Proceedings of the Ocean Drilling Program Scientific Results*, **107**, 513-533.

Rohling, E.J., Jorissen, F.J. & De Stigter, H.C. 1997. 200 year interruption of Holocene sapropel formation in the Adriatic Sea. *Journal of Micropaleontology*, **16**, 97-108.

Ruddiman, W., F., Raymo, M. & McIntyre A. 1986. Matuyama 41,000 years cycles: North Atlantic Ocean and Northern Hemisphere ice sheet. *Earth and Planetary Science Letters*, **80**, 117-129.

Ruggieri, G. & Sprovieri, R. 1976. Messinian salinity crisis and its paleogeographical implications. *Palaeogeography, Palaeoclimatology, Palaeoecology*, **20**, 13-21.

Schulz, M. & Stattegger, K. 1997. Spectral analysis of unevenly spaced paleoclimatic time series. *Computers and Geosciences*, **23**, 929-945.

Shackleton, N.J., Cita, M.B. 1979. Oxygen and Carbon isotope stratigraphy of benthic foraminifers at site 397: detailed history of climatic change during the late Neogene. *Initial Report of the Deep sea Drilling Project*, **47**, 433-445.

Sierro, F.J., Flores, J.A., Francés, G., Vasquez, A., Utrilla, R., Zamarreno, I., Erlenkeuser, H. & Barcena M.A. 2003. Orbitally-controlled oscillations in plantktic communities and cyclic changes in western Mediterranean hydrography during the Messinian. *Palaeogeography, Palaeoclimatology, Palaeoecology*, **190**, 289-316.

Spaak, P. 1983. Accuracy in correlation and ecological aspects of the planktonic foraminiferal zonation of the Mediterranean Pliocene. *Utrecht Micropaleontology Bullettin*, **28**, 1-160.

Sprovieri, R. 1993. Pliocene-early Pleistocene astronomically forced and chronology of Mediterranean calcareous plankton bio-events. *Rivista Italiana di Paleontologia e Stratigrafia*, **99**, 371-414.

Sprovieri, R., Di Stefano, E., Howell, M., Sakamoto, T., Di Stefano, A. & Marino, M. 1998. Integrated calcareous plankton biostratigraphy and cyclostratigraphy at site 964. *Proceeding of the Ocean Drilling Program, Scientific Results*, **160**, 155-165.

Sprovieri, M., Caruso, A., Foresi, L., Bellanca, A., Neri, R., Mazzola, S. & Sprovieri, R. 2002. Astronomical calibration of the upper Langhian/lower Serravallian record of Ras il-Pelegrin section (Malta island, central Mediterranean). In: Iaccarino S. (ed.), Integrated stratigraphy and paleoceanography of the Mediterranean Middle Miocene. *Rivista Italiana di Paleontologia e Stratigrafia*, **108**, 183-193.

Suc, J.P., Bertini, A., Leroy, S. A.G. & Subaalyova, D. 1997. Towards the lowering of the Pliocene/Pleistocene boundary to the Gauss-Matuyama reversal. *Quaternary International*, **40**, 37-42.

Van Couvering, J.A, Castratori D., Cita, M.B., Hilgen, F.J. & Rio, D. 2000. The base of the Zanclean Stage and of the Pliocene Series. *Episodes*, **23**, 179-187.

Weedon, G.P. 2003. *Time- Series Analysis and Cyclostratigraphy. Examining stratigraphic records of environmental cycles*. Cambridge University Press, Cambridge, UK,. 1-259.

Zachariasse, W.J., Zijderveld J.D.A., Langereis C.G., Hilgen F.J. & Verhallen P.J.J.M. 1989. Early Late Pliocene Biochronology and surface water temperature variations in the Mediterranean. *Marine Micropaleontology*, **14**, 339-355.

Zachariasse, W.J., Gudjonsson, L., Hilgen, F.J., Langereis, C.G., Lourens, L.J., Verhallen, P.J.J.M. & Zijderveld J.D.A. 1990. Late Gauss to early Matuyama invasions of *Neogloboquadrina atlantica* in the Mediterranean and associated record of climatic change. *Paleoceanography*, **5**, 239-252.

Zhisheng, A., Kutzbach, J.E., Prell, W.L. & Porter S.C. 2001. Evolution of Asian monsoons and phased uplift of the Himalaya-Tibetan plateau since Late Miocene

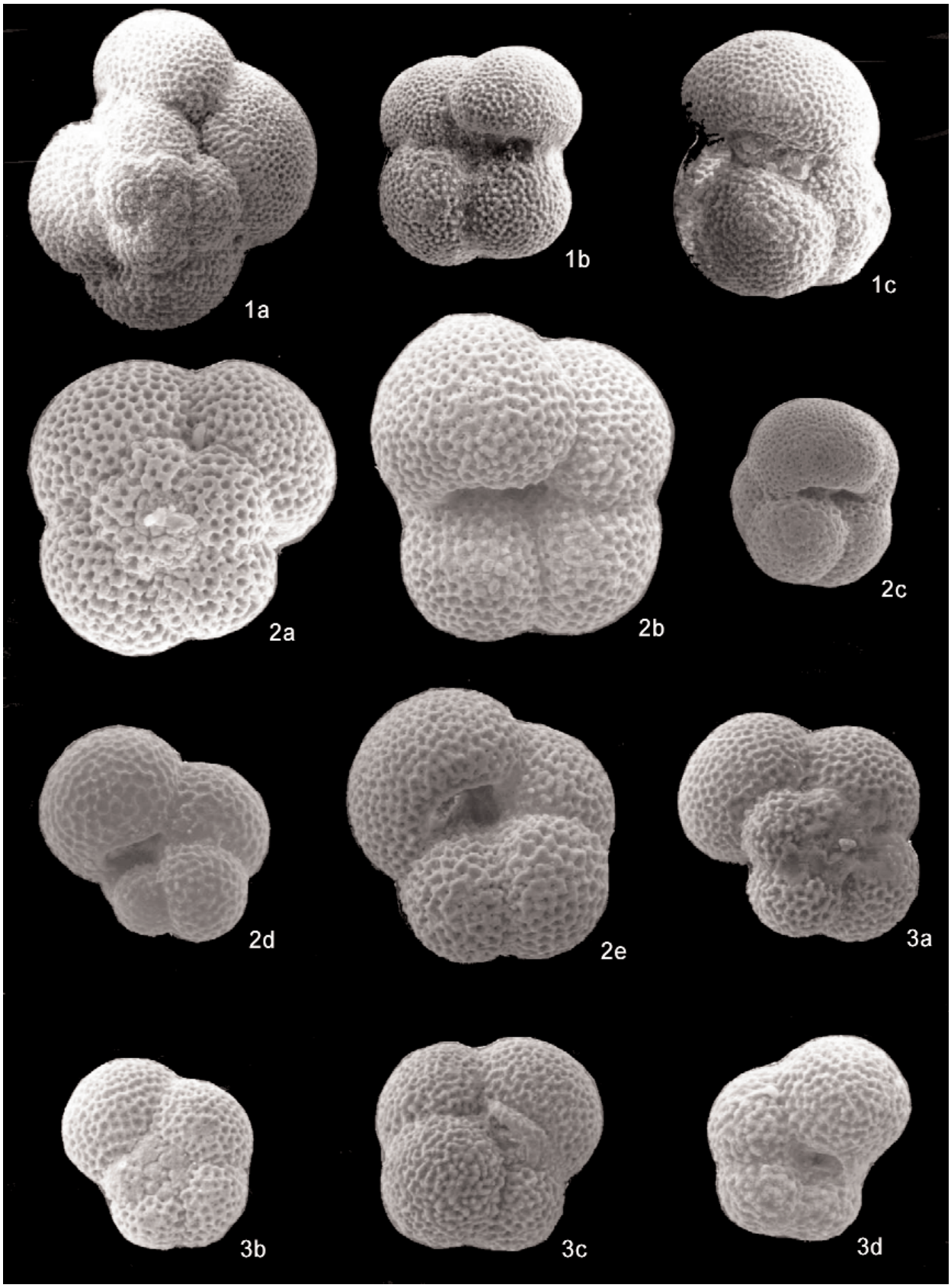


**Plate 1.** 1a. *Neogloboquadrina atlantica* spiral view , x80 1b. umbilical view, 1c. lateral view, x60 (sample FR 0 18), 2a. *Neogloboquadrina pachyderma* right coiling spiral view, x110; 2b. *Neogloboquadrina pachyderma* right coiling umbilical view, x110 (sample FR 200); 2c,d,e. *Neogloboquadrina pachyderma* right coiling umbilical view, x60 (sample FR 300); 3a. *Neogloboquadrina pachyderma* left coiling spiral view, x60 (sample FR 325); 3b,c. *Neogloboquadrina pachyderma* left coiling umbilical view, x60 (sample FR 325).

# Chamber elongation in Early Cretaceous planktonic foraminifera: a case study from the Lower Hauterivian-Lower Aptian Rio Argos succession (southern Spain)

*RODOLFO COCCIONI*[*], *ANDREA MARSILI and ALBERTO VENTURATI*

Istituto di Geologia e Centro di Geobiologia dell'Università degli Studi di Urbino "*Carlo Bo*", Campus Scientifico, Località Crocicchia, 61029 Urbino. [*]e-mail: cron@info-net.it

**ABSTRACT**

Chamber elongation in Early to Late Cretaceous planktonic foraminifera has been recently interpreted as an adaptation to low oxygen levels in the upper water column. In the well-dated uppermost Hauterivian-Lower Aptian of the Rio Argos sections (southern Spain) which contains also the equivalent of the $C_{org}$-rich Faraoni Level, we found several samples yielding planktonic foraminifera with radially elongated chambers. These elongated forms became a consistent component of foraminiferal assemblages in several stratigraphic intervals. Several lines of evidence suggest that water oxygenation could not have been the only controlling factor governing the development of elongate chambers. It is most likely an interplay of several influential factors (i.e., dissolved oxygen concentration, temperature, salinity, nutrients, type of food, trace elements) that was responsible for such a morphological adaptation.

**keywords**. planktonic foraminifera, chamber elongation, Early Cretaceous, Rio Argos, southern Spain.

## INTRODUCTION

Planktonic foraminifera with radially elongated chambers were a consistent component of foraminiferal assemblages at different levels within the Cretaceous, especially in coincidence with the deposition of remarkable organic layers which are evidence of dysoxic to anoxic conditions at the sea floor.

The chamber elongation of Early to early Late Cretaceous planktonic foraminifera has been recently interpreted as an adaptive response to oxygen depletion in the upper water column (BouDagher-Fadel *et al*., 1997; Magniez-Jannin, 1998; Aguado *et al*., 1999; Cobianchi *et al*., 1999; Luciani *et al*., 2001; Premoli Silva *et al*., 1999; Bellanca *et al*., 2002). In fact, following BouDagher-Fadel *et al*. (1997) and Magniez-Jannin (1998), the acquisition of high surface area-to-volume ratio is regarded as the simplest way to improve gas exchange with sea water and to take in sufficient amounts of oxygen for the metabolic needs of the organism.

The paleoceanographic significance of planktonic foraminifera with radially elongated chambers is still ambiguous, however, these forms are also interpreted in analogy with Eocene hantkeninids, to live at or near oxygen-depleted sea surface waters (Banner & Desai, 1988; Boersma *et al*., 1987; BouDagher-Fadel *et al*., 1997; Premoli Silva & Sliter, 1999).

We have quantitatively investigated in greater detail on the elongated chambered planktonic foraminifera from the well-dated uppermost Hauterivian-Lower Aptian sections along the Rio Argos near Caravaca (southern Spain) (Figs 1, 2) where several layers were found to yield some to few "clavate" forms (Coccioni & Premoli Silva, 1994). In particular, the Rio Argos succession as a reference for the Hauterivian/Barremian Boundary was chosen for its completeness, fossil richness and excellent outcrop (Rawson, 1996). Coccioni & Premoli Silva (1994), Hoedemaeker (1995, 2002), Hoedemaeker & Leereveld (1995), Leereveld (1997) and Company *et al*. (2003a, b) have contributed with biostratigraphic (ammonite, planktonic foraminiferal, and preliminary nannoplankton, dinoflagellated cyst and calpionellid data) and sequence stratigraphic studies on the succession.

*In*: Coccioni R., Galeotti S., & Lirer F., (eds), 2004. Proceedings of the First Italian Meeting on Environmental Micropaleontology. *Grzybowski Foundation Special Publication*, 9, 37-47.

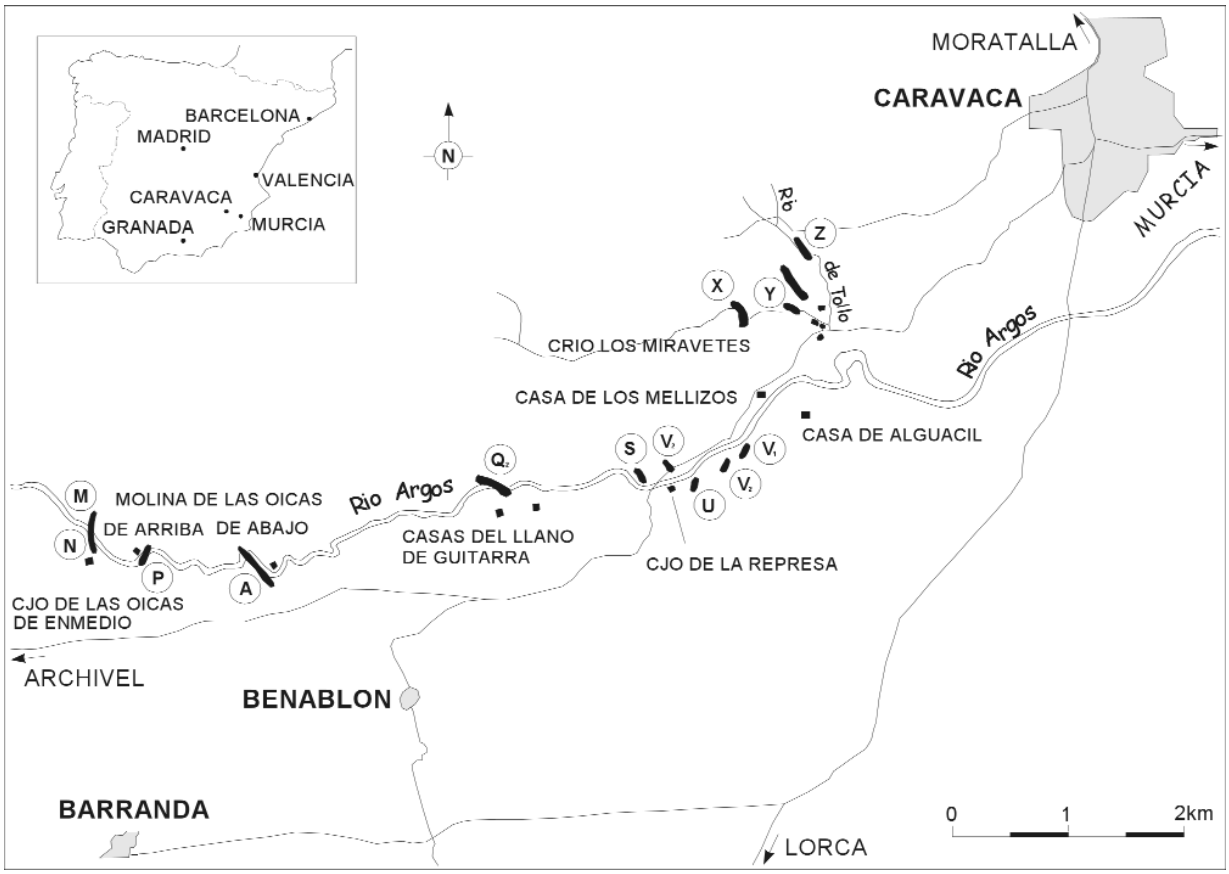


**Figure 1.** Location map of the Rio Argos sections (modified after Hoedemaeker & Leevereld, 1995).

## MATERIAL AND METHODS

Four hundred and eight-two samples of marly, marly-limestone and limestone layers of the Lower Hauterivian to Lower Aptian interval were analysed for their planktonic foraminiferal content. Ninety of them were previously studied also by Coccioni & Premoli Silva (1994).

Spacing is not constant and ranges from some decimetres to 5 meters. Marly and soft marly-limestone samples of almost the same weight were disaggregated with hydrogen peroxide and washed through a > 32 μm mesh sieve. Planktonic foraminifera from the hard marly limestone and limestone samples were successfully extracted, by concentrated acetic acid largely following the laboratory procedure proposed by Lirer (2000).

The fraction greater than 63 μm was split with a microsplitter into subsamples containing at least 300 specimens each, which were all picked, counted and mounted on micropaleontological slides. Preservation is fair to very poor; specimens are mainly recrystallized and original walls are never preserved. Specimens with radially elongated chambers were distinguished and separated from the entire planktonic foraminifera assemblage (Fig. 3). On the basis of the elongated chamber morphology in the outer whorl we distinguished three morphological categories among the planktonic foraminifera with radially elongated chambers as follows:

1) subclavate to clavate chambers;
2) pointed at the end chambers;
3) bulbous terminations-bearing chambers (Fig. 4).

In order to quantify the relative abundance of the elongated forms, we have defined three abundance classes: less than 5%, 5-10% and more than 10%. The generic classification adopted here follows mainly Loeblich & Tappan (1988), Verga & Premoli Silva (2002), and Verga (2004).

The stratigraphic range of the identified species with radially elongated chambers and their relative abundance are plotted on fig. 3. We followed the zonation scheme proposed by Coccioni & Premoli Silva (1994) and modified according to the recent Early Cretaceous planktonic foraminiferal taxonomic concepts. The total organic carbon content (TOC) was also measured using a LECO IR-122 analyser at the University of P. and M. Curie of Paris.

## GEOLOGICAL AND PALEONTOLOGICAL FRAMEWORK

The thick, well exposed and tectonically little disturbed Lower Cretaceous Rio Argos succession is located in the frontal parts of the Subbetic Zone of the Betic Cordillera and crops out along the meandering Rio Argos and its tributaries west of

Caravaca, Province of Murcia, southeast Spain (Fig. 1). It encompasses the entire Berriasian-Upper Albian interval, except for a hiatus comprising the Upper Aptian-Middle Albian. Twenty-five parallel and partly overlapping sections (indicated with the letters A to Z) were measured whereby each bed was numered. The Rio Argos succession consists of a rather monotonous cyclic alternation of olive-grey marly micritic limestone beds and dark-grey, shaly marlstone interbeds (Fig. 2). Several slumped intervals occur in the succession. In the middle part of the Barremian strata, a few olisthostromes are intercalated. In the Upper Barremian and Aptian strata, distal siliciclastic turbidites are frequent. On account of these turbidites, 2 formations have been distinguished (van Veen, 1969): the Miravetes Formation without turbidites (from bed Z1 to V63) and Argos Formation with turbidites (from bed V63 upwards). The entire Lower Cretaceous Rio Argos succession was deposited within a basinal pelagic environment. Several paleoecological arguments suggest deposition in an upper bathyal paleoenvironment varying between 200 and 400 m: nektonic ammonites constitute 99% of the megafossil content (see Hoedemaeker, 1998). The ammonite fauna is dominated by phylloceratids, lytoceratids, haploceratids and desmoceratids. Such a domination characterized depths below 200 m (Ziegler, 1967). Besides frequent bioturbation, large *Zoophycos* feeding burrows are present throughout the succession. This so-called '*Zoophycos* ichnofacies' is commonly interpreted to indicate depths below the neritic environments (Pemberton *et al*., 1992). These depths are in accordance with the general scarcity of benthic megafossils and foraminifera. In conclusion, the depth of the sea was estimated to be in the order of 300-400 m (Hoedemaeker & Leereveld, 1995). Remarkably, the Rio Argos succession includes the uppermost Hauterivian Faraoni Level which is a $C_{org}$-rich stratigraphic interval recognised in several basins of the Mediterrranean Tethys as expression of a short-lived oxygen-deficient event (Baudin *et al*., 1999, 2002a, b). At Rio Argos, the 250 cm-thick Faraoni Level equivalent (beds 148 to 151 in section A) consists of three limestone beds sandwiched between marlstone layers (Company *et al*., 2003a, b). It corresponds to an important episode of organic-matter preservation (TOC up to 2.56%) (see Baudin *et al*., 2002b and unpublished data) and falls within the lower part of the *Mortilleti* Ammonite Subzone (Company *et al*., 2003a, b) (Fig. 2). A small positive excursion of $\delta^{13}C$ in carbonates which implies an episode of increased organic carbon storage in marine sedimemts is recorded associated with the Faraoni Level equivalent together with the first step in the extensive ammonite renewal that took place during the latest Hauterivian (Company *et al*., 2003a, b).

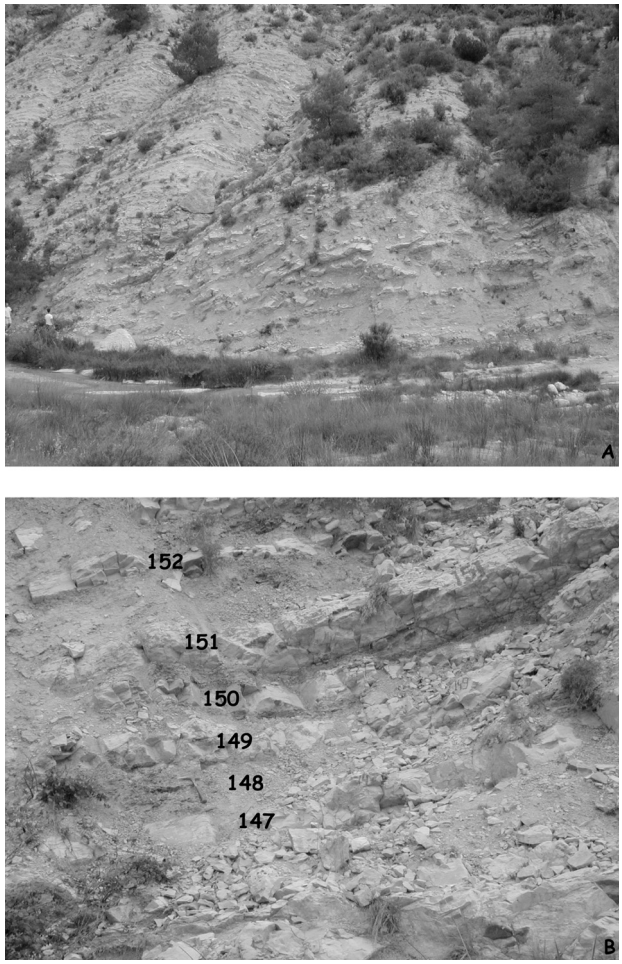


**Figure 2.** A) Typical alternation of Upper Hauterivian-Lower Barremian marls, marly limestones, and limestones at Rio Argos. B) The Faraoni Level equivalent (beds 148 to 151 according to Company *et al*., 2003a, b) at Rio Argos. Hammer as a scale.

## RESULTS

### PLANKTONIC FORAMINIFERAL ASSEMBLAGE COMPOSITION AND BIOSTRATIGRAPHY

The planktonic foraminifera observed in the Rio Argos sections are unevenly distributed throughout the succession. In the basal portion they are generally rare and occur in very few samples. Higher in the succession, from the Early Barremian Caillaudianus Ammonite Zone upward, they increase in abundance and diversity, and are more constantly present. However, poor assemblages composed of few specimens and species still occur up to the top, as do layers barren of planktonic foraminifera (see also Coccioni & Premoli Silva, 1994).

Several events and changes of assemblage composition, correlated to the ammonite zones, then to stages, were recognised in the studied interval. In particular, in stratigraphic order (see Fig. 3):

1) Through the Lower Hauterivian and lower part of the Upper Hauterivian, planktonic foraminifera occur in very few samples. Assemblages are very poor and comprised of small specimens (< 125

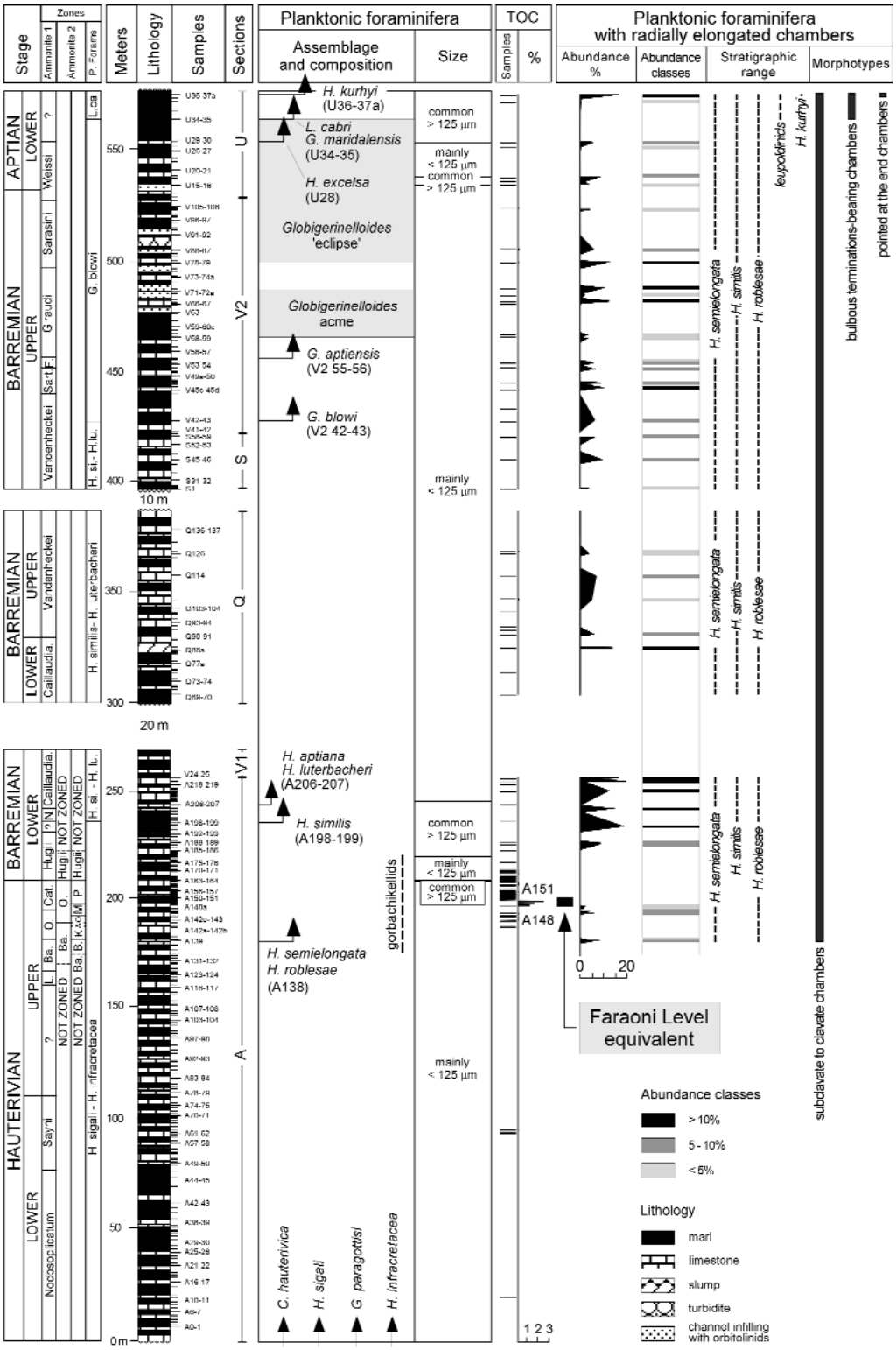


**Figure 3.** Lithostratigraphic log with sample numbers and ammonite and planktonic foraminiferal zonations of sections A, V1, Q, S, V2, and U (Lower Hauterivian-Lower Aptian) plotted against the planktonic foraminiferal assemblage and composition, TOC record, and stratigraphic distribution and relative abundance of the radially elongated chamber species at Rio Argos. Sections A, V1, S, and the lower part of Section V2 belong to the Miravetes Formation; the upper part of Section V2 (from sample V2 63) and Section U belong to the Argos Formation. The first elongated chambered morphotypes appear just below the Faraoni Level equivalent. In the uppermost Hauterivian-Lower Aptian several discrete intervals containing high proportions of radially elongated chambered forms were recognised. Ammonite zones: 1) Hoedemaeker (2002); 2) Company *et al*. (2003a, b). Planktonic foraminiferal zones modified after Coccioni & Premoli Silva (1994) and taking into account the taxonomic reorganization proposed by Verga (2004). Abbreviations: L. = *Ligatus*, Ba. = *Balearis*, O. = *Ohmi*, Cat. = *Catulloi*, N. = *Nicklesi*, Caillaudia. = *Caillaudianus*, Sart. = *Sartousiana*, F. = *Feraudianus*, B. = *Binelli*, K. = *Krenkeli*, A. = *Angulicostatus*, M = *Mortilleti*, P. = *Picteti*, H. si.-H. lu. = *Hedbergella similis - Hedbergella luterbacheri*, L. ca. = *Leupoldina cabri*. For discussion of data, see text.

μm) belonging to very few species (*Caucasella hauterivica*, *Globigerinelloides gottisi*, *Hedbergella infracretacea*, and *H. sigali*).

2) The first forms with radially elongated chambers (*Hedbergella roblesae*, *H. semielongata*) appear in sample A138 from the uppermost Hauterivian *Balearis* Ammonite Zone, *Binelli* Subzone. From here upward, assemblages with elongated chambers alternate with assemblages consisting of subglobular to globular chambered morphotypes.

3) Remarkably, *H. semielongata* and *H. roblesae* also occur just below (sample A138 from the top of the *Binelli* Ammonite subzones, samples A139 and A139-140 from the base of the *Binelli* Ammonite subzone, and samples A145, 146, and A147 from the *Omhi* Ammonite Zone, *Ohmi* Subzone) and at the very base (sample A148a) of the Faraoni Level equivalent.

4) High numbers of gorbachikellids occur in a discrete stratigraphical interval (samples A135 to A183) which includes the Faraoni Level equivalent.

5) The planktonic foraminiferal population displays a first increase in size (specimens frequently > 125 μm) in sample A163 from the *Ohmi* Ammonite Zone, *Picteti* Subzone. Remarkably, this faunal change occurs at the same time when, according to Company *et al*. (2003), an extensive ammonite renewal takes place and the increase in the proportion of wide-canal nannoconids reachs its climax.

6) In the lowermost Barremian, from the middle part to the *Hugii* Ammonite Zone trough the base of the *Caillaudianus* Ammonite Zone, the planktonic foraminiferal population shows a marked change demonstrated by an overall increase in abundance and in size (specimens frequently > 125 μm), by a better state of preservation and by the appearance of new species. In this interval, begin to appears *Hedbergella similis* (sample A198-199) and *Hedbergella aptiana* and *Hedbergella luterbacheri* (sample A206-207).

7) *Globigerinelloides blowi* and *Globigerinelloides aptiensis* first appear at the top of the *Vandenheckei* Ammonite Zone in the Upper Barremian (sample V2 42-43) and at the base of the *Giraudi* Ammonite Zone (sample V2 55-56), respectively. Representatives of the genera *Globigerinelloides* are particularly common in the middle part of the *Giraudi* Zone, identifying a *Globigerinelloides* acme.

8) The *Sarasini-Weissi* Ammonite zonal interval (uppermost Barremian-lowermost Aptian) is characterized by small size assemblages devoid of *Globigerinelloides* species, identifying a *Globigerinelloides* 'eclipse'. At the top of this interval, planktonic foraminifera increase in overall size. Moreover, *Hedbergella excelsa* first occurs (sample U28) followed by the first appearance of *Globigerinelloides maridalensis* and *Leupoldina cabri* in sample U34-35 and *Hedbergella kurhyi* in sample U36-37a.

In the Rio Argos succession seven species with radially elongated chambers were recognised. In order of appearance they are *Hedbergella semielongata* and *H. roblesae*, *H. similis*, *Leupoldina cabri*, *L. pustulans pustulans*, and *L. pustulans quinquecamerata*, and *H. kurhyi* (Pl. 1). Radially elongated chamber morphotypes increase in abundance (up to 16% of the entire assemblage) several times from the uppermost Hauterivian troughout the Lower Aptian (see Fig. 3). Higher numbers occur in the Lower Barremian (*Nicklesi* and *Caillaudianus* Ammonite Zones), in the Upper Barremian (*Sartousiana*, *Giraudi* and *Sarasini* Ammonite Zones) and in the Lower Aptian (*L. cabri* planktonic foraminiferal Zone). Based on the elongated chamber morphology we distinguished three morphological categories as follows: 1) subclavate to clavate chambers (*Hedbergella roblesae*, *H. semielongata*, and *H. similis*), 2) pointed at the end chambers (*H. kurhyi*)

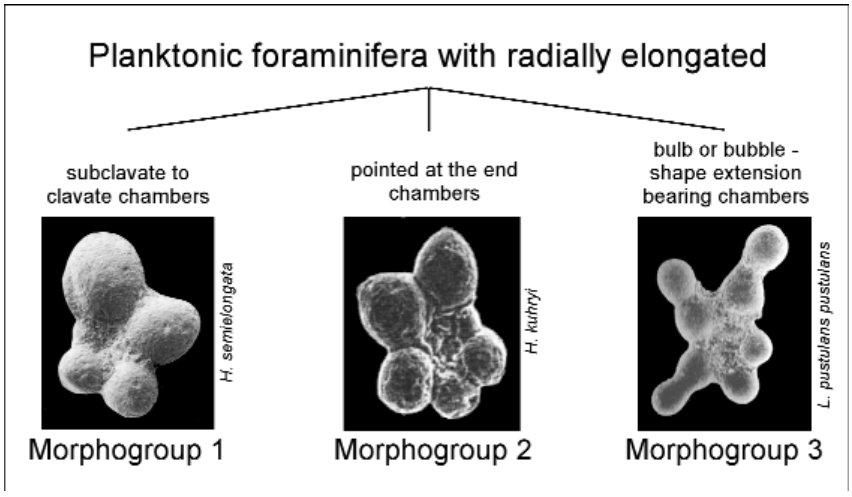


**Figure 4.** Morphogroups of Early Cretaceous planktonic foraminifera with radially elongated chambers recognised at Rio Argos.

and 3) bulbous terminations-bearing chambers (*Leupoldina cabri*, *L. pustulans pustulans* and *L. pustulans quinquecamerata*) (Fig. 4). The subclavate to clavate chamber morphotypes are the most representative in the studied interval with *Hedbergella semielongata* dominating in numbers. The pointed at the end chambers and bulbous terminations-bearing chambers morphotypes are present in the basal Aptian (*Leupoldina cabri* planktonic foraminiferal Zone) only (see Fig. 3). According to the biozonation of Coccioni & Premoli Silva (1994) and taking into account the taxonomic reorganization proposed by Verga & Premoli Silva (2002, 2003a, b) and Verga (2004), four planktonic foraminiferal zones have been identified within the studied interval (from bottom to top) (see Fig. 3):

1) *Hedbergella sigali - Hedbergella infracretacea* Zone (sample A0-1 to sample A197-198);

2) *Hedbergella similis - Hedbergella luterbacheri* Zone (sample A198-199 to sample to V2 41-42);

3) *Globigerinelloides blowi* Zone (sample V 42-43 to sample U29-30);

4) *Leupoldina cabri* Zone (sample U34-35 to sample U36-37a).

## ORGANIC CARBON AND RADIALLY ELONGATED CHAMBERED FORMS

Magniez-Jannin (1998) suggested a close relationship between the occurrence of planktonic foramifera with radially elongated chambers and the development of hypoxic conditions which she roughly estimated from the TOC content of the sediment.

Accordingly, the TOC content of several, selected samples from the studied succession was measured. TOC content values are generally very low ranging from 0 to 2.56%, the highest value occurring in the lowermost part the Faraoni Level equivalent (sample A148e) (see Fig. 3). For each sample, TOC content values were plotted against the percentage of planktonic foraminifera with radially elongated chambers (Fig. 5). No correlation between these parameters has been recognised.

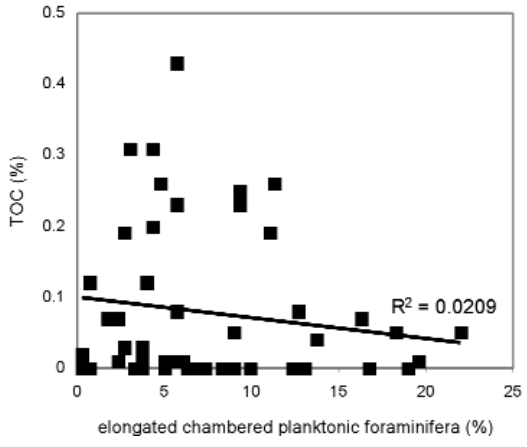


**Figure 5.** Dispersion diagram of TOC content against planktonic foraminifera with radially elongated chambers. No positive correlation is found between the TOC content and the abundance and occurrence of elongated chambered forms.

## DISCUSSION

According to some recent papers (BouDagher-Fadel *et al*., 1997; Magniez-Jannin, 1998; Aguado *et al*., 1999; Cobianchi *et al*., 1999; Luciani *et al*., 2001; Premoli Silva *et al*., 1999; Bellanca *et al*., 2002), the elongation of the chambers in Early Cretaceous foraminifera was probably associated with reduced oxygenation of the water column. In fact, if in a hypothetical marine scenario the seawater becomes dysoxic, more extrathalamous cytoplasm, capable of gas exchange with the seawater to maintain intake of sufficient quantities of oxygen for the metabolic needs of the planktonic foraminifera, would be needed. Therefore, the relative amount of extrathalamous cytoplasm had to be increased in other ways. One simple way of doing this would be to modify the chamber shape, reducing chamber-volume, elongating and flattening the chambers or both.

The paleoceanographic significance of planktonic foraminifera with "clavate" morphology is still ambiguous, however, these forms are also interpreted by Boersma *et al*., (1987), Premoli Silva & Sliter (1999), in analogy with Eocene hantkeninids, to inhabit at or near oxygen-depleted sea surface waters, where the warmth and oxygenation of surface waters permitted survival with a low test porosity. As reported in Bé (1965) and BouDagher-Fadel *et al*. (1997), recent planktonic foraminifera as *Globigerina* and *Hastigerina*, both with subglobular chambers live and float at or near the sea-surface waters. In contrast, *Beella* and *Hastigerinopsis*, which have radially elongated chambers are being found to inhabit deep waters environments. According to BouDagher-Fadel *et al*. (1997), during the Early Cretaceous the Praehedbergellidae with globular to subglobular chambers (e.g., *Blefluscuiana*, *Gorbachikella*, *Praehedbergella*) are interpreted to inhabit the most superficial waters. However, the praehedbergellids with radially elongated chambers (e.g., *Lilliputianella*, *Claviblowiella*, *Leupoldina*) are interpreted to have occupied both the lower, fully oxygenated waters as well as deeper waters with less oxygen, below the level of wave-air mixing and in which photosynthetic oxygenation also became much reduced.

At Angles (Vocontian Basin, southeastern France), elongated chambered morphotypes (*Clavihedbergella* sp., *C. eocretacea*, *Hedbergella similis*, and *Leupoldina cabri*) appeared on four occasions in the Lower Cretaceous succession either when dysoxic conditions prevailed in bottom and probaly in intermediate sea waters (Magniez-Jannin, 1998). Following Aguado *et al*. (1999), at Cau (southeastern

Spain), forms with radially elongated chambers (*Clavihedbergella saundersi*, *Leupoldina protuberans*, *Lilliputinalella bizonae*, *L. longorii*, *L. kuhryi*, *L. roblesae*, and *Schackoina cabri*) occur with high percentage across the Selli Level equivalent (Coccioni *et al*., 1987) which is the sedimentary record of the late Early Aptian Oceanic Anoxic Event (OAE) 1a (Arthur *et al*., 1990) that led to the widespread deposition of organic carbon ($C_{org}$)-rich sediments.

In the Coppitella and Le Batterie sections (Gargano Promontory, southern Italy), very rare to common elongated chambered specimens of *Clavihedbergella eocretacea*, *C. semielongata*, *Globigerinelloides cepedai*, *Hedbergella kuhryi*, *H. similis*, *Leupoldina. cabri*, and *L. pustulans* were found just below and just above the Selli Level equivalent which contains only few specimens of *C. eocretacea* (Cobianchi *et al*., 1999; Luciani *et al*., 2001).

In the Cismon core (southern Alps of Italy), the species occurring with some consistency throughout the Selli Level equivalent interval are hedbergellids and gorbachikellids/favusellids (Premoli Silva *et al*., 1999). However, a discrete leupoldinids-rich interval was identified above the base of the Selli Level equivalent. Higher in the Selli Level equivalent, leupoldinids seem to alternate with *Hedbergella similis*, and above the selli Level equivalent common leupoldinids occur along with *Hedbergella similis*, *Globigerinelloides cepedai* and *G. saundersi*, all with clavate chambers (Premoli Silva *et al*., 1999; Coccioni & Luciani, 2003).

According to Bellanca *et al*. (2002), at Calabianca (nortwestern Sicily, Italy), the planktonic foraminiferal assemblages from the Selli Level equivalent are dominated by clavate hedbergellids associated with rare leupoldinids alternating with normal faunal assemblages. However, the highest numbers of leupoldinids and clavihedbergellids were found above the Selli Level equivalent.

In the Rio Argos succession, only the very base of the $C_{org}$-rich Faraoni Level equivalent which was deposited under oxygen-depleted conditions contain some specimens of *Hedbergella semielongata*. Conversely, the planktonic foraminifera with radially elongated chambers are common to abundant just below and well above it. In addition, higher numbers of radially elongated chambered forms are even found in samples displaying lower values of TOC.

Remarkably, the radiation of radially elongated chambered morphotypes appears to have taking place at the same time as significant changes in the planktic ecosystem which appear to be related to sea-level changes and increase in primary productivity (see also Company *et al*., 2003).

At Gubbio (central Italy), high numbers of schakoinids occur just below and above the Bonarelli Level which is the sedimentary record of the latest Cenomanian OAE2 (Arthur *et al*., 1990) that led to the near-worldwide deposition of organic matter-rich sediments (Coccioni & Luciani, in press).

All these lines of evidence suggest that water oxygenation could not have been the only controlling factor governing the development of planktonic foraminifera with radially elongated chambers. Most likely an interplay of several influential factors (i.e., dissolved oxygen concentration, temperature, salinity, nutrients, trace elements) was responsible for such a morphological adaptation.

## SUMMARY AND CONCLUSIONS

The analysis of the planktonic foraminiferal assemblages from the Lower Hauterivian-Lower Aptian Rio Argos succession reveals the following:

(1) At different stratigraphic levels, planktonic foraminifera with radially elongated chambers became a consistent component of foraminiferal assemblages (up to 16% of the entire assemblage). Higher numbers occur in the Lower Barremian (*Nicklesi* and *Caillaudianus* Ammonite Zones), in the Upper Barremian (*Sartousiana*, *Giraudi*, and *Sarasini* Ammonite Zones) and in the Lower Aptian (*L. cabri* planktonic foraminiferal Zone).

(2) Based on last chambers morphology we distinguished three distinctive morphological categories as follow: 1) subclavate to clavate chambers, 2) pointed at the end chambers and 3) bulbous terminations-bearing chambers. The subclavate to clavate chamber morphotypes are the most abundant in the studied succession with the species *H. semielongata* dominating in numbers.

(3) The origin of the Cretaceous elongated chambered morphotypes occurs at the top of the uppermost Hauterivian *Binelli* Ammonite subzone of the *Balearis* Ammonite Zone and remarkably predates the short-lived oxygen-deficient event recorded by the Faraoni Level equivalent. In fact, close to this OAE occurred a new gradual diversification in planktonic foraminiferal evolutionary trend, with the first radiation of elongated forms (*H. semielongata*, *H. roblesae*) that occupied new ecological niches.

(4) Several lines of evidence and comparison with the patterns recognised at different stratigraphic levels and settings suggest that water oxygenation could not have been the only controlling factor governing the development of elongate chambers in Early Cretaceous planktonic foraminifera.

In fact, no correlation is found between the TOC content and the abundance of the elongated chambered forms. Most likely an interplay of several physical-chemical factors (i.e., dissolved oxygen concentration, temperature, salinity, nutrients, type of food, trace elements) was responsible for the development of such a morphological adaptation. Further investigations are still needed to understand this life strategy process.

**ACKNOWLEDGEMENTS**
We thank F. Baudin for courteously supply some samples from the Faraoni Level equivalent together with unpublished TOC data. The paper benefited greatly from the careful reviews of Malcolm B. Hart and Michael A. Kaminski. This research was financially supported by MIUR COFIN 2001 and MIUR ex 60% to RC.

**TAXONOMIC NOTES**
A short list of the most important synonyms for each species with radially elongated chambers is included.

Genus ***Leupoldina*** Bolli, 1957
***Leupoldina cabri*** (Sigal, 1952)
Plate 1, fig. 14

1952 *Schackoina cabri* Sigal, p. 20, text-fig 20.
1957 *Leupoldina protuberans* Bolli, p. 277, pl. 2, figs 2, 5-13, non figs 1, 3, 3a, and 4.
1974 *Leupoldina cabri* (Sigal). Longoria, p. 90, pl. 2, figs 1-12.
1994 non *Leupoldina cabri* (Sigal). Coccioni & Premoli Silva, p. 683, pl. 14, figs 15-16.
1995 *Leupoldina cabri* (Sigal). BouDagher-Fadel *et al*., p. 147, pl. 4, fig. 8, non fig. 9.
1997 *Schackoina cabri* Sigal. Bou-Dagher-Fadel *et al*., p. 185, p. 10.6, figs 8-9, 14, non figs 10-13.
1997 *Leupoldina protuberans* Bolli. BouDagher-Fadel *et al*., p. 184, pl. 10.6, figs 1-2, 6-7.
1998 non *Schakoina (Leupoldina) cabri* (Sigal). Moullade *et al*., p. 223, pl. 6, figs 9, 11-12.
1999 non *Schakoina cabri* Sigal. Aguado *et al*., p. 676, figs 9, 16-20.
2002 *Leupoldina cabri* (Sigal). Verga & Premoli Silva, p. 208, pl. 7, figs 1-12; p. 209, pl. 8, figs 1-6.
2004 *Leupoldina cabri* (Sigal). Verga, p. 7-9, figs 1.4.1-12, 1.5.1-6.

***Leupoldina pustulans pustulans*** Bolli, 1957
Plate 1, figs 15-16

1957 *Schackoina pustulans pustulans* Bolli, p. 274, pl. 1, figs. 1, 3, 3a, non figs 2, 4.
1957 *Leupoldina protuberans* Bolli, p. 277, pl. 2, figs 1, 3, 3a.
1974 *Leupoldina pustulans* (Bolli). Longoria, p. 90, pl. 3, figs 4-5, non fig. 3; pl. 8, non fig. 7.
1994 *Leupoldina pustulans* (Bolli). Coccioni & Premoli Silva, p. 663; pl. 14, figs 17-18.
1994 *Leupoldina cabri* (Sigal). Coccioni & Premoli Silva, p. 683, pl. 14, fig. 15-16.
1995 *Leupoldina protuberans* Bolli. BouDagher-Fadel, p. 148, pl. 4, figs 3-5.
1997 *Schackoina cabri* Sigal. BouDagher-Fadel *et al*., p. 185, pl. 10.6, figs 10, 12.
1997 *Leupoldina protuberans* Bolli. BouDagher-Fadel *et al*., p. 184, pl. 10.6, figs 3, 5.
1998 *Schakoina (Leupoldina) cabri* Sigal. Moullade *et al*., p. 223, pl. 6, figs 9, 11-12.
1999 *Leupoldina protuberans* Bolli. Aguado *et al*., p. 676, figs 9.9-15.
1999 *Leupoldina cabri* (Bolli). Aguado *et al*., p. 676, figs 9.16-20.
2002 *Leupoldina pustulans pustulans* Bolli. Verga & Premoli Silva, p. 204, pl. 4, figs 1-15; p. 206, pl. 5, fig. 1.
2004 *Leupoldina pustulans pustulans* Bolli. Verga, p. 9-10, figs 1.1.1-15, 1.2.1.

***Leupoldina pustulans quinquecamerata*** Bolli, 1957
Plate 1, fig. 17

1957 *Schackoina pustulans quinquecamerata* Bolli, p. 274, pl. 1, fig. 7a-b.
1957 *Leupoldina protuberans* Bolli, p. 277, pl. 2, fig. 4.
1997 *Schackoina cabri* Sigal. BouDagher-Fadel *et al*., p. 185, pl. 10.6, fig. 13.
1997 *Leupoldina protuberans* Bolli. BouDagher-Fadel *et al*., p. 184, pl. 10.6, fig. 4.
2002 *Leupoldina pustulans quinquecamerata* (Bolli). Verga & Premoli Silva, p. 206, pl. 5, figs 2-12; p. 207, pl. 6, figs 1-4.
2004 *Leupoldina pustulans quinquecamerata* (Bolli, 1957). Verga, p. 10, figs 1.3.1.

Genus ***Hedbergella*** Brönnimann & Brown, 1958
***Hedbergella kuhryi*** Longoria, 1974
Plate 1, figs 11-12

1974 *Hedbergella kuhryi* Longoria, p. 60, pl. 14, figs 1-6.
1988 *Lilliputianella kuhryi* (Longoria). Banner & Desai, p. 169, pl. 8, fig. 5.
1994 *Clavihedbergella eocretacea* Neagu. Coccioni & Premoli Silva, p. 699-670, fig 9. 16-18.
1995 *Lilliputianella kuhryi* (Longoria). BouDagher-Fadel, p. 144, pl. 4, figs 7.
1997 *Lilliputianella kuhryi* (Longoria). BouDagher-Fadel *et al*., p. 165, pl. 9.2, figs 7-10.

***Hedbergella roblesae*** (Obregòn de la Parra, 1959)
Plate 1, figs 9-10

1959 *Globigerina roblesae* Obregòn de la Parra, p. 149, pl. 4, figs 10-11.
1974 *Hedbergella roblesae* (Obregòn de la Parra). Longoria, p. 65-66, pl. 16, figs 1-3, 4-6; pl. 20, figs 10-11.
1974 *Hedbergella semielongata* Longoria, p. 66-68, pl. 21, figs 4-5.
1988 ?*Lilliputianella bizonae* (Chevalier). Banner & Desai, p. 168, pl. 7, figs 12, 15.
1994 *Clavihedbergella semielongata* (Longoria). Coccioni & Premoli Silva, p. 670-671, fig 9. 19-21, fig 10. 1-3.
1997 *Lilliputianella roblesae* (Obregòn de la Parra). BouDager-Fadel *et al*., p. 165-166, pl. 9.3, figs 1-7.
1999 *Lilliputianella roblesae* (Obregòn de la Parra). Aguado *et al*., figs 7. 13-21.
1999 *Lilliputianella bizonae* (Obregòn de la Parra). Aguado *et al*., figs 7. 22-24.
2004 *Hedbergella roblesae* (Obregòn de la Parra). Verga, p. 80-81, figs 9.3.1-10, 9.4.1-10.

***Hedbergella semielongata*** Longoria, 1974
Plate 1, figs 1-8

1974 *Hedbergella semielongata* Longoria, p. 66-68, pl. 20, figs 12-13; pl. 21, figs 1-3, non figs 4-5.

1975 *Clavihedbergella eocretacea* Neagu, p. 112-113, pl. 89, figs 1-2, 5-6, 9-10, non figs 3-4.
1993 non *Lilliputianella eocretacea* (Neagu). Banner *et al*., p. 15, pl. 6, figs 8.
1994 *Clavihedbergella eocretacea* Neagu. Coccioni & Premoli Silva, p. 669-670, fig 9. 10-15.
1997 *Lilliputianelloides eocretaceous* (Neagu). BouDagher-Fadel *et al*., p. 163, pl. 9.1, figs 1-4.
2004 *Hedbergella semielongata* Longoria. Verga, p. 81-82, figs 9.1.1-10, 9.2.1-8.

### ***Hedbergella similis*** Longoria, 1974
Plate 1, fig. 13

1971 *Clavihedbergella subcretacea* (Tappan). Gorbatchick, pl. 30(X), fig 3..
1974 *Hedbergella similis* Longoria, p. 68-69, pl. 16, figs 10-21, pl. 18, figs 12-13; pl. 23, figs 14-16.
1988 *Lilliputianella similis* (Longoria). Banner & Desai, p. 169-170, pl. 8, fig. 8, non fig. 9.
1993 non *Lilliputianella similis* (Longoria). Banner *et al*., p. 15, pl. 8, figs 8a-c.
1993 *Lilliputianella eocretacea* (Neagu). Banner *et al*., p. 15, pl. 6, figs 8.
1994 *Hedbergella similis* Longoria. Coccioni & Premoli Silva, p. 678-679, figs 13.1-3, non figs 13.4-9.
1997 *Lilliputianella globulifera* (Kretchmar & Gorbachik). BouDagher-Fadel *et al*., p. 165, pl. 9.2, figs 1-3.
2004 *Hedbergella similis* Longoria. Verga, p. 82-83, figs 9.9.4-10.

## REFERENCES


Aguado, R., Castro, J.M., Company, M. & de Gea, G.A., 1999. Aptian-bio-events - an integrated biostratigraphic analysis of the Almadich Formation, Inner Prebetic Domain, SE Spain. *Cretaceous Research*, **20**, 663-683.

Arthur, M.A., Brumsack, H.-J., Jenkyins, H.C., & Schlanger, S.O. 1990. Stratigraphy, geochemistry, and paleoceanography of organic carbon-rich Cretaceous sequences, In: Ginsburg, R. N., and Beaudoin, B. (eds.), *Cretaceous Resources, Events and Rhythms*. Kluwer Academic Publishers, 75-119.

Banner, F.T. & Desai, D. 1988. A review and revision of Jurassic-Early Cretaceous Globigerinina, with especial reference to the Aptian assemblages of Speeton (North Yorkshire, England). *Journal of Micropaleontology*, **7**, 143-185.

Banner, F.T., Copestake, P. & White, M.R. 1993. Barremian-Aptina Praehedbergellidae of the North Sea area: a reconnaissance. *Bulletin of the Natural History Museum*, Geology Series **49**, 1-30.

Baudin, F., Bulot, L.G., Cecca, F., Coccioni, R., Gardin, S. & Renard, M. 1999. Un équivalent du "Niveau Faraoni" dans le Bassin du Sud-Est de la France, indice possible d'un évenement anoxique fini-hauterivien étundu à la Téthys méditerranéenne. *Bulletin de la Societé Géologique de France*, **170**, 487-498.

Baudin, F., Cecca, F., Galeotti, S. & Coccioni, R. 2002a. Palaeoenvironmental controls of the distribution of organic matter within a Corg-rich marker bed (Faraoni level, uppermost Hauterivian, central Italy). *Eclogae Geologicae Helvetiae*, **95**, 1-13.

Baudin, F., Cecca, F., Gardin, S., Rafelis, M., Renard, M. & Coccioni, R. 2002b. L'évenément anoxique fini-Hauterivien (Niveau Faraoni) est-il-enregistré dans la Zone Sub-Bétique et en dehors de la Téthys méditerranéenne? *Documents du Laboratoire de Géologie de Lyon*, **156**, 30-31.

Bé, A.W.H. 1965. The influence of depth on shell growth in *Globigerinoides sacculifer* (Brady). *Micropaleontology*, **11**, 81-97

Bellanca, A. Erba, E., Neri, R., Premoli Silva, I., Sprovieri, M., Tremolada, F. & Verga, D. 2002. Palaeoceanographic significance of the Tethyan "Livello Selli" (early Aptian) from the Hybla Formation, northwestern Sicily; biostratigraphy and high-resolution chemostratigraphic records. *Palaeogeography, Palaeoclimatology, Palaeoecology*, **185**, 175-196.

Boersma, A., Premoli Silva, I. & Shackleton, N.J. 1987. Atlantic Eocene planktonic foraminiferal paleohydrographic indicators and stable isotope paleoceanography. *Paleoceanography*, **2**, 287-331

Bolli, H.M. 1957. The foraminiferal genera Schackoina Thalmann, emended and Leupoldina, n. gen. in the Cretaceous of Trinidad B.W.I. *Eclogae Geologicae Helvetiae*, **50**, 271-278.

BouDagher Fadel, M.K. 1995. The planktonic foraminifera of the Early Cretaceous of Tunisia compared to those of western and central Tethys. *Palaeopelagos*, **5**, 137-170

BouDagher Fadel, M.K., Banner, F.T. & Whittaker, J.E. 1997. *The Early Evolutionary History of Planktonic Foraminifera*. Chapman & Hall, England, 1-269.

Brönnimann, P. & Brown N.K. Jr. 1958. *Hedbergella*, a new name for a Cretaceous planktonic foraminiferal genus. *Journal of the Washington Academy of Sciences*, **48**, 15-17.

Cobianchi, M., Luciani, V. & Menegatti, A. 1999. The Selli Level of the Gargano Promontory, Apulia, southern Italy: foraminiferal and calcareous nannofossil data. *Cretaceous Research*, **20**, 255-269.

Coccioni, R. & Luciani, V. 2003. What happened to Cretaceous planktonic foraminifera during times of severe environmental stress?: case studies from the Selli (OAE1a, late Early Aptian) and Bonarelli (OAE2, latest Cenomanian) events. Bioevents: their stratigraphical records, patterns and causes. Caravaca de la Cruz, June 3rd-8th 2003, 98.

Coccioni, R. & Luciani, V. in press. Planktonic foraminifera and environmental changes across the Bonarelli event (OAE2, latest Cenomanian) in its type: a high-resolution study from the Tethyan reference Bottaccione section (Gubbio, central italy). *Journal of Foraminiferal Research*.

Coccioni, R. & Premoli Silva, I. 1994. Planktonic foraminifera from the Lower Cretaceous of Rio Argos sections (southern Spain) and biostratigraphic implications. *Cretaceous Research*, **15**, 645-687.

Coccioni, R., Nesci O., Tramontana, M., Wezel, F.C. & Moretti, E. 1987. Descrizione di un livello-guida "radiolaritico-bituminoso-ittiolitico" alla base delle Marne a Fucoidi nell'Appennino umbro-marchigiano. *Bollettino della Società Geologica Italiana*, **106**, 183-192.

Company, M., Aguado, R., Jimenez de Cisneros, C., Sandoval, J., Tavera J.M., & Vera J.A. 2003a. Biotic changes at the Hauterivian/Barremian boundary in the Mediterranean Tethys. Field-trip guide to agost (K/T) and Rio Argos (Hauterivian/Barremian) sections. Bioevents: their stratigraphical records, patterns and

causes. Caravaca de la Cruz, June 3rd-8th 2003, 15-28.
Company, M., Sandoval, J. & Tavera J.M. 2003b. Ammonite biostratigraphy of the uppermost Hauterivian in the Betic Cordillera (SE Spain). *Geobios*, **36**, 685-694.
Gorbatchik, T.N. 1971. On Early Cretaceous Foraminifera from Krimea. *Voprosy Mikropaleontologii,* **14**, 125-139. (In Russian, English abstract).
Hoedemaeker, P.J. 1995. Ammonite distribution around the Hauterivian-Barremian boundary along the Rio Argos (Caravaca, SE Spain). *Géologie Alpine, Mem. H.S.* n° 20 (1994), 219-277.
Hoedemaeker, P.J. 1998. Correlating the uncorrelatables: A Tethyan-Boreal correlation of pre-Aptian Cretaceous strata. In: Michalik, J. (ed.), *Tethyan/Boreal Cretaceous correlation*. Publishing House of the Slovak Academy of Sciences, Bratislava, 235-283.
Hoedemaeker, P.J. 2002. Correlating the uncorrelatables: A Tethyan-Boreal correlation of pre-Aptian Cretaceous strata. In: Michalik, J. (ed.), *Tethyan/Boreal Cretaceous correlation*. Publishing House of the Slovak Academy of Sciences, Bratislava, 235-283.
Hoedemaeker, P.J., & Leereveld, H. 1995. Biostratigraphy and sequence stratigraphy of the Berresian-lowest Aptian (Lower Cretaceous) of the Rio Argos succession, Caravaca, SE Spain. *Cretaceous Research*, **16**, 195-230.
Jenkyns, H.C. 1980. Cretaceous anoxic events from continents to oceans. *Journal of the Geological Society London*, **137**, 171-188.
Leereveld, H. 1997. Hauterivian-Barremian (Lower Cretaceous) dinoflagellate cyst stratigraphy of the western Mediterranean. *Cretaceous Research*, **18**, 421-456.
Lirer, F. 2000. A new technique for retrieving calcareous microfossils from lithified lime deposits. *Micropaleontology*, **46**, 365-369.
Loeblich, A.R. & Tappan, H. 1988. *Foraminifera genera and their classification*. Van Nostrand Reinhold Co., New York, 1-970.
Longoria, J.F. 1974. Stratigraphic, morphologic and taxonomic studies of Aptian planktonic foraminifera. *Revista Espanola de Micropaleontologia*, Numero Extraordinario, 5-107
Luciani, V., Cobianchi, M., & Jenkyns, H.C. 2001. Biotic and geochemical reponse to anoxic events: the Aptian pelagic succession of the Gargano Promontory (southern Italy). *Geological Magazine*, **138**, 277-298.
Magniez-Jannin, F. 1998. L'élongation des loges chez les foraminifères planctoniques du Crétacé inférieur: une adaptation à la sous-oxygénation des eaux? *C. R. Acad. Sci. Paris. Sciences de la terre et des planètes/Earth & Planetary Sciences*, **326**, 207-213.
Moullade, M., Tronchetti, G., Kuhnt, W., & Masse, J.P. 1998. Les Foraminifères benthiques et planctoniques du stratotype historique de l'Aptien infèrieur dans la region de Cassis - La Bedoule (SE France). *Géologie Méditerranéenne*, Tome XXV, 187-225.
Moullade, M., Bellier, J.-P., & Tronchetti, G. 2002. Hierarchy of creiteria, evolutionary process and taxonomic simplification in the classification of Lower Cretaceous planktonic foraminifera. *Cretaceous Research*, **23**, 111-148.
Neagu, T. 1975. Monographie de la faune des Foraminifères éocrétacés du coloir de la Dimbovicioara, de Codlea et des Monts Persani (Couches de Carhaga). *Memoires de l'Intitut de Géologie et Géophysique*, **25**, 1-141.
Obregón de la Parra, J. 1959. Foraminiferos de la Formación La Peña. *Boletin de la Asociation Mexicana de Geólogos Petroleros*, **11**(3-4), 135-154.
Pemberton, S.G., Maceachern, J.A. & Frey, R. W. 1992. Trace fossil/facies models: environmental & allostratigraphic significance. In: Walker, R.S., & James, W.P. (eds.), *Facies Models: Response to Sea Level Change*. St John's Geological Association of Canada, 47-72.
Premoli Silva, I. & Sliter, W.V. 1999. Cretaceous paleoceanography: Evidence from foraminiferal evolution. In: Barrera, E. & Johnson, C. (eds.), Evolution of the Cretaceous Ocean-Climate System. *Geological Society of American Special Pubblication,* **332**, 301-328
Premoli Silva, I., Erba, E., Salvini, G., Locatelli, S. & Verga, D. 1999. Biotic changes in Cretaceous oceanic anoxic events of the Tethys. *Cretaceous Research*, **29**, 352-370.
Rawson, P.F. 1996. The Barremian Stage. In: Rawson, P.F., Dhondt, A.V., Hancock, J.M., & Kennedy, W.J. (eds.), Proceedings of the Second International Symposium on Cretaceous Stage Boundaries. *Bulletin de l'institut Royal des Sciences Naturelles de Belgique*, **66**, 25-30.
Schlanger, S.P. & Jenkyins, H.C. 1976. Cretaceous oceanic anoxic events: causes and consequences. *Geologie en Mijnbouw*, **55**, 179-184.
Sigal, J. 1952. Aperçu stratigraphique sur la Micropaléontologie du Crétacé. *XIX Congrés Géologique International* (Série1), Alger, 26, 3-47.
Van Veen, G.W. 1969. *Geological investigations in the region of Caravaca, south-easter Spain*, Published Ph.D. Thesis, University of Amsterdam, 1-143.
Verga, D. & Premoli Silva, I. 2002. Early Cretaceous planktonic foraminifera from the Tethys: the genus *Leupoldina*. *Cretaceous Research*, **23**, 189-212.
Verga, D. & Premoli Silva, I. 2003a. Early Cretaceous planktonic Foraminifera from the Tethys. The small-sized representatives of the genus *Globigerinelloides*. *Cretaceous Research*, **24**, 305-334.
Verga, D. & Premoli Silva, I. 2003b. Early Cretaceous planktonic Foraminifera from the Tethys. The large, many-chambered representatives of the genus *Globigerinelloides*. *Cretaceous Research*, **24**, 661-690.
Verga, D., 2004. *The first evolutionary radiation of planktonic Foraminifera in the Valanginian-Aptian interval: taxonomical, biostratigraphycal and paleoecological implications*. PhD Thesis, Earth Sciences, University of Milan, Italy, 134 pp. (unpublished).
Ziegler, B. 1967. Ammoniten-Ökologie am Beispiel des Oberjura. *Geologische Rundschau*, **56**, 439-464.

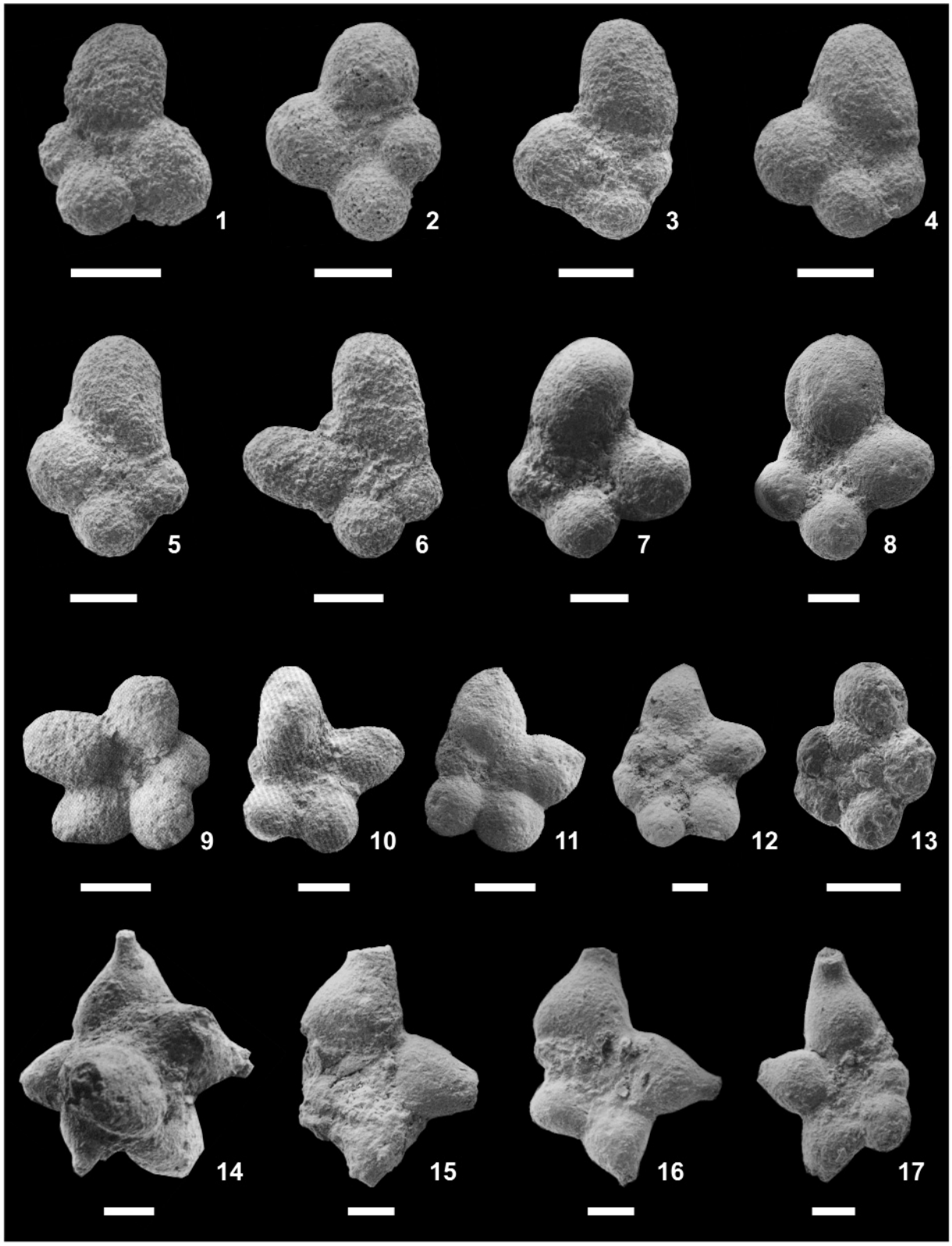


**PLATE 1**. Planktonic foraminifera with radially elongated chambers from the uppermost Hauterivian-Lower Aptian Rio Argos succession: 1. *Hedbergella semielongata*, sample A138; 2. *Hedbergella semielongata*, sample A145; 3. *Hedbergella semielongata*, sample A139; 4. *Hedbergella semielongata*, sample A139; 5. *Hedbergella semielongata*, sample A138; 6. *Hedbergella semielongata*, sample A138; 7. *Hedbergella semielongata*, sample A206-207; 8. *Hedbergella semielongata*, sample A207-208; 9. *Hedbergella roblesae*, sample U34-35; 10. *Hedbergella roblesae*, sample A207-208; 11. *Hedbergella kuhryi*, sample U36-37a; 12. *Hedbergella kuhryi*, sample U36-37a; 13. *Hedbergella similis*, sample A218-219; 14. *Leupoldina cabri*, sample U34-35; 15. *Leupoldina pustulans pustulans*, sample U34-35; 16. *Leupoldina pustulans pustulans*, sample U36-37a; 17. *Leupoldina pustulans quinquecamerata*, sample U36-37a. Scale bar = 100 μm.

# Middle Miocene Paleoceanography of the western Equatorial Atlantic Ocean (Leg 154, Site 926): evidence from benthic foraminifera

*ELISA GUASTI* [1]* *SILVIA IACCARINO*[2] *and TANJA KOUWENHOVEN*[3]
1. Department of Geosciences, Bremen University, P.O. Box 330 440, 28334 Bremen, Germany.
2. University of Parma, Parco Area delle Scienze, 43100 Parma, Italy
3. Utrecht University, Faculty of Geosciences, Utrecht, The Netherlands
* corresponding author; e-mail: eguasti@uni-bremen.de

**ABSTRACT**

Benthic foraminiferal data are presented of the Ceara Rise, ODP Leg 154, Site 926 in the western Equatorial Atlantic Ocean. The data cover part of the Middle Miocene: the time span between ~14.4 and ~8.8 Ma. During this period the Ceara Rise was, just as today, located at bathyal to abyssal water depths. Using benthic foraminiferal and geochemical data in combination with the preliminary benthic stable oxygen isotope data of Shackleton & Hall (1997) we reconstructed paleoceanographic changes and perturbations in the bottom-water environments. The abundance patterns of benthic foraminifera, notably *Nuttallides umbonifera*, *Cibicides wuellerstorfi* and *Astrononion pusillum* indicate cooling of the deep waters, and may constitute evidence of water masses of northern and southern provenance reaching the Ceara Rise in discrete periods during the course of the Middle Miocene. A series of oxygen isotopic excursions was reported during the Middle Miocene: so-called Mi-events, related to expansion of the Antarctic ice sheets. Of these Mi-events, we find the expression of Mi5 (astronomically calibrated at ~11.8-11.3 Ma in the Mediterranean) in our data as a period of perturbations of longer-lasting trends in the deep-water evolution. This period marks a prominent lithological transition at the Ceara Rise.

***keywords***. Middle Miocene, western equatorial Atlantic, benthic foraminifera, paleoceanography, water-mass distribution

## INTRODUCTION

The Middle Miocene is an important period in Cenozoic climatic and oceanographic evolution and is characterised by profound paleoenvironmental and paleogeographic change in the Atlantic and global oceanographic system.

During the Middle Miocene the transition probably occurred toward a thermohaline circulation system similar to the modern one (Woodruff & Savin, 1989; Roth *et al*., 2000; Nisancioglu *et al*., 2003). From the early Miocene, the Atlantic Ocean was mainly characterised by the influx of warm saline Tethyan Outflow Water (TOW: Woodruff & Savin, 1989; Ramsay *et al*., 1998) and by Northern Component Water (NCW: Wright & Miller, 1996; Ramsay *et al*., 1998). Circulation evolved toward dominance of the North Atlantic Deep Water (NADW), also related to the closure of America's central corridor (Woodruff & Savin, 1989; Roth *et al*., 2000; Nisancioglu *et al*., 2003). During the Middle Miocene, the paleoceanographic setting is also characterised by the intensification of the deep Southern Component Water (SCW, Flower & Kennett, 1994), in relation to the expansion of the Antarctic ice cap (Miller *et al*., 1991; Flower & Kennett, 1994).

The Middle Miocene geological record of some deep sea sites in the Atlantic ocean (South Atlantic: Hsü *et al*., 1984; Ceara Rise: King *et al*., 1997; Caribbean basin: Roth *et al*., 2000) and in the Pacific ocean (Lyle *et al*., 1995) is characterised by dissolution events, due to an increased input of Southern source corrosive pore/bottom waters and the relative shoaling of the lysocline.

Important events characterised the foraminiferal world during the Middle Miocene. In particular a turnover in the benthic fauna was described (Schnitker, 1980; Miller & Katz, 1987; Woodruff, 1992), with the occurrence of new species. The contrast between the water temperatures in the tropical and polar regions increased, together with the formation of a deep biotic provincialism (Flower & Kennett, 1994), evidenced mainly by planktonic foraminifera (Thunell & Belyea, 1982).

The importance of benthic foraminifera as tools to study the modern and past ocean is widely docu-

*In*: Coccioni R., Galeotti S., & Lirer F., (eds), 2004. Proceedings of the First Italian Meeting on Environmental Micropaleontology. *Grzybowski Foundation Special Publication*, 9, 49-62.

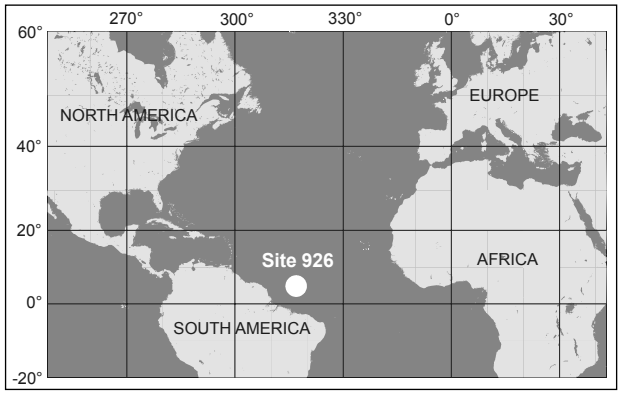


**Figure 1**. Location map of Site 926.

mented, above all to monitor deep water-mass circulation, oxygen variations of bottom waters and organic flux supply. Many studies reveal a close relationship between benthic foraminiferal assemblages and water masses, in relation with their chemical and physical characteristics (Lohmann, 1978; Miller & Katz, 1987; Woodruff & Savin, 1989; Iaccarino & Gaboardi, 1990; Boltovskoy *et al*., 1992; Smart & Ramsay, 1995; Yasuda, 1997; Schmiedl *et al*., 1997). Moreover, organic matter supply is one of the factors which exert important control on the distribution of benthic assemblages (Gooday, 1993; Loubère & Fariduddin, 1999; Van der Zwaan *et al*., 1999) Detailed studies of the assemblages allow a better understanding of the paleoproductivity system in the area.

The purpose of this study is to reconstruct the paleoceanographic features of the western Equatorial Atlantic Ocean, and improve the knowledge of the changes in deep-water circulation during the Middle Miocene. For this purpose we studied the benthic foraminiferal assemblages from Leg 154, Site 926 at the Ceara Rise. The continuity of the sedimentary record, and the richness of the well-preserved fauna together with the location along the corridor of the NADW and the AABW, render the Ceara Rise a suitable area for paleoceanographic reconstruction.

## MATERIAL AND METHODS

### *Geological and oceanographic setting*

During Ocean Drilling Program Leg 154, five Sites were drilled in the western equatorial Atlantic Ocean, along a transect from Site 925 at 3040 metres depth to Site 929 at 4355 metres depth. The Ceara Rise is an aseismic rise, which represents the conjugate of Sierra Leone Rise in the eastern Atlantic Ocean; it was formed at the Mid-Atlantic Ridge, about 80 Ma ago during a period of intensive volcanic activity (Shackleton *et al*., 1997). After its formation, it was affected by continuous subsidence and then covered by a thick sedimentary sequence of pelagic and siliceous sediments (Kumar & Embley, 1977). The area consists of a series of NW-SE oriented platforms, the tops of which reach about 3200 metres below sea level, surrounded by a seafloor at 4500 metres water depth. Due to the proximity of the North Brazilian coast, the area N, W and S-W of Ceara Rise is covered by Amazon fan deposits. At N-E and E, the Ceara abyssal plane is located, at 4500-4700 metres depth, which is characterised by a rough and irregular surface.

For this paper samples were studied from Site 926 (Fig. 1). Site 926 is the southernmost Site of Leg 154, at 343.15′ N, 4254.50′ W and is presently located on a plateau of 3598 metres deep. In the present-day oceanographic setting, surface waters at the Ceara Rise are represented by the North Equatorial Counter Current (NECC) and by the Northern Brazilian Current (NBC), which contribute to the transfer of saline warm waters from the Equatorial zone to the North Atlantic. The deep-water circulation at Ceara Rise is characterised by a northern source water mass, the North Atlantic Deep Water (NADW) and by a southern source water mass, the Antartic Bottom Water (AABW). At the present day the boundary of these currents at the Ceara Rise corresponds to the depth of the lysocline (Van Leeuwen, 1989) at about 4100 metres.

### *Lithology and age model*

The lithological record of Site 926 shows an evident sedimentary cyclicity, characterised by an alternation of marls and marly limestones with different contents of calcium carbonate. The interval from 310 mcd (metres composite depth) to 268 mcd is characterised by poorly bioturbated light marly limestones and dark, greenish-grey marls. In the whitish layers the carbonate content ranges from 70% to 90%, and from 5% to 30% in the greenish-grey layers (Fig.2). Within core 26, at 268 mcd, the greenish marls are substituted by brown-reddish marly layers. The interval from 268 to 226 mcd is characterised by whitish bioturbated carbonate-rich marls alternating with limestones and brown-reddish marls. The carbonate content in the whitish layers ranges from 70% to 90%, while in the brown-reddish layers it has a mean value of 50%.

The sedimentary cyclicity is well reflected by the magnetic susceptibility, colour and natural gamma ray emission (Curry *et al*., 1995; Turco *et al*., 2002). In particular susceptibility is characterised by the precessional cyclicity (Shackleton & Crowhurst, 1997). The magnetic susceptibility record has been used to establish an astronomical time scale for the last 14 Ma (0 to 2.5 Ma: Bickert *et al*., 1997; 2.5 to 5.0 Ma: Tiedemann & Franz, 1997; 5.0 to 14 Ma: Shackleton & Crowhurst, 1997). An accurate astrobiochronological time scale for the interval between 5 and 14 Ma has been provided by high-resolution calcareous nannofossil assemblages (Backman & Raffi, 1997). For the studied interval, a precise astronomical time

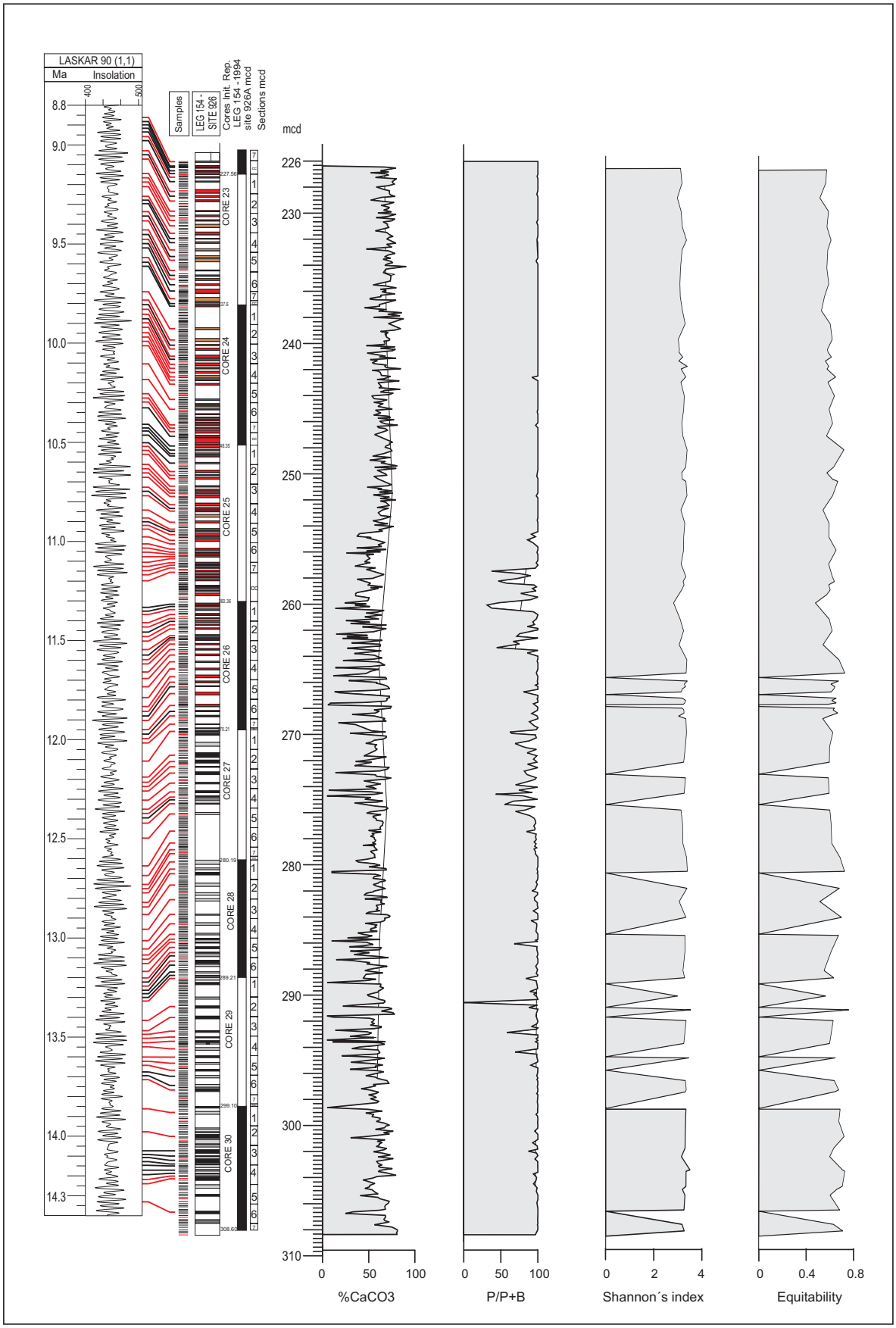


**Figure 2**. Carbonate content ($CaCO_3$ %) and Plankton/Benthos ratio (Turco *et al.*, 2002), Shannon´s index and equitability are plotted against the lithological record of Site 926. Lithological cycles are correlated to Northern Hemisphere summer insolation curve on the base of the astronomical tuning of Shackleton & Crowhurst (1997).

scale has been proposed by Shackleton & Crowhurst (1997), which allows estimation of an age of 14.45 to 8.86 Ma. Moreover, the astronomical time scale has been used to calibrate the calcareous plankton (foraminifera and nannofossils) bioevents (Turco *et al*., 2002).

***Sampling and benthic foraminifera***

Samples were studied from Site 926 between 226 and 310 mcd (metres composite depth), including cores 22 (926B-22H-5) to 30 (926A-30H-cc) for a total studied thickness of 83 metres (Fig. 2).

The cores have been sampled in the ODP Repository at Bremen, where 684 samples were collected with 10-20 cm sample spacing, and a temporal resolution of 10-21 Ky. Most of the samples were collected from Hole 926A; for some intervals samples have been collected from Hole 926B (226.58 to 227.53 mcd; 247.43 to 248.33 mcd; 258.14 to 260.40 mcd; and 269.98 to 270.27 mcd). Of these samples, 118 were used to study the benthic foraminifera.

First some 80 samples were studied with a sample spacing of 1 metre, to make an inventory of the events along the record. Considering biochronologically and paleoecologically important intervals, more samples were studied: one every 10 centimetres in cycles from 265.78 to 269.29 mcd and one every 20 centimetres in cycles from 240.88 to 243.39, from 249.92 to 251.02, and from 258.36 to 258.97 mcd. Additional samples were also counted in the greenish-dark layers (from 273.56 to 275.89 mcd, and from 285.87 to 308.2 mcd).

The samples were processed using standard laboratory procedures. They were washed in water and sieved into two size fractions (mesh sizes 63 μm and 125 μm). An Otto micro splitter was used to obtain a representative aliquot, preferentially containing 200-300 benthic foraminiferal specimens in the fraction >125 μm. These specimens were identified, counted and permanently stored in Chapman slides. Preservation of benthic foraminifera is generally very good in the whitish and reddish layers. Samples from greenish-grey layers are generally characterised by a scarcity or total absence of benthic foraminifera; specimens are usually very small, with a shell characterised by large pores, which may be related to dissolution.

Benthic foraminifera were identified at specific or supraspecific level. Some taxa have been classified at genus level, because they occur just as young specimens (*Lenticulina* spp., *Gyroidina* sp. 2) or because identification on basis of literature was uncertain (*Gyroidina* sp. 1, *Epistominella* sp.). Unilocular specimens of *Nodosariacaee* have been lumped in lagenids.

The percentage of planktonic species in the total foraminiferal association (%P) was calculated as 100*P/(P+B), in order to reconstruct paleodepth and track sea level changes. As %P is usually about 99%, this precludes a reconstruction of depositional depth as based on %P (see Van der Zwaan *et al*., 1990).

Relative frequencies of the taxa were calculated. The initial dataset, containing 95 taxa and all samples, was used to calculate Shannon's diversity index, and equitability (see Buzas & Gibson, 1969; Murray, 1991). Twenty samples contained less than 150 specimens, and have been excluded from further calculations. Subsequently, the dataset was condensed. We used taxa with relative frequency >4%, to perform hierarchical cluster analysis and principal component analysis, using standard SPSS statistical software. Taxa with lower relative frequencies were omitted from statistical analysis, because the signal would be obscured by too many taxa showing very minor variations in abundance over time. Statistical analysis has been performed considering samples from the whitish marls, discarding the greenish and reddish intervals, as we focus on capturing long-term trends, and not on differences between lithologies.

## RESULTS

***Benthic faunal trends***

A major faunal turnover is not observed at Site 926. The curves of the Shannon diversity index and equitability show a similar absence of any long-term trend (Fig.2). The record is, however, characterised by two main phases: from the bottom part of the record up to ~265 mcd the general and quite constant trend is interrupted by the occurrence of samples barren (or nearly barren) of benthic foraminifera; these samples are derived from the greenish-grey levels. In the upper part of the record, above 265 mcd, these barren or nearly barren intervals do not occur. This is coincident with a dominant change in lithology: the greenish marls are replaced by reddish layers intercalated in the light marls.

Some numerically important and representative taxa also show major trends. Taxa showing increasing abundances through time are for instance *Nuttallides umbonifera* and *Astrononion pusillum*. *N. umbonifera* presents an upwards increasing trend, with highest occurences of 19% at 259.7 mcd, 21.4% at 229.20 mcd, 13.8% at 240.88 mcd. *A. pusillum* shows very low abundances from the bottom of the record up to 268 mcd, where it increases quite instantaneously, reaching abundances exceeding 10% (12.3% at 267.01 mcd). The maximum abundance (14.5%) is at 241.46 mcd. This taxon does not occur between 266.13 mcd and 258.72 mcd.

In the middle part of the record, between 269 and 260 mcd, *Epistominella exigua, Epistominella* sp. and *Eponides pusillus* reach the highest abundances. *E. exigua* is one of the most abundant species of the assemblage, with highest occurrences between 270

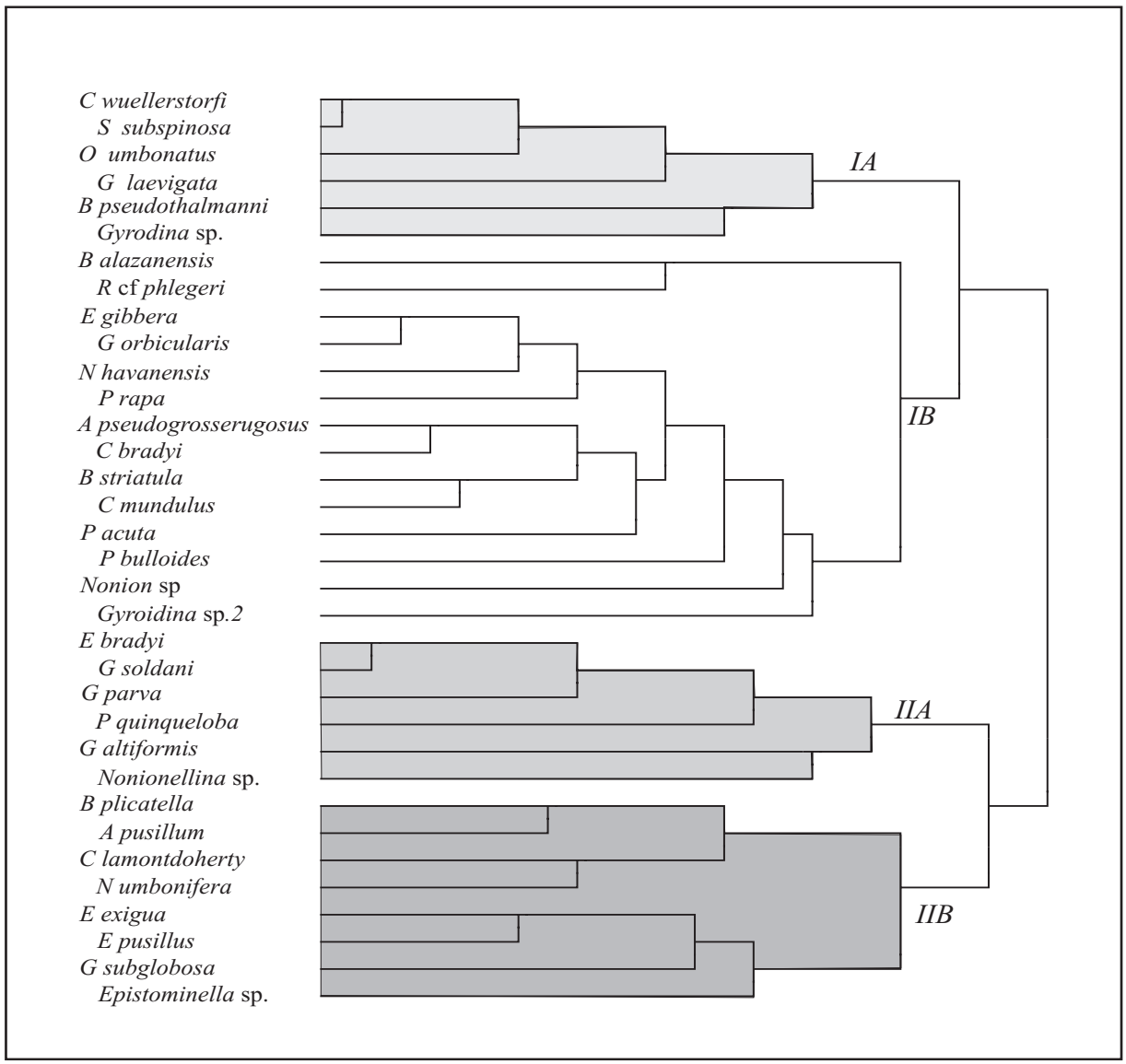


**Figure 3**. Dendrogram derived from hierarchical cluster analysis (within group, Pearson correlation) of relative frequency of 4% and more in the whitish levels. Two main groups and four clusters are indicated and discussed in the text.

and 260 mcd, and between 288 and 282 mcd. *Epistominella* sp. is quite abundant in the central part of the record with peaks of 4.3 % and 5.1% at 268.08 mcd and 261.62 mcd, while it is rare or absent in the uppermost and lowermost part. *Eponides pusillus* is nearly absent in the whole record, but it is relatively abundant in an interval between 255.33 and 277.40 mcd, with a maximum of 10.5% at 260.37 mcd.

Decreasing trends towards the top of the record are displayed by *Cibicides wuellerstorfi, Cibicidoides mundulus, C. bradyi,* and *Eggerella bradyi.* Moreover, *C. wuellerstorfi* shows its first occurrance at 306 mcd. Its abundance decreases upwards after a maximum of 17.4% at 290.62 mcd.

### *Statistical analysis*

Statistical analyses were performed on the samples taken from the whitish marls, which represent an undisturbed open marine environment, in order to capture the main faunal trends through time. The initial dataset was condensed, and only taxa were considered with percentages larger than 4% in any one sample. No new closed sum was calculated, in order to avoid overrepresentation of remaining taxa.

Hierarchical cluster analysis resulted in the dendrogram of Figure 3, which divides the species into two main groups, contained in clusters I and II. Cluster I groups species with a generally upwards decreasing trend (e.g., *Bulimina alazanensis*, *Cibicides wuellerstorfi*, *Cibicidoides bradyi*, *C. mundulus*, *Oridorsalis umbonatus*). Cluster II groups species with the opposite, upwards increasing trend (e.g., *Astrononion pusillum*, *Cibicidoides lamontdohertyi*, *Nuttallides umbonifera*). These clusters can be subdi-

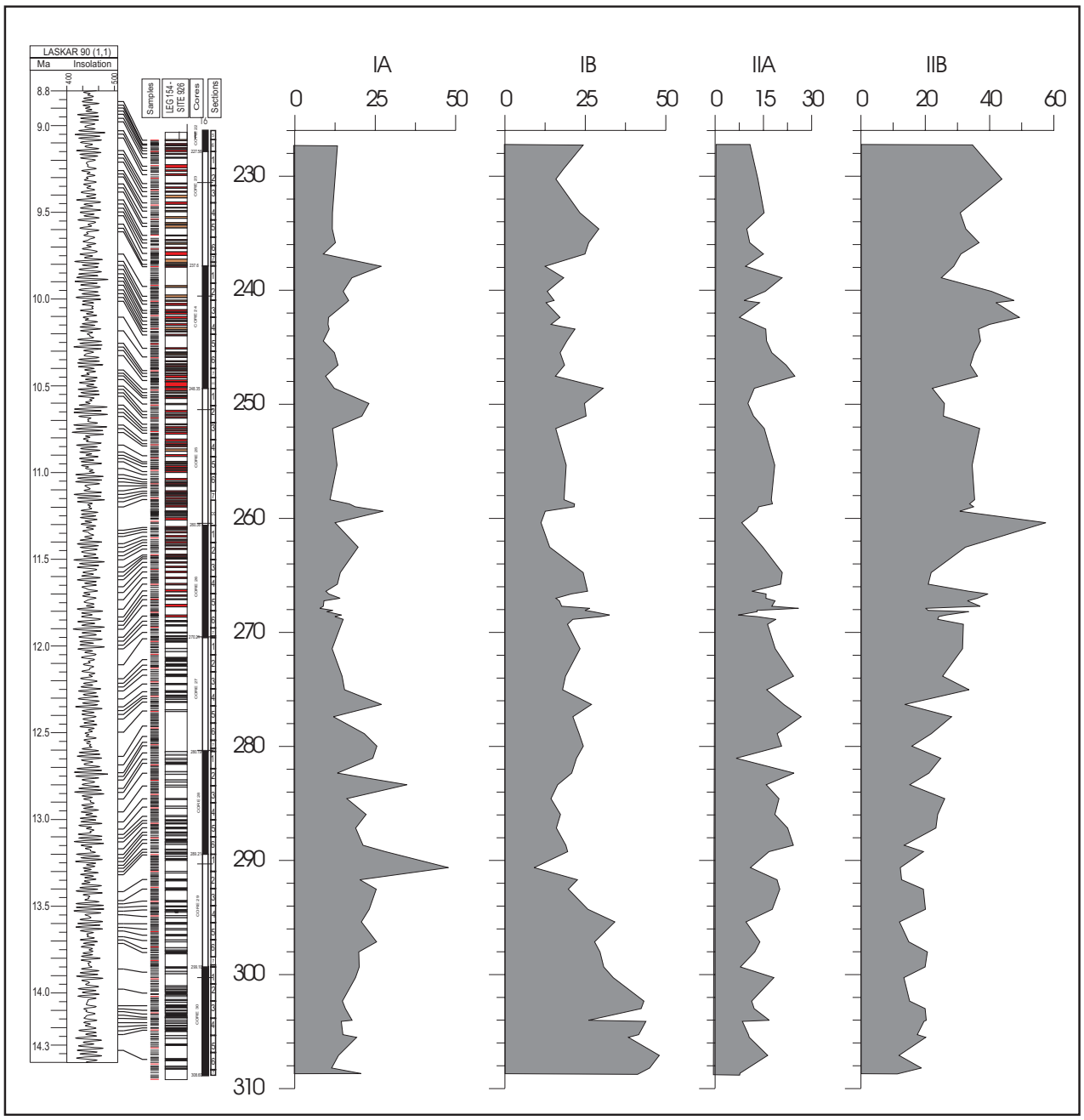


**Figure 4**. Relative frequencies of the four main clusters are summed and plotted against the lithological record.

vided into sub-clusters (IA, IB, IIA, IIB). *Eponides pusillus*, *Epistominella* sp. and *Epistominella exigua* are represented in sub-cluster IIB, together with *Globocassidulina subglobosa* (Fig. 3). The abundances of the species within the same sub-clusters have been summed and are graphically represented in Figure 4.

Using the same condensed dataset, a principal component analysis has been carried out (see Davis, 1976). The first axis (PCA1) explains 13.2% of the variance and is discussed here (Fig. 5). The PCA 1 curve has a general trend from positive values at the base toward negative values at the top of the studied interval. The transition from positive to negative values occurs in an interval from 270 to 259 mcd.

## DISCUSSION

### *Benthic faunal trends*

*General considerations and paleobathymetry*

The benthic assemblages of Site 926 consist of typical deep-sea mud dwelling faunas. As a whole, the assemblages do not reflect wide diversity fluctuations along the interval, and many important species, such as *Epistominella exigua*, *Nuttallides umbonifera*, *Globocassidulina subglobosa*, *Cibicides wuellerstorfi*, and *Oridorsalis umbonatus* occur throughout the record. Overall, benthic foraminifera indicate normal marine conditions, with exception of the dark greenish levels in the lower part of the record.

The assemblages represent a typical bathyal to abyssal environment (e.g., Van Morkhoven *et al*.,

1986; Iaccarino & Gaboardi, 1990; Rathburn & Corliss, 1994; Yasuda, 1997), based on taxa such as *C. wuellerstorfi*, *C. mundulus*, *N. umbonifera* and *E. exigua*. The assemblages recorded along the sequence show no wide variation in paleobathymetry. The reconstruction of depositional depth as based on %P indicates a paleodepth exceeding 1200 m, as in general %P exceeds 99% (see Van der Zwaan *et al*., 1990). Sea-level fluctuations will not be immediately apparent in benthic foraminiferal faunas at this depth. A constant subsidence related to cooling of the ocean crust after the formation of the Ceara Rise is not reflected in P/B ratios, or in the benthic faunas. Low %P values (around 50%) and low $CaCO_3$ content recorded in some intervals (from 296 to 286 mcd, from 278 to 270 mcd, and from 264 to 258 mcd), are probably due to dissolution and not to temporary shallowing (see also Turco *et al*., 2002).

*Dark and red levels*

Dark greenish-grey levels from Cores 30 to 27 are characterised by scarce residue, the scarcity or absence of benthic fauna and low calcium carbonate content. They occur mainly grouped in specific intervals, between 305 and 302 mcd, 290 and 286 mcd, and between 276 and 268 mcd. At the base of Core 26, at 268 mcd, the dark-greenish layers are gradually replaced by reddish layers. The first six red layers show the same characteristics as the greenish layers below. Within this group a single reddish layer occurs, which is rich in well-preserved fauna. Despite this one, the initial group of reddish layers is comparable to the greenish-grey levels in being very poor or barren of benthic fauna, and having a low calcium carbonate content.

Due to the scarcity and the bad preservation of the benthic fauna in the dark greenish layers, the P/B ratio values in these layers are not reliable. Benthic specimens are usually very small, often broken, and the wide pores on the tests indicate dissolution. This may be related to the rise of the lysocline by intensification of southern source deep water and/or to corrosive bottom/pore waters.

In some of the samples taken in these dark levels, it has been possible to find a certain number of specimens. The assemblage is generally formed by the same species that characterise the whole record, mainly *N. umbonifera*, *E. exigua*, *G. subglobosa*, *O. umbonatus*, and *Pullenia* spp.

Samples within the upper part of Core 26 and Cores 25 to 22 (265.52 – 226.25 mcd) show comparable features in the red and white levels: high amounts of washed residue and foraminifera. There is no clear evidence of dissolution, the tests of the benthic foraminifera are well preserved, not fragmented and the P/B ratio is always larger than 99%.

***Species distributions and conditions at the sea floor***

Many authors (e.g., Schnitker, 1980; Miller & Katz, 1987; Woodruff, 1992) describe a Middle Miocene benthic fauna turnover, characterised by the occurrence of new species still present in the modern ocean, as for instance *C. wuellerstorfi* (Miller & Katz, 1987). In the Pacific Ocean, this taxon evolved probably since 15.3 Ma according to Woodruff (1992) (and is present since the Oligocene according to Boltovskoy *et al*., 1992). This evolution precedes the most intensive period of Middle Miocene benthic turnover. At Site 926, *C. wuellerstorfi* appears to enter the record at 306 mcd, corresponding to an approximate age of 14.3 Ma. However, as 306 mcd is almost the base of the record, we cannot be certain that this level represents the true entry of *C. wuellerstorfi*. Our record of Site 926 probably postdates the major period of benthic faunal turnover of the Middle Miocene.

Although a major benthic faunal turnover is not recorded at Site 926, important shifts in species abundances do occur (Figs. 4, 5). An upward increasing abundance of *N. umbonifera* is evident. Lohmann (1978) interpreted the increasing relative abundance of this species to reflect low bottom-water temperatures related to AABW. The occurrence of *N. umbonifera* has also been related to corrosive (carbonate-undersaturated) bottom waters (e.g., Corliss, 1983; Woodruff, 1992; Mackensen, 1992; Yasuda, 1997; Schmiedl *et al*., 1997; Fariduddin & Loubère, 1997).

Decreasing abundances are displayed by taxa of cluster IB between 310 and 290 mcd and taxa of cluster IA between 290 and 270 mcd (Fig. 4). Of cluster IB, several taxa were related to raised organic flux, e.g., *C. bradyi*, *Bolivina striatula*, *Ehrenbergina gibbera*. Decreasing abundances of these taxa point to the development of more oligotrophic conditions, which is in line with the increasing abundance of taxa in cluster IA at the same time: *C. wuellerstorfi* (Mackensen *et al*., 1995) and *O. umbonatus* (Rathburn & Corliss, 1994) are related to more oligotrophic conditions. Moreover, the decrease of *C. wuellerstorfi* can also be attributed to a lowering of bottom-water temperatures (Lohmann, 1978).

The first Principal Component axis (PCA1) explains 13.2% of the variance in the data set. *C. wuellerstorfi* is one of the species that loads the axis prominently. The PCA1 curve is compared with the benthic foraminiferal $\delta^{18}O$ curve proposed by Shackleton & Hall (1997) for Site 926 (Fig. 5). Isotope analysis in 3 intervals (from 288 to 280 mcd, from 270 to 262 mcd and from 238 to 228 mcd) shows a more or less continuous upward increasing trend toward higher values. In the same interval the PCA1 curve shows a regular trend toward lower values. Together with the species patterns and the variation of the $\delta^{18}O$ of benthic foraminifera, this allows us to

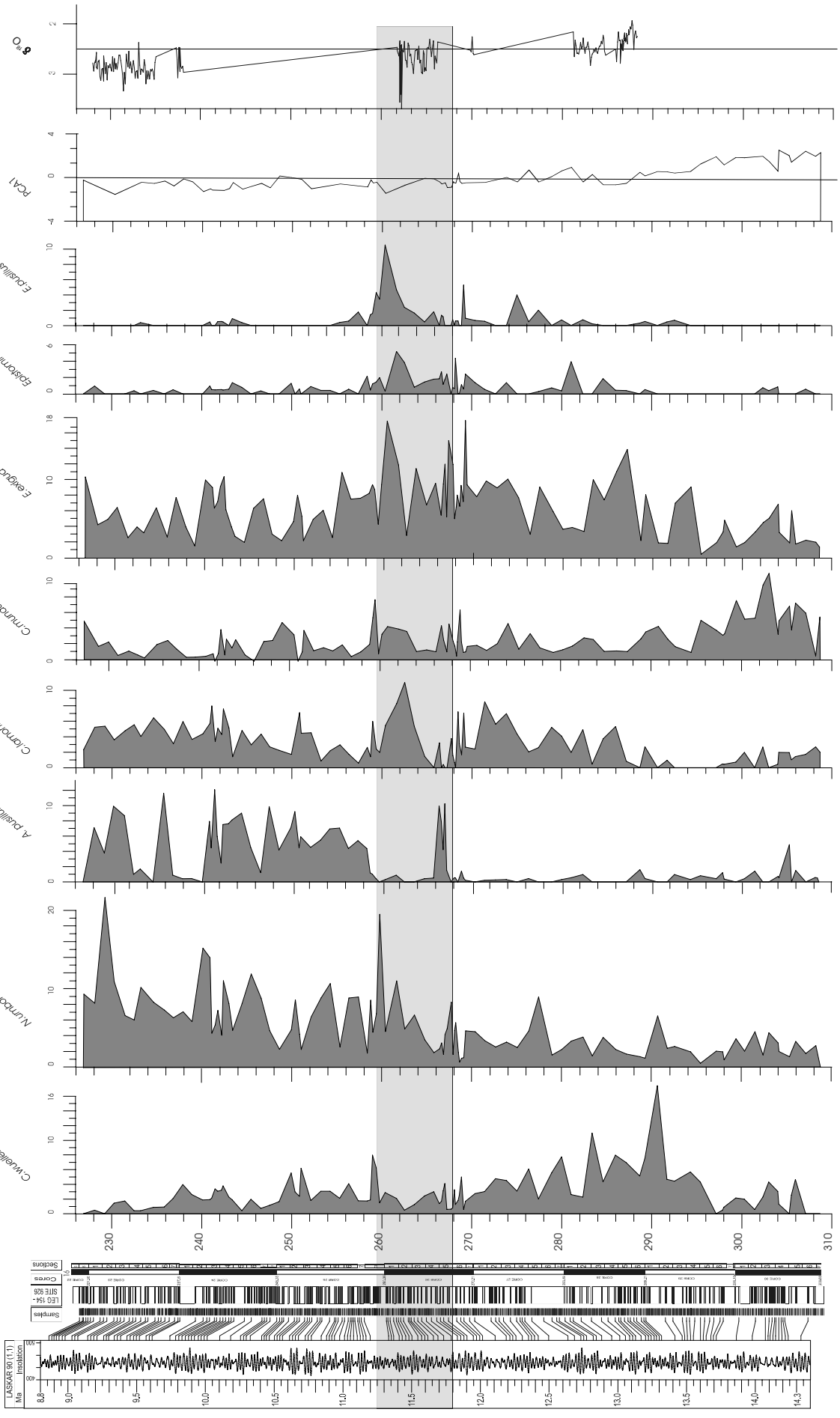


**Figure 5**. Sample score pattern on the first principal component (PCA1) plotted with the relative frequency data of the most abuntant taxa and the oxygen isotope record, derived from benthic foraminifera by Shackleton & Hall (1997).

interpret the PCA1 curve as temperature variation, that is, a decrease of the bottom-water temperature. This temperature decrease may be related to a general global cooling.

Between 270 and 260 mcd the conditions at the seafloor changed rapidly and repeatedly, as is evidenced by fluctuations in the relative frequency of *Astrononion pusillum*, and the temporary increase in the frequencies of *Epistominella* sp., *E. exigua*, and *Eponides pusillus*. The latter species have been related to a pulsed supply of organic matter to the sea floor (Gooday, 1993; Smart *et al*., 1994; Thomas & Gooday, 1996; Ohkushi *et al*., 2000). As food pulses are related to seasonal variations in surface water productivity, this would imply that the trophic regime in the waters overlying the Ceara Rise was characterised by increased seasonal contrast during this interval.

### *Species distributions and water masses*

*General considerations*

A relationship between the distribution of the benthic assemblages in the deep basins on the one hand and the water masses, with specific chemical and physical properties on the other is widely documented (Lohmann, 1978; Corliss, 1979; Kennett, 1982; Murray, 1984; Schnitker, 1984; Miller & Katz, 1987; Van Leeuwen, 1989; Iaccarino & Gaboardi, 1990; Woodruff, 1992; Woodruff & Savin, 1989; Boltovskoy *et al*., 1992; Smart & Ramsay, 1995; Yasuda, 1997; Schmiedl *et al*., 1997). According to many authors the distribution of benthic foraminifera is a useful tool to study the water mass changes over time and to recognize their corridors (e.g., Corliss, 1983; Iaccarino & Gaboardi, 1990; Yasuda, 1997). Considering the physical characteristics, a water mass is a relatively homogeneous body, characterised by conservative properties such as temperature, $\delta^{18}O$, and salinity, while other parameters such as oxygen, carbon dioxide, $\delta^{13}C$ and nutrient concentrations are less conservative properties and can be related to local environmental conditions (e.g., Broecker & Peng, 1982; Van Leeuwen, 1989). However, to correlate the faunal assemblages with environmental parameters is generally quite difficult (see also Murray, 1984, 1991). In the literature, the relation between some species and the deep water mass varies in relation with the studied area and the subjective interpretation of the authors. For instance *G. subglobosa* is related to AABW by Van Leeuwen (1989) and by Iaccarino & Gaboardi (1990), to NADW by Lohmann (1978), Corliss (1983), and by Yasuda (1997); *E. exigua* is related to AABW by Iaccarino & Gaboardi (1990) and to NADW by Boltovskoy *et al*. (1992), but more recently this taxon has also been related to phytodetritus input (Gooday, 1993; Schmiedl *et al*., 1997; Yasuda, 1997) and pulsed input of organic matter (Gooday, 1993; Smart *et al*., 1994; Thomas & Gooday, 1996; Ohkushi *et al*, 2000). *C. wuellerstorfi* is related to AABW by Iaccarino & Gaboardi (1990) and to NADW by Lohmann (1978), Corliss (1983) and by Boltovskoy *et al*. (1992). Fresh organic matter also influences the distribution of *C. wuellerstorfi* (e.g., Mackensen *et al*., 1993). Other species such as *B. alazanensis*, *Bolivinita pseudothalmanni* belong to the NADW according to Schmiedl *et al*. (1997).

*N. umbonifera* is related to carbonate undersaturated water of the AABW according to many authors (e.g., Lohmann, 1978; Corliss, 1983; Murray, 1984; Miller & Katz, 1987; Iaccarino & Gaboardi 1990; Woodruff, 1992; Mackensen, 1992; Yasuda, 1997). Woodruff (1992) relates C. *wuellerstorfi, C. kullenbergi* and *G. subglobosa* to the NADW.

Referring to Schnitker (1980), Murray (1984) considers different taxa characterising the NADW, depending on the zone. For instance, the deepest western part of the Atlantic ocean is characterised by the occurrence of *E. exigua*, the eastern part by *C. wuellerstorfi*; while the less deep waters are characterised by *Uvigerina peregrina* at both sides. In the studied interval, the abundance of *Uvigerina* spp. is generally quite low, probably due to the depth of the basin.

*The benthic assemblages of Site 926 and water masses*

Taking literature data into account (see previous section), many of the species present in the record of Site 926 can be related to either to NADW (or NCW) or to AABW (or SCW) or both, making this attempt at reconstruction quite complicated. Mackensen (1992) described late Middle to early Late Miocene assemblages from the Kerguelen Plateau and, comparing his data with those from Corliss (1983) concluded that the *N. umbonifera* assemblage was related to a carbonate-undersaturated, AABW-like water mass, and the *Astrononion pusillum* assemblage (including *C. wuellerstorfi* and *G. subglobosa*) to an aged, NADW-like water mass. Based on these occurrences the author dated the first NADW-like waters reaching Kerguelen Plateau around 11 Ma. Following this conclusion, it would appear that in the upper part of the record of Site 926 we see NCW reaching the Ceara Rise in a short period around 12 Ma, and more consistently, though frequently interrupted, after 11.2 Ma. Not in contrast with this, Wright *et al*. (1992) and Wright & Miller (1996) find evidence for a Northern Component water mass in the Atlantic from 12.5 Ma onwards. Their conclusion was based on Atlantic and Pacific $\delta^{13}C$ and $\Delta^{13}C$ data.

### *Antarctic glaciations and Mi-events*

Miller *et al*. (1991), Wright *et al*. (1992), and Flower & Kennett (1994) considered a number of Miocene oceanic events related to increasing $\delta^{18}O$ values: Mi-

events. The Mi-events were explained by phases of expansion of the Antarctic ice sheet (Miller *et al*., 1991; Wright *et al*., 1992; Flower & Kennett, 1994). The interval we studied is in part coeval with these expansions of the Antarctic ice sheet during the Miocene. Three of the so-called Mi-events fall within the time-span covered by our data: Mi 3, Mi 4, and Mi5 (dated at ~13.6 Ma, ~12.5 Ma, and ~11.2 Ma by Miller *et al*., 1991). In our data we can probably recognize one of these so-called Mi-events: the Mi5 (Fig. 5). In the PCA curve the transition from positive to negative values corresponds with an increase in the $\delta^{18}O$ values of Shackleton & Hall (1997). This interval might be related to the Mi5, calibrated by Turco *et al*. (2001) between 11.8 and 11.3 Ma at Monte Gibliscemi (Sicily). The base of the Mi5 corresponds to the transition from the grey-greenish layers to the red ones (~270 mcd). In this period we see several temporary shifts in species abundances (Fig. 5) that can be related to variations in deep-water characteristics. *Epistominella* sp., *E. exigua* and *Eponides pusillus* show maximum abundances. *C. wuellerstorfi* and *N. umbonifera* show opposite trends, and *A. pusillum* is nearly absent. These abundance patterns can be explained by a period of dominance of southern-source water masses reaching the Ceara Rise, associated with increased seasonal contrast. These phenomena may be related to the expansion of the Antarctic ice sheet.

## SUMMARY AND CONCLUSIONS

The benthic foraminiferal data of the Ceara Rise, Site 926 in the western Equatorial Atlantic Ocean, reflect changing paleoceanographic conditions in the time span between ~14.4 and ~8.8 Ma. These changes are probably related to the deep water masses reaching the Ceara Rise at lower bathyal to abyssal water depths, and to the expansion of the Antarctic ice sheet. The lithological alternation in the lower part of the record (~310-270 mcd) is characterised by intercalation of dark greenish layers showing low $CaCO_3$ contents and scarcity or absence of benthic foraminifera. Around 270 mcd the dark greenish layers are gradually replaced by reddish strata that contain well-preserved benthic foraminiferal faunas. The interval between ~270 and 260 mcd shows fluctuations in the benthic foraminiferal abundances that may be related to the Mi5 event. Following this event, the abundance patterns of *N. umbonifera*, *C. wuellerstorfi* and *A. pusillum* indicate cooling, and maybe water masses of mixed composition reaching the Ceara Rise. The Mi5 event, astronomically calibrated in Monte Gibliscemi (Sicily) as occurring between 11.8 and 11.3 Ma, is reflected in our data and corresponds to the transition from dark greenish to reddish marly strata intercalated in the lithology. During the same interval a period of increased seasonal contrast seems to occur. Over the whole period considered, the abundance patterns of *C. wuellerstorfi* and *N. umbonifera,* together with the increasing benthic $\delta^{18}O$ values indicate a temperature decrease.

## TAXONOMIC NOTES

***Anomalinoides pseudogrosserugosus*** (Colom, 1945)
*Anomalina pseudogrosserugosa* Colom, 1945, p.290, pl. 31, figs. 19-30.
*Anomalina pseudogrosserugosa* Colom. - Tjalsma 1983, p. 739, pl. 7, figs. 3a-4c.
*Anomalinoides pseudogrosserugosus* (Colom). - 1982, Atlas of foraminiferi Padani (Agip).

***Astrononion pusillum*** Hornibrook, 1961
*Astrononion pusillum* Hornibrook, 1961, p. 96, pl.12, figs. 229, 236.
*Astrononion pusillum* Hornibrook. - Mackensen, 1992, p. 670, pl. 2, figs. 11,12.

***Bolivina plicatella*** Cushman, 1939
cf. *Bolivina plicatella* Cushman, 1930, p. 46, pl.8 fig. 10a, b.

***Bolivina striatula*** Cushman, 1922
*Bolivina striatula* Cushman, 1922, pl. 3, pp. 43-44.

***Bolivinita pseudothalmanni*** Boltovskoy & Giussani de Kahn, 1981
*Bolivinita pseudothalmanni* Boltovskoy & Giussani de Kahn, 1981, p. 44.

***Bulimina alazanensis*** Cushman, 1927
*Bulimina alazanensis* Cushman, 1927, p. 161, pl. 25, fig. 4.
*Bulimina alazanensis* (Cushman). - Phleger, Parker & Peirson, 1953, p. 32, pl. 6, fig. 23.
*Bulimina alazanensis* (Cushman). - Tjalsma & Lohmann, 1983, p. 24, pl. 14, fig. 4.

***Cibicidoides bradyi*** (Trauth, 1918)
*Truncatulina bradyi* Trauth, 1918, p. 235.
*Cibicides bradyi* (Trauth). - Pflum & Frerichs, 1976, pl. 3, figs. 6, 7.
*Cibicidoides bradyi* (Trauth). - Miller & Katz, 1987, p. 135, pl. 7, figs.2a-c.

***Cibicidoides lamontdohertyi*** Miller & Katz, 1987
*Cibicidoides lamontdohertyi* Miller & Katz, 1987, pl. 9, figs. 1a-3c.

***Cibicidoides mundulus*** (Brady, Parker & Jones, 1888)
*Truncatulina mundula* Brady, Parker & Jones 1888, p. 228, pl. 45, figs. 25 a-c.
*Cibicidoides mundulus* (Brady, Parker & Jones). - Loeblich & Tappan, 1955, figs. 4a-c.

***Cibicides wuellerstorfi*** (Schwager, 1866)
*Anomalina wuellerstorfi* Schwager, 1866, vol. 2, p. 258, pl. 7, figs. 105, 107.
*Planulina wuellerstorfi* (Schwager). - Phleger, Parker & Peirson, 1953, p. 49, pl. 11, figs. 1, 2.

*Planulina wuellerstorfi* (Schwager). - Lohmann, 1978, p. 26, pl. 4, figs. 1-4.

***Eggerella bradyi*** (Cushman, 1911)
*Verneuilina bradyi* Cushman, 1911, p. 54, pl. 87, fig. 3.
*Verneuilina bradyi* Cushman. – Cushman, 1933, p.120, pl.12, fig. 5.
*Eggerella brady* (Cushman). - Phleger & Parker, 1951, p. 6, pl. 3, figs. 1, 2.
*Eggerella brady* (Cushman). – Miller, 1983, p. 435, pl. 5, fig. 5.

***Ehrenbergina gibbera*** Galloway & Heminway, 1941
*Ehrenbergina serrata* Reuss var. *gibbera* Galloway and Heminway 1941, p. 427, pl. 32, figs. 5a-d.
*Ehrenbergina gibbera* Galloway & Heminway. – Douglas, 1973, pl. 10, figs. 4, 5.
*Ehrenbergina gibbera* Galloway & Heminway. - Miller & Katz, 1987, p. 2, figs 5 a-b.

***Epistominella exigua*** (Brady, 1884)
*Pulvinulinella exigua* Brady, 1884, p. 696, pl. 103, figs. 13-14.
*Epistominella exigua* (Brady). - Phleger, Parker & Peirson, 1953, p. 43, pl. 9, fig. 35, 36.
*Epistominella exigua* (Brady). - Todd, 1965, p. 30, pl.10, fig.1.

***Eponides pusillus*** Parr 1950
*Eponides pusillus* Parr, 1950, p. 360, pl. 14, fig.16.
*Eponides pusillus* Parr. - Phleger, Parker & Peirson, 1953, p. 41, pl. 9, figs. 5, 6.
*Nuttallides pusillus pusillus* (Parr). - van Leeuwen R. J.W., 1989, pl. 14, figs. 4-12.

***Globocassidulina subglobosa*** (Brady, 1881):
*Cassidulina subglobosa* Brady, 1881, p. 60.
*Cassidulina subglobosa* Brady. - Brady, 1884, p. 430, pl. 54, fig. 17.
*Cassidulina subglobosa* (Brady). - Barker, 1960, p.112, pl. 54, fig.17.
*Globocassidulina subglobosa* (Brady). - Tjalsma & Lohmann 1983, p. 31, pl. 16, fig. 9.
*Globocassidulina subglobosa* (Brady). - Miller & Katz, 1987, pl. 3, fig. 4.

***Gyroidina altiformis*** R.E. & K.C. Stewart, 1930
*Gyroidina soldani* d'Orbigny var. *altiformis* R.E. & K.C. Stewart, 1930 p. 67, pl. 9, fig. 2.

***Gyroidina laevigata*** d'Orbigny, 1826
*Gyroidina laevigata* d'Orbigny, 1826, p. 278.
*Gyroidinoides laevigatus* (d'Orbigny). - Atlas of foraminiferi Padani (Agip), 1982, tav. XXXIX, fig. 7.

***Gyroidina orbicularis*** d'Orbigny, 1826
*Gyroidina orbicularis* d'Orbigny, 1826, p. 278, mod. 13.
*Gyroidina orbicularis* d'Orbigny. - Parker, Jones & Brady, 1865, pl. 3, fig. 85.
*Gyroidina orbicularis* d'Orbigny. - Loeblich & Tappan, 1964, p. C750, pl. 614, figs. 5, 6.

***Gyroidina parva*** Cushman & Renz, 1941
*Gyroidina parva* Cushman & Renz, 1941, p. 23, pl. 4, fig. 2.

***Gyroidina soldanii*** d'Orbigny, 1826
*Gyroidina soldanii* d'Orbigny, 1826, p. 278.
*Gyroidina soldanii* d'Orbigny. - Cushman, 1929, p. 38, pl. 8, figs. 3-8.
*Gyroidina soldanii* d'Orbigny. - Longinelli, 1956, pl. 14, figs. 16a, b.

***Nonion havanense*** Cushman & Bermudez, 1937
*Nonion havanense* Cushman & Bermudez, 1937, p. 19, pl. 2, figs. 13-14.
*Nonion havanense* Cushman & Bermudez. - Tjalsma & Lohmann, 1983, p. 17, pl. 7, figs. 6a-b.
*Nonion havanense* Cushman & Bermudez. - Miller & Katz, 1987, p.129, pl. 4, figs 7a-b.

***Nonionellina* sp.**
*Nonionellina* sp. 1987, Miller & Katz, p. 129, pl. 4, figs 1a-c.

***Nuttallides umbonifera*** (Cushman, 1933)
*Pulvinulinella umbonifera* Cushman, 1933, p. 90, pl. 9, fig. 9.
*Epistominella? umbonifera* (Cushman). - Phleger, Parker & Peirson, 1953, p. 43, pl. 9, figs. 33, 34.

***Oridorsalis umbonatus*** (Reuss, 1851)
*Rotalina umbonata* Reuss, 1851, vol. 3, p. 75, pl. 5, fig. 35.
*Oridorsalis umbonatus* (Reuss). - Wright, 1978, p. 716, pl. 6, figs. 15-19.

***Pleurostomella acuta*** Hantken 1875
*Pleurostomella acuta* Hantken, 1875, p. 44.
*Pleurostomella acuta* (Hantken). - Kaiho, 1991, p. 75, fig. 7, no. 11.

***Pleurostomella alternans*** Schwager, 1866
*Pleurostomella alternans* Schwager, 1866, p. 238, pl. 6, figs. 79, 80.
*Pleurostomella alternans* Schwager.- McFadyen, 1930, p. 63, pl. 1, figs. 25 a, b.
*Pleurostomella alternans* Schwager. - Christodolou, 1960, p. 57, pl. 7, figs. 30, 31.

***Pleurostomella rapa*** Gümbel, 1868
*Pleurostomella rapa* Gümbel, 1868, p. 630.
*Pleurostomella rapa* (Gümbel). - Atlas of foraminiferi Padani (Agip), 1982, tav. XXXVII, fig. 10.

***Pullenia bulloides*** (d'Orbigny, 1846)
*Nonionina bulloides* d'Orbigny, 1846, p. 107, pl. 5, figs. 9, 10.
*Pullenia bulloides* (d'Orbigny). - Dieci, 1959, p. 87, pl. 7, fig. 16.
*Pullenia bulloides* (d'Orbigny). - Christodolou, 1960, p. 56, pl. 2, figs. 11, 12.

***Rectuvigerina phlegeri*** Le Calvez, 1959
cf. *Rectuvigerina phlegeri*, Le Calvez, 1959, 23, p. 263, pl. 1, fig. 11.

**ACKNOWLEDGEMENTS**

E. Turco, F. Lirer, L. Foresi, F. Sgarrella, B. Russo, G. Bonaduce, R. Mazzei, G. Salvatorini and E. Vecchio are thanked for sampling the cores. F. Lirer and E. Turco are also thanked for the interesting discussions and for helping us in drawing the figures. G.J. van der Zwaan is thanked for his constructive suggestions. T. Bickert and T. Westerhold are thanked for the useful discussion. S. Heal is thanked for checking the English spelling and grammar. We are grateful to R. Sprovieri and an anonymous reviewer for their helpful and thoughtul reviews. This study was supported by the Italian Ministry of University and Scientific and Technologic Research (MURST) (COFIN98 to S. Iaccarino) and partly by the National Council of Research (CNR) (Contribution no. 98.00253.CT.05/115.07271 to S. Iaccarino).

**REFERENCES**

Agip, 1982. *Foraminiferi padani*. II Edizione. 52 Plates. AGIP Mineraria S.p.A., San Donato Milanese (Milano).

Barker, R.W. 1960. Taxonomic notes on the species figured by H. B. Brady in his Report on the Foraminifera dredged by H. M. S. Challenger during the years 1873-1876. S*ociety Ec Pal. and Min., Spec. Publ*. **9**.

Backman, J. & Raffi, I. 1997. Calibration of Miocene nannofossil events to orbitally-tuned cyclostratigraphies from Ceara Rise. *Proceedings of the Ocean Drilling Program, Scientific Results*, **154**, 179-217.

Bickert, T., Curry, W.B. & Wefer, G. 1997. Late Pliocene to Holocene (2.6-0 Ma) western equatorial Atlantic deep-water circulation: inferences from benthic stable isotopes. *Proceedings of the Ocean Drilling Program, Scientific Results*, **154**, 239-253.

Boltovskoy, E. & Giussani de Kahn, G. 1981. Cinco nuevos taxones en Orden Foraminiferida. *Hidrobiologia*, (Comun. Mus. Argent. C. Nat.), **2**(5), 43-51.

Boltovskoy, E., Watanabe, S., Totah, V.I. & Vera Ocampo, J. 1992. Cenozoic benthic bathyal foraminifers of DSDP Site 548 (North Atlantic). *Micropaleontology*, **38**(2), 183-207.

Broecker, W.S. & Peng, T.H., 1982. *Tracers in the sea*. Eldigio Press, 690 pp.

Brady, H.B. 1881. Notes on some of the reticularian *Rhizopoda* of the Challenger Expedition, Pt. 3, *Quart. J. Micr. Sci.*, **21**, London.

Brady, H.B. 1884. Report on the Foraminifera dredged by H.M.S. Challenger, during the years 1873-1876. In: Report on the Scientific Results of the Voyage of H.M.S. Challenger during the years 1873-1876. *Zoölogy*, **9**, 814 pp., London.

Brady, H.B., Parker, W.K. & Jones, T.R. 1888. On some foraminifera from the Abrohlos Bank. *Zool. Soc. Trans. London England*, **12**.

Buzas, M.A. & Gibson, T.G. 1969. Species diversity: Benthonic foraminifera in Western North Atlantic. *Science*, **163**, 72-75.

Christodolou, G. 1960. Geologische und mikropaläontologische Untersuchungen auf der Insel Karphatos (Dodekanesos), *Paläontographica, Abt. A*, **115**, 143 pp.

Colom, G. 1945. Notas sobre foraminiferos fósiles. *R. Soc. Española Hist. Nat. Bol*., **43**, 290 pp.

Corliss, B.H. 1979. Taxonomy of Recent deep-sea benthic foraminifera from the Southeast Indian Ocean. *Micropaleontology*, **25**(1), 1-19.

Corliss, B.H. 1983. Distribution of Holocene deep-sea benthonic foraminifera in the southeast Indian Ocean: inferred bottom-water routes and ecological implications. *Marine Geology*, **31**, 115-138.

Curry, W.B., Shackleton, N.J., Richter, C. & Bralower, T.J. 1995. *Proceedings of the Ocean Drilling Program, Initial Reports,* **154**, 1111 pp.

Cushman, J.A. 1911. A monograph of the Foraminifera of the North Pacific Ocean, Pt. 2: Textulariidae, *U. S. Nat. Mus. Bull*., **71**, 108 pp. Washington D.C.

Cushman, J.A. 1922. Shallow-water Foraminifera of the Tortugas region. *Carnegie Inst. Washington, Publ. No* **311** (Dept. Mar. Biol. Pap., 17), 1-85.

Cushman, J.A. 1927. Some characteristic Mexican fossil foraminifera. *Journal of Paleontology*, **1**.

Cushman, J.A. 1929. The Foraminifera of the Atlantic Ocean, Pt. 6: Miliolidae, Ophtalmidiidae and Fisherinidae, *U. S. Nat. Mus. Bull.* **104**.

Cushman, J.A. 1930. The Foraminifera of the Choctawhatchee Formation of Florida. *Florida State Geological Survey Bulletin.*, **4**.

Cushman, J.A. 1933. Foraminifera, their classification and economic use. *Cushman Laboratory Foraminiferal Research, Spec. Publ*., **4**, 349 pp.

Cushman, J.A. & Bermudez, P.J. 1937. Further new species of foraminifera from the Eocene of Cuba. Contr. *Cushman Laboratory Foraminiferal Research*, **13**.

Cushman, J.A. & Renz, H.H. 1941. New Oligocene-Miocene Foraminifera from Venezuela. *Contr. Cushman Laboratory Foraminiferal Research*, **17**(1), 1-27.

Davis, J.C. 1973. *Statistics and Data Analysis in Geology*. John Wiley & Sons, Inc., 646 pp.

Dieci, G. 1959. I foraminiferi Tortoniani di Montegibbio e Castelvetro. *Paleontographia Italica*, **54**, 113 pp.

d´Orbigny, A.D. 1826. Tableau méthodique de la classe des Céphalopodes. *Ann. Sci. Nat.* Paris, série 1, **7**, 245-315.

d´Orbigny, A.D. 1846 Foraminifères, in R. de la Sagra, Histoire physique, politique et naturelle de l'Île de Cuba. Atlas, 12 Pl.

Douglas, R. 1973. Benthonic foraminiferal biostratigraphy in the central North Pacific, Leg 17, DSDP. *Deep Sea Drilling Project, Initial Reports*, **17,** 591-695.

Flower, B.P. & Kennett, J.P. 1994. The middle Miocene climatic transition: East Antartic ice sheet development, deep ocean circulation and global carbon cycling. *Palaeogeography, Palaeoclimatology, Palaeoecology,* **108**, 537- 555.

Galloway, J.J. & Heminway, C.E. 1941. The Tertiary Foraminifera of Puerto Rico. *New York Acad. Sc.*, **3**, 431 pp.

Gooday, A.J. 1993. Deep-sea benthic foraminiferal species which exploit phytodetritus: Characteristic features and controls on distribution. *Marine Micropaleontology*, **22**, 187- 205.

Gümbel, C.W. 1868. Beiträge zur Foraminiferenfauna der nordalpinen Eocängebilde. *K. Bayer. Akad. Wiss. Abh.*, Cl.II, 10, Pt. **2**, 581-730.

Hantken, M. von 1875. Die Fauna der Clavulina Szabói

Schichten, Teil 1, Foraminiferen, Magy. Kir. Földt int. évkönyve, (Mitt. Jahrb. K. Ung. Geol. Anst.), **4**.

Hornibrook, N. de B. 1961. Tertiary Foraminifera from Oamaru District (N.Z.). *New Zealand Geological Survey. Paleontological Bulletin*, **34**(1), 194 pp.

Hsü, K.J., McKenzie, J.A. & Oberhänsli, A. 1984. South Atlantic Cenozoic Paleoceanography. *Deep Sea Drilling Project, Initial Reports,* **73**, 771-785.

Iaccarino, S. & Gaboardi, S. 1990. Deep Water benthic foraminifera in the Indian Ocean (ODP LEG 116). *Memorie della Societa´ Geologica Italiana* **44**, 145-155.

Kaiho, K. 1991. Global changes of Paleogene aerobic/anaerobic benthic foraminifera and deep-sea circulation. *Palaeogeography, Palaeoclimatology, Palaeoecology*, **83**, 65-85.

Kennett, J.P. 1982. *Marine Geology*. Prentice Hall. 813 pp.

Kennett, J.P. & Barker, P.F. 1997. Latest Cretaceous to Cenozoic climate and oceanographic developments in the Weddel Sea Antarctica: an ocean-drilling perspective. *Proceedings of the Ocean Drilling Program, Scientific Results*, **113**, 937- 960.

King, T.A., Ellis, W.G., jr., Murray, D.W., Shackleton, N.J. & Harris, S. 1997. Miocene evolution of carbonate sedimentation at the Ceara Rise: a multivariate data/proxy approach. *Proceedings of the Ocean Drilling Program, Scientific Results,* **154**, 117-134.

Kouwenhoven, T.J. 2000. *Survival under stress: benthic foraminiferal patterns and Cenozoic biotic crises*. Geologica Ultraiectina, **186**, 206 pp.

Kumar, N. & Embley, R.W. 1977. Evolution and origin of Ceara Rise: An aseismic rise in the western equatorial Atlantic. *Geological Society of America Bulletin*, **88**, 683-694.

Le Calvez, Y. 1959. Rec. Tranv. Inst. Peches Maritimes, **23**.

Loeblich, A.R. & Tappan, H. 1955. *Revision of some recent foraminiferal genera*. Smithsonian Institute Misc. Coll., Washington, D. C.

Loeblich, A.R. & Tappan, H. 1964. Sarcodina, chiefly "Thecamoebians" and Foraminifera. 1, 2, In: R. C. Moore (Ed.). *Treatise on Invertebrate Paleontology*, pt. C, Protista 2, The Geological Society of America and the University of Kansas Press.

Lohmann, G.P. 1978. Abyssal benthonic foraminifera as hydrographic indicators in the Western South Atlantic Ocean. *Journal of Foraminiferal Research*, **8**(1), 6-34.

Longinelli, A. 1956. Foraminifera del Cambriano e Piacenziano di Rosignano marittimo e della Val di Cecina, *Paleontographia Italica*, nov. ser., **19**: 116 pp.

Loubère, P. 1997. Benthic foraminiferal assemblage formation, organic carbon flux and oxygen concentrations on the outer continental shelf and slope. *Journal of Foraminiferal Research*, **27**(2), 93- 100.

Loubère, P. & Fariduddin, M. 1999. Benthic Foramnifera and the flux of organic carbon to the Seabed; in Sen Gupta, B.K. (Ed.). *Modern Foraminifera*. Kluwer Academic Publishers: 161-179.

Lyle, M., Dadey, K.A., & Farrell, J.W. 1995. The late Miocene (11-8 Ma) eastern Pacific carbonate crash: evidence for reorganization of deep-water circulation by the closure of Panama Gateway. *Proceedings of the Ocean Drilling Program, Scientific Results*, **138**, 821-838.

Mackensen, A. 1992. Neogene benthic foraminifers from the southern Indian Ocean (Kerguelen Plateau): biostratigraphy and paleoecology. *Proceedings of the Ocean Drilling Program, Scientific Results*, **120**, 649-673.

Mackensen, A., Hubberten, H.W., Bickert, T., Fischer, G. & Fütterer, D.K 1993. The $\delta^{13}C$ in benthic foraminiferal tests of *Fontbotia wuellerstorfi* (Schwager) relative to the $\delta^{13}C$ of dissolved inorganic carbon in Southern Ocean deep water: implications for glacial ocean circulation models. *Paleoceanography*, **8**(5), 587-610.

Mackensen, A., Schmiedl, G., Harloff, J. & Giese, M. 1995. Deep-sea foraminifera in the South Atlantic Ocean: Ecology and assemblage generation. *Micropaleontology*, **41**(4), 42- 358.

MacFadyen, W.A. 1930. *Miocene Foraminifera from the clysmic area of Egypt and Sinai Egypt*, Geological Survey, Cairo.

Miller, K.G. 1983. Eocene- Oligocene paleoceanography of the deep Bay of Biscay: benthic foraminiferal evidence. *Marine Micropaleontology*, **7**, 403-440.

Miller, K.G & Katz M.E., 1987. Oligocene to Miocene benthic foraminiferal and abyssal circulation changes in the North Atlantic. *Micropaleontology*, **33**(2), 97-149.

Miller, K.G., Wright, J.D. & Fairbanks, R.G. 1991. Unlocking the Ice House: Oligocene- Miocene Oxygen Isotopes, Eustasy and Margin Erosion. *Journal of Geophysical Research*, **96** (B4), 6829- 6848.

Murray, J. with contribution of Weston, J.F. 1984. Paleogene and Neogene Benthic Foraminifers from Rockall plateau. *Deep Sea Drilling Project, Initial Reports*, **81**, 503- 534.

Murray, J.W. 1991. *Ecology and palaeoecology of benthic foraminifera*. Longman Scientific & Technical, England, 397 pp.

Nisancioglu, K.H., Raymo, M.E. & Stone, P.H. 2003. Reorganization of Miocene deep water circulation in response to the shoaling of the Central American Seaway. *Paleoceanography*, **18**(1), 1-12.

Ohkushi, K., Thomas, E. & Kawahata, H. 2000. Abyssal benthic foraminifera from the northwestern Pacific (Shatsky Rise) during the last 298 kyr. *Marine Micropaleontology*, **38**, 119-147.

Parker, W.K., Jones, T.R. & Brady, H.B. 1865. On the nomenclature of the Foraminifera. Pt. 12: The species enumerated by d´Orbigny in the "Annales des Sciences Naturelles", 7, 1826, *Annals and Magazine of Natural History*, ser. 3, **16**, 15-41.

Parr, W.J. 1950. *Foraminifera*. B: A.N.Z. Antartic Reserch Expedition 1929- 1931. Repts. Adelaide, **5**, 360 pp.

Pflum, C.E. & Frerichs, W.E. 1976. Gulf of Mexico deep-water foraminifers. *Cushman Foundation Foraminiferal Research*, Spec. Publ., **14**, 1-125.

Phleger, F.P. & Parker, F.L. 1951. Ecology of Foraminifera Northwest Gulf of Mexico. *Geological Society of America Mem*. New York, **46**, 64 pp.

Phleger, F.P., Parker, F.L. & Peirson, J.F. 1953. North Atlantic Foraminifera. Rep. Swedish Deep Sea Exped., Vol. VII, Sediment cores from the North Atlantic Ocean, Mar. For. Lab., Scripps Inst. Ocean., California.

Ramsay, A.T.S., Smart, C.W. & Zachos, J.C. 1998. A model of early to middle Miocene deep Ocean circulation for the Atlantic and Indian Oceans. *Geological Society of London*, Special Publications, **131**, 55- 70.

Rathburn, A.E. & Corliss, B.H. 1994. The ecology of

living (stained) deep-sea benthic foraminifera from the Sulu Sea. *Paleoceanography,* **9** (1), 87-150.

Reuss, A.E. 1851. Über die fossilen Foraminiferen und Entomostraceen des Septarientonen der Umgegend von Berlin, *Deutsch. Geol. Gesellsch. Zeitschr*., **3**, 49-91.

Roth, J.M., Droxler, A.W. & Kameo, K. 2000. The Caribbean carbonate crash at the middle to late Miocene transition: linkage to the establishment of the modern global conveyor. *Proceedings of the Ocean Drilling Program, Scientific Results*, **165**, 249-273.

Schmiedl, G., Mackensen, A. & Muller, P.J. 1997. Recent benthic foraminifera from the eastern South Atlantic Ocean: dependence on food supply and water masses. *Marine Micropaleontology*, **32**, 49-287.

Schnitker, D. 1980. Global Paleoceanography and its Deep Water Linkage to the Antartic Glaciation. *Earth Science Reviews*, **16**, 1- 20.

Schnitker, D. 1984. High resolution records of benthic foraminifers in the late Neogene of the Northeastern Atlantic, *Deep Sea Drilling Project, Scientific Results*, **81**, 611- 622.

Schwager, C. 1866. Fossile Foraminiferen von Kar-Nicobar, Novara Exp., 1857-1859. Geol. Theil, **2**, 187-268.

Shackleton, N.J. & Crowhurst, S. 1997. Sediment fluxes based on an orbitally tuned time scale 5 Ma to 14 Ma, site 926. *Proceedings of the Ocean Drilling Program, Scientific Results*, **154**, 69-82.

Shackleton, N.J. & Hall, M.A. 1997. The late Miocene stable isotope record, Site 926. *Proceedings of the Ocean Drilling Program, Scientific Results*, **154**, 367-374.

Shackleton N.J., Curry, W.B., Richter C. & Bralower T.J. 1997. Shipboard Scientific Party. *Proceedings of the Ocean Drilling Program, Scientific Results*, **154**, 532 pp.

Smart, C.W. & Ramsay, A.T.S. 1995. Benthic foraminiferal evidence for the existence of an early Miocene oxygen- depleted oceanic water mass? *Journal of the Geological Society*, London, **152**, 735- 738.

Smart, C.W., King, S.C., Gooday, A.J., Murray, J.W. & Thomas, E. 1994. A benthic foraminiferal proxy of pulsed organic matter paleofluxes. *Marine Micropaleontology*, **23**, 89-99.

Stewart, R.E. & Stewart, K.C. 1930. Post- Miocene foraminifera from the Ventura Quadrangle, Ventura County, *Journal of Paleontology*, **4**(1).

Thomas, E. & Gooday, A.J. 1996. Cenozoic deep-sea benthic foraminifers: Tracers for changes in oceanic productivity? *Geology*, **24**(4), 355-358.

Thunell, R. & Belyea, P. 1982. Neogene planktonic foraminiferal biogeography of the Atlantic Ocean. *Micropaleontology*, **28**(4), 381- 398.

Tiedemann, R. & Franz, S.O. 1997. Deep- water circulation, chemistry, and terrigenous supply in the equatorial Atlantic during the Pliocene, 3.3- 2.6 Ma and 5-4.5 Ma. *Proceedings of the Ocean Drilling Program, Scientific Results*, **154**, 299-318.

Tjalsma, R.C. 1983. Eocene to Miocene benthic foraminifera from DSDP Site 516 Rio Grande Rise, South Atlantic. *Deep Sea Drilling Project, Initial Reports*, **72**, 731-755.

Tjalsma, R.C. & Lohmann, G.P. 1983. Paleocene-Eocene bathyal and abyssal benthic foraminifera from the Atlantic Ocean. *Micropaleontology* Special Publication, **4,** i-iii, 1-90.

Trauth, F. 1918. Das Eozänvorkommen bei Radstadt im Pongau und seine Beziehungen zu den gleichalteringen Ablagerungen beu Kirchberg am Wechsel und Wimpassing am Leithagebirge. *Denkschr. K. Akad. Wissensch. Wien, Math. –Nat. Cl.*, **95**, 171-278.

Turco, E., Hilgen, F.J., Lourens, L.J., Shackleton, N.J. & Zachariasse, W.J. 2001. Punctuated evolution of global climate cooling during the late Middle to early Late Miocene: High- resolution planktonic foraminiferal and oxygen isotope records from the Mediterranean. *Paleoceanography*, **16**(4), 405- 423.

Turco, E., Bambini, A. M., Foresi, L., Iaccarino, S., Lirer, F., Mazzei, R. & Salvatorini, G. 2002. Middle Miocene high-resolution calcareous plankton biostratigraphy at Site 926 (Leg 154, equatorial Atlantic Ocean): paleoecological and paleobiogeographical implications. *Geobios*, *Mémoire Spécial*, **24**, 257-276.

Van der Zwaan, G.J., Jorissen, F.J. & de Stigter, H.C. 1990. The depth dependency of planktonic/benthic foraminiferal ratios: constraints and applications. *Marine Geology*, **95**, 1-16.

Van der Zwaan, G.J., Duijnstee, I.A.P., den Dulk, M., Ernst, S.R., Jannink, N.T. & Kouwenhoven, T.J. 1999. Benthic foraminifers: proxies or problems? A review of paleoecological concepts. *Earth Science Reviews*, **46**, 213-236.

Van Leeuwen, R.J.W. 1989. Sea-floor distribution and late Quaternary faunal patterns of planktonic and benthic foramnifers in the Angola basin. *Utrecht Micropaleontological Bulletin*, **38**, 287 pp.

Van Morkhoven, F. P. C. M., Berggren, W. A. & Edwards, A.S. 1986. *Cenozoic cosmopolitan deep-water benthic foraminifera*. Bull. Cent. Rech. Explor.- Prod. Elf Aquitaine, Mem. **11**, 421 pp.

Wright, R. 1978. Neogene paleobathymetry of the Mediterranean based on benthic foraminifers from DSDP leg 42A. *Initial Reports, Deep Sea Drilling Project*, **42**, 837-846.

Wright, J.D., Miller, K.G. & Fairbanks, R.G. 1992. Early and Middle Miocene stable isotopes: implications for the deepwater circulation and climate. *Paleoceanography*, **7**(3), 357-389.

Wright, J.D. & Miller, K.G. 1996. Control of North Atlantic Deep Water circulation by the Greenland-Scotland Ridge. *Paleoceanography*, **11**(2), 157-170.

Woodruff, F. 1992. Deep-sea Benthic Foraminifera as Indicators of Miocene Oceanography. *Tokai University Press*: 55-66.

Woodruff, F. & Savin, S. M. 1989. Miocene Deepwater oceanography. *Paleoceanography* **4**(1), 87- 140.

Yasuda, H. 1997. Late Miocene-Holocene paleoceanography of the Western Equatorial Atlantic: evidence from deep-sea benthic foraminifers. *Proceedings of the Ocean Drilling Program, Scientific Results*, **154**, 395-432.

# Response of foraminiferal assemblages to the Neogene-Quaternary tectono-sedimentary evolution of the Tyrrhenian margin (Latium, central Italy)

*FABRIZIA IAMUNDO, LETIZIA DI BELLA and MARIA GABRIELLA CARBONI*
Earth Science Department, "La Sapienza" University, P.le A. Moro, 5- 00185 Roma, Italy

**ABSTRACT**

The purpose of this paper is to reconstruct the paleoenvironmental evolution during Plio-Pleistocene of the central Latium coast (Italy) through foraminiferal assemblages. Several sections and boreholes have been assigned to a time interval from Zanclean (*Globorotalia margaritae* Zone) to Emilian (*Globigerina cariacoensis* Zone).
R-mode hierarchical clustering and Principal Component Analysis have been performed using the relative abundance of the benthic foraminiferal taxa on approximately two hundred Pleistocene samples. The statistical results point to a shallowing-upward trend from circalittoral (Piacenzian-Gelasian *p.p.*: *Globorotalia aemiliana* Zone) to infralittoral environment (Emilian: *Globigerina cariacoensis* Zone). The paleobathymetrical evolution corresponds to an uplift of structural highs such as the Tor Caldara high.
Principal Component Analysis provides us with information on different trophic conditions highlighted in this time interval. The data collected indicate an oligotrophic and well-oxygenated environment during Piacenzian-Gelasian *p.p.* (*Globorotalia aemiliana* Zone). Eutrophic and poorly oxygenated conditions at the sea bottom, probably connected to the continental inflow, were present in the Rome basin during the Emilian (*Globigerina cariacoensis* Zone). The P/B ratio confirms the paleobathymetrical evolution of the entire area from the Pliocene to the Pleistocene.

***keywords***: Benthic foraminifers, Statistical analyses, Plio-Pleistocene, Central Italy.

## INTRODUCTION

A significant number of universities have spent various decades studying the Neogene-Quaternary basins along the Tyrrhenian margin of the Apennine chain in Central Italy. During the Plio-Pleistocene, this area was affected by complex tectonic phases, repeated subsidence episodes and differentiated uplift phenomena. In addition, an extensional regime in the basins contributed to give rise to intense volcanic activity since the Pliocene, resulting in several volcanic districts distributed along a narrow belt which runs parallel to the coast (Cavinato *et al*., 1994).

The Tuscany-Latium Tyrrhenian margin of the Italian peninsula represents the east border of the northern Tyrrhenian Sea, a stretched region characterised by continental crust less than 25 km thick, high heat flow and wide volcanic provinces (Sartori, 1989). This area is characterised by a system of NW-SE basins (Fig. 1) filled with thick sequences of marine clastic deposits dating from Messinian to Early Pleistocene (Funiciello *et al*., 1976; Ambrosetti *et al*., 1978; Bartolini *et al*., 1983). During this period extensional tectonics progressively moved east north-eastward following compressional phases related to the building up of the Apenninic chain (Elter *et al*., 1975; Patacca *et al*., 1991). The NE-SW oriented stretching regime was accompanied by a NW-SE normal fault system and by the formation of basins, which are linked by the NE-SW transfer fault zones. These fault zones bound narrow and deep half-graben basins (Faccenna *et al*., 1994) characterised by complex paleomorphology and often separated by structural highs. This *horst* and *graben* tectonic style became active since the Late Miocene (Ambrosetti *et al*., 1978; Funiciello & Parotto, 1978; Faccenna *et al*., 1994), as evidenced also by gravimetric data (Toro, 1978; Di Filippo & Toro, 1980, 1995). All the above-referred tectono-sedimentary events, which controlled the sedimentary processes in this period, determined a complicated square of different situations. In addition, the limited number of outcrops do not facilitate the reconstruction of the stratigraphy and paleoenvironmental evolution of the studied area. For the strong urbanization the dearth of data involves in particular the area south of Rome. In the 1980's, certain authors (Dai Prà & Arnoldus Huyzenveld, 1984; Malatesta & Zarlenga,

*In*: Coccioni R., Galeotti S., & Lirer F., (eds) 2004. Proceedings of the First Italian Meeting on Environmental Micropaleontology. *Grzybowski Foundation Special Publication*, 9, 63-76.

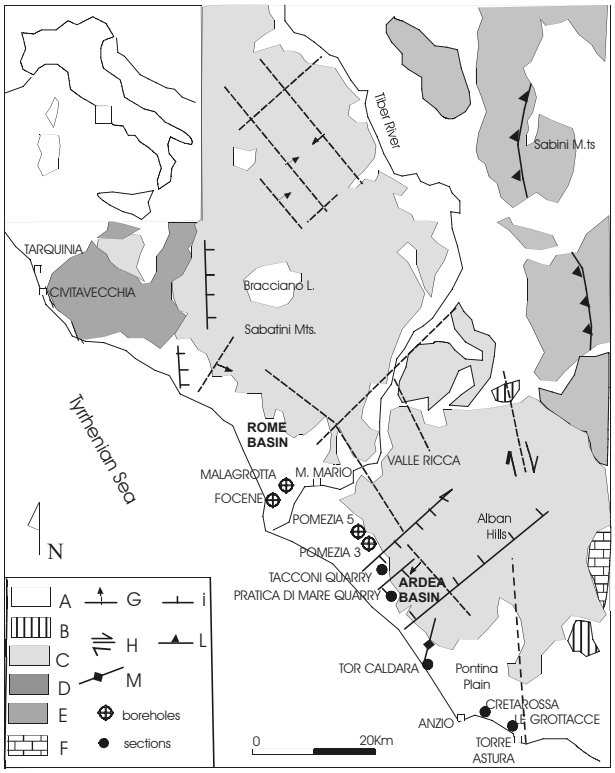


**Figure 1**. Structural sketch of the Central Italy Tyrrhenian margin (from Marra et al., 1995). A) sedimentary sequences of the "neo-autochthonous" cycles (Messinian-Pleistocene); B) travertine deposits (Quaternary); C) volcanic sequences (Plio-Pleistocene); D) Tolfa units (Upper Cretaceous-Eocene); E) Sabina units (Upper Triassic-Upper Miocene); F) Lepini Mts. units (Cretaceous); G) main buried faults, the arrow indicates the downthrow limb; H) strike-slip faults; I) normal faults; L) thrust faults; M) anticline axis.

1985; 1986) tried to synthesise the geomorphologic and stratigraphic data which characterised the Latium coast. Carboni & Di Bella (1997) reconstructed the stratigraphical succession outcropping between Tor Caldara and Anzio through foraminiferal records.

This study focused on two basins, Rome and Ardea, which constitute prime example of this geological setting. The Rome basin goes from the Cornicolani Mountains in the east to the present coastline in the west, and from the Sabatini Mountains in the north to Pomezia in the south (Fig. 1). The beginning of the sedimentation process commenced in the Early Pliocene (Zanclean-Piacenzian *p.p.*, *Globorotalia puncticulata* Zone) (Bonadonna 1968; Carboni, 1975), and continued until the Early Pleistocene (Emilian, *Globigerina cariacoensis* Zone) (Marra & Rosa, 1995; Marra *et al*., 1995).

The Ardea basin, which constitutes the deepest Neogene Tyrrhenian basin, is limited in the north by the Rome basin, in the east by the Alban Hills and in the south by the Pontina Plane. In the southern sector an anticline, whose axis lies close to Tor Caldara (Segre, 1957), divides a little secondary basin (Astura sub-basin) as evidenced by the analysis of seismic profiles (Faccenna *et al.*, 1994).

The purpose of this study is to reconstruct the kinematic setting of the extensional basins along the Tyrrhenian margin using quantitative benthic foraminiferal data and P/B ratio that provide direct indications on water depth, oxygenation, and trophic conditions**.** Progress made by studies on Recent benthic foraminiferal assemblages fully demonstrates their potential value as a tool for the reconstruction of marine paleoenvironmental processes. Although the use of benthic foraminiferal assemblages as a proxy for many physical parameters is limited (Murray, 2001), they gave an excellent response to oxygen content and organic matter distribution. The co-variation between oxygen-organic flux and depth makes the benthic foraminiferal assemblages distribution a valid tool to recognise bathymetrical changes (Van der Zwaan *et al.*, 1999). A statistical approach was adopted to understand particular water mass conditions. These analyses highlight the major water-depth variations, evidenced by the trend of faunal changes, related to the combined effects of tectonic and climate.

## MATERIAL AND METHODS

The geological structure of the studied area determined the selection of two important sections (Tor Caldara, Fig. 2 and Tacconi Quarry, Fig. 3) normal to strike in the Ardea basin and four boreholes in the Rome basin (Focene, Malagrotta, Pomezia 3 and Pomezia 5, Fig. 3). Twenty-nine additional single samples were collected to cover a large part of the area.

Tor Caldara is a composite section consisting of Pliocene clays and sandy clays and transgressively overlain by Pleistocene silty-clayey sands. At the top of the Pliocene sequence, sedimentation is marked by a facies change characterised by the deposition of sands and frequent intercalations of biocalcarenites. The base of the Early Pleistocene sequence shows a cemented sandy level containing *Arctica islandica*. Altogether, thirty-four samples were collected.

At the Tacconi Quarry (33 samples in all), a Lower Pleistocene section is outcropping composed of Santernian grey clay at the bottom, and Emilian grey-yellow clayey sands at the top.

The marine sediments of the Pomezia boreholes (37 samples) have been assigned to the Emilian. The upper 30 m of continental and volcanic deposits, which are present in the two cores, can be assigned to the "Ponte Galeria Formation". Some samples (Pomezia 3: P68-P49; Pomezia 5: P32, P23 and from P28 to P25) were excluded from the statistical analyses since such samples were affected by a strong reworking of Pliocene taxa (*Globorotalia puncticulata, Globigerinoides obliquus*).

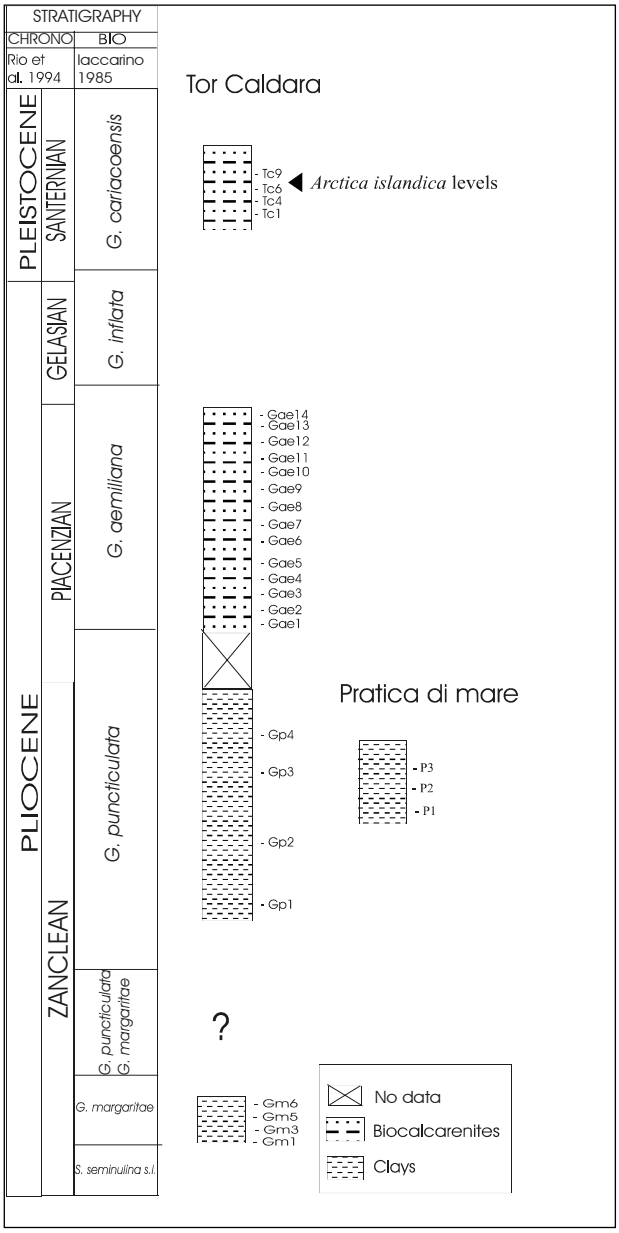


**Figure 2.** Lithological, bio and cronostratigraphical scheme of the Pliocene sites: Tor Caldara and Pratica di Mare sections.

The Malagrotta borehole was drilled at 25 m a.s.l. in the northeastern portion of the studied area (43 samples). This borehole recovered 134.5 m of mainly clayey and sandy Emilian marine sediments.

The Focene borehole, located at 3 m a.s.l. in the northwestern sector, is 125.50 meters deep and 41 samples were collected therefrom. The lower 60 m are made up of Emilian clays, in which two sandy intervals, probably linked to storm events, were identified (between -106.5 and -104 meters and between -92 and -86 meters a.s.l.). The samples collected in these intervals were not used for statistical analysis because their foraminiferal assemblages were deemed as displaced. The top 60 meters were also excluded because constituted by brackish-continental sediments.

Three Lower Pliocene samples consisting of alternations of grey and yellow clays were collected in the Pratica di Mare Quarry (Fig. 2).

Twenty-six single samples were collected in the coast between Anzio and F. Astura, which belong to Santernian (Cretarossa: A1–E2) and Emilian (Le Grottacce: E2-T2)(Fig. 3).

The nearly 200 samples were washed through a 90 m sieve and, subsequently, 300 specimens of benthic foraminifers were selected and identified from each sample. Planktonic foraminifers were contemporaneously identified and counted.

The results of quantitative analysis were processed using a statistical program (SPSS 9.0) in order to perform the hierarchical clustering (R-mode Cluster Analysis - CA) and the Principal Component Analysis. For CA, the distance was assumed in percentage by adopting the Pearson correlation and clusters were calculated by using the Average Linkage method. In order to simplify the matrix, the data set, originally containing 185 taxa, was condensed to 53 taxa. Some species with homogeneous environmental significance were grouped on the basis of their taxonomy, so that only species or groups more abundant than 3% in at least one sample were considered for the statistical analysis. The list of species groups utilised for the analysis is reported in Table 1. This study excluded the Pliocene (Zanclean) samples (basal part of Tor Caldara section and Pratica di Mare section) from the multivariate analysis because of the higher value of plankton, which might alter the statistical results.

The paleoenvironmental reconstruction is based on literature of the Mediterranean basin (Blanc-Vernet, 1969; Jorissen, 1988; Murray, 1991; Sgarrella & Moncharmont-Zei, 1993). The paleobathymetric interpretation follows published zonation studies for the Mediterranean area (Wright, 1978; Murray, 1991; Sgarrella & Moncharmont-Zei, 1993).

In order to reconstruct the paleobathymetric evolution of the basin, the P/B ratio was used on both the Pliocene and Pleistocene samples. The paleowater depth is frequently estimated as the mean ratio between planktic and benthic foraminifera. Recent studies on the Mediterranean Sea have shown a valid correlation between the P/B ratio and water depth (De Rijk *et al*., 1999).

Assuming that normal marine conditions prevailed at the time of deposition and that dissolution has not affected the sampled material, the formula suggested by Van der Zwaan *et al*., (1990):

$$\text{depth (m)} = e^{(3.58718+(0.03534*\%P))}$$

was used in this study. Results will be compared to the bathymetrical data based on benthic foraminiferal taxa.

**Table 1.** List of species groups utilised for the statistical analysis

| Groups | Included species |
|---|---|
| *Ammonia beccarii* group | *A. parkinsoniana, A. tepida, A. inflata, A. beccarii* |
| *Amphicoryna* spp | *A. scalaris, A. sublineata* |
| *Bolivina* spp. | *B. catanensis, B. aenariensis, B. punctata, B. alata, B. subspinescens, B. spathulata, B. dilatata* |
| *Bulimina costata* group | *B. inflata, B. costata* |
| *Bulimina marginata* group | *B. basispinosa, B. elegans marginata, B. etnea, B. marginata* |
| *Bulimina sublimbata* group | *B. fusiformis, B. lappa, B. elongata, B. sublimbata* |
| *Cibicidoides* spp. | *C. refulgens, C. ungerianus, C. robertonianus, C. pseudoungerianus* |
| *Elphidium* spp. | *E. advena, E. granosum, E. decipiens, E. complanatum, E. crispum, E. macellum, Elphidium sp.* |
| *Fissurina* spp. | *F. aperta, F. apiculata, F. castanea, F. longirostris, F. lucida, F. marginata, F. orbignyana, F. piriformis, F. quadricostulata* |
| *Florilus* spp. | *F. boueanus, F. citai* |
| *Globobulimina* spp. | *G. ovata, G. affinis, G. ovula, G. pyrula, G. pupoides* |
| *Gyroidina* spp. | *G. soldanii, G. neosoldani, G. altiformis, G. longispira, G. umbonata* |
| *Heterolepa* spp. | *H. floridana, H. bellincionii* |
| *Lagena* spp. | *L. clavata, L. semistriata, L. striata* |
| *Lenticulina* spp. | *L. calcar, L. peregrina, L. gibba, L. rotulata* |
| *Melonis* spp. | *M. barleeanus, M. pompilioides* |
| *Pullenia* spp. | *P. bulloides, P. quinqueloba* |
| *Pyrgo* spp. | *P. bulloides, P. depressa, P. oblonga* |
| *Quinqueloculina* spp. | *Q. oblonga, Q. seminulum, Q. stalkeri, Q. viennensis, Q. laevigata, Q.* cf. *vulgaris* |
| *Sigmoilopsis* spp. | *S. celata, S. schlumbergeri* |
| *Spiroloculina* spp. | *S. canaliculata, S. excavata, S. depressa* |
| *Textularia* spp. | *T. conica, T. soldani, T. pala, Textularia* sp. |
| *Uvigerina costata* group | *U. pygmaea, U. peregrina, U. mediterranea* |

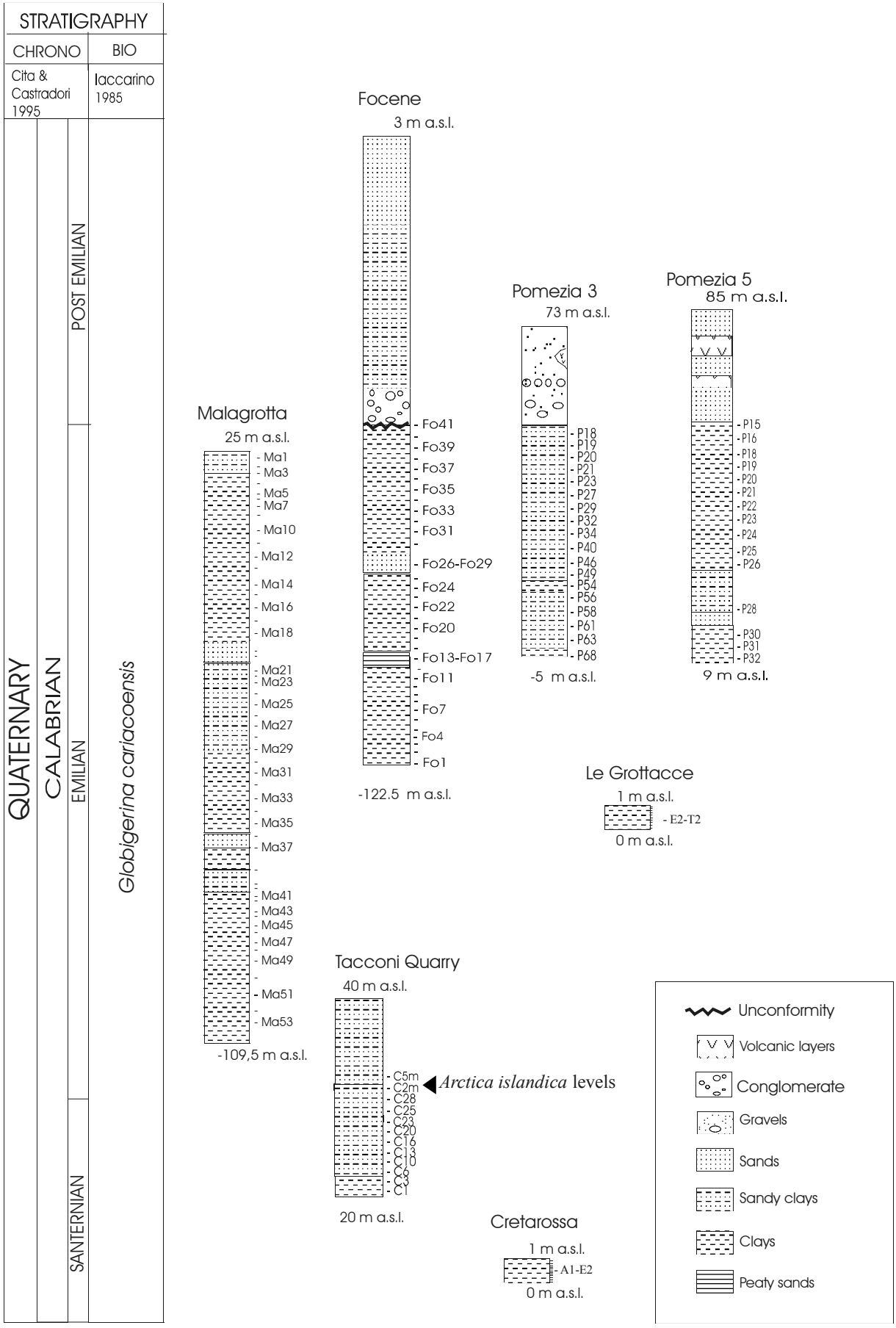


**Figure 3.** Lithological, bio and cronostratigraphical scheme of Pleistocene sites: Pomezia, Malagrotta and Focene (boreholes) and Tacconi and Le Grottacce (sections).

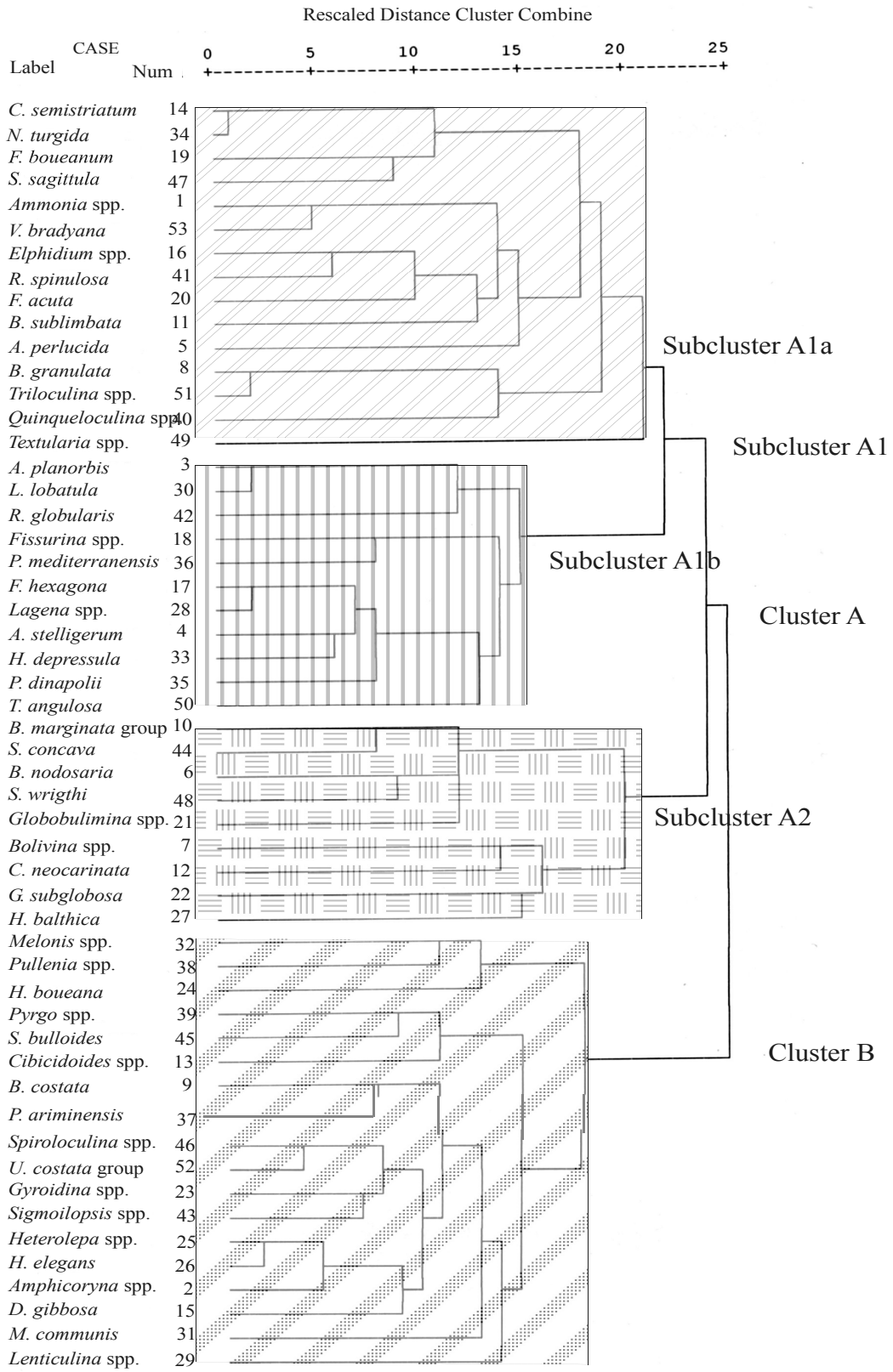


**Figure 4**. Dendrogram resulting from R-mode cluster analysis.

## BIOSTRATIGRAPHY

The sediments studied here were located in a chronostratigraphic scheme, resulting from the adoption of the subdivision of the Plio-Pleistocene (Rio *et al.*, 1994; Cita & Castradori, 1995). The zonal scheme of Iaccarino (1985) was utilised for the micropaleontological data.

The more ancient sediments, assigned to the *Globorotalia margaritae* Zone (Zanclean), cropped out

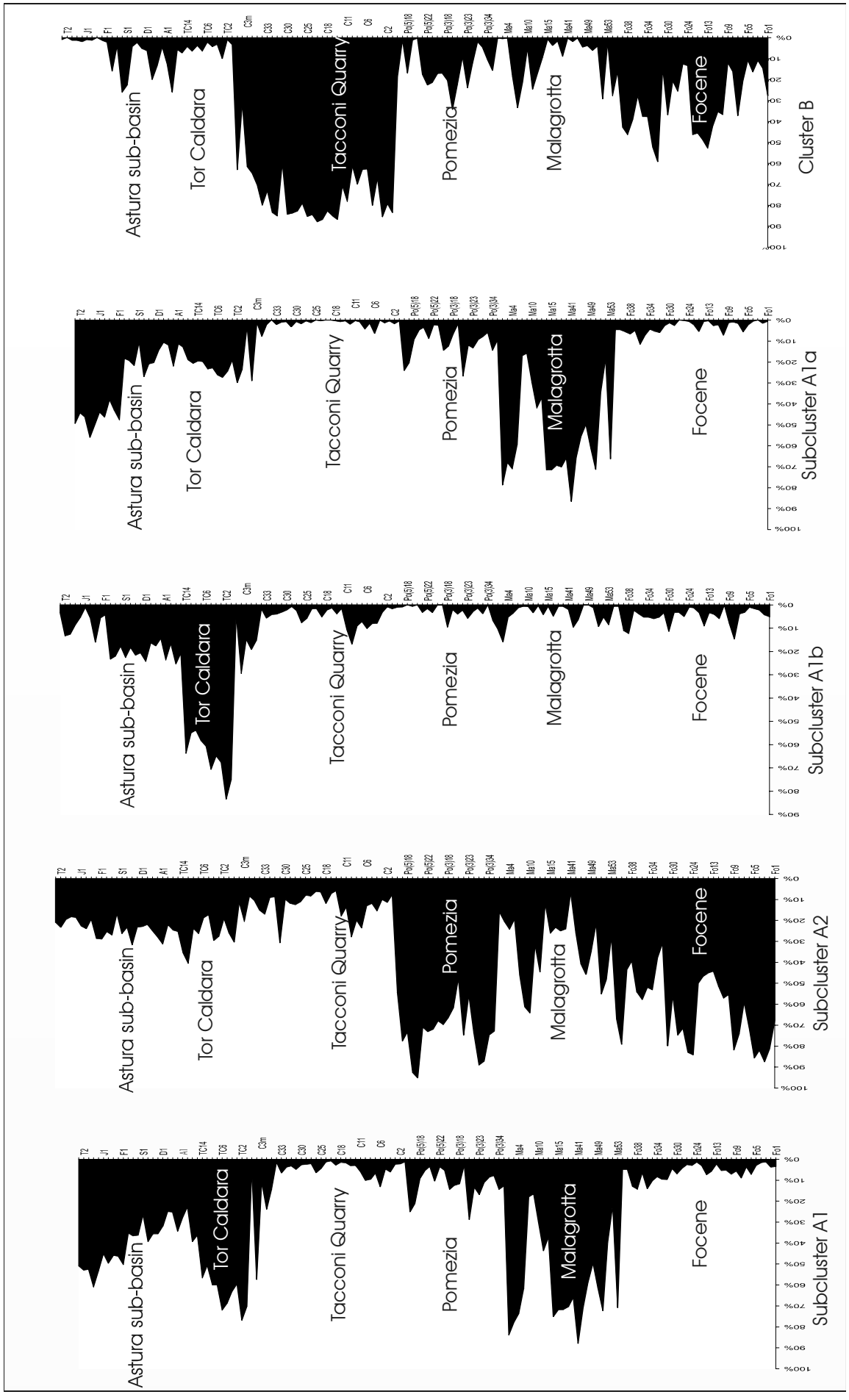


**Figure 5**. Plot of the clusters and subclusters against samples.

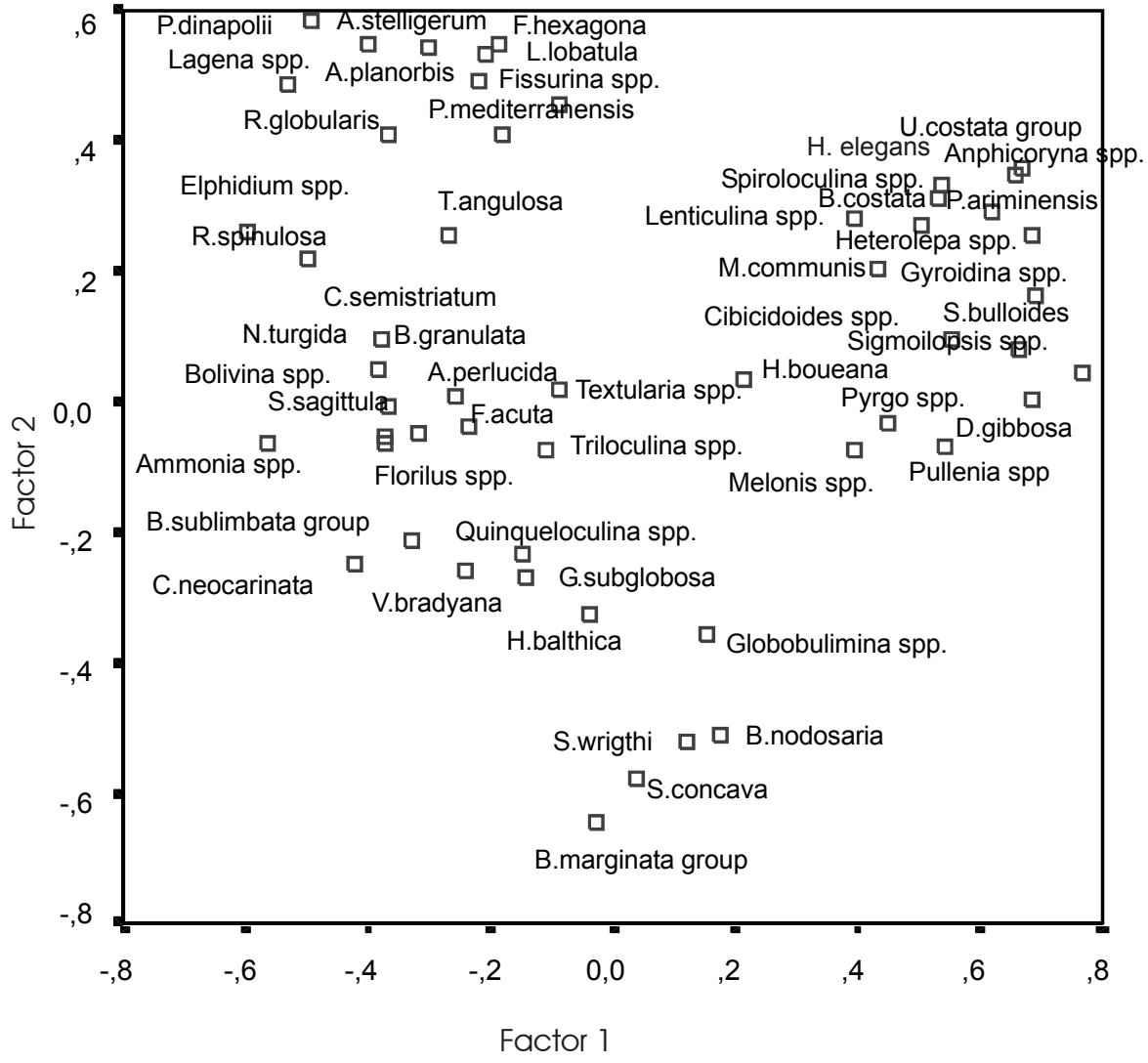


**Figure 6**. Bivariate plot of taxa on the first and second principal factors.

exclusively in the Ardea basin and constitute the nucleus of the Tor Caldara anticline (Fig. 2). The sediments belonging to the *Globorotalia margaritae-Globorotalia puncticulata* Zone (Zanclean) are recorded only in the Pratica di Mare area (Malatesta & Zarlenga, 1985). This biozone, probably because of human barriers or as a result of a depositional hiatus, was not found along the coast. The basal portion of both the *Globorotalia puncticulata* Zone (Zanclean) and the *Globorotalia aemiliana* Zone (Piacenzian-Gelasian *p.p.*) sediments cropped out in the Anzio area. The boundary between these two biozones is not identified due to the presence of anthropic barriers. Only the *Globorotalia puncticulata* Zone was recorded in the Pratica di Mare Quarry (Fig. 2).

Sediments assigned to the Gelasian portion of the *Globorotalia inflata* Zone, owing to a stratigraphic hiatus, are absent along the coast and in the Pratica di Mare Quarry.

The Lower Pleistocene (*Globigerina cariacoensis* Zone- Santernian and Emilian) subhorizontal sediments transgressively overlay the Pliocene sequence along the coast both in the Ardea and Rome basins (Figs. 2,3).

## RESULTS AND ANALYSES

### Hierarchical clustering

R-mode Hierarchical Cluster analysis was used in order to group benthic foraminifera together into few assemblages corresponding to faunal communities, thereby enabling a paleoecological reconstruction to be carried out.

Two main clusters, A and B, were distinguished and in the first two subclusters were highlighted: A1 (itself divisible in A1a and A1b) and A2 (Fig. 4).

On the basis of the paleoecological information provided by the taxa present in the clusters, clusters A and B appear to reflect different bathymetric zones, whereas the subclusters A1a, A1b and A2 also indicate different oxygen concentrations at the

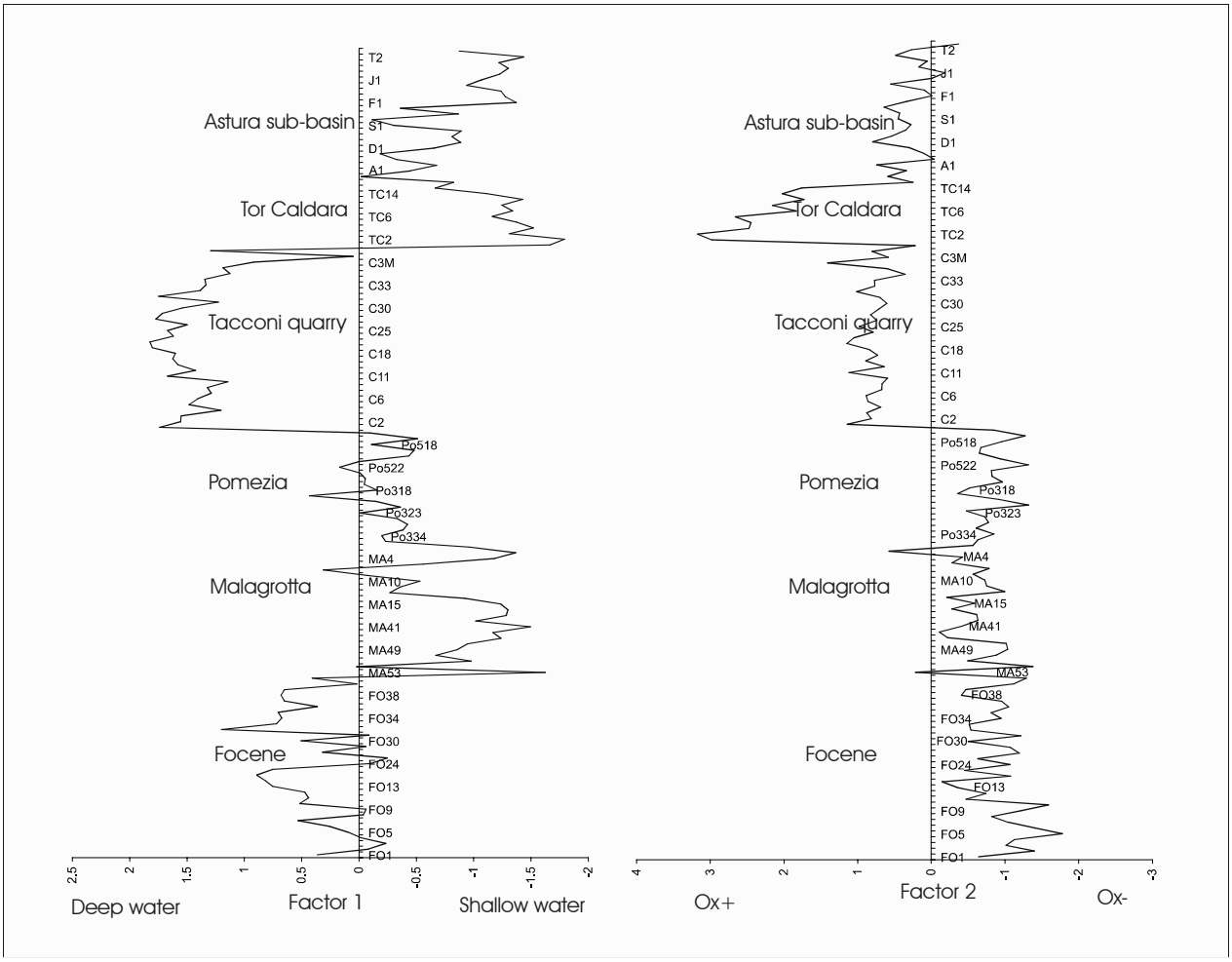


**Figure 7**. The two factors plotted against the samples.

sea-bottom. The clusters and subclusters are plotted along the sections and the boreholes in Fig. 5.

Cluster A consists of species typical of shallow water environments (between infralittoral and upper circalittoral zone).

Subcluster A1, predominant in the Malagrotta and Tor Caldara samples (about 70%) and characterised by a percentage of approximately 50% in the Astura sub-basin, combines taxa which are typical of the infralittoral zone: the *Ammonia beccarii* group, *Triloculina* spp., *Quinqueloculina* spp., *Rosalina globularis*, *Haynesina depressula*, etc.

In minor subcluster A1a, *Valvulineria bradyana, Nonionella turgida, Reussella spinulosa,* which are typical forms of stressed oxygen conditions frequently linked to river runoff, prevail (Jorissen, 1987; Bergamin *et al*., 1999). This group of species prevails in the Malagrotta section (70%) and it is less significant in the Tor Caldara samples (20%).

Subcluster A1b contains, among others *Lobatula lobatula, R. globularis, Asterigerinata planorbis* and *Planorbulina mediterranensis,* species known as epiphytic and typical of oligotrophic environments (Langer, 1988; Sgarrella & Moncharmont-Zei, 1993). This subcluster is extremely infrequent in all the samples studied hereunder except with respect to the Tor Caldara samples where subcluster A1b constitutes approximately 70% of the total assemblage. The distribution of subcluster A1a and A1b in the Tor Caldara and Malagrotta sections shows that the differences between such subcluster are more related to trophic conditions than to water depths.

Subcluster A2, which presents the highest values (about 80%) in the northern part of the sites studied hereunder (the Focene and the Malagrotta boreholes and Pomezia cores), shows taxa which are frequent in the upper circalittoral zone: the *Bulimina marginata* group, *Globobulimina* spp., *Bolivina* spp., *Cassidulina neocarinata,* etc. This kind of benthic assemblage is associated with low-oxygen bottom waters (Van der Zwaan & Jorissen, 1991; Barmawidjaja *et al*., 1992; Sen Gupta & Machain-Castilllo, 1993).

Cluster B, composed of deep-water species (lower circalittoral-epibathyal zone): *Planulina ariminensis*, the *Uvigerina costata* group, *Sphaeroidina bulloides, Hoeglundina elegans*, *Amphicoryna* spp. etc., shows the highest frequencies (up to 80%), in the Tacconi Quarry, high percentages (about 50%) are also present in the Focene core; whereas the

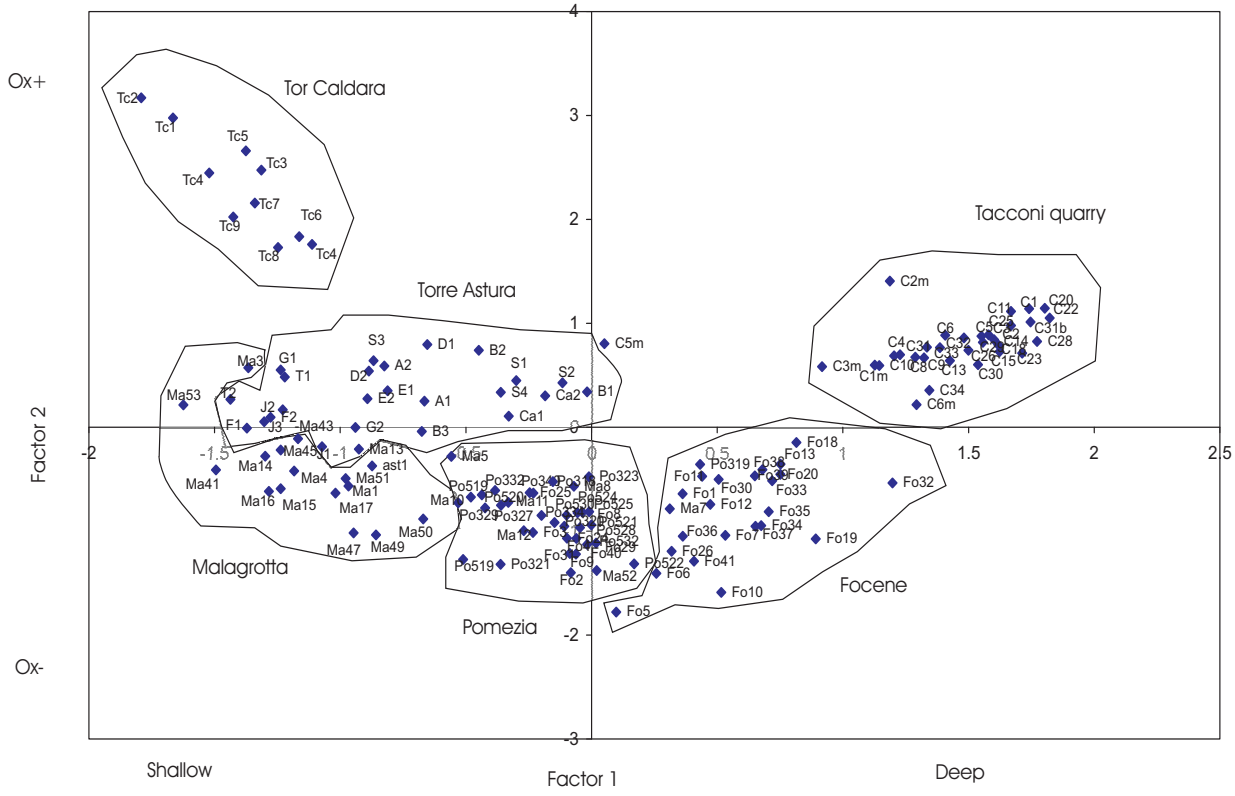


**Figure 8**. Bivariate plot of samples on the first and second principal factors.

Santernian Tor Caldara samples show the lowest values.

**Principal Component Analysis**

A standardised PCA was performed on the same data set (Fig. 6). The first and the second factor explain 27.95% of the variance (17.68% and 10.27% respectively). The other factors are not considered because they are too low.

The first factor is loaded positively by the *Uvigerina costata* group, *H. elegans*, *Gyroidina* spp., *S. bulloides*, *Sigmoilopsis* spp., *Amphicoryna* spp., *Bulimina costata*, *Pullenia* spp., etc.

*Bulimina costata* is a taxon reported from the circalittoral zone, which becomes abundant in deeper water environments (Sgarrella & Moncharmont Zei, 1993). *Gyroidina* spp. become present below 150-200 m (Wright, 1978). Also *S. bulloides* and *Amphicoryna* spp. are frequent in the circalittoral-bathyal zone.

The first factor is negatively loaded by *Elphidium* spp, *Ammonia* spp, *R. globularis*, *Astrononion stelligerum*, etc. These species are indicators of shallow water environments (infralittoral zone - Murray, 1991). As a result the first factor is loaded positively by taxa typical of deep water environments (circalittoral zone) and negatively by shallow water (infralittoral) taxa.

Plotting factor 1 scores (Fig. 7) results in strongly negative values for the Tor Caldara section (TC1-TC14), the Astura sub-basin samples (Le Grottacce, Cretarossa: A1-T2) and the Malagrotta samples (Ma1-Ma53), while this factor is moderately negative for the Pomezia samples (Po334-Po518). Positive values are present in the Focene section (Fo1-Fo41) and the highest recorded values are relative to Tacconi Quarry section (C1-C6m).

The resulting trend indicates a complicated paleomorphology of the Latium coast basins during the Early Pleistocene. The deepest water environment was located in the Tacconi Quarry and Focene areas while shallow water conditions were present in the Malagrotta and Tor Caldara sites.

The second factor is loaded positively by oxyphilic species such as *H. elegans* (Schönfeld, 2001) and by taxa characterised by an epiphytic style of life (*L. lobatula, A. planorbis, R. globularis, P. mediterranensis*, etc.). This factor is loaded negatively with species that are typical of poorly oxygenated or eutrophic environments (*Bulimina marginata* group, *C. neocarinata, V. bradyana, Globobulimina* spp., etc.). It seems to be indicative of variations in bottom water oxygenation. The oscillating trend of the values shows a cyclic variation of this parameter during time.

Plotting the factor 2 scores (Fig. 7) shows strongly positive values with respect to the Tor Caldara section (TC1-TC14), moderately positive values for the Tacconi Quarry section (C1-C6m) and for the Astura samples (A1-T2), while this factor is negative with respect to all other samples. The Emilian northern boreholes (Pomezia, Malagrotta and Focene) are

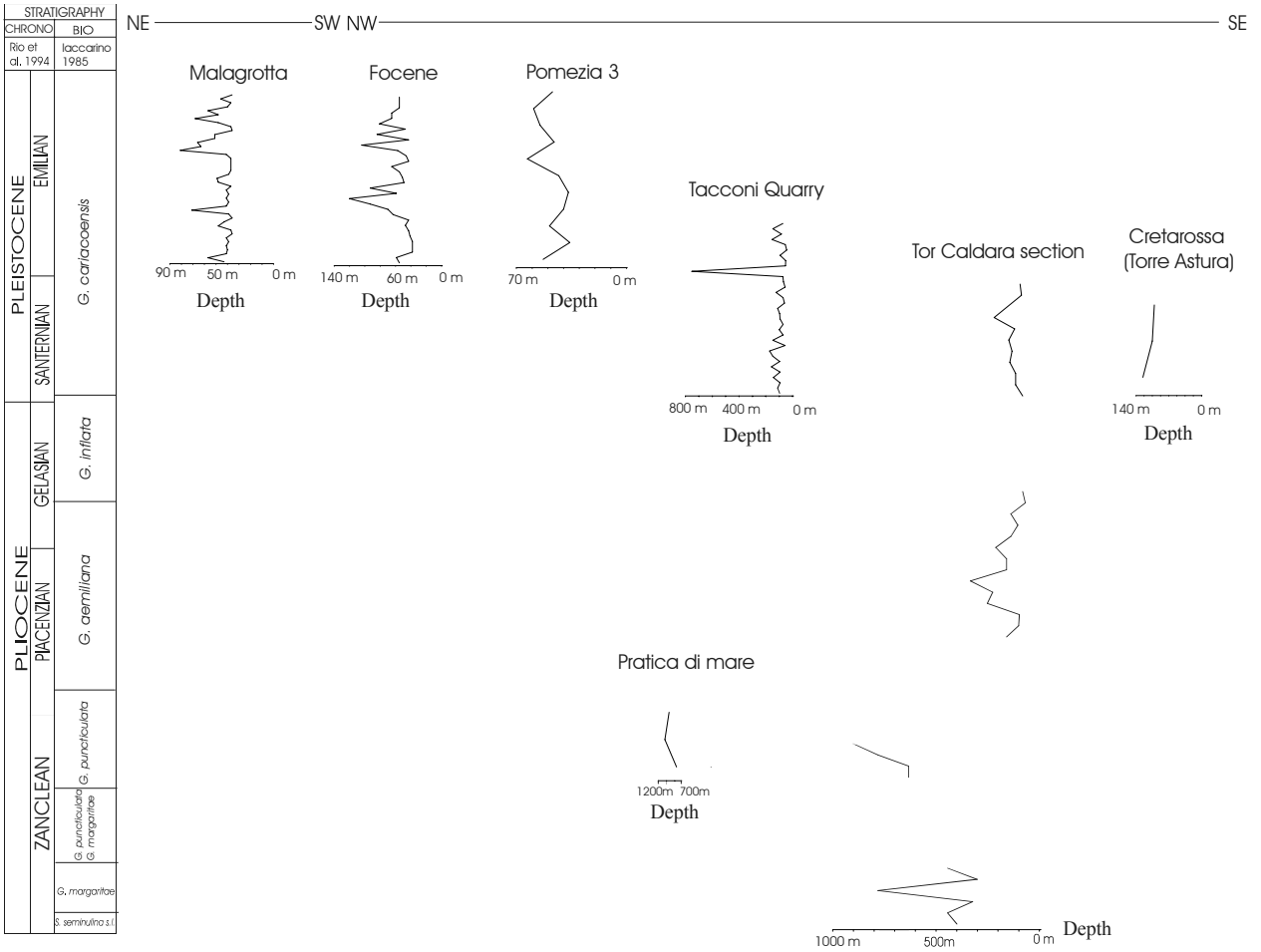


**Figure 9**. Paleobathymetry based on P/B ratio during Pliocene-Pleistocene along the coast from NE-SW and NW-SE.

clearly characterised by poorly oxygenated conditions.

Plotting sample scores along the two factors three major clusters enables us to identify (Fig. 8): samples TC1-TC14 (Tor Caldara) characterised by factor 1 strongly negative and factor 2 strongly positive; samples C1-C6m (Tacconi Quarry) characterised by factor 1 strongly positive and factor 2 positive; and, finally, all the other samples (Malagrotta, Focene, Astura sub-basin and Pomezia). In the latter more heterogeneous group other subclusters can be singled out: the Astura sub-basin samples are characterised by factor 1 negative and low positive values of factor 2 and the samples related to the Malagrotta, Pomezia and Focene sites, where factor 2 is always negative and factor 1 is negative, zero and positive.

The northern sites, characterised by eutrophic conditions, show a deepening between Malagrotta and Focene. The Pomezia sections represent an intermediate paleobathymetry. The southern samples, characterised by oligotrophic conditions, represent shallower water conditions in the Tor Caldara section and deeper water conditions in the Tacconi Quarry.

**Plankton/Benthos ratio**

Calculated paleodepths with respect to the six studied sections are illustrated in Figure 9. The deepest water conditions are registered in the Pliocene sediments of the Pratica di Mare (*Globorotalia puncticulata* Zone) and in the contemporaneous samples of the Tor Caldara section. The P/B ratio indicates a bathymetry equal to approximately 1000 m.

The *Globorotalia aemiliana* Zone, which is present only in the Tor Caldara section, shows a shallower condition, suggested also by the benthic assemblages (depositional depth about 200 m).

The Santernian sediments present in the Astura sub-basin (only the Cretarossa site was reported in the illustration as an example) show a depth of about 120 metres, a depth that is significantly shallower than the one registered in the Pleistocene portion of Tor Caldara (less than 70 m).

Even if benthic assemblage and the PCA suggest that the Tacconi Quarry section was deposited in a deeper water environment (more than 200 m), its fluctuating values are lower than those present in the contemporaneous Astura sub-basin and Tor Caldara section. This condition was probably caused by microfauna displacement related to secondary factors such as storm events or flow of

reworked and/or displacement sediments coming from structural highs.

The Emilian sections, even if the oscillating trends suggest disturbances during deposition, indicate a water depth of about 70 meters in the Pomezia and Malagrotta sections, while deeper water conditions are present in the Focene section with a bathymetry of about 120 metres.

This set of data confirms the usefulness of Plankton/Benthos ratios in evaluating paleodepth with respect to Pliocene sediments. For the Pleistocene deposits, this method is less valid because of the synsedimentary tectonic activity affecting these basins. In addition, a comparison of Pleistocene plankton/benthos ratio values and Factor1 of the PCA did not provide satisfactory results, giving a further confirmation of the tectonic disturbances. To obtain a better bathymetric assignment, it is necessary that the P/B ratio information be supported by data derived from the total benthic assemblages.

## DISCUSSION

The faunal assemblages allow us to identify three different paleoenvironmental settings which evolved from the Early Pliocene to the Early Pleistocene.

Benthic faunal assemblages characterising a deep-water environment (epibathyal zone) are present from the *Globorotalia margaritae* Zone to the *Globorotalia puncticulata* Zone (Zanclean). At the same time, slightly suboxic conditions were developed homogeneously along the whole of the Tyrrhenian margin from Tuscany to southern Latium (Barberi *et al.*, 1994; Iamundo *et al.*, 2002). This conclusion is in agreement with P/B ratios indicating a water depth of about 1000 m.

The Piacenzian-Gelasian *p.p.* (*Globorotalia aemiliana* Zone) is characterised by a paleomorphological complication due to the differential uplifting of several areas as evidenced by environmental changes. Three different sectors can be distinguished: in the northern Tyrrhenian area (Radicofani, Albegna, Tarquinia and Chiani-Tevere basins) this phase led to the deposition of sands, which are typical of the infralittoral zone, and biocalcarenites, locally called "Calcari ad Amphistegina" (Conti *et al.*, 1983; Barberi *et al.*, 1994; Iaccarino *et al.*, 1994). The deepest sectors of the Rome, Ardea and lower Tiber Valley basins were subjected to sedimentation typical of the epibathyal zone (Arias *et al.*, 1990; Marra *et al.*, 1995). The Sabatini area (Buonasorte *et al.*, 1991; Carboni & Palagi, 1998b) and the structural highs in the Ardea Basin (Tor Caldara and Pratica di Mare) were instead characterised by sedimentation typical of the circalittoral zone, with well oxygenated conditions (Iamundo *et al.*, 2002). This conclusion is in line with P/B ratios indicating a water depth of about 200 m.

During the Gelasian (*Globorotalia inflata* Zone), the tectonic uplifting reached its acme with the emersion of several areas. The only two sites where the sedimentation is continuous are the deepest part of the Tiber Valley Basin (Valle Ricca, Monterotondo) (Carboni et *al.*, 1993) and the Ardea structural low (Tacconi Quarry), where a circalittoral environment persisted, even though the percentage of low-oxygen tolerant species (*Bulimina marginata* group, *Bolivina* spp. and *C. neocarinata*) (Jorissen, 1987) increased.

As a result of an intense tectonic phase leading to strong subsidence, marine conditions were established in the Santernian (*Globigerina cariacoensis* Zone *p.p.*). Two different environments, an infralittoral and a circalittoral one, can be distinguished. The former, recognised in northern Latium (Tarquinia Basin, Barberi *et al.*, 1994; Carboni & Palagi, 1998a), in some sectors of the Rome and of the lower Tiber Valley basins and in the whole Anzio structural high (Tor Caldara), is characterised by the abundance of *L. lobatula*, *Ammonia* spp., *Elphidium* spp., *P. mediterranensis*, *A. planorbis* and *R. globularis*, which testify a vegetated and well oxygenated sea floor. The P/B ratio indicates a paleodepth of less then 70 m. The latter is found in the Sabatini area (Carboni & Palagi, 1998b), in the lowest part of the Tiber Valley, in the Rome Basin, in the Alban Hills (Funiciello & Parotto, 1978), in the deepest sector of the Ardea Basin (Tacconi Quarry), and in the area located between Anzio and Torre Astura. The faunal assemblages show relatively deep water, oxic or slightly suboxic environment. The P/B ratio indicates a water depth of about 150 m.

During the Emilian (*Globigerina cariacoensis* Zone *p.p.*) the uplifting of the northeastern areas continued: no sediments attributed to this period were recognised in north Latium, and north-east of Rome. Nevertheless subsidence allowed the accumulation of thick deposits in the Ardea Basin and in the Rome Basin where the uplift of the Monte Mario structure (Marra *et al.*, 1995) represented a barrier for the sea ingression in the eastern sector. The gradual shallowing from west to east (i.e. from lower circalittoral zones to the transition circalittoral-infralittoral zone) is well evidenced by the comparison between the benthic assemblages from the Focene and Malagrotta boreholes. Emilian circalittoral sediments are present in the whole Ardea Basin, testifying the subsidence that influenced the entire sector during this period. The analysis of Emilian foraminiferal assemblages also gives evidence of the establishment of low oxygen conditions at the sea floor (an increase in abundance of the *Bulimina marginata* group, *C. neocarinata*, *Globobulimina* spp. and *V. bradyana*) probably due to

the large amount of organic material carried from rivers from the northeastern emerged areas.

## CONCLUSIONS

The statistical analyses enabled us to document a differentiated bathymetrical evolution in different portions of the basins during the Early Pliocene/Early Pleistocene interval. These results allowed us to identify the setting and evolution of structures (structural highs) linked to the tectonic differential uplifting of the areas. The paleoecological changes identified by foraminiferal assemblages constitute a reliable tool to reconstruct the tectonic phases of a basin; good results are confirmed by geological, geophysical and gravimetric evidence.

The most evident phenomenon is the complication of the paleogeographical setting from the Early Pliocene to the Early Pleistocene, due to the superimposition of the Tyrrhenian coast uplifting over the previous tectonic structures combined with climatic effects. This uplift, migrating from northwest to southeast, originated different stratigraphical settings with more continuous and longer-lasting sedimentation in southern areas. Along the Tyrrhenian Latium margin both lithological and microfaunistic data evidenced, independently from local uplift, one more important event at a regional level, corresponding to the Late Pliocene hiatus (*Globorotalia inflata* Zone). This event is linked both to the tectonics and to a sea level lowering ensuing from climate cooling recorded in the Mediterranean (Thunell *et al.*, 1990). The two effects cannot be easily separated; nevertheless the climatic changes are well evidenced by variations in foraminiferal assemblages with an increased proportion of cool water taxa such as *C. neocarinata* (Hald & Varren, 1987; Mackensen & Hald, 1988).

The Early Pleistocene is characterised by a new cycle in the western part of the basins that began in the Early Santernian and ended in the Emilian. This cycle represents the last marine event that closed the marine sedimentation along the whole Tyrrhenian margin before the definitive emersion of the area.

## ACKNOWLEDGMENTS

Authors thank the referees, Prof. R. Coccioni and Prof. R. Spejer, for their useful advice. This work was supported by COFIN 2002 (grant 812125).

## REFERENCES

Ambrosetti, P., Carboni, M.G., Conti, M.A., Costantini, A., Esu, D., Gandin, A., Girotti, O., Lazzarotto, A., Mazzanti, R., Nicosia, U., Parisi, G. & Sandrelli, F. 1978. Evoluzione paleogeografica e tettonica dei bacini tosco umbro laziali nel Pliocene e nel Pleistocene inferiore. *Memorie della Società Geolologica Italiana*, **19**, 573-580.

Arias, C., Bigazzi, G., Bonadonna, F., Iaccarino, S., Urban, B., Dal Molin, M., Dal Monte, L. & Martolini, M. 1990. Valle Ricca Late Neogene stratigraphy (Lazio Region, Central Italy). *Paleobiologie continentale*, Montpellier, **XVII**, 61-80.

Barberi, F., Buonasorte, G., Cioni, R., Fiordelisi, A., Foresi, L., Iaccarino, S., Laurenzi, M.A., Sbrana, A., Vernia, L. & Villa, I.M. 1994. Plio-Pleistocene geological evolution of the geothermal area of Tuscany. *Memorie Descrittive della Carta Geologica D'Italia*, **XLIX**, 9-22.

Barmawidjaja, D.M., Jorissen, F.J., Puskaric, S. & Van der Zwaan, G.J. 1992. Microhabitat selection by benthic foraminifera in the northern Adriatic Sea. *Journal Foraminiferal Research*, **22** (4), 297-317.

Bartolini, C., Bernini, Carloni, G., Castaldini, P., Costantini, A., Federici, P., Francavilla, F., Gasperi, G., Lazzarotto, G., Mazzanti, A., Papani, G., Pranzini, G., Rau, G., Sandrelli, F. & Vercesi, P.L. 1983. Carta neotettonica dell'Appennino settentrionale. *Note illustrative Bollettino della Società geologica Italiana*, **101**, 523-549.

Bergamin, L., Di Bella, L. & Carboni, M.G. 1999. *Valvulineria bradyana* (Fornasini) in organic matter-enriched environment (Ombrone River Mouth, Central Italy). *Il Quaternario*, **12**, 51-56.

Blanc-Vernet, L. 1969. Contribution a l'étude des Foraminifères de Mediterranée. *Thèse de Doctorat Etat. Travaux de la Station Marine d' Eudoùme*, **64** (48), 281 pp.

Bonadonna, F.P. 1968. Studi sul Pleistocene del Lazio V. La biostratigrafia di Monte Mario e la "Fauna Malacologica Mariana" di Cerulli-Irelli. *Memorie della Società Geologica Italiana*, **7**, 261-321.

Buonasorte, G., Carboni, M.G. & Conti, A. 1991. Il substrato plio-pleistocenico delle vulcaniti sabine: considerazioni stratigrafiche e paleoambientali. *Bollettino della Società Geologica Italiana*, **110**, 35-40.

Carboni, M.G. 1975. Biostratigrafia di alcuni affioramenti pliocenici del versante tirrenico dell'Italia Centrale. *Geologica Romana*, **14**, 63-85.

Carboni, M.G. & Di Bella, L. 1997. The Plio-Pleistocene of the Anzio coast (Rome). *Bollettino della Società Paleontologica Italiana*, **36** (1-2), 135-159.

Carboni, M.G., Di Bella, L. & Girotti, O. 1993. Nuovi dati sul Pleistocene di Valle Ricca (Monterotondo, Roma). *Il Quaternario*, **6** (1), 39-48.

Carboni, M.G. & Palagi, I. 1998a. The Neogene-Quaternary deposits of the coastal belt between the Tafone and Marta Rivers (Northern Latium). *Bollettino della Società Paleontologica Italiana*, **37** (1), 41-60.

Carboni, M.G. & Palagi, I. 1998b. Biostratigrafia del sottosuolo plio-pleistocenico a sud del lago di Bracciano: il sondaggio Sabatini 9. *Il Quaternario*, **11** (1), 107-114.

Cavinato, G.P., Cosentino, D., De Rita, D., Funiciello, R. & Parotto, M. 1994. Evoluzione tettonico-sedimentaria dei bacini intrappenninici e correlazione con l'attività vulcano-tettonica dell'Italia centrale. *Memorie Descittive della. Carta Geologica d'Italia,* **49**, 63-76.

Cita, M. B. & Castradori, D. 1995. Rapporto sul workshop " Marine sections from the gulf of Taranto (Southern Italy) usable as potential stratotypes for the GSSP of the Lower, Middle and Upper Pleistocene" (29 Settembre- 4 Ottobre 1994). *Bollettino della Società Geologica Italiana*, **114**, 319-336.

Conti, M.A., Parisi, G. & Nicosia U. 1983. Un orizzonte ad *Amphistegina* nel Pliocene di Orvieto e sue implicazioni neotettoniche. *Bollettino della Società Geologica Italiana,* **102**, 113-122.

Dai Prà, G. & Arnoldus Huyzendveld, A. 1984. Lineamenti stratigrafici, morfologici e pedologici della fascia costiera dal fiume Tevere al fiume Astura (Lazio, Italia Centrale). *Geologica Romana*, **23**, 1-12.

De Rijk, S., Troelstra, S.R. & Rohling, E.J. 1999. Benthic foraminiferal distribution in the Mediterranean Sea. *Journal Foraminiferal Research*, **29** (2), 93-103.

Di Filippo, M. & Toro, B. 1980. Analisi gravimetrica delle strutture geologiche del Lazio meridionale. *Geologica Romana*, **19**, 285-294.

Di Filippo, M. & Toro, B. 1995. Gravity features. In: Trigila R. (Ed.), *The Volcano of the Alban Hills*, Rome, 213-219.

Elter, P., Giglia, G., Tongiorgi, M. & Trevisan, L. 1975. Tensional and compressional areas in the recent (Tortonian to Present) evolution of North Apennines. *Bollettino di Geofisica Teorica Applicata*, **17**, 3-18.

Faccenna, C., Funiciello, R., Bruni, A., Mattei, M. & Sagnotti, L. 1994. Evolution of a transfer-related basin: the Ardea basin (Latium, central Italy). *Basin Research*, **6**, 35-46.

Funiciello, R. Locardi, E. & Parotto, M. 1976. Lineamenti geologici dell'area sabatina orientale. *Bollettino della Società Geologica Italiana*, **95**, 831-849.

Funiciello, R. & Parotto, M. 1978. Il substrato sedimentario dell'area dei Colli Albani. Considerazioni geochimiche e paleogeografiche sul margine tirrenico dell'Appennino centrale. *Geologica Romana*, **17**, 233-287.

Hald, M. & Varren, T.O. 1987. Foraminiferal stratigraphy and environment of Late Weichselian deposits on the continental shelf off Troms, Northern Norway. *Marine Micropaleontology*, **12**, 129-160.

Iaccarino, S. 1985. Mediterranean Miocene and Pliocene planktic foraminifera. In Bolli H.H., Sanders J.B. & Perch-Nielsen K. (eds.), "*Plankton Stratigraphy*", 283-314.

Iaccarino, S., Vernia, L., Battini, P. & Gnappi, G. 1994. Osservazioni stratigrafiche sul bordo orientale del bacino di Radicofani (Toscana meridionale). *Memorie Descrittive della Carta Geologica D'Italia*, **XLIX**., 151-168.

Iamundo, F., Di Bella, L. & Carboni, M.G. 2002. Benthic foraminiferal assemblages of a Plio-Pleistocene section (Tor Caldara, Rome): statistical approach for paleoenvironment reconstruction. Giornate di Paleontologia 2002 Verona-Bolca-Priabona 6-8/6/2002. Abstract book, p. 30

Jorissen, F.J. 1987. The distribution of the benthic foraminifera in the Adriatic Sea. *Marine Micropaleontology*, **12** (1), 21-48.

Jorissen, F.J. 1988. Benthic Foraminifera from the Adriatic Sea; priciples of phenotypic variation. *Utrecht Micropaleontological Bulletin*, **37**, 174 pp.

Langer, M.R. 1988. Recent epiphytic Foraminifera from Vulcano (Mediterranean Sea). *Revue de Paléobiologie*, Benthos 86', *Special Publication*, **2**, 827-832.

Malatesta, A. & Zarlenga, F. 1985. Il Quaternario di Pomezia (Roma) e la sua fauna marina. *Bollettino della Società Geologica Italiana*, **104**, 503-514.

Malatesta, A. & Zarlenga, F. 1986. Evoluzione paleogeografico-strutturale Plio-pleistocenica del basso bacino Romano a Nord e a Sud del Tevere. *Memorie della Società Geologica Italiana*, **35**, 75-85.

Marra, F., Carboni, M.G., Di Bella, L., Faccenna, C., Funiciello, R. & Rosa, C. 1995. Il substrato plio-pleistocenico nell'area romana. *Bollettino della Società Geologica Italiana*, **114**, 195-214.

Marra, F. & Rosa, C. 1995. Stratigrafia e assetto geologico dell'area romana. *Memorie Descrittive della Carta Geologica D'Italia*, **L**, 49-118.

Mackensen, A. & Hald, M. 1988. *Cassidulina teretis* Tappan and *C. laevigata* d'Orbigny: their modern and Late Quaternary distribution in Northern Seas. *Journal of Foraminiferal Research*, **18**, 16-24.

Murray, J.M. 1991. *Ecology and Paleoecology of Benthic Foraminifera*. Longman Scientific & Technical Eds., New York, 397 pp.

Murray, J.M. 2001. The niche of benthic foraminifera, critical thresholds and proxies. *Marine Micropaleontology*, **41**, 1-7.

Patacca, E., Sartori, R. & Scandone, P. 1991. Tyrrhenian basin and Apenninic arcs: kinematic relations since Late Tortonian time. *Memorie della Società Geologica Italiana*, **45**, 425-451.

Rio, D., Sprovieri, R. & Di Stefano, E. 1994. The Gelasian Stage: a proposal of a new Chronostratigraphic unit of the Pliocene series. *Rivista Italiana di Paleontologia Stratigrafica*, **100** (1), 103-124.

Sartori, R. 1989. Evoluzione neogenico-recente del bacino tirrenico e i suoi rapporti con la geologia delle aree circostanti. *Giornale di Geologia*, **51** (2), 1-39.

Schönfeld, J. 2001. Benthic Foraminifera and pore-water oxygen profiles: a re-assessment of species boundary conditions at the Western Iberian margin. *Journal Foraminiferal Research*, **31**, 86-107.

Segre, A.G. 1957. Nota sui rilevamenti eseguiti nel Foglio 158 Latina della Carta Geologica d'Italia. *Bollettino del Servizio Geologico D'Italia*, **78**, 569-583.

Sen Gupta, B.K. & Machain-Castillo, M.L. 1993. Benthic foraminifera in oxygen-poor habitats. *Marine Micropaleontology*, **20**, 183-201.

Sgarrella, F. & Moncharmont-Zei, M. 1993. Benthic Foraminifera of the Gulf of Naples (Italy): systematics and autoecology. *Bollettino della Società Paleontologica Italiana*, **32** (2), 145-264.

Thunnel, R., Williams, D., Tappa, E., Rio, D. & Raffi, I. 1990. Pliocene-Pleistocene stable isotope record for Ocean Drilling Program Site 653, Tyrrhenian basin: Implications for the paleoenvironmental history of the Mediterranean Sea. *Proceedings of the Ocean Drilling Program, Scientific Results*, **107**, 387-399.

Toro, B. 1978. Anomalie residue di gravità e strutture profonde nelle aree vulcaniche del Lazio settentrionale. *Geologica Romana*, **17**, 35-44.

Van der Zwaan, G.J., Jorissen, F. J. & de Stigter, H.C. 1990. The depth dependency of planktonic/benthic foraminiferal ratios: Constraints and applications. *Marine Geology*, **95**, 1-16.

Van der Zwaan, G.J. & Jorissen, F.J. 1991. Biofacial patterns in river-induced shelf anoxia. In Tyson, R.V. & Pearson, T.H. (Eds.), "Modern and Ancient Continental Shelf Anoxia". *Geological Society Special Publication*, **58**, 65-82.

Van Der Zwaan, G.J., Duijnstee, I.A.P., Der Dulk, M., Ernest, S.R., Jannink, N.T. & Kouwenhoven, T.J. 1999. Benthic foraminifers: proxies or problems? A review of paleoecological concepts. *Earth Science Reviews*, **46** (1-4), 213-235.

Wright, R. 1978. Neogene benthic foraminifers from DSDP Leg 42a, Mediterranean Sea. *Initial Reports of the Deep Sea Drilling Project* **42**(1), 709-72.

# Paleoclimatic changes in the Serravallian record of the Mediterranean area

*FABRIZIO LIRER[1]*, ANTONIO CARUSO[2], LUCA MARIA FORESI[3], SILVIA IACCARINO[1] and PAOLA IACUMIN[1]*

1. Dipartimento di Scienze della Terra, Università di Parma, Parco Area delle Scienze 157/A, 43100 Parma, Italy
* Current address: IAMC (Istituto Ambiente Marino Costiero - sede Geomare - CNR). Calata Porta di Massa, Interno porto di Napoli, 80133 Napoli; e-mail: flirer@gms01.geomare.na.cnr.it
2. Dipartimento di Geologia e Geodesia, Università di Palermo, Corso Tukory 131, 90134 Palermo, Italy
3. Dipartimento di Scienze della Terra, Università di Siena, Via Laterina 8, 53100 Siena, Italy

**ABSTRACT**

Planktonic foraminiferal and oxygen isotope records of the astronomically tuned S. Nicola composite section (Tremiti Islands, Mediterranean basin) provide new insight into the paleoclimatic evolution during the Middle to early Late Miocene (between 12.60 and 11.10 Ma). The application of PCA (Principal Component Analysis) to high-resolution data enabled us to examine the interactions among the foraminiferal proxies and to identify a series of paleoclimatic events of long and short duration that took place in the Mediterranean basin during the late Serravallian. The long term trend in PCA-1 score plot shows that the faunal composition of the studied sedimentary record changed significantly at 11.80 Ma. This change coincides with the significant shift from negative to positive loading in PCA-1 and it has been correlated with the onset of the Mi5 event, which in the Mediterranean area is testified by the first influx of neogloboquadrinids. Such a major change is preceded by other minor events at 12.38, 12.21, and 12.00 Ma, which indicate the progressive deterioration from warm to colder climatic conditions. The most evident step coincides with a sharp decrease in abundance of surface species at 12.00 Ma and the relative increase of intermediate species, suggesting a contraction of the habitat of warm faunas and increasingly eutrophic conditions. This cooling (of sea surface water) is also supported by a gradual shift in the bulk $\delta^{18}O$ from –2.38‰ (12.374 Ma) to -0.28‰ (11.963 Ma). The comparison between oxygen isotope oscillations and the eccentricity records revealed a good correspondence of the light $\delta^{18}O$ values to eccentricity maxima. In addition, the vanishing from the Mediterranean of the neogloboquadrinids between 11.54 Ma and 11.21 Ma has been related to the intensification of monsoon activity with an increase in runoff. This hypothesis is supported by more negative values in $\delta^{18}O$. The Mediterranean results are compared with those from the Equatorial and North Atlantic Ocean.

**keywords**. paleoclimatology, planktonic foraminifera, stable isotope, late Middle Miocene, Mediterranean.

## INTRODUCTION

Since the Cretaceous and beyond, through studies of sedimentary archives, it has become increasingly apparent that the Earth's climate system has experienced continuous change, during which the global ocean has evolved from a circum-tropical to circum-Antarctic surface circulation and from a halothermal to the thermohaline deep-water circulation of today (Kennett & Barker, 1990; Roth *et al*., 2000; Zachos *et al*., 2001). Following the cooling and the expansion of the Antarctic continental ice-sheet in the earliest Oligocene, a permanent ice sheet developed in Antarctica (Zachos *et al*., 2001). This ice sheet persisted until the late part of the Oligocene (26 to 27 Ma, see Zachos *et al*., 2001), when a warming trend reduced the extent of Antarctic ice. It follows that the late Oligocene to Miocene constitutes a key interval in the global climatic evolution of the Cenozoic. The transition from relative global warmth of the Late Oligocene-Early Miocene to the Neogene «ice-house» world took place through a series of major changes in climate, polar ice volume, and ocean circulation (Roth *et al*., 2000; Mutti, 2000). During this period, global ice volume remained low and bottom water temperatures trended slightly higher (Wright & Miller, 1992; Miller *et al*., 1991) with the exception of several short periods of glaciation (Mi- events).

During the Early Miocene (about 22-16 Ma, Billups & Scrag, 2002), the relatively warm Atlantic

*In*: Coccioni R., Galeotti S., & Lirer F., (eds) 2004. Proceedings of the First Italian Meeting on Environmental Micropaleontology. *Grzybowski Foundation Special Publication*, 9, 77-96.

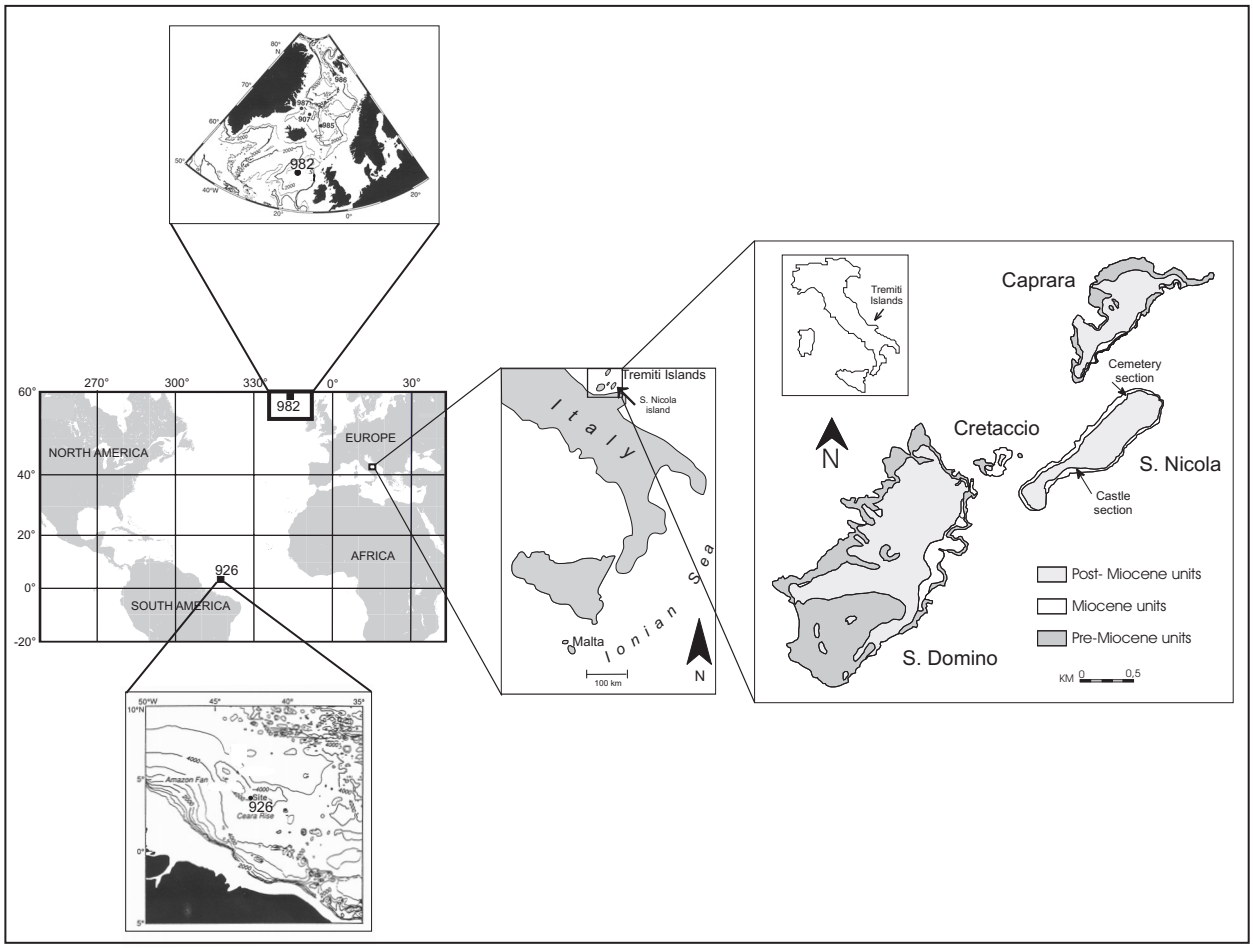


**Figure 1.** Study area: Location map of S. Nicola composite Section (Tremiti Island), Leg 154, Site 926 (Equatorial Atlantic Ocean), Leg 162, Site 982B (North Atlantic Ocean).

bottom water temperatures suggest that Antarctica was not yet covered by an extensive, permanent ice cap, and that there was only a seasonal ice cover in the northern hemisphere. However, from the early Middle Miocene, global temperatures cooled dramatically as the Earth entered its Ice House phase; in fact, the major phase of East Antarctic ice sheet growth took place between 15 Ma and 13 or 12 Ma (Zachos at al., 2001; Billups & Schrag, 2002; Winkler *et al*., 2002), with a deep ocean cooling of about 3°C (Shackleton & Kennett, 1975; Savin *et al*., 1985; Miller *et al*., 1987; Zachos *et al*., 2001; Billups & Schrag, 2002).

The late Middle to early Late Miocene (12 Ma-11 Ma) is considered a period of stable climatic conditions after a previous stage from 15-13 Ma during which the global climate changed to colder conditions with increased zonality (Flower & Kennett, 1994; Zachos at al., 2001). At this time, the ocean climate system evolved into modern state conditions dominated by strong meridionality and vertical thermal gradients and dominance of high-latitude deep water source (Kennett, 1977; Miller *et al*., 1987, 1991; Woodruff & Savin, 1989, 1991; Flower & Kennett, 1993; Roth *et al*., 2000).

Possible factors contributing to this climate transition include: 1) tectonic events that altered atmospheric and oceanic circulation, such as the opening and closing of oceanic gateways. The uplift rate of the Himalayas increased and the Mediterranean sea became isolated from the Indian Ocean, as a result of the collision of Arabia with Iran and Turkey (Woodruff & Savin, 1989; Miller *et al*., 1991; Jacobs *et al*., 1996; Mutti, 2000); 2) forcing factors that contributed to the cooling via reduced greenhouse effect, which increased weathering (Raymo & Ruddiman, 1992; Raymo, 1994) and/or organic carbon burial rates (Vincent & Berger, 1985).

Nevertheless, much of the long-term and short-term change in climate is generated by periodic oscillations in Earth's orbital parameters (eccentricity, obliquity and precession) that affect the distribution and amount of incident solar energy (Beaufort, 1994; Lourens & Hilgen, 1997; Turco *et al*., 2001; Zachos *et al*., 2001).

This period (late Middle to early Late Miocene) of relatively stable climatic conditions, is characterised by two well-known short term increases in benthic foraminiferal $\delta^{18}O$ values (Mi5 and Mi6 events), which reflect continental ice sheet growth and bot-

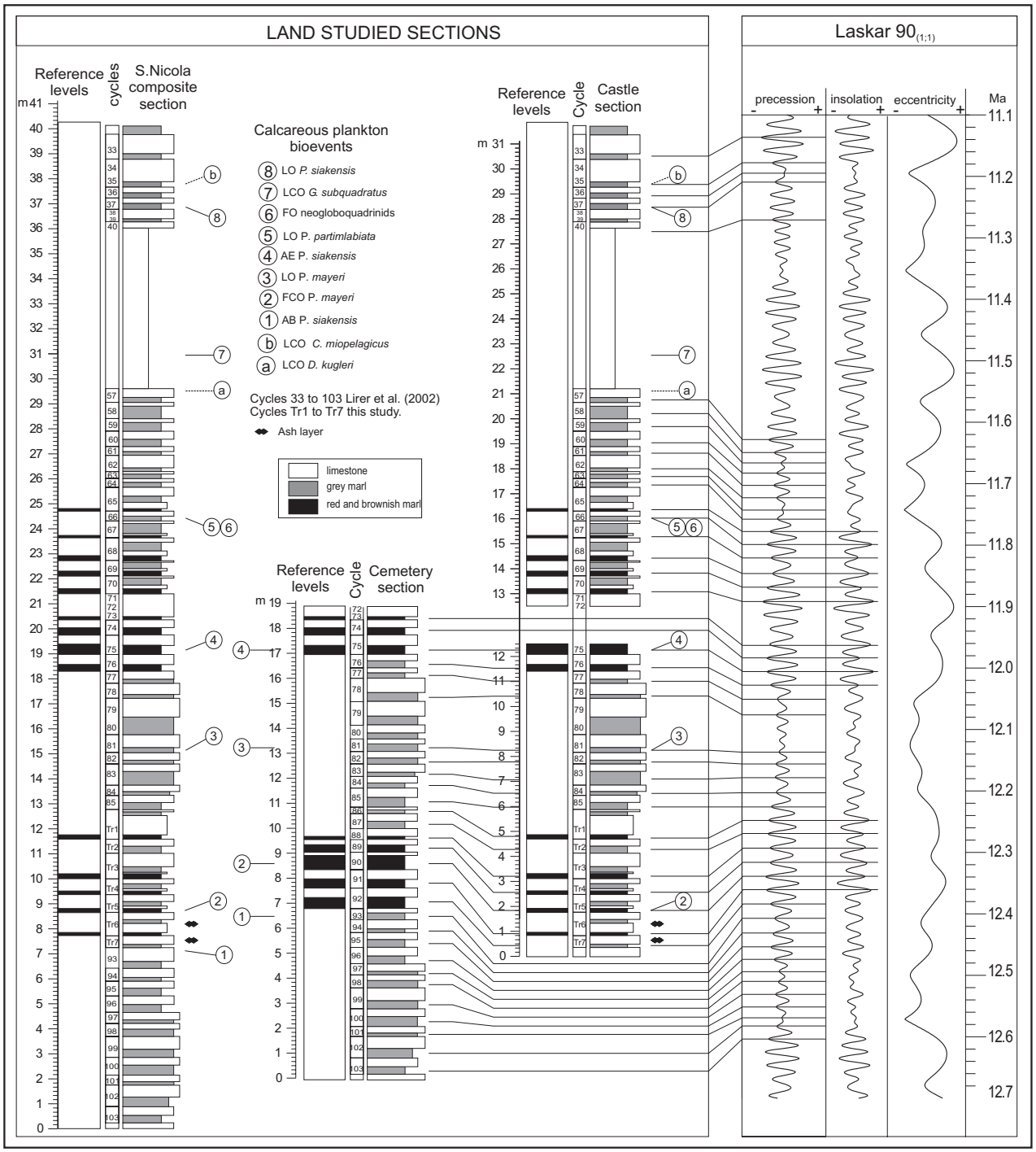


**Figure 2.** Integrated stratigraphic correlation of the Cemetery and Castle sections within the astronomical tuned integrated stratigraphic framework. LO: Last Occurrence; LCO: Last Common Occurrence; FO: First Occurrence; AE: Acme end; AB: Acme base.

tom water cooling (Miller *et al*., 1991). Because of the lack of continuous marine sedimentary records spanning the Middle to early Late Miocene, the timing of Miller's Mi5 and Mi6 events and their possible relationship to astronomic parameters are uncertain. Recently, Turco *et al*. (2001) producing a detailed study of the Monte Gibliscemi section (Sicily), astronomically calibrated by Hilgen *et al*. (2000), gave the precise timing and interpretation of Mi5 and Mi6 events (Miller *et al*., 1991) recorded in the Mediterranean area.

The present study refers to the latest Middle Miocene (latest Serravallian) paleoclimatic evolution of eastern Mediterranean and more precisely, of the southern Adriatic Sea (Tremiti Islands, S. Nicola composite section). Our results are based on the application of Principal Component Analysis (PCA) to the high-resolution planktonic foraminiferal record. This analysis enabled us to examine the interactions among the variables (foraminiferal species)

**Table 1**. Stratigraphic position and astronomical ages of the sedimentary cycles after Lirer et al. (2002).

| Data by Lirer *et al*. 2002 | | | Data this work | | | Data by Lirer *et al*. 2002 | | | Data this work | | |
|---|---|---|---|---|---|---|---|---|---|---|---|
| **Section** | **lithologic Cycle** | **Age (ky)** | **Section** | **lithologic Cycle** | **Age (ky) this work** | **Section** | **Cycle** | **Age (ky)** | **Section** | **Cycle** | **Age (ky)** |
| Castle | 33 | 11,137 | Castle | 33 | 11,137 | Castle\Cemetery | 78 | 12,079 | Castle\Cemetery | 78 | 12,079 |
| Castle | 35 | 11,180 | Castle | 35 | 11,180 | Castle\Cemetery | 79 | 12,100 | Castle\Cemetery | 79 | 12,100 |
| Castle | 36 | 11,197 | Castle | 36 | 11,197 | Castle\Cemetery | 80 | 12,120 | Castle\Cemetery | 80 | 12,120 |
| Castle | 37 | 11,211 | Castle | 37 | 11,211 | Castle\Cemetery | 81 | 12,139 | Castle\Cemetery | 81 | 12,139 |
| Castle | 39 | 11,253 | Castle | 39 | 11,251 | Castle\Cemetery | 82 | 12,158 | Castle\Cemetery | 82 | 12,158 |
| | | | Castle | 40 | 11,271 | Castle\Cemetery | 83 | 12,179 | Castle\Cemetery | 83 | 12,179 |
| Castle | 56 | 11,608 | | | | Castle\Cemetery | 84 | 12,204 | Castle\Cemetery | 84 | 12,204 |
| Castle | 57 | 11,630 | Castle | 57 | 11,630 | Castle\Cemetery | 85 | 12,227 | Castle\Cemetery | 85 | 12,227 |
| Castle | 58 | 11,651 | Castle | 58 | 11,651 | Castle\Cemetery | 86 | 12,249 | Castle | TR1 | 12,249 |
| Castle | 59 | 11,669 | Castle | 59 | 11,669 | Cemetery | 87 | 12,271 | Castle | TR2 | 12,271 |
| Castle | 60 | 11,685 | Castle | 60 | 11,685 | Cemetery | 88 | 12,294 | Castle | TR3 | 12,294 |
| Castle | 61 | 11,704 | Castle | 61 | 11,704 | Cemetery | 89 | 12,318 | Castle | TR4 | 12,318 |
| Castle | 62 | 11,725 | Castle | 62 | 11,725 | Cemetery | 90 | 12,341 | Castle | TR5 | 12,341 |
| Castle | 63 | 11,743 | Castle | 63 | 11,743 | Cemetery | 91 | 12,363 | Castle | TR6 | 12,363 |
| Castle | 64 | 11,759 | Castle | 64 | 11,759 | Cemetery | 92 | 12,385 | Castle | TR7 | 12,385 |
| Castle | 65 | 11,779 | Castle | 65 | 11,779 | Cemetery | 93 | 12,409 | Cemetery | 93 | 12,409 |
| Castle | 66 | 11,800 | Castle | 66 | 11,800 | Cemetery | 94 | 12,434 | Cemetery | 94 | 12,434 |
| Castle | 67 | 11,822 | Castle | 67 | 11,822 | Cemetery | 95 | 12,455 | Cemetery | 95 | 12,455 |
| Castle | 68 | 11,848 | Castle | 68 | 11,848 | Cemetery | 96 | 12,476 | Cemetery | 96 | 12,476 |
| Castle | 69 | 11,871 | Castle | 69 | 11,871 | Cemetery | 97 | 12,495 | Cemetery | 97 | 12,495 |
| Castle | 70 | 11,893 | Castle | 70 | 11,893 | Cemetery | 98 | 12,512 | Cemetery | 98 | 12,512 |
| Castle | 71 | 11,914 | Castle | 71 | 11,914 | Cemetery | 99 | 12,532 | Cemetery | 99 | 12,532 |
| Cemetery | 73 | 11,963 | Cemetery | 73 | 11,963 | Cemetery | 100 | 12,553 | Cemetery | 100 | 12,553 |
| Cemetery | 74 | 11,985 | Cemetery | 74 | 11,985 | Cemetery | 101 | 12,571 | Cemetery | 101 | 12,571 |
| Cemetery | 75 | 12,006 | Cemetery | 75 | 12,006 | Cemetery | 102 | 12,585 | Cemetery | 102 | 12,585 |
| Castle\Cemetery | 76 | 12,009 | Castle\Cemetery | 76 | 12,009 | Cemetery | 103 | 12,605 | Cemetery | 103 | 12,605 |
| Castle\Cemetery | 77 | 12,053 | Castle\Cemetery | 77 | 12,053 | | | | | | |

**Table 2.** All planktonic foraminifera recognised in the S. Nicola composite section.

| Planktonic foraminifera | |
|---|---|
| *Globigerina falconensis* (Blow) | *Globigerinoides subquadratus* (Brojnniman) |
| *Globigerina bulloides* d'Orbigny | *Globigerinoides trilobus* (Reuss) |
| *Globigerina eamesi* (Blow) | *Globigerinoides obliquus obliquus* Bolli |
| *G. foliata* Bolli | *Globigerinoides bulloideus* Crescenti |
| *Globigerina praebulloides* Blow | *Globorotalia scitula gigantea* Blow |
| *Globoturborotalita woodi* Jenkins | *Globorotalia scitula* (Brady) |
| *Globoturborotalita apertura* (Chshman) | *Paragloborotalia siakensis* (Le Roy) |
| *Globoturborotalita decoraperta* (Takayanagi & Saito) | *Paragloborotalia mayeri* (Cushman & Ellisor) |
| *Globoturborotalita druryi (*Akers) | *Paragloborotalia partimlabiata* (Ruggeri & Sprovieri) |
| *Globoturborotalita nepenthes* (Todd) | *Globorotalia menardii* s.l. |
| *Globigerinita glutinata* (Egger) | *Globorotalia* aff. *menardii* (Parker, Jones & Brady) |
| *Globigerinita uvula* (Ehrenberg) | *Globorotalia praemenardii praemenardii* Cushman & Stainforth |
| *Globoquadrina dehiscens* (Chapman, Parr & Collins) | *Globorotalia miozea miozea* Finlay |
| *Dentoglobigerina baromoenenis* (Le Roy) | *Orbulina suturalis* (Bronnimann) |
| *Globigerinella pseudobesa* (Salvatorini) | *Orbulina bilobata* (d'Orbigny) |
| *Globigerinella obesa* (Bolli) | *Turborotalita quinqueloba* (Natland) |
| *Orbulina universa* d'Orbigny | *Neogloboquadrina atlantica praeatlantica* Foresi, Iaccarino & Salvatorini |
| *Dentoglobigerina altispira altispira* (Cushman & Jarvis) | *Neogloboquadrina atlantica atlantica* (Berggren) |
| *Dentoglobigerina altispira globosa* (Bolli) | *Neogloboquadrina acostaensis* (Blow) |
| *Globigerinoides bolli* (Blow) | *Globigerinopsis aguasayensis* Bolli |
| *Globigerinoides sacculifer* (Brady) | *Catapsydrax parvulus* (Bolli) |
| *Globigerinoides quadrilobatus* (d'Orbigny) | *Clavatorella sturanii* (Giannelli & Salvatorini) |

and identify a series of paleoclimatic events of long and short duration that took place in the Mediterranean area during the latest Middle Miocene (Serravallian).

In addition, stable isotope analyses on bulk sediments were performed to integrate the planktonic foraminiferal data. In order to produce a more complete framework of the Middle Miocene period and to evaluate the degree of synchroneity and diachroneity of the paleoclimatic events between the Mediterranean and the oceanic records, we compared the Mediterranean data with those from Site 926 (Leg 154, Equatorial Atlantic Ocean), recently published by Turco *et al*. (2002), and Site 982B (Leg 162, North Atlantic Ocean), (Lirer, in progress).

## GEOLOGICAL SETTING AND LITHOLOGY OF THE STUDIED SECTION

This study has been performed on the Tremiti Islands, located in the southern Adriatic Sea, belonging to the Adria microplate which is bounded by the Hellenids to the east, and by the Apennines to the west (Channell *et al*., 1979; Platt *et al*., 1989; Gambini & Tozzi, 1996).

The sedimentary sequence cropping out on the Tremiti Islands, extends from the Paleogene to the Quaternary (Selli, 1971; Foresi *et al*., 2001; Iaccarino *et al*., 2001, among others). The Neogene succession is mostly represented by the Cretaccio Formation (Selli, 1971; Pampaloni, 1988; Iaccarino *et al*., 2001) whose sedimentation depth has been estimated about 1,000 meters by Russo *et al*. (2002).

The present study focuses on the S. Nicola composite Section which consists of two subsections (the Castle and Cemetery sections), cropping out on S. Nicola Island (Fig. 1), correlated to each other through biostratigraphic datum planes (calcareous plankton bioevents, Foresi *et al*., 2002a) (Fig. 2). These sections have been sampled and logged along different trajectories because of small faults. The detailed logging provides a continuous record for the entire investigated sequence (Lirer *et al*., 2002).

The section shows a sedimentary cyclicity characterised by clusters of a cyclic alternation of marls and marly limestones, distinguishable by the colour (grey/red) of the marly beds (Fig. 2). The basic small-scale cycle is a couplet (0.50-1.0 m thick) consisting of an indurated whitish marly limestone and a softer gray marl (Fig. 2). Red colored beds are often (but not always) intercalated in the limestones (Fig. 2). The red layers are considered sapropel equivalent and therefore correlate with precession minima (Lirer *et al*., 2002). The S. Nicola composite section has been astrochronologically calibrated between 12.605 Ma and 11.137 Ma (Lirer *et al*., 2002). The discover of distinct classic quadripartite cycles at the base of the Castle Section (0.50 to 5.8 m, cycles TR1-TR7) and from 13 m to 18.8 m (cycles 70-65) (Fig. 2) provided an up-to-date astronomical tuning. These small-scale cycles, well described in the lower Pliocene of Sicily (Hilgen, 1991a; 1991b), are quadripartite due to the intercalation of an additional grey-coloured, $CaCO_3$-poor marly-bed between the whitish, more indurated and carbonate-rich beds

**Table 3**. Comparision between the $\delta^{18}O$ and $\delta^{13}C$ values from the bulk-rock composition, the lithology and the time (my).

| Age (Ma) | LITHOLOGY | $\delta^{13}C$(V-PDB) | $\delta^{18}O$(PDB) |
|---|---|---|---|
| 12,383 | $CaCO_3$-rich marly limestones | -1,25 | -2,05 |
| 12,374 | $CaCO_3$-rich marly limestones | -0,93 | -1,69 |
| 12,355 | $CaCO_3$-rich marly limestones | -0,64 | -1,52 |
| 12,342 | $CaCO_3$-poor red marls | -0,53 | -1,22 |
| 12,31 | $CaCO_3$-rich marly limestones | -0,6 | -0,85 |
| 12,276 | $CaCO_3$-rich marly limestones | -1,03 | -1,71 |
| 12,242 | $CaCO_3$-rich marly limestones | -0,91 | -1,77 |
| 12,222 | $CaCO_3$-poor grey marls | -1,24 | -2,38 |
| 12,18 | $CaCO_3$-poor grey marls | -1,15 | -1,99 |
| 12,132 | $CaCO_3$-rich marly limestones | -0,99 | -1,61 |
| 12,0942 | $CaCO_3$-rich marly limestones | -1,16 | -1,68 |
| 12,025 | $CaCO_3$-poor red marls | -1,29 | -1,4 |
| 11,988 | $CaCO_3$-poor red marls | -2,13 | -1,09 |
| 11,98 | $CaCO_3$-rich marly limestones | -1,56 | -0,7 |
| 11,963 | $CaCO_3$-poor red marls | -1,35 | -0,28 |
| 11,952 | $CaCO_3$-poor red marls | -2,78 | -1,73 |
| 11,943 | $CaCO_3$-rich marly limestones | -0,97 | -0,17 |
| 11,929 | $CaCO_3$-rich marly limestones | -1,2 | -0,17 |
| 11,926 | $CaCO_3$-rich marly limestones | -1,19 | -0,44 |
| 11,9 | $CaCO_3$-rich marly limestones | -0,95 | -0,55 |
| 11,889 | $CaCO_3$-poor red marls | -1,59 | -1,86 |
| 11,865 | $CaCO_3$-rich marly limestones | -0,34 | -0,1 |
| 11,814 | $CaCO_3$-rich marly limestones | -0,7 | -0,39 |
| 11,771 | $CaCO_3$-poor grey marls | -1,79 | -1,91 |
| 11,765 | $CaCO_3$-rich marly limestones | -1,39 | -1,48 |
| 11,725 | $CaCO_3$-poor grey marls | -1,55 | -1,95 |
| 11,717 | $CaCO_3$-rich marly limestones | -1,15 | -1,23 |
| 11,71 | $CaCO_3$-rich marly limestones | -0,95 | -0,91 |
| 11,697 | $CaCO_3$-poor grey marls | -1,53 | -1,70 |
| 11,68 | $CaCO_3$-rich marly limestones | -1,01 | -1,05 |
| 11,671 | $CaCO_3$-rich marly limestones | -0,22 | -0,09 |
| 11,656 | $CaCO_3$-rich marly limestones | -0,64 | -0,38 |
| 11,643 | $CaCO_3$-rich marly limestones | -0,33 | -0,04 |
| 11,621 | $CaCO_3$-rich marly limestones | -0,39 | -0,11 |
| 11,5956 | homogeneous marls | -0,77 | -0,37 |
| 11,5864 | homogeneous marls | -1,44 | -1,36 |
| 11,568 | homogeneous marls | -1,14 | -0,85 |
| 11,5496 | homogeneous marls | -1,06 | -1,12 |
| 11,5224 | homogeneous marls | -1,34 | -1,64 |
| 11,4976 | homogeneous marls | -1,69 | -2,15 |
| 11,4728 | homogeneous marls | -0,33 | -0,77 |
| 11,4356 | homogeneous marls | -1,17 | -1,45 |
| 11,3612 | homogeneous marls | -1,71 | -1,93 |
| 11,3116 | homogeneous marls | -1,55 | -1,67 |
| 11,247 | homogeneous marls | 1,76 | 0,22 |

(Fig. 2). As the other basic cycles they were found to have an average duration of 21 ky and have been interpreted in terms of climatic variations induced by precessional cycles. Therefore, in the present work the labelling of the sedimentary cycles (Tab. 1) slightly differs from that of Lirer *et al*. (2002). For more details about the tuning see Lirer *et al*. (2002).

Diffractometric analyses carried out between cycle Tr2 and cycle Tr7, showed the presence of an ash layer between cycle Tr6 and cycle Tr7 (Fig. 2).

## MATHERIAL AND METHODS

### *Planktonic foraminifera*

Planktonic foraminiferal analysis has been performed on a total number of 469 samples collected at a mean interval of 10 cm, with a temporal resolution on the order of 4-5 ky. Quantitative analysis was carried out on splits of the > 125 μm fraction. Taxon abundance is expressed as a percentage of the total planktonic fauna.

To perform this analysis we preferred: 1) to avoid counting the fraction <125μm which is mainly composed by juvenile specimens not easy to determine. In this way the percentage of small-size adult forms (i.e., *T. quinqueloba*) is altered; 2) to adopt taxonomic units which group taxa very similar in morphology and/or phylogenetically related (see Foresi *et al*., 2002a).

For a reliable quantitative analysis it is necessary to adopt a wide taxonomic concept, which remains unchanged even under poor preservational conditions and taxonomical problems. For this reason we introduced some supraspecific categories (Foresi *et al*., 2002a), reducing the number of species really present in the planktonic foraminiferal data set. The categories used in this paper are reported in table 2 and the percentages of planktonic foraminiferal abundance versus time are plotted in Figure 3.

The planktonic assemblage is abundant and the preservation is generally better in the grey/red marly layers than in the whitish limestones, where foraminifera are often filled or sometimes even recrystallized. The percentages of foraminiferal fragments and indeterminable specimens are very low and do not alter the composition of the assemblage.

### *Stable isotope analyses*

Forty-five samples were analysed for their oxygen and carbon isotope composition of the (bulk) calcium carbonate. The samples are collected in the whitish $CaCO_3$-rich marly limestones and in the red $CaCO_3$ –poor marls (Tab. 3).

The samples, previously powdered, were analysed according to well-established techniques (McCrea, 1950; Epstein *et al*., 1953), which include a preliminary roasting *in vacuo* at 350°C for about 45 minutes to pyrolize the organic matter, an overnight reaction of $CaCO_3$ with 100% $H_3PO_4$ to produce $CO_2$, and its measurement in a Finnigan Delta S mass spectrometer for the determination of the $^{18}O/^{16}O$ and $^{13}C/^{12}C$ ratios. The isotope measurements on purified $CO_2$ samples were carried out by means of a double-inlet system mass spectrometer versus a laboratory standard ($CO_2$ from a very pure Carrara marble periodically calibrated versus NBS-19 and NBS-20 standards). The results obtained are reported in terms of per mil deviation ( units) relative to the PDB-1 isotope standard (both oxygen and carbon). The mean value of the standard deviation is close to ±0.04 ‰ (1).

### *Statistical Analysis*

The statistical approach to obtain the highest amount of informations among the wide data set, is the Principal Component Analysis (PCA). This method involves a mathematical procedure that transforms a number of (possibly) correlated variables into a (small) number of uncorrelated variables called principal components. The first principal component accounts for as much as possible of the variability in the data as possible, and each succeeding component accounts as much as possible of the remaining variability as possible. The standardised Principal Component Analysis (PCA) applied to our data, has been used to extract the main components from the planktonic foraminiferal abundance pattern.

In addition, the Cluster Analysis (Pearson correlation) has been applied to find a relation between different variables and to sort out the variables in clusters.

## PRINCIPAL COMPONENT AND CLUSTER ANALYSIS

Standard SPSS computer software (realise 10.0) was used to run statistical analyses on relative frequency data, as an aid to define planktonic assemblages. The original data set contains 45 variables (see Tab. 2), consisting of species and categories of species. For a hierarchical cluster analysis, indeterminate forms and species occurring in frequency below 2% were omitted, obtaining 23 categories. The reduced data set was introduced into factor analysis, with the purpose of describing the major trends in planktonic faunal development. Unrotated factor scores of the first two axes were considered.

The first principal component PCA-1 describes 16.9% of the total variance (Tab. 4). Taxa with negative loading are those which show a progressively upward decrease in percentage (the *Dentogloboquadrina altispira* gr., *Globoquadrina dehiscens dehiscens*, *Globigerinella obesa*, *Orbulina* spp.) or taxa mainly occurring in the lower part of the studied section (*Paragloborotalia mayeri*, *P. partimlabiata*,

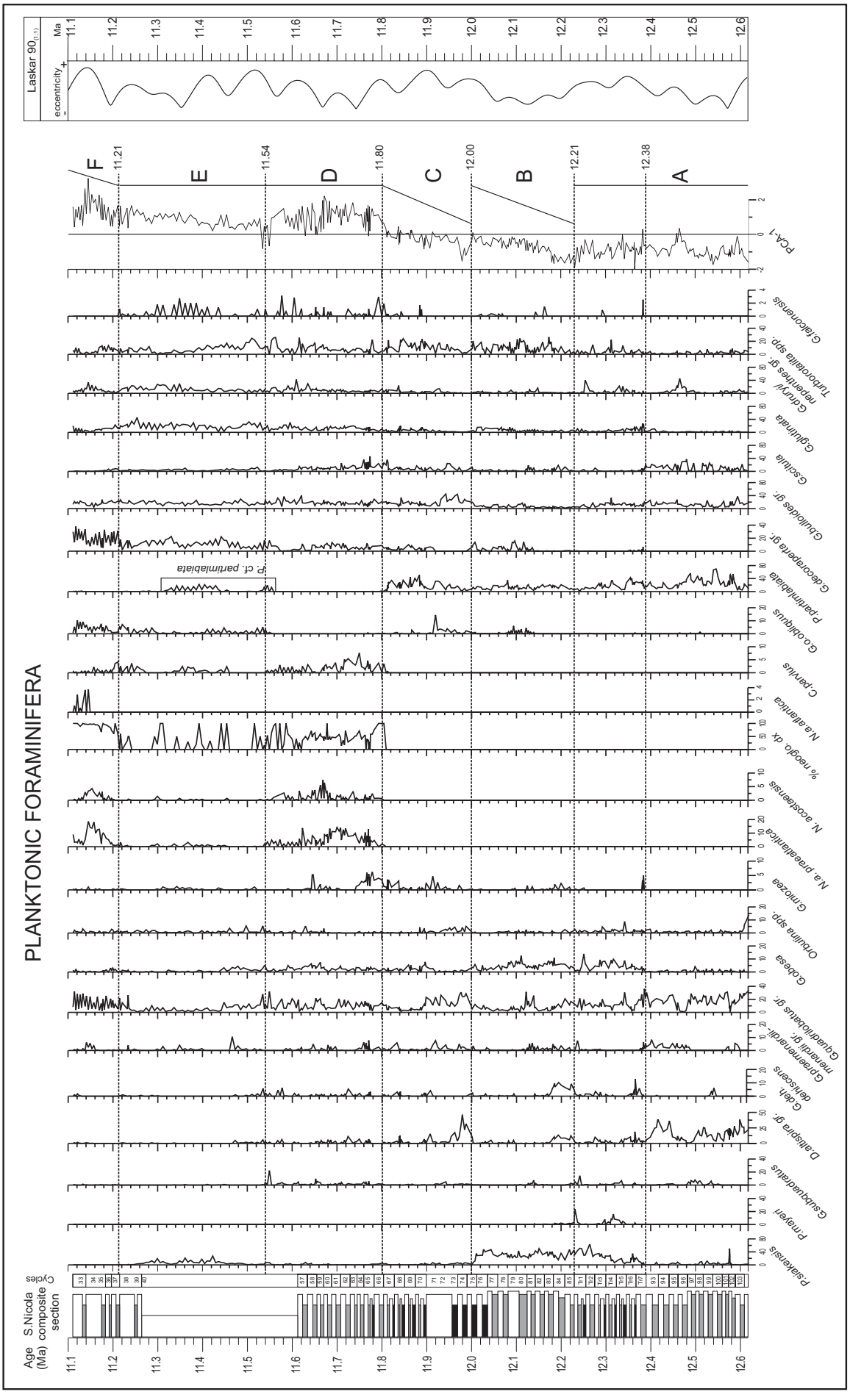


**Figure 3**. Quantitative distribution of planktonic foraminifera (as % of the total planktonic foraminiferal assemblage) plotted versus the PCA-1 score plot and the eccentricity curve of Laskar et al. (1993).

**Table 4.** Statistical Analysis results: loadings of planktonic foraminiferal taxa on the first principal component axis (PCA-1) resulting from a principal component analysis carried out on the total census data.

| Variables | PCA-1 |
|---|---|
| *G. falconensis* | 0,160303 |
| *G. glutinata* | 0,586936 |
| *G. miozea* | 0,251032 |
| *G. obliquus obliquus* | 0,24366 |
| *C. parvulus* | 0,529417 |
| *G. bulloides* gr. | 0,399372 |
| *N. acostaensis* | 0,566355 |
| *N a. praeatlantica* | 0,671334 |
| *N. atlantica atlanatica* | 0,222497 |
| *G. druryi-nepenthes* gr. | 0,53146 |
| *Turbolotalita* spp. | 0,248104 |
| *G. decoraperta* gr. | 0,702487 |
| *G. obesa* | -0,284267 |
| *G. quadrilobatus* gr. | -0,340435 |
| *Orbulina* spp. | -0,269703 |
| *G. scitula* | -0,008963 |
| *P. partimlabiata* | -0,600616 |
| *P. mayeri* | -0,228418 |
| *P. siakensis* | -0,44222 |
| *G. menardii-praemenardii* | -0,016074 |
| *D. altispira* gr. | -0,522631 |
| *G. dehiscens dehiscens* | -0,315968 |
| *G. subquadratus* | -0,188563 |
| Variance | 16,9% |

and *P. siakensis*), (Fig. 3). Taxa having positive loading show a progressive increase in percentage in the upper part of the studied record (*Catapsydrax parvulus*, *Globigerinoides obliquus obliquus*, *Globigerinita glutinata*, the *Globoturborotalita decoraperta* gr., the *G. druryi/nepenthes* gr., and neogloboquadrinids) (Fig. 3).

The planktonic foraminiferal assemblage clearly reflects the long-term change in the faunal pattern. In fact, *P. siakensis*, *G. obesa* and the *D. altispira* gr. dominate the lower part of PCA-1 (negative loading) while, on the contrary, the neogloboquadrinids, *G. obliquus obliquus* and the *G. decoraperta* gr. dominate the upper part of PCA-1 (positive loading). The change from assemblage with negative loading to assemblage with positive loading occurs through different steps superimposed on the overall long-term trend.

The long-term trend of PCA-1 score plot (Fig. 3) reveals that the faunal composition changes significantly at 11.8 Ma, in correspondence of the first influx of the neogloboquadrinids (*Neogloboquadrina acostaensis* and *N. atlantica praeatlantica*) (Hilgen *et al*., 2000; Lirer *et al*., 2002; Foresi *et al*., 2002a), coinciding with the onset of the Mi5 event (Turco *et al*., 2001) and in correspondence of the exit from the Mediterranean of *P. siakensis* at 11.21 Ma (Fig. 3). The short-term fluctuations in PCA-1 score plot reflect periodic changes in the plankton communities, forced by astronomical oscillations of the orbital parameters.

The hierarchical cluster analysis (Pearson correlation) performed on our taxa (23 variables), produced two different clusters (Fig. 4): cluster I groups *C. parvulus, Globorotalia scitula*, *G. miozea*, the *G. praemenardii-menardii* gr., the *Globigerina bulloides* gr. *G. falconensis*, *Globigerinoides obliquus obliquus, G. glutinata*, the *G. decoraperta* gr., the *G. druryi/nepenthes* gr., *Neogloboquadrina acostaensis*, *N. atlantica praeatlantica*, and *Turborotalita* spp. which show an upward increase; cluster II groups warm water forms (*D. altispira* gr., *G. dehiscens dehiscens*, *Orbulina* spp., *G. obesa*, *P. mayeri*, *P. partimlabiata*, *P. siakensis*, the *Globigerinoides quadrilobatus* gr. and *G. subquadratus* ) which progressively decrease in the upper part of the section studied. In this cluster, *P. partimlabiata* and *P. siakensis* belong to the same cluster but different subclusters.

Within cluster I, a small cluster Ia is detectable (Fig. 4). This cluster includes *G. miozea*, the *G. praemenardii-menardii* gr., *G. scitula* and *G. falconensis* which show abundance peaks in correspondence of the first influx of the neogloboquadrinids (Fig. 3).

The PCA-2 and PCA-3 have been omitted because the low values in the total variance render very difficult their interpretation.

## FAUNAL CHANGES

The main changes in the planktonic foraminiferal abundance pattern are related to the distribution of taxa having biostratigraphic significance (Fig. 3). The taxa (more or less continuously present) like the *G. bulloides* gr. the *G. decoraperta* gr., the *G. druryi-nepenthes* gr., *G. glutinata*, and *Turborotalita* spp. show an overall increase upward. Among the taxa having a discontinuous distribution, *G. falconenis*, *G. obliquus obliquus*, *G. subquadratus*, *G. miozea*, the *G. praemenardii-menardii* gr., *Orbulina* spp., *P. mayeri, P. siakensis*, *P. partimlabiata*, the *D. altispira* gr., and *G. dehiscens dehiscens*, *G. obesa* rhythmically or occasionally reach significant percentages.

From 12.62 Ma to 11.80 Ma, the negative loading is dominated by warm assemblages while from 11.80 Ma upwards, the positive loading is associated with an assemblage mainly dominated by typical cool water taxa (Fig. 3 and Tab. 3).

Six intervals (A to F) were distinguished in the long-term trend of PCA-1.

The lowest interval A, between 12.62 Ma (base of the section) and 12.21 Ma shows several oscillations in PCA-1 score plot (Fig. 3), reflecting short-term

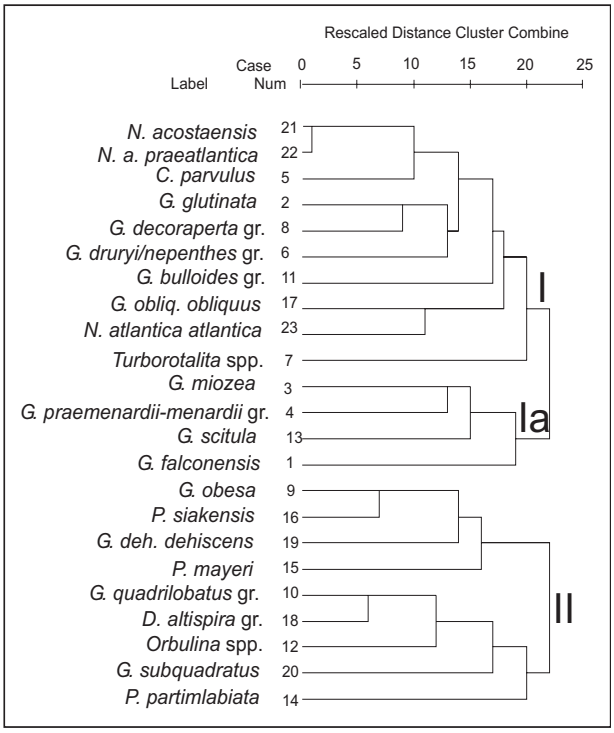


**Figure 4.** Dendrogram resulting from cluster analysis.

changes in faunal composition. This interval is mainly composed by *P. siakensis*, the *D. altispira* gr., the *G. quadrilobatus* gr., *G. obesa* and minor by *G. dehiscens dehiscens*, the *G. praemenardii-menardii* gr. and *Orbulina* spp.. In particular the *G. quadrilobatus* gr., *G. obesa* and *Orbulina* spp. are living species proliferating in surface, nutrient-depleted warm-oligotrophic waters (Bé, 1977; Hemleben *et al*., 1988; Rohling & Gieskes, 1989; Pujol & Vergnaud-Grazzini, 1995) and were abundant during the sapropel deposition in the Late Miocene-Pliocene (Sierro *et al*., 1999, 2003 and reference therein), while the fossil species *P. siakensis*, the *D. altispira* gr., the *G. praemenardii-menardii* gr. and *G. dehiscens dehiscens* were abundant in tropical Miocene oceans (Keller, 1985; Savin *et al*., 1985; Turco *et al*., 2002). As previously reported, these warm taxa, excluding the *G. quadrilobatus* gr., show a discontinuous distribution reaching high abundance values only in short intervals (Fig. 3).

As concerns the long-term trend of warm taxa, the *D. altispira* gr. and the *G. quadrilobatus* gr. are abundant in the lower part of this interval, while *P. siakensis* and *G. obesa* are more common in the upper part (between 12.38 Ma and 12.21 Ma) (Fig. 3). This vicariance is clearly visible also in the subsequent interval B (Fig. 3).

The cool water taxa are represented by *G. scitula* and the *G. bulloides* gr. which presently bloom during spring and winter in the western Mediterranean (Cifelli, 1974; Thunell, 1978; Rohling & Gieskes, 1989; Pujol & Vergnaud-Grazzini, 1995); in particular, *G. scitula* is a bathypelagic species and *G. bulloides* lives in upwelling regions (Hemleben *et al*., 1988). The first species vicariant with *G. glutinata* is present between 12.62 Ma and 12.38 Ma, while the second one is continuously common from the base up to the top of interval A (Fig. 3). Interval A is also characterised by *P. partimlabiata* which is continuously common to abundant throughout. This taxon which shows an opposite trend to the *D. altispira* gr. and *P. siakensis*, reaches maximum values when the PCA-1 has the most negative loading suggesting a temperate (intermediate) habitat for *P. partimlabiata* (Fig. 3). The cluster analysis, which places *P. partimlabiata* and *P. siakensis* in the same cluster but in different subclusters, supports this hypothesis. Therefore, in this interval cooler and warmer water taxa co-exist but the latter show the highest percentages.

In the subsequent interval B, from 12.21 to 12.00 Ma (Fig. 3), the influence of cool water taxa is more visible; the PCA-1 score plot shows a progressive increase from more negative to less negative values. Although *P. siakensis* and *G. obesa* are continuously present, the *G. decoraperta* gr., the *G. bulloides* gr. and *Turborotalita* spp. (this taxon reach highest concentrations in upwelling regions or in areas of vigorous vertical mixing in water column, see Reynolds & Thunell, 1986) show a sharp increase in abundance reaching a mean value of 30-40% of the total fauna (Fig. 3). By contrast, the *G. quadrilobatus* gr. shows a decrease in abundance (Fig. 3). As in the previous interval *G. glutinata* and *G. scitula* have an opposite trend (Fig. 3).

The subsequent interval C (Fig. 3), from 12.00 Ma to 11.80 Ma, is marked by a drop in the abundance of *P. siakensis* and an increase in *P. partimlabiata*. This interval shows a further cooling trend as testified by the progressive increase in abundance of *G. scitula*, *Turborotalita* spp., the *G. bulloides* gr. and the *G. decoraperta* gr., and by contrast, the progressive decrease or absence of typical Middle Miocene warm water taxa (Fig. 3). The negative loading of the PCA-1 score plot moving towards positive loading might indicate a fast transition to a pronounced climatic cooling at around 11.80 Ma (Fig. 3).

Interval D, from 11.80 Ma to 11.54 Ma, has a positive loading in the PCA-1 score plot, mainly controlled by the first influx of the neogloboquadrinids. The extant neogloboquadrinids living today, reach their highest concentration in stratified water and are abundant at depth, during spring and winter in western Mediterranean when the DCM (Depth Clorophil Maximum) develops (Thunell, 1978; Rohling & Gieskes, 1989; Pujol & Vergnaud Grazzini, 1995; Sierro *et al*., 2003).

As described by Foresi *et al*. (2002a) and according to Hilgen *et al*. (2000) and Turco *et al*. (2001) the earliest neogloboquadrinids have random coiling and are dominated by *Neogloboquadrina atlantica*

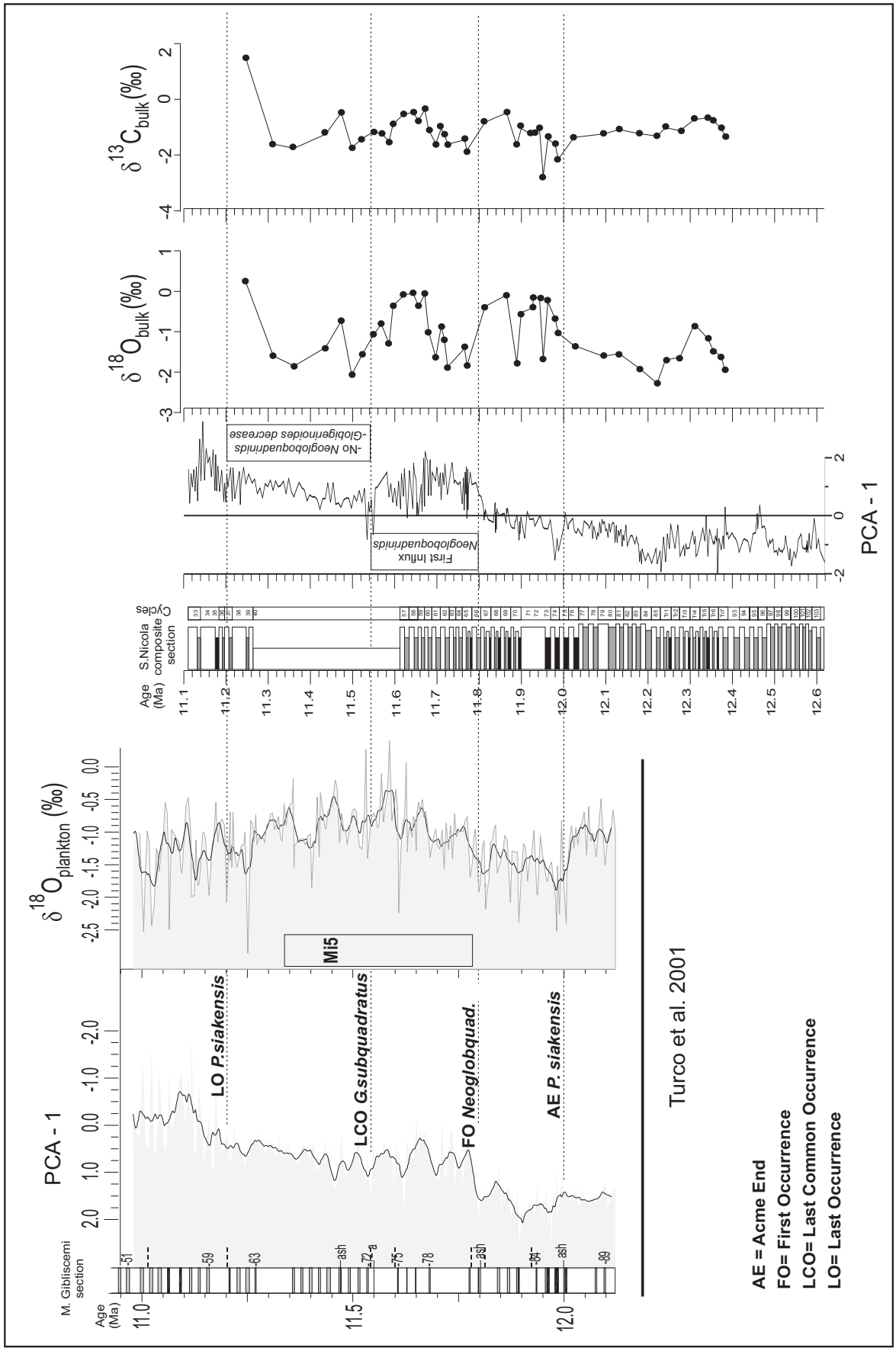


**Figure 5**. Comparison between the score plot of PCA-1, the planktonic oxygen isotope records of Turco *et al.* (2001) and the score plot of PCA-1 and the oxygen and carbon isotope records of bulk-rock of the present work plotted versus time (Ma). See Figure 2 for the age model.

*praeatlantica*, associated with *Neogloboquadrina*-four chambers of Hilgen *et al*. (2000), and *N. acostaensis* s.s. (Fig. 3).

The overlying interval E, from 11.54 Ma to 11.21 Ma (Fig. 3) is characterised by the absence of neogloboquadrinids and by a drastic decrease in the abundance of *G. quadrilobatus* group, while the cool water species, the *G. bulloides* gr., *G. glutinata*, the *G. decoraperta* gr., the G. *druryi-nepenthes* gr. and *Turborotalita* spp. remain abundant (Fig. 3).

The latest interval F, from 11.21 Ma up to 11.12 Ma is characterised by the exit from the Mediterranean area of *P. siakensis* and by the second influx of dextral coiled neogloboquadrinids and later on by the first arrival of *Neogloboquadrina atlantica atlantica* (Fig. 3). This interval is also characterised by a further increase in typical subtropical water taxa like *G. obliquus obliquus* and the *G. decoraperta* gr., and wide fluctuations of the *G. quadrilobatus* gr. (Fig. 3).

## ISOTOPE DATA

The stable isotope results reflect the bulk-rock composition and even though bulk values reflect a mixing of carbonate from different sources, it has been shown that as it concerns calcareous oozes, the isotopic composition derived from bulk analyses closely resembles the record derived from single foraminiferal analyses (Shackleton & Hall, 1984; Shackleton *et al*., 1993). In fact the bulk isotopic composition is a function of the abundance of calcareous nannofossils, benthic and planktonic foraminifera.

The stable isotope data are reported numerically in Table 2 and graphically in Figure 5. The low number of the samples measured prevents a detailed interpretation of the curve. The time resolution between samples is about 30-40 kyr between 12.40 Ma and 12.00 Ma and about 10 kyr between 12.00 Ma and 11.95 Ma encompassing the Mi5 event (Fig. 5).

The oxygen isotope record shows a total range of 2.6 ‰, from –2.38‰ to +0.22‰ with a mean value of –1.14 ± 0.70 ‰. The pattern of the values is quite similar to that obtained by Turco *et al*. (2001) from Mediterranean deep marine sediments of the same age (Fig. 5).

This result confirms that the $\delta^{18}O$ isotopic values from the S. Nicola composite Section are mainly function of calcareous planktonic composition. In addition, the P/B+Bx100 ratio ranging between 94% and 98% supports this result.

Despite the low resolution of the $\delta^{18}O$ record, the oxygen isotope curve shows two main groups of values, the most negative with a mean value of about -1.7±0.2 ‰, the less negative around -0.2±0.2‰ and three distinct intervals are visible (Fig. 5).

In the interval between 12.40 Ma and 12.00 Ma the $\delta^{18}O$ signal is marked by light values suggesting a general warm condition (excluding the less negative $\delta^{18}O$ value at 12.31 Ma, Tab. 2) supported by the negative PCA-1 score plot (interval mainly dominated by warm water taxa, see Fig. 3).

In the overlying interval, between 12.00 Ma and 11.55 Ma the oxygen isotope record reveals a long interval mainly characterised by more positive $\delta^{18}O$ values (mean value of -0.43‰) (Fig. 5). This interval seems to reflect the progressive cooling observed in the planktonic assemblage: first, at 12.00 Ma (AE of *P. siakensis*) and later on at 11.80 Ma (first influx of the neogloboquadrinids) (Fig. 3), clearly evident in the PCA-1 score plot (Fig. 5). The two sharp negative excursions at 11.952 Ma (cycle 73) and at 11.889 Ma (cycle 70) and between 11.77 Ma and 11.70 Ma (cycle 65 to cycle 61) (Tab. 2), which seem not support this cooling, reflect the $\delta^{18}O$ signal generally lighter than the red/grey marly layers (sapropel equivalent).

The subsequent interval between 11.55 Ma and 11.25 Ma (third interval) is characterised by high fluctuations in $\delta^{18}O$ from –2.15‰ to +0.22‰. The oxygen isotope curve shows that this interval is mainly characterised by more negative $\delta^{18}O$ values than the first interval (see Fig. 5). Comparing our data with those from the M. Gibliscemi section (Turco *et al*., 2001), the two trends look quite comparable (Fig. 5).

The variation of the $\delta^{18}O$ values in these intervals is quite large and cannot be only ascribed to a decrease in the sea surface temperature. In fact, these isotopic shifts would require a change of the water temperature of 5.5 to 8 °C which is unlikely for two main reasons: the relatively short time intervals and the enormous impact that these temperature changes should have had on the marine fauna. There is no evidence of such an impact. Changes in the oxygen isotopic composition of seawater are the only alternative cause to be taken into account. The most negative $\delta^{18}O$ values could be referred to periods of sensible inflow of continental waters and the transition towards more positive values could be referred to a decreasing inflow of continental water or, alternatively, to an increasing evaporation effect. One should bear in mind that nowadays the excess evaporation in the Mediterranean is more than one meter of water per year and that the impact of this process on the $\delta^{18}O$ of seawater ranges between about +0.5‰ in the western basin to about+1.5‰ in the eastern basin (Garrett *et al*., 1993).

The partial positive relationship existing between $\delta^{18}O$ and $\delta^{13}C$ well agrees with the hypothesis of a variable contribution of runoff associated to a variable contribution of $\delta^{12}C$ enriched in dissolved carbon that is characteristic of the continental water masses.

The same positive correlation was found in diffe-

**Table 5**. Selected surface and intermediate planktonic species prefering a specific depth as their primary habitat (Gasperi & Kennett, 1992).

| Planktonic foraminifera |
|---|
| surface species |
| *Dentoglobigerina altispira* gr. |
| *Globigerinoides* spp. |
| *Paragloborotalia siakensis* |
| *Orbulina* spp. |
| intermediate species |
| *Globorotalia menardii* |
| *Globoquadrina dehiscens dehiscens* |
| Neogloboquadrinids spp. |
| *Globigerina druryi/nepenthes* |
| *Globigerina bulloides* gr. |

rent Mediterranean cores of Quaternary age by Devaux (1985), Vergnaud-Grazzini *et al*. (1986, 1988) and in cores of Middle Miocene age from the Pacific (Flower & Kennett, 1993).

The two rather abrupt negative values of $\delta^{18}O$ at ll.889 Ma and ll.952 Ma combined with the similar changes in the carbon isotopic composition which varies between –2.78 and -1.59‰ with a mean value of –2.185±0.76 (Fig. 5) are not in favour of a strong climatic change.

## VARIATION OF EUTROPHIC-OLIGOTROPHIC CONDITIONS

In order to better constrain and better understand the change from warm to cold climatic conditions, the ratio between the warm-oligotrophic planktonic foraminifera (*Orbulina* spp., the *G. quadrilobatus* gr.) and the cold-eutrophic (neogloboquadrinids, *G. glutinata*, the *G. bulloides* gr., *Turborotalita* spp.) plus warm-oligotrophic planktonic species was calculated (Fig. 6).

When the ratio is 0, the assemblage is dominated by cold-eutrophic planktonic foraminifera, while the ratio is 1 when warm-oligotrophic planktonic foraminifera form nearly 100% of the association. This index (Sierro *et al*., 2003) provides a good record for the estimation of the progressive but constant deterioration of the climate from 12.62 Ma up to 11.12 Ma (Fig. 6). In fact, even if several oscillations are present, the straight-line trend shows a gradual upward decrease of the warm water taxa in the total assemblage.

According to Sierro *et al*. (1999, 2003), the maximum values of the ratio (highest values of warm-oligotrophic planktonic foraminifera) occur in the red layers (sapropels equivalent) supporting the hypothesis of warm surface water during their deposition. Starting from this tie point, clearly evident in our sedimentary record (Fig. 7), we tentatively tried to interpret the response of the planktonic assemblage in terms of lithological changing. We focused our interpretation to the middle part of the studied section between cycle Tr7 and cycle 77 (Fig. 7).

In the quadripartite cycles, in proximity of the middle-upper part of the red layers where higher values of warm-oligotrophic foraminifera occur, *P. siakensis* has low values. The white carbonate beds above the red or grey layers are characterised by an abundance of *P. siakensis* and by the increase in abundance of the *G. bulloides* gr., *Turborotalita* spp., *G. glutinata*, the *G. druryi/nepenthes* gr. and *G. scitula* (Fig. 7).

The grey layers intercalated with the white carbonate beds are characterised by the increase of *G. scitula*, and *P. partimlabiata,* and decrease of *P. siakensis* as in the red marls. These data indicate that *P. siakensis* is not a typical oligotrophic taxon, reaching the maximum abundance values in the white carbonate beds, where generally eutrophic conditions prevail. The increase in *P. partimlabiata* occurs just below the transition between white carbonate and grey beds.

During low amplitude summer insolation (cycle 85 to cycle 77, in Fig. 7), when the interference between obliquity and precession occurs, the sedimentary cycles are characterised by thicker and more prominent white carbonate beds. In this case, where the red layers (sapropel equivalent) are not recorded, the maxima of warm-oligotrophic planktonic foraminifera occur mainly within the white carbonate beds (i.e. cycles 77, 78, 79, 81, 82, 83, 84, 85) (Fig. 7). At present this relation is not evident.

## SURFACE AND INTERMEDIATE FORAMINIFERA

Planktonic foraminiferal species are known to prefer a specific depth as their primary habitat (Fairbanks *et al*., 1982; Hemleben *et al*., 1988). Therefore, changes in depth and shape of the ther-

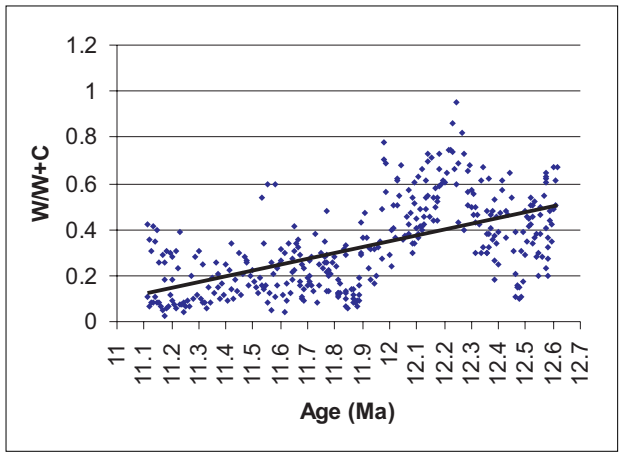


**Figure 6.** Warm-oligotrophic/warm-oligotrophic plus cold-eutrophic foraminifera plotted versus time (Ma). See Figure 2 for the age model.

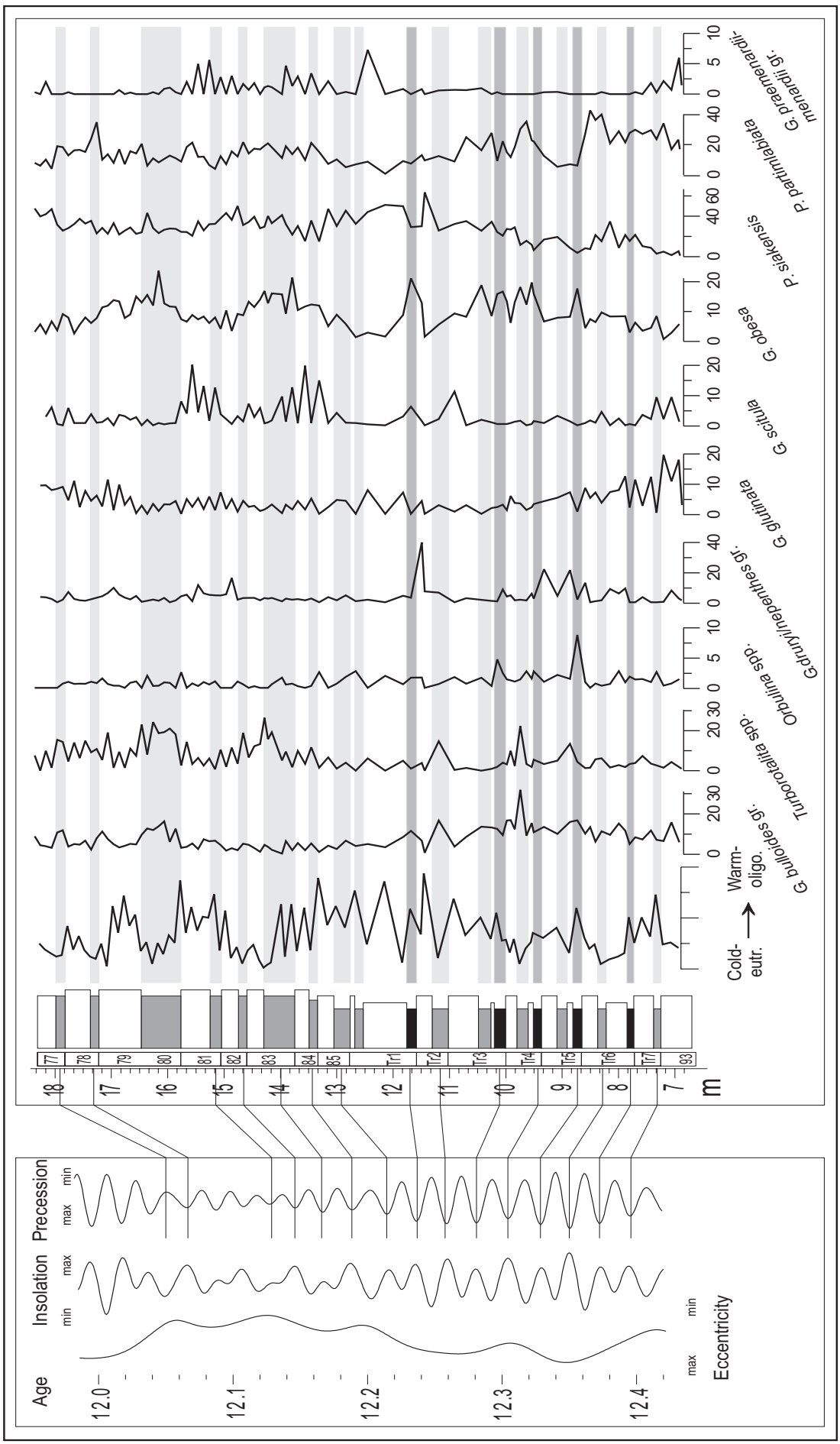


**Figure 7**. Long and short term trend of 10 planktonic foraminiferal species and distribution of the warm-oligotrophic foraminifera plotted against selected astronomically calibrated lithological cycles (cycles 93-77).

mocline are expected to affect the composition of the planktonic foraminiferal assemblage (Chaisson & Ravelo, 1997; Ravelo & Fairbanks, 1992) as well as their $\delta^{18}O$ value (Chaisson & Ravelo, 1997; Fairbanks *et al*., 1982).

The living habitat of Miocene planktonic foraminifera has been provided by Keller (1985), Gasperi & Kennett (1992) and Hemleben *et al*. (1988), who collected information from the isotopic analyses of various species of this time interval. Surface and intermediate water planktonic foraminifera are reported in Table 5.

Plotting separately these species we obtained two curves (Fig. 8b) which show an opposite trend at about 11.96 Ma. The surface species are more abundant in the lower part of the section and the intermediate in the upper part of the section. The peaks are controlled by the distribution of the *G. quadrilobatus* gr. and the *D. altispira* gr. (see the negative peaks between 12.45 and 12.50 Ma and the positive peaks between 11.96 and 12.00 Ma). Moreover, we plotted separately the warm and cold intermediate species and the two curves show the same trend as the previous one: the warm intermediate species are dominant in the lowest part of the section.

The interval from 12.62 Ma to 11.96 Ma is mainly dominated by surface species (Fig. 8b) and in particular by warm intermediate species (the *G. praemenardii-menardii* gr. and *G. dehiscens dehiscens*) (Fig.8c). In particular, from 12.62 Ma to 12.30 Ma (interval of eccentricity minimum), surface (mainly the *G. quadrilobatus* gr. and the *D. altispira* gr.) and intermediate (*G. bulloides* gr.) taxa show wide fluctuations, while from 12.30 Ma to 11.95 Ma the surface species (Fig. 8b) are dominant. Nevertheless from 12.03 Ma up to 11.95 Ma the intermediate species (and in particular the cold intermediate species, Fig. 8c) start to increase in abundance (Fig. 8b).

At 11.96 Ma the surface-dweller species drop down in abundance and the assemblages are replaced by cold intermediate species (neogloboquadrinids, the *G. druryi/nepenthes* gr. and the *G. bulloides* gr.) (Fig.8b and c) which continuously increase up to 11.60 Ma. From 11.60 Ma up to 11.22 Ma the cold intermediate species remain the most abundant but show a visible decrease. In the uppermost part of the section the cold species show again a remarkable increase in abundance (Fig. 8c).

In order to better constrain and understand the water mass changes, we compared the PCA-1 score plot, the bulk-rock $\delta^{18}O$ record, and the abundance curves of the surface and intermediate species (Figs. 8a, b and c).

The interval from 12.62 Ma to 11.96 Ma is characterised by surface dwellers and by warm intermediate species pointing to overall warm conditions as indicated by the PCA-1 score plot (Fig.8a) and by the trend of the $\delta^{18}O$ which in this interval shows the most negative values. In the upper part of the interval, the progressive change of the $\delta^{18}O$ values, from more negative to less negative and the score plot of PCA-1 are in agreement with the increase of cold intermediate species (Fig. 8c) and indicate an upward change to cooler conditions (Fig. 8b).

From 11.96 Ma to 11.80 Ma upward, the assemblage composition as the score plot of PCA-1 and the $\delta^{18}O$ values indicate a remarkable change that is interpreted as a strong cooling of the surface water masses recalling at the surface the cold intermediate species.

In the interval from 11.96 Ma up to the top of the section, both the planktonic assemblage and the score plot of PCA-1 confirm the lowering of the surface temperature of the water-mass. In particular from 11.60 Ma to 11.20 Ma the two curves show the same trend. Also the $\delta^{18}O$ values even if show wide fluctuations between 11.54 Ma and 11.21 Ma (Fig. 8b), interpreted as an intensification of runoff, are less negative than in the previous interval. To understand the nature of such fluctuations we excluded all the samples from the red/grey layers (sapropel equivalent) analysing only the samples from the white carbonate beds. The obtained smothed curve of $\delta^{18}O$ shows higher values between 11.25 Ma and 11.60 Ma following more closely the curve of the cold intermediate species. This relationship confirms that the increase of cold intermediate species is clearly function of the sea surface cooling (Fig. 8b, c).

## COMPARISON BETWEEN MEDITERRANEAN, EQUATORIAL AND NORTH ATLANTIC OCEANS

In order to attempt a paleoceanographic reconstruction of the late Middle Miocene of the Atlantic-Mediterranean area the different data (ecologic, climatic, biostratigraphic) from the Mediterranean area (Hilgen *et al*., 2000; Lirer *et al*., 2002; Foresi *et al*., 2002a) and Site 926 (Turco *et al*., 2002) are compared. Additionally, the preliminary biostratigraphic results of a high-resolution study (Lirer, in progress) recorded in Site 982B Leg 182 (Fig. 1) has been considered assuming that the Mediterranean age model can be applied to the North Atlantic realm.

To achieve this reconstruction we used the following biostratigraphic events: the LO of *G. peripheroronda*, FO and LO of *P. partimlabiata*, FO and LO of *P. mayeri*, FO of *N. atlantica praeatlantica* and FO of *N. acostaensis*.

In the North Atlantic Ocean, the FO of *N. atlantica praeatlantica* occurs within the short range of *P. mayeri* (12.38-12.14 Ma) and predates the FO of *N. acostaensis*. In the Mediterranean area the FO of *N. atlantica praeatlantica* and the FO of *N. acostaensis*

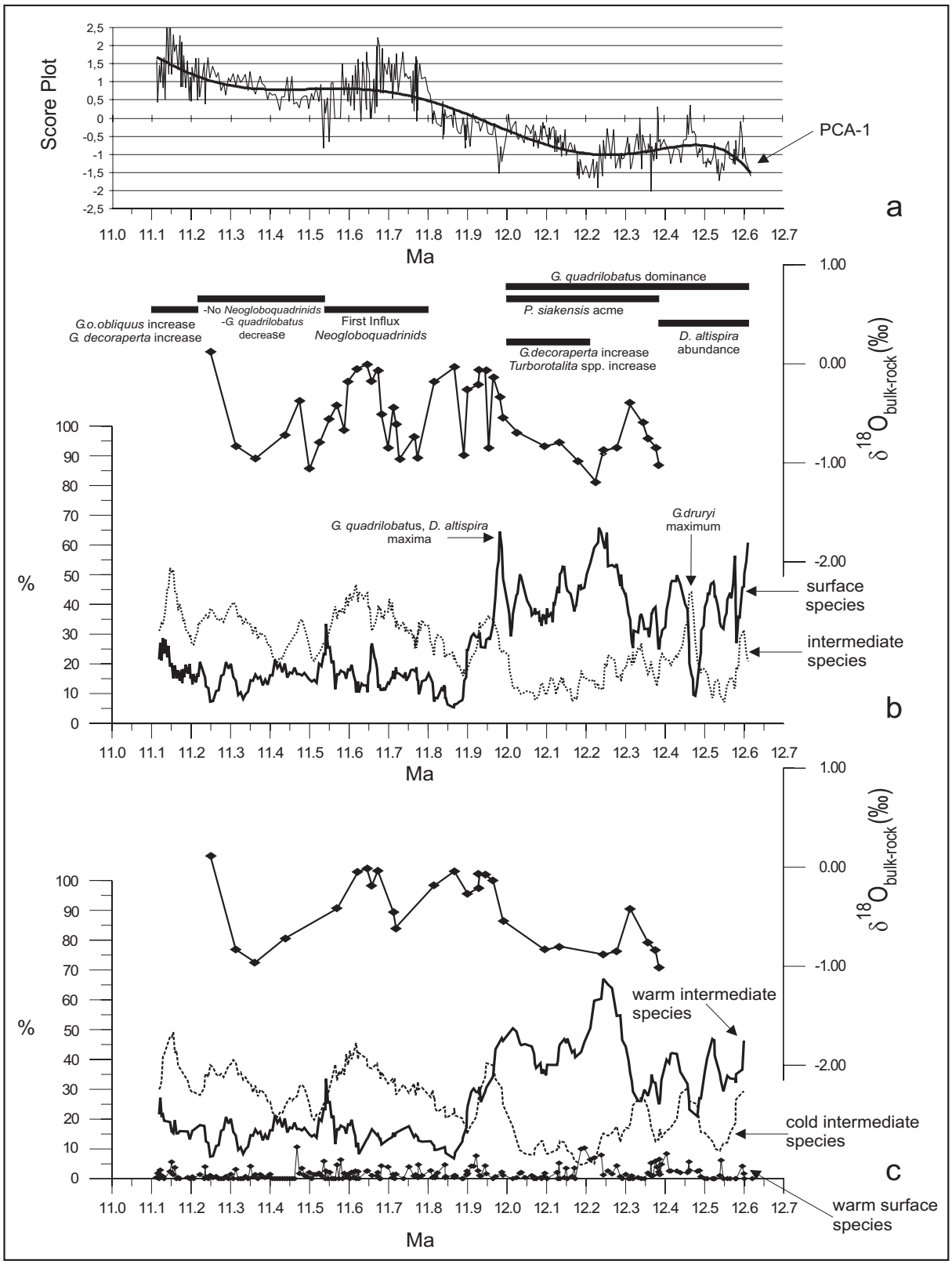


**Figure 8**. ***a***: PCA-1 score plot curve plotted versus time (Ma) with superimposed a polyline; ***b***: Comparison between the oxygen stable isotope record (thick line with diamonds), the intermediate species smoothed with a 8 point moving average (dotted line): *G. praemenardii-menardii* gr., *G. dehiscens dehiscens*, neogloboquadrinids , *G. druryi/nepenthes* gr., *G. bulloides* gr. and surface species smoothed with a 8 point moving average (thick line): *D. altispira* gr., *Globigerinoides* spp., *P. siakensis*, *Orbulina* spp; ***c***: Comparison between the oxygen stable isotope record (thick line with diamonds), warm surface species (thin line with dark diamonds): *D. altispira* gr., *Globigerinoides* spp., *P. siakensis*, *Orbulina* spp., the warm intermediate species smoothed with a 8 point moving average (thick line): *G. praemenardii-menardii* gr., *G. dehiscens dehiscens,* and the cold intermediate species smoothed with a 8 point moving average (dotted line): neogloboquadrinids , *G. druryi/nepenthes* gr., *G. bulloides* gr.. In this last graphic (c) we excluded the samples falling in the red and grey layers.

occur at the same level. Both in the Mediterranean and North Atlantic Ocean, the FO of *N. acostaensis* coincides with the LO of *P. partimlabiata* (11.80 Ma, Lirer *et al*., 2002; Foresi *et al*., 2002a). In the Equatorial Atlantic Ocean *P. mayeri* and *N. atlantica praeatlantica* are absent and are replaced by the lineage of *G. foshi*.

In the Equatorial Atlantic Ocean the high abundance of warm water species (*P. siakensis*, *Sphaerodinellopsis* spp. and the *G. foshi* gr.) indicates warm surface water mass which prevents habitat of the neogloboquadrinids (in fact, *N. acostaensis* the only representative of the group, first occurs only at 9.89 Ma, Turco *et al*., 2002) and the increase of the other cool water taxa (*G. obliquus obliquus* and the *G. decoraperta* gr.).

At the time of LCO/LO of *G. subquadratus*, which is considered a synchronous event between Equatorial Atlantic Ocean and the Mediterranean (this bioevent is dated at 11.54 Ma in the Mediterranean, Lirer *et al*., 2002; Foresi *et al*., 2002a; Hilgen *et al*., 2000; at 11.55 Ma in the Equatorial Atlantic Ocean, Turco *et al*., 2002) we can suppose that its habitat (shape and depth of the thermocline) was quite similar in the two basins.

The main difference is that the presence in the Mediterranean since 11.80 Ma of cold intermediate species (Fig. 9) is indicative of a stable thermocline, while in the Equatorial Atlantic Ocean the planktonic fauna is completely dominated by warm surface species, indicating a shallower thermocline.

As reported by Turco *et al*. (2001), the exit of *P. siakensis* at 11.21 Ma from the Mediterranean Sea is presumably coeval with that of the North Atlantic. The sharp decreases at 11.10 Ma (100 ky later) of this taxon in the Equatorial Atlantic Ocean (Site 926), (Turco *et al*., 2002; Chaisson & Pearson, 1997) could correspond to the LO of *P. siakensis* in the Mediterranean and could be the response to the progressive cooling of water masses (increase of the subtropical water taxa *G. obliquus obliquus* and the *G. decoraperta* gr.).

These events point to a more pronounced global cooling and seem to indicate the definitive establishment of cool conditions, previously created by the Ice-House phase. However according to Turco *et al*. (2001) this datum is contradicted by the oxygen isotope record.

The effects of this cooling at 11.10 Ma are also visible in the North Atlantic (Leg 151- Site 909C in Winkler *et al*., 2002) variation within clay mineral distribution and increased accumulation rate and in the South Ocean (Leg 120-Site 747 in Billups & Schrag, 2002) major mid-Miocene sea level regression (TB3.1) which corresponds to a sharp decrease in the Mg/Ca ratio and in the $\delta^{18}O_{sw}$.

## CONCLUSION

A complex high-resolution record of Middle Miocene planktonic foraminiferal assemblage changes complemented with stable isotopic data is documented herein from the S. Nicola composite section.

The interval between 12.62 Ma to 12.21 Ma is characterised by overall warm conditions testified also by the subordered intermediate species which are mainly represented by warm water taxa.

From 12.21 Ma when *P. siakensis* disappears, to 11.80 Ma (intervals B and C) the planktonic foraminfera show a pattern indicating a gradual but constant cooling culminating at 11.80 Ma.

Our data substantiate that the climatic cooling at 11.80 Ma, coinciding with the onset of the Mi5 event of Miller (already recognized by Turco *et al*., 2001), is preceded by a stable and long warmer period showing a gradual but progressive change in faunal composition towards colder conditions.

The abundance of neogloboquadrinids in interval D between 11.80 and 11.54 Ma suggests an increase of winter surface water productivity associated with upwelling, spring bloom or DCM development (Ravelo *et al*., 1990; Reynolds & Thunell, 1986; Pujol & Vergnaud-Grazzini, 1995; Tolderlound & Bè, 1971; Fairbanks *et al*., 1982), (Fig. 3). According to Turco *et al*. (2001) the first influx of neogloboquadrinids is related to global cooling as a response to the Mi5 event.

The planktonic assemblage of interval E, from 11.54 Ma to 11.21 Ma can be explained by the intensification of monsoons, with runoff intensification producing a decrease in surface salinities. The monsoon intensification is mainly controlled by eccentricity maxima (precession minima), when high amplitude oscillation occurs in summer insolation. During precession minima the maximum of sea surface temperature and oligotrophic conditions occurs as indicated by the high abundance of *G. quadrilobatus*. This hypothesis is confirmed by the lowest oxygen isotope values and by the positive relationship between $\delta^{18}O$ and $\delta^{13}C$ (Fig. 5).

The cooling trend observed in the Mediterranean area, as well as in the Equatorial Atlantic Ocean, North Atlantic Ocean and Southern Ocean, between 11.21 Ma and 11.10 Ma, shows the definitive establishing of cool conditions toward the Ice-House phase and the temporary disappearance of warm-water taxa from the Mediterranean.

These data support the hypothesis of the southward contraction of the faunal bio-provinces with the inflow of cold North Atlantic water in the Mediterranean (Turco *et al*., 2001). This contraction probably started before the first influx of neogloboquadrinids at 11.80 Ma (Hilgen *et al*., 2000; Lirer *et al*., 2002; Foresi *et al*., 2002a) and more precisely at 12.00 Ma (or 12.21 Ma). In the Equatorial Atlantic Ocean the high abundance of surface warm species

until 11.10 Ma (Turco *et al*., 2002) indicates that the cooling is delayed by 780 ky.

This change has been related to the climate cooling which led to the Ice-House phase with the formation of the EAIS-East Antarctic Ice-sheet (Zachos *et al*., 2001; Winkler *et al*., 2002), characterised by a contraction of warm faunal provinces (Turco *et al*., 2001).

## ACKNOWLEDGEMENTS

We thank E. Turco and L. Capotondi for stimulating discussion on Mediterranean climatic events, A. Vinci for diffractometric analyses, and S. Davanzo and E. Selmo for isotopic analyses. Furthermore we would like to thank I. Premoli Silva for constructive reviews. This study is supported by the Ministero dell'Università e Ricerca Scientifica (MURST-COFIN 2002).

## REFERENCES

Bè, A.W.H. 1977. An ecologic, zoogeographic and taxonomic review of recent planktonic foraminifera. In: Ramsay, A.T.S. (ed.), *Oceanic Micropaleontology*, **1**, 1-100, Academic Press.

Beaufort, L. 1994. Climate importance of the modulation of the 100 kyr cycle inferred from 16 m.y. long Miocene records. *Paleoceanography*, **9**, 821-834.

Billups, K. & Schrag, D.P. 2002. Paleotempeatures and ice volume of past 27 Myr revisited with paried Mg/Ca and $^{18}O/^{16}O$ measurements on benthic foraminifera. *Paleoceanography*, **17**, 1-11.

Chaisson, W.P. & Peirson, P.N., 1997. Planktonic foraminifer biostratigraphy at Site 925: Middle Miocene-Pleistocene. *Proceedings of the Ocean Drilling Program, ScientificResults*, **154**, 3-31.

Chaisson, W.P. & Ravelo, A.C. 1997. Changes in upper water-column strcture at site 925, late Miocene-Pleistocene: Planktonic foraminifer assemblage and isotopic evidence. *Proceedings of the Ocean Drilling Program, ScientificResults*, **154**, 255-268.

Channell, J.E.T., D'Argenio, B. & Horwath, F., 1979. Adria, the African promontory, in Mesozoic Mediterranean paleogeography. *Earth Science Review*, **15**, 213-292.

Devaux, C., 1985. *Foraminifères et isotope légers, indicateurs stratigraphiques et environmentaux de la dernière déglaciation quaternaire, Golfe de Cadix-mer d'Alboran*. Thesis Univ. Bordeaux.

Epstein, S., Buchsbaum, H.A., Lowenstam, H.A. & Urey, H.C. 1953. Revised carbonate-water isotopic temperature scale. *Bulletin Geological Society of America*, **64**, 1315-1325.

Fairbanks, R.G., Sverdlove, M., Free, R., Wiebe, P.H., & Bè, A.W.H. 1982. Vertical distribution and isotopic fractionation of living planktonic foraminifera from the Panama Basin. *Nature*, **298**, 841-844.

Flower, B.P. & Kennett, J.P. 1993. Middle Miocene ocean-climate transition: High resolution oxygen and carbon isotopic records from Deep Sea Drilling Project Site 588A, southwest Pacific. *Paleoceanography*, **8**, 811-843.

Flower, B.P. & Kennett, J.P. 1994. The middle Miocene climatic transition: east Antartic ice sheet development, deep ocean circulation and global carbon cycling. *Paleogeography, Paleoclimatology, Paleoecology*, **108**, 537-555.

Foresi, L.M., Iaccarino, S., Mazzei, R. & Salvatorini, G. 1998. New data on middle to late Miocene calcareous plankton biostratigraphy in the Mediterranean area. *Rivista Italiana di Paleontologia e Stratigrafia*, **104**, 95-114.

Foresi, L-M., Iaccarino S., Mazzei, R., Salvatorini, G., Bambini A.M. 2001. Il plancton calcareo (Foraminiferi e nannofossili) del Miocene delle Isole Tremiti. *Paleontografia Italica*, **88**, 1-64.

Foresi, L.M., Bonomo, S., Caruso, A., Di Stefano, A., Di Stefano, E., Iaccarino, S.M., Lirer, F., Mazzei, R., Salvatorini, G., & Sprovieri, R. 2002a. High resolution calcareous plankton biostratigraphy of the Serravallian succession of the Tremiti Islands (Italy). In: Iaccarino, S., (ed.), Integrated Stratigraphy and Paleoceanography of the Mediterranean Middle Miocene. *Rivista Italiana di Paleontologia e Stratigrafia*, **108**, 257-273.

Foresi, L.M., Bonomo, S., Caruso, A., Di Stefano, E., Salvatorini, G., & Sprovieri, R. 2002b. Calcareous plankton high resolution biostratigraphy (foraminifera and nannofossils) of the uppermost Langhian – lower Serravallian Ras Il-Pellegrin section (Malta). In: Iaccarino, S., (ed.), Integrated Stratigraphy and Paleoceanography of the Mediterranean Middle Miocene. *Rivista Italiana di Paleontologia e Stratigrafia*, **108**, 195-210.

Foresi, L.M., Iaccarino, S. & Salvatorini, G. 2002b. *Neogloboquadrina atlantica praeatlantica*, new subspecies from late Middle Miocene. In: Iaccarino S. (ed.), Integrated Stratigraphy and Paleoceanography of the Mediterranean Middle Miocene *Rivista Italiana di Paleontologia e Stratigrafia*, **108**, 325-336.

Gambini, R. & Tozzi, M. 1996. Tertiary geodynamic evolution of the Southern Adria microplate. *Terra Nova*, **8**, 593-602.

Garrett, C., Outerbridge, R., & Thompson, K. 1993. Interannual variability in Mediterranean heat budget and buoyancy fluxes, *Journal of Climatology*, **6**, 900-910.

Gasperi, J.T. & Kennett, J.P. 1992. Miocene planktonic foraminifers at DSDP Site 289: depth stratification using isotopic differences. In: Berger W.H. *et al*., 1993. *Proceedings of the Ocean Drilling Program, Scientific Results*, **130**, 323-325, College Station TX.

Hemleben, Ch., Spindler, M. & Anderson, O.R. 1988. *Modern Planktonic Foraminifera*. Springer Verlag, 363 pp.

Hilgen, F.J. 1991a. Astronomical calibration of Gauss to Matuyama sapropels in the Mediterranean and implication for Geomagnetic Polarity Time Scale. *Earth and Planetary Science Letters*, **104**, 226-244.

Hilgen, F.J. 1991b. Extension of the astronomically calibrated (polarity) time scale to the Miocene/Pliocene boundary. *Earth and Planetary Science Letters*, **107**, 349-368.

Hilgen, F.J., Krijgsman, W., Raffi, I., Turco, E., & Zachariasse, W.J. 2000. Integrated stratigraphy and astronomical calibration of the Serravallian/Tortonian boundary section at Monte Gibliscemi (Sicily, Italy). *Marine Micropaleontology*, **38**, 181-211.

Iaccarino, S., Foresi, L.M, Mazzei, R. & Salvatorini, G. 2001. Calcareous plankton biostratigraphy of the Miocene sediments of the Tremiti Islands (southern Italy). *Rivista Espanola de Micropaleontologia*, **33**, 237-

248.

Jacobs, E., Weissert, H., Shields, G. & Stille, P. 1996. The Monterey event in the Mediterranean: A record from shelf sediments of Malta. *Paleoceanography*, **11**, 717-728.

Keller, G. 1985. Depth stratification of planktonic foraminifers in the Miocene ocean. In: Kennett J.P. (ed.), The Miocene Ocean - Paleoceanography and Biogeography. *Geological Society of America*, **163**, 177-195.

Kennett, J.P. 1977. Cenozoic evolution of Antartic glaciation, the circum-Antartic ocean, and their impact on global paleoceanography. *Journal of Geophysical Research*, **82**, 3843-3859.

Kennett, J.P. & Barker, P.F. 1990. Latest Cretaceous to Cenozoic climate and oceanographic developments in the Weddel Sea, Antarctica: An ocean-drilling perspective. *Proceedings of the Ocean Drilling Program, Scientific Results*, **113**, 937-960.

Laskar, J., Joutel, F. & Boudin, F. 1993. Orbital precessional, and insolation quantities for the Earth from – 20 Myr to + 10 Myr. *Astronomy and Astrophysics*, **270**, 522-533.

Lirer, F., Caruso, A., Foresi, L.M., Sprovieri, M., Bonomo, S., Di Stefano, A., Di Stefano, E., Iaccarino, S. M., Salvatorini, G., Sprovieri, R., & Mazzola, S. 2002. Astrochronological calibration of the Upper Serravallian/Lower Tortonian sedimentary sequence at Tremiti Islands (Adriatic Sea, Southern Italy). In: Iaccarino S. (ed.), Integrated Stratigraphy and Paleoceanography of the Mediterranean Middle Miocene. *Rivista Italiana di Paleontologia e Stratigrafia*, **108**, 241-256.

Lourens, L.J. & Hilgen, F.J. 1997. Long-periodic variations in the Earth's obliquity and their relation to third-order eustatic cycles and late Neogene glaciations. *Quaternary International*, **40**, 43-52.

McCrea, J.M. 1950. The isotopic chemistry of carbonates and a paleotemperature scale. *Journal of Chemical Physics,* **18**, 849-857.

Miller, K.G, Fairbanks, R.G. & Mountain, G.S. 1987. Tertiary oxygen isotope synthesis, sea level history, and continental margin erosion. *Paleoceanography*, **2**, 1-19.

Miller, K.G, Wright, J.D. & Fairbanks, R.G. 1991. Unlocking the ice house: Oligocene-Miocene oxygen isotopes, eustasy and margin erosion. *Journal of Geophysical Research*, **96B**, 6829-6848.

Mutti, M. 2000. Bulk $\delta^{18}O$ and $\delta^{13}C$ records from Site 999, Colombian Basin, and Site 1000, Nicaraguan Rise (latest Oligocene to middle Miocene): diagenesis, link to sediment parameters, and paleoceanography. *Proceedings of the Ocean Drilling Program, Scientific Results*, **165**, 275-283.

Pampaloni, M.L. 1988. Il Paleogene-Neogene delle Isole Tremiti (Puglie, Italia meridionale): stratigrafia e analisi paleoambientale. *PhD thesis*, 165pp.

Platt, J., Behermann, H., Cunningham, P.C., Dewey, J.F., Helman, H., Parish, M., Shepley, M.G., Wallis, S. & Weston, P.J. 1989. Kinematics of the Alpine arc and the motion history of Adria. *Nature*, **337**, 158-161.

Pujol, C. & Vergnaud-Grazzini, C. 1995. Distribution patterns of live planktic foraminifers as related to regional hydrography and productive systems of the Mediterranean Sea. *Marine Micropaleontology*, **25**,187-217.

Raymo, M.E. 1994. The Himalayas, organic carbon burial, and climate in the Miocene. *Paleoceanography*, **9**, 399-404.

Raymo, M.E. & Ruddiman, W.F. 1992. Tectonic forcing of late Cenozoic climate. *Nature*, **359**, 117-122

Ravelo, A.C. & Fairbanks, R.G. 1992. Oxygen isotopic composition of multiple species of planktonic foraminifera: records of the modern photic zone temperature gradients. *Paleoceanography*, **7**, 815-831.

Ravelo, A.C. & Fairbanks, R.G., Philander, G. 1990. Reconstruction tropical Atlantic hydrography using planktonic foraminifera and an ocean model. *Paleoceanography*, **5**, 409-431.

Reynolds, L.A. & Thunell, R.C. 1986. Seasonal production and morphologic variation of *Neogloboquadrina pachyderma* (Ehrenberg) in the northeast Pacific. *Micropaleontology*, **32**, 1-18.

Rohling, E.J. & Gieskes, W.W.C. 1989. Late Quaternary changes in Mediterranean Intermediate Water density and formation rate. *Paleoceanography*, **4**, 531-545.

Roth J.M., Droxler, A.W. & Kameo, K. 2000. The Carribean carbonate crash et middle to late Miocene transition: linkage to the establishment of modern global ocean conveyor. *Proceedings of the Ocean Drilling Program, Scientific Results*, **165**, 249-273.

Russo, B., Sgarrella, F., Gaboardi, S. 2002. Benthic foraminifera as indicators of paleoecological bottom conditions in the middle Serravallian-basal Tortonian Tremiti sections (eastern Mediterranean, Italy). In: Iaccarino, S.M. (ed.), Integrated Stratigraphy and Paleoceanography of the Mediterranean Middle Miocene. *Rivista Italiana di Paleontologia e Stratigrafia*, **108**, 275-287.

Savin, S.M, Abel, L., Barrera, E., Hodell, D., Keller, G., Kennett, J.P., Killingley, J., Murphy, M., & Vincent, E. 1985. The evolution of Miocene surface and near-surface marine temperatures: Oxygen isotopic evidence. In: Kennett J.P. (ed.), The Miocene Ocean - Paleoceanography and Biogeography. *Geological Society of America,* **163**, 49-82.

Selli, R. 1971. Isole Tremiti e Pianosa. In: Cremonini G., Elmi C., & Selli R. Foglio 156: S. Marco in Lamis, *Note illustrative alla Carta Geologica di Italia, scala 1:100.000.*

Shackleton, N.J. & Kennett, J.P. 1975. Paleotemperatures history of the Cenozoic and the initiation of Antarctic glaciation: oxygen and carbon isotope analyses in DSDP sites 277, 279 and 281. *Initial Reports, Deep Sea Drilling Project*, **29**, 743-755.

Shackleton, N.J. & Hall, M.A. 1984. Carbon isotope data from Leg 74 sediments. *Initial Reports, Deep Sea Drilling Project*, **74**, 613-619.

Shackleton, N.J., Hall, M.A., Pate, D., Meynadier, L., & Valet, J.P. 1993. High resolution stable isotope stratigraphy from bulk sediment. *Paleoceanography*, **8**, 141-148.

Sierro, F.J., Flores, J.A., Francés, G., Vàzquez, A., Utrilla, R., Zamarreno, I., Erlenkeuser, H., Barcena, M.A. 2003. Orbitally-controlled oscillations in planktic communities and cyclic changes in western Mediterranean hydrography during the Messinian. *Paleogeography, Paleoclimatology, Paleoecology*, **190**, 289-316.

Sierro, F.J., Flores, J.A., Zamarreno, I., Vàzquez, A., Utrilla R., Francès G., Hilgen F.J, Krijgsman W. 1999.

Messinian pre-evaporite sapropels and precession-induced oscillations in western Mediterranean climate. *Marine Geology*, **153**, 137-146.

Thunell, R.C. 1978. Distribution of recent planktonic foraminifera in surface sediments of the Medioterranean Sea. *Marine Micropaleontology*, **3**,147-173.

Tolderlund, D.S. & Bé, A.W.H. 1971. Seasonal distribution of planktonic foraminifera in the western North Atlantic. *Micropaleontology*, **17**, 297-329.

Turco, E., Bambini, A.M., Foresi, L.M., Iaccarino, S., Lirer, F., Mazzei, R. & Salvatorini, G. 2002. Middle Miocene high-resolution calcareous plankton biostratigraphy at Site (Leg 154, equatorial Atlantic Ocean): paleoecological and paleobiogeographical implications. *Geobios*, special volume **24**, 257-276.

Turco, E., Hilgen, F.J, Lourens, L.J., Shackleton, N.J & Zachariasse, W.J. 2001. Punctuated evolution of global climate cooling during the late Middle to early Late Miocene: High-resolution planktonic foraminiferal and oxygen isotope records from the Mediterranean. *Paleoceanography*, **16**, 405-423.

Vergnaud-Grazzini, C., Borsetti, A.M., Cati, F., Colantoni, P., D'Onofrio, S., Saliege, J.F., Sartori, R. & Tampieri, R. 1988. Palaeoceanographic record of the Last Deglaciation in the Strait of Sicily. *Marine Micropaleontology*, **13**, 1-21.

Vergnaud-Grazzini, C., Devaux, M. & Znaidi, J. 1986. Stable isotope "anomalies" in Mediterranean Pleistocene records. *Marine Micropaleontology*, **10**, 147-173.

Vincent, E. & Berger, W.H. 1985. Carbon dioxide and polar cooling in the Miocene: The Monterey Hypothesis. In Sundquist E.T., and Broecher W.S. (eds), The Carbon Cycle and Atmospheric CO2: Natural Variations Archean to Present. *Geophysical Monography Serie*, **32**, 455-468.

Winkler, A., Wolf-Welling, T.C.W., Stattegger, K. 2002. Clay mineral sedimentation in high northern latitude deep-sea basins since the Middle Miocene (ODP Leg 151, NAAG). *Journal of Earth Sciences* (Geol. Rundsch), **91**, 133-148.

Woodruff, F. & Savin, S., 1991. Mid-Miocene isotope stratigraphy in the deep sea: High-resolution correlations, paleoclimatic cycles, and sediment preservation. *Paleoceanography*, **6**, 755-806.

Woodruff, F. & Savin, S. 1989. Miocene deep water oceanography. *Paleoceanography*, **4**, 87-140.

Wright, J.D. & Miller, K.G. 1992. Miocene stable isotope stratigraphy, Site 747, Kerguelen Plateau. *Proceedings of the Ocean Drilling Program, Scientific Results*, **120**, 855-866.

Zachos, J., Pagani, M., Sloan, L., Thomas, E., & Billups, K. 2001. Trends, Rhythms, and Aberrations in Global Climate 65 Ma to present. *Science*, **292**, 686-693.

ISBN: 83-912385-5-5

**IMEM-1**

This book presents a collection of papers presented at the 1st Italian Meeting on Environmental Micropaleontology (IMEM) which was held in Urbino in June, 2002. This Meeting was the first in this series and was the precursor to following meetings. The main theme of IMEM-1 was "Micropaleontology applied to environmental and paleoenvironmental research". The papers included in the book present recent advances in the use of foraminifera in environmental and paleoenvironmental recontructions. As it deals with foraminifera from the past and the present, it will be of interest to any Micropaleontologist working in Environmental Micropaleontology.